EVALUATION OF THE QUASI-STEADY-STATE METHOD FOR THE ASSESSMENT OF ENERGY USE IN SCHOOL BUILDINGS

Barbara WAUMAN

Supervisor:
Prof. dr. ir. arch. Dirk Saelens
dr. Ir. Hilde Breesch

Members of the Examination Committee:
Prof. dr. A. Bultheel, chair
Prof. dr. ir. arch. F. De Troyer, (assessor)
Prof.dr. ir. arch. G. Verbeeck, (assessor, UHasselt)
dr. ir. arch. K. Allacker
Prof.Ir. W. Boydens (UGent)
Prof. Ing. V. Corrado (Politecnico di Torino)

Dissertation presented in partial fulfilment of the requirements for the degree of Doctor in Engineering Science

September 2015

Voor papa

Voorwoord

"The finish line is only the beginning of a whole new race." - Unknown

Vandaag, na bijna 6 jaar, is het dan eindelijk zo ver, ik mag het dankwoord schrijven, van mijn doctoraat dan nog wel. Wie had dat ooit gedacht? Velen geloofden het allicht heel wat eerder dan ikzelf. Omdat het zonder de steun van die velen dan ook nooit zover gekomen was, zet ik ze hier met veel plezier graag even in de kijker.

Mijn promotor, Dirk, bedankt! Jouw veelzijdige (praktijk)kennis, oog voor detail en kritische ingesteldheid waren van onschatbare waarde. Jouw werklust en drijfveer waren vaak de extra (nodige) duw in de rug naar hogere toppen die ik alleen ongetwijfeld nooit had bereikt. Het was een enorm leerrijke ervaring om met jou te kunnen samenwerken. Bedankt!
Hilde, zonder jou was er simpelweg geen doctoraat geweest. Bedankt om mij deze kans te geven en steeds in mij te blijven geloven! Je was een fantastische co-promotor en collega, een onmisbare steun op professioneel maar ook op persoonlijk vlak. Om het te zeggen met je eigen woorden "Ik ben er fier op je eerste doctoraatstudent te mogen zijn! Ik ben er zeker dat er nog veel zullen volgen."

Alle alle (ex)collega's van Gent, wat vormen jullie een ongelooflijk fijn team! Al was het de laatste jaren iets meer van op een afstand, de KAHO - *of mag ik dit niet meer zeggen?* - blijft ook nu nog steeds, na 15 jaar, mijn tweede thuis. Bedankt hiervoor!
Micheline, Gerda, Lieselot, Ine, Veerle, Peter(s), Frans en Alexis, bedankt voor de waardevolle aanmoedigingen en steun onderweg. Luc, bedankt voor de unieke kans die je mij gaf en om in mij te geloven.

Alle collega's van de afdeling bouwfysica in Leuven, bedankt! Het duurde misschien iets langer als outsider uit het Gentse maar al snel werd ook voor mij het labo een *derde* thuis. Een fijne werkplek, leuke samenwerking, afgewisseld met op tijd en stond een gezellige koffieklets, een stukje (appel)taart, een zomerse BBQ of pizza's uit de labo oven.
Ruben, bedankt voor de wijze raad, de gezellige treinritten, de aanmoedigende post-its op mijn scherm en verlichtende emailtjes als het weer eens zwart werd voor mijn ogen. Het ga je ontzettend goed in je zoektocht!
Jelle, Mieke en Wout... het werk zit erop, het is gedaan!!! Bedankt voor alles, jullie waren ECHT onmisbaar vanaf dag één: onuitputtelijke bronnen van kennis en wijsheid (?!?), luisterende oren, steun en toeverlaat, heerlijke collega's maar misschien wel nog het meest van alles als gezellige babbelaars, ongelooflijk fijn gezelschap op een emiritaatsviering of andere avondjes weg en hopelijk

vrienden voor het leven. Mieke, ik had me geen betere partner on the road kunnen bedenken!

Naast alle collega's zijn er natuurlijk nog een hele hoop vrienden en familie die hun steen(tje) hebben bijgedragen. Zij wisten tot op vandaag eigenlijk niet juist waarom ik zoveel keren achter de schermen verdween.
Mama, bedankt voor alle kansen, het onmetelijke geduld, het delen van de hoge toppen maar ook - *en misschien wel vooral* - het opvangen van de diepe dalen. Bedankt voor de geweldige en zorgeloze thuis die ons gaf/geeft, je ongelooflijke enthousiasme als mama van 3 maar ook als marraine van 6 - *en binnenkort zelfs 7!* Bedankt om er steeds te zijn voor 2!
Lieselotte, wat een zus! Bedankt om de spil te zijn bij onze familiale gebeurtenissen, bedankt voor alle steun, ontspannende babbels maar in het bijzonder voor de tweede, onmisbare thuis die je onze kindjes gaf wanneer ik er vaak - *te veel?* - niet was.
Alle andere (schoon)familieleden, vrienden en vriendinnen, en in het bijzonder Noémie, voor de virtuele koffiebreaks, maffe skypegesprekjes en de wederzijdse PhD-peptalk vanuit Lissabon, Melbourne of Oostende, en Inge voor de ontspannende avondjes weg, de mama-talks en het inspireren, stimuleren en delen van onze reisplannen. Bedankt!

En dan zijn er nog de 3 mannen van mijn leven ...
Cis en Mon, gewoon bedankt om er te zijn, om te zijn wie jullie zijn, 2 fantastische kereltjes! Ik ben ongelooflijk trots op jullie! Het laatste jaar hebben jullie mama veel moeten missen maar dat maken we nu dubbel en dik goed!!
En tenslotte Oli, de persoon die het de laatste maanden ongetwijfeld het hardst heeft moeten verduren. Ik heb veel van je gevraagd. Je hebt minstens even hard gezwoegd als ik en dit zonder enige extra titel. Daarom, papa der papa's maar vooral partner der partners, bedankt om er steeds opnieuw voor ons te zijn, om me te laten zijn wie ik ben en het beste in mezelf naar boven te halen. Je bent gewoonweg onmisbaar!

De klus is geklaard! Het zit erop! Nu ligt de weg open om even alleen nog maar te genieten met ons 4, met een ticket naar de zon ... .

Barbara, 23 oktober 2015

Abstract

In Flanders, a monthly, *quasi-steady-state* calculation tool is used for energy rating and certification of building designs. To guarantee the EPB Directive's effectiveness, the obtained *quasi-steady-state* calculation results must be accurate and reliable. Possible inaccuracies may however occur due to inaccuracies of the implemented input data or by inaccurate model simplifications. This research focuses specifically on the evaluation of the accuracy of the calculation method for school buildings in Flanders. In doing so, the accuracy of the use of (**i**) standardised boundary conditions and default input data, (**ii**) correlation-based correction factors to account for the thermal transient behaviour and system intermittency and (**iii**) default fixed subsystem efficiencies to calculate the energy use is studied.

First, an uncertainty and sensitivity analysis are performed to reveal the impact of the choice of the standardised input data on the energy performance assessment. Second, the accuracy of the monthly method for energy demand calculations itself is analysed and modified to the use of school buildings. *Dynamic* and *quasi-steady-state* calculation results are compared to assess the accuracy of the implementation of the dynamic behaviour in the monthly method. The correlation-based correction factors are adapted accordingly using regression analysis techniques. Finally, a series of integrated, dynamic building and HVAC system simulations is performed to assess the reliability of the simplified, sequential subsystem calculation approach used for the energy use calculations.

The following modifications are suggested to fit the EPR results better to the output of dynamic building simulations, ordered based on their priority. (**i**) The implementation of a more diverse room type profile, including representative boundary conditions for amongst others occupancy rates and schedules, internal heat gains, etc. based on the specific use and characteristics of Flemish schools, should be considered. (**ii**) The integrated, dynamic building and HVAC system simulations confirm the reliability of the simplified calculation approach. A revision of the tabulated efficiencies is however suggested, based either on the results of dynamic simulations or on the alternative calculation approach as described in EN 15316. Finally, (**iii**) it is suggested to implement newly derived values for the utilisation and intermittency factor, specifically adapted to the typically school use.

Korte inhoud

Om de energieprestatie van gebouwontwerpen te beoordelen, wordt in Vlaanderen gebruik gemaakt van een maandelijkse, *quasi-statische* berekeningsmethode. De nauwkeurigheid van deze resultaten is cruciaal voor de doeltreffendheid van het energiebeleid (EPBD). Hierbij spelen zowel de juistheid van de gebruikte randvoorwaarden en gebruikerskarakteristieken als de betrouwbaarheid van berekeningsmethode zelf een belangrijke rol. Deze studie bestudeert specifiek de nauwkeurigheid van de berekeningsmethode voor schoolgebouwen in Vlaanderen. Hiertoe is de impact bestudeerd van het gebruik van (**i**) gestandaardiseerde, maandgemiddelde randvoorwaarden, (**ii**) geïmplementeerde correlatie-factoren om dynamische effecten en de thermische traagheid van schoolgebouwen in te rekenen en (**iii**) jaargemiddelde systeemrendementen op het resultaat van de energie-prestatie-berekening.

Eerst is de impact van de randvoorwaarden op de energievraag bepaald aan de hand van een onzekerheids- en sensitiviteitsanalysis. Vervolgens is de nauwkeurigheid van de berekeningsmethode voor energievraag bestudeerd. Op basis van een vergelijking van *dynamische* en *quasi-statische* resultaten en gebruik van regressieanalyse zijn nieuwe waarden voor de correlatie-factoren afgeleid. Tenslotte is met behulp van geïntegreerde, dynamische simulaties de vereenvoudigde methode voor de berekening van het eindenergiegebruik voor verwarming geëvalueerd.

Gebaseerd op deze resultaten worden volgende aanpassingen voorgesteld aan de *quasi-statische* berekeningsmethode om maximale compatibiliteit met dynamische simulatieresultaten te bekomen, opgesomd in volgorde van belangrijkheid. (**i**) Er wordt voorgesteld om de mogelijkheid te creëren om een breder spectrum van schoollokalen in de methode in te voeren, alsook bijhorende realistische gebruikstypologieën (oa. interne warmtewinsten, gebruiksduur kunstverlichting) te gebruiken die zijn afgetoetst aan het reële gebruik van Vlaamse scholen. (**ii**) Dynamisch simulaties tonen aan dat voor de onderzochte selectie van verwarmingssystemen, de vereenvoudigde berekeningsmethode die gebruik maakt van jaargemiddelde systeemrendementen betrouwbare resultaten oplevert. Een aanpassing van de huidige, getabelleerde systeemrendementen wordt echter aangeraden. Uit de studie blijkt dat zowel dynamische simulatieresultaten als de alternatieve berekeningsmethode uit EN 15316 hiervoor als referentie kunnen dienen. (**iii**) Tenslotte wordt voorgesteld om de correlatie-factoren die dynamische effecten en thermische traagheid inrekenen specifiek aan te passen aan de typologie en het gebruik van schoolgebouwen.

Contents

Nomenclature

Acronyms

ACH	Air changes per hour
AGIOn	Agency for School infrastructure
AHU	Air handling unit
ASHP	Air source heat pump
ASO	General secondary education (in Dutch)
BEMS	Building energy management system
BSO	Vocational secondary education
CAV	Constant air volume
CEN	European Committee for Standardisation
DCV(-IR)	Demand control ventilation(-Infra red)
EAHX	Earth air heat exchanger
EE	Elementary effect
EESB	Energy efficient school buildings
EPBD	Energy performance of buildings directive
EPR	Energy performance regulation
GSHP	Ground source heat pump
GSHX	Ground source heat exchanger
HRV	Heat recovery device
HT	High temperature regime
HVAC	Heating, ventilation and air conditioning
IAQ	Indoor air quality
IDA	Indoor air
IHG	Internal heat gains
KSO	Art secondary education
LHC	Latin Hypercube
LT	Low temperature regime
MCA	Monte Carlo analysis
MW	Mineral wool

NPC	Net present cost
NPD	Normalised lighting power density
NTU	Number of transfer units
OSB	Oriented strand board
PE	primary energy use
PHPP	Passive House Planning Package
PLR	Part load ratio
POF	Partial operation time factor
PUR	Polyurethane
RA	Relative absence factor
RMSE	Root mean square error
SA	Sensitivity analysis
SFP	Specific fan power
TRNSYS	Transient system simulation
TRV	Thermostatic radiator valve
TSO	Technical secondary education
UA	Uncertainty analysis
VAT	Value added tax
VAV	Variable air volume
VSD	Frequent speed drive
WWR	Window-to-wall ratio

Roman symbols

a	Correlation based numerical parameter	-
	Correction factor	-
A	Surface area	m^2
b	Correlation based correction factor	-
c	Specific heat capacity	J/(kg.K)
	Correlation based correction factor	-
C	Heat capacitance	J/K
d	(Effective) thickness	m
	Discount rate	-
dT	Relative overheating	-
E	Energy (except quantity of heat)	kWh
	Energy cost	€; €/m^2
f	Fraction	-
	Conversion factor	-
	Correction factor	-

F	Temperature fraction for radiation	-
	Probability distribution	-
g	Solar factor of glazing	-
G	Air flow rate	m^3/h, ACH
h	Heat transfer coefficient	W/(m^2.K)
	Height	m
	Heat transfer coefficient	W/K
I	Investment cost	€, €/m^2
L	Length	m
m	Mass	kg
$\dot{m}$	Mass flow rate	m^3/h
M	Maintenance costs	€, €/m^2
n	Air tightness level	ACH, h^{-1}
	Number	-
	Radiator exponent	-
P	Power (except thermal power)	W
q	Heat flux density	W/m^2
	Specific heat design heat load	W/m^2
Q	Quantity of heat	J, kWh, kWh/(m^2.a)
r	Price increase	-, %
	Temperature adjustement factor	-
R	Thermal resistance	(m^2.K)/W
	Replacement costs	€, €/m^2
t	Time	s, h, a
T	Temperature	°C, Kelvin
U	Overall heat transmission coefficient	W/(m^2.K)
V	Volume	m^3
	Residual value	€
$\dot{V}$	Air flow rate	m^3/h
W	Auxiliary (electrical) energy use	J, kWh

Greek symbols

α	absorption coefficient	-
β	part load ratio of the heating (distribution) system	-
γ	heat balance/gain loss ratio	-
δ	relative error	-
ε	emissivity	-
	effectiveness	-
η	efficiency	-
λ	thermal conductivity	W/(m.K)
	air to fuel ratio	-
ξ	window-to-floor ratio	-
μ	average	N.A.
ρ	reflectance	-
	density	kg/mcub
σ	standard deviation	N.A.
τ	Thermal transmittance	-
	Time constant of the building	h
	Correlation based numerical parameter	-
θ	Temperature	°C
χ	Control signal	-
ϕ	Thermal power	W
	Heat flow	W
ψ	Linear thermal transmittance	W/(m.K)

1 Introduction

1.1 Background and problem statement

Energy efficiency and good indoor environmental quality are important issues in schools. While the Flemish educational system ranks highly [1, 2], the quality of the school buildings is generally poor [3, 4]. Research results of the organisation for economic co-operation and development (OECD) on the state of education world wide [5] show that investments in educational infrastructure in Flanders are below the averages. The chronic shortage of funds results in an aging and outdated building stock with often inadequately maintained and degraded lighting, heating and (if present) ventilation systems [6] which, in turn, cause high energy use [7, 8, 9], high related energy costs and poor indoor climate conditions [10, 11, 12].

Recent large scale monitoring of the quality of Flemish school buildings revealed that 59% of the schools buildings are built before *1970* and thus prior to the introduction of building energy efficiency policy [6]. Only 6% is recently built (> 2008) [6]. The school building stock is thus largely outdated which results consequently in a high energy use: Flemish schools use on average 240 $kWh_{prim}/(m^2.a)$ [9]. In parallel, various studies [10, 11, 12] confirm the generally poor conditions of the indoor environment in (Flemish) schools. According to large scale questioning, 20% of the users of school buildings are dissatisfied with the indoor environmental conditions [12]. Indoor temperatures are often uncontrollable resulting in bad thermal comfort in winter in 40% of the questioned schools while 70% of the schools suffer from bad thermal comfort and overheating in summer. At the same time, the indoor air quality in class rooms is often insufficient [11, 10]. Hens et al. [11] measured the indoor air quality in 19 class rooms, in 18 different schools. In 17 of the observed rooms, CO_2levels of more than 1500 ppm (*i.e.* the threshold limit value for IDA-class 3 as set in [13]) were found, while in nine class rooms, even the average CO_2levels exceeded that limit [11]. A more

recent large scale study, in which the indoor air quality of 90 class rooms was measured [10], revealed CO_2 concentrations higher than 900 ppm in *89%* of the cases. The peak CO_2 concentration was 2701 ppm [10].
Based here upon, one may conclude that the overall quality of the current school building stock is rather poor, both in terms of comfort as energy efficiency. Over the last years however, a strong trend towards increased indoor environmental quality and reduced energy use in schools is noticed in Flanders. Large-scale indoor air monitoring and sensibility campaigns in schools are set up [14]. Moreover, improved ventilation strategies for class rooms are introduced resulting generally in an improvement of the indoor air quality [15, 16]. Simultaneously, the building energy policy has become increasingly stringent. The key part is the introduction of the *'Energy Performance of Buildings Directive'* (EPBD) [17], first published in *2002* and followed by a more stringent recast *2010/31/EU* in *2010* [18]. Since the implementation of the EPBD in 2006 in Flanders, the number of energy efficient non-residential buildings has increased constantly [19, 20]. The evolution towards more energy efficient schools in particular is strengthened by the approval of the *'Directive for Energy Performance in School Buildings'* dd.*07/12/2007* [21]. In this Directive, amongst others the criteria for Flemish passive schools are set forward:

1. annual net energy need for heating $\leq$ 15 kW/(m^2.a)
2. annual net energy need for cooling $\leq$ 15 kW/(m^2.a)
3. maximum air tightness level $n_{50} \leq$ 0.6 ACH
4. maximum E-level = 55 (primary energy performance level as calculated by *EPR* [22])

At the same time, financial initiatives are introduced by the Flemish government - aside from the regular financing procedures - to reduce the backlog in modernised school infrastructure and to assist schools by implementing the energy policy in the school building practice. The first initiative is the DBFM-project which is responsible for **d**esigning, **b**uilding, **f**inancing and **m**aintaining approximately 200 new energy efficient school building projects spread over Flanders [6]. It involves an investment of €1.5 billion and aims at reducing the energy use in schools and to sensitise pupils for the need to save energy. The second initiative offers additional funding (235 €/m^2) to finance (part of the) extra investments in 24 passive 'pilot' school projects (> 65000 m^2, spread over the Flemish region and covering all educational forms) which will be used as a reference for contemporary (and future) high performance school building practice.

To assess the energy performance compliance (EPBD) of the newly built schools in Flanders, an obligatory software tool [23, 22]) is used which calculates the energy performance of a building design in three consecutive steps: **(i)** the calculation of the net energy demand, **(ii)** the calculation of the delivered energy to the heating and cooling systems as the division of the energy demand by the annually averaged, tabulated subsystem efficiencies for generation, storage, distribution, control and emission and **(iii)** the calculation of the primary energy use by adding the auxiliary energy needed for all system components and converting it to primary energy, taking into account renewable energy sources and national conversion factors which represent the conversion step from energy source to energy carrier. The energy balances are hereby calculated in steady-state conditions on a monthly time-base so dynamic effects such as climatic conditions, operational schedules or (system) intermittency are taken into consideration in a simplified way by time weighted averaged values and

empirically determined correction factors. Furthermore, a simplified approach is used for the interaction between **(i)** the various building zones (*i.e.* a multi-zonal approach is applied without taking into account thermal coupling between the considered building zones) and **(ii)** the building and HVAC systems. Finally, as the *EPR* calculation method is used in the context of building regulation, standardised boundary conditions and default input data are used to allow for objective evaluation and mutual comparison of the various (school) building designs.

To ensure the objectives of the building energy policy and guarantee the EPB Directive's effectiveness, the obtained *quasi-steady-state* calculation results must be accurate and reliable. Moreover, as the EPR tool is used for the execution of cost-optimal studies [24, 25] in the context of EPBD [18] and hence is used as a supporting tool for energy policy decision making, the calculation results should be realistic to avoid inaccurate cost-optimal design solutions and inefficient energy saving measures which could affect in turn the evolutions and trends on the building market [26]. Within that context, various studies can be found which investigate the accuracy of the use of monthly, *quasi-steady-state* calculation methods for energy rating purposes [27, 28, 29, 30, 31, 32, 33, 34, 31, 35]. No clear consensus however has been reached. Some studies state that the monthly, *quasi-steady-state* calculation method is well suitable to assess accurately the energy performance of a building (design) [28, 27, 29, 30, 31] while other studies are found which reveal significant discrepancies between *static* and *dynamic* energy calculation results, especially for intermittently used buildings such as schools [28, 29, 30, 32, 33, 34, 31, 35]. These discrepancies are explained by inaccuracies of the implemented standardised boundary conditions and input data, inaccuracies of the heat transfer/gain calculations or by inherent model assumptions and simplifications of the monthly, *quasi-steady-state* calculation method [28, 29, 30, 32, 33, 34, 31, 35].

Among the list of likely causes of inaccuracies, three are specifically influenced by the use and typology of school buildings:

- The **deterministic** values for amongst others operational schedules, ventilation characteristics and internal heat gains as used in the *EPR* calculation tool are not always representative for the current Flemish school's use. Some of the semi-empirical data that are used are outdated due to current changes and trends (*i.e.* occupant density rates vary in time, user's schedules may changes due to the shift towards 'Open schools'[1] [36]) while other data are inaccurate (*i.e.* default values as set in the European CEN/EPB standard [37] are applied whereas real **boundary conditions** often depend strongly on national or regional customs (*i.e.* school opening hours differ strongly between various countries or regions) or too general (*i.e.* no diversification is made in the calculation tool between offices and school buildings).
- The **implementation of the transient thermal behaviour of the building** in the *quasi-steady-state* calculation method - and in particular the use of numerical correlation-based correction factors as currently applied in the *EPR* calculation tool - are inaccurate and should be adapted to the typical use and the typology of the considered (school) building [32, 33, 34, 38].

[1] 'Open schools' are defined as a local collaboration between different sectors, whereby one or more schools work together to create a broad learning and living environment in an effort to maximise development opportunities for all children and youngsters. This ambition inherently means a more intensive use of space outside the regular school opening hours, on Wednesday afternoons, in weekends etc.

- The **tabulated subsystem efficiencies** used to assess the final energy use in *EPR* might (over)simplify the dynamic and nonlinear interaction of the building and systems, and might neglect the mutual interplay between the various subsystems [39, 40, 41, 42].

Other likely causes of inaccuracies such as the (simplified) calculation of the heat transfer to the soil, the calculation of solar heat gains, the long-wave radiation to the sky, the choice of the calculation time step (*i.e.* hourly, monthly or seasonal), ignoring the thermal coupling between various building zones, etc. are as important for the accuracy of the outcome of the calculations though are independent of the specific use and typology of the building.

In this context, the overall aim of this research is to **evaluate the accuracy of the monthly, *quasi-steady-state* calculation method** as currently applied in Flanders for energy rating and certification of building (designs) in a regulatory context and **revise** the method wherever necessary **to fit it better to the typical use and characteristics of school buildings**.

1.2 Research objectives

Within the framework of the above elaborated problem statement, the overall objective of this dissertation is to obtain more accurate energy use assessment results by fitting the results of the monthly, *quasi-steady-state* calculation method to the results of *dynamic* simulations in TRNSYS. The research is hereby focusing specifically on (contemporary) school buildings and the impact of their typical users' characteristics on the results of the energy use calculations.

To obtain the general research aim, following consecutive research objectives are set:

- To **develop** of a representative set of **reference school buildings** which are used as a basis for analysing the (contemporary) Flemish school building stock.
- To define a set of **representative, standardised boundary conditions, typical for Flemish schools,** and assess the impact on the *quasi-steady-state* energy calculation results.
- To **study the energy demand and the thermal behaviour** of school buildings by *dynamic* simulations and **refine the *quasi-steady-state* calculation method** - and in particular the applied numerical correlation-based correction factors - **in line with these simulation results**.
- To **estimate the interaction of the building and the coupled HVAC systems** by integrated *dynamic* simulations and define the **effects of this interaction on the HVAC system performance and overall system efficiency**.
- To assess **the impact of the suggested changes to the method on a cost-optimal school design** in order to emphasise the need to revise the *quasi-steady-state* calculation method.

1.3 Dissertation outline

In ***Chapter 2***, the contemporary Flemish school building stock is described. An analysis is made of the typical architectural characteristics of the current school building practice: representative building sizes, geometries, shapes and room type profiles are defined based on literature review and

an exhaustive statistical survey of recently built or renovated school projects. Furthermore, typical characteristics related to **(i)** the use and operational profile, **(ii)** the construction and building envelopes and **(iii)** the HVAC systems and lighting concepts in schools are studied. Subsequently, this information is combined into a number of reference school buildings which are used along the rest of the research study.

Overall, two main methods exist for energy performance compliance checking: *quasi-steady-state* methods, which calculates the heat balance in steady-state conditions over a sufficiently long time (often a month) and *dynamic* methods, which calculate the heat balance with shorter time steps (typically 1 h or less). The basic principles of both methods are discussed in ***Chapter 3***. First, the monthly, *quasi-steady-state* method as described in *EN ISO 13790* [37] is analysed. Subsequently, a comparison with equivalent (inter)national standards on the *quasi-steady-state* calculation is made (*EPR* [22], *DIN V 18599* [43], NEN 7120 [44]). Next, a short summary of the calculation procedures for energy use for heating as described in *EPR* [22] and *EN 15316* [45] is given. The specific calculation algorithms and tabulated input values used for the calculations of each part of the heating system are discussed. Third, the algorithm for *dynamic* simulations as applied in the simulation tool `TRNSYS` is discussed. Fourth and final, an overview is given of measures taken to guarantee compatibility and consistency between the application and results of the *static* and *dynamic* methods.

In the next two chapters, the likely causes of the differences between *dynamic* and *static* calculation methods to predict energy demand are studied, focusing in particular on the influence of typical characteristics of school buildings. The first part (***Chapter 4***) analyses the use of standardised input data and boundary conditions and their impact on the energy assessment results. A provisional list of input data is developed based on the existing European (*EN 12464* [46], *EN 13779* [13], *EN 15251* [47], *EN ISO 7730* [48], *EN ISO 13790* [37]), Belgian (*EPR* [22]), German (*DIN V 18599* [43]) and Dutch (*NEN 7120* [44]) standards concerning energy performance, ventilation and comfort. The impact on the energy demand calculations due to the variations of the input data as found in literature is demonstrated in an uncertainty analysis (UA) using the Monte Carlo analysis method (MCA) combined with the Latin Hypercube Sampling technique (LHS). Afterwards, a sensitivity analysis (SA) is performed, using the method of Morris, to determine the relative importance of each investigated boundary condition. Once the predominant boundary conditions are depicted, surveys are performed to gather exact information on these specific parameters and subsequently new, more realistic boundary conditions can be determined, wherever necessary, to be used in the context of the building energy regulation.
In the second phase (***Chapter 5***), the accuracy of the *quasi-steady-state* method itself - and more in particular the implementation of dynamic effects - is analysed and modified to the use of school buildings. The influence of typical school buildings' characteristics on the energy demand are studied by *dynamic* simulations. New values for the utilisation factors used for the heating and cooling balance are derived using regression analysis techniques. Furthermore, the impact of system intermittency on the energy demand is simulated and the calculation approaches used to implement these effects in the *quasi-steady-state* method are evaluated. Based on the results of *dynamic* simulations and additional regression analyses, new values for the numerical, correlation-based parameters as used

in *EN ISO 13790* [37] and in *NEN 7120* [44] to account for system intermittency are set.

In ***Chapter 6***, the influence of both the buildings' characteristics and the selection of the HVAC system components on the HVAC system performance in schools is analysed. To that end, integrated building and HVAC system simulations of a typical school building model are conducted in TRNSYS. 18 school model design variants, defined by varying building characteristics, are coupled with a selection of four traditional but commonly found HVAC systems in contemporary schools. A radiator, a floor and an all-air heating system, all supplied by a condensing gas boiler, are simulated. Subsequently, it is evaluated if these affects are accounted for accurately by the *EPR* calculation standard [22]. Next, it is investigated if an alternative calculation approach either based on the CEN/EPBD standard *EN 15316* [49] or on the results of dynamic simulations could offer more accurate calculation results for the final energy use for heating compared to the *EPR* calculation standard [22].

Finally, in ***Chapter 7***, a cost-optimal study is performed to assess the impact of the changes to the monthly, *quasi-steady-state* calculation method as set in *Chapter 4* to *Chapter 6* on a cost-optimal school design. The impact of the suggested changes of the calculation method is studied on both the determination of the Pareto-optimal school designs and on the hierarchy of a restricted list of energy saving measures of the building envelope. The cost-optimal study presented along this research study is performed only to reveal the impact of the suggested changes to the energy calculation method. Consequently, no general conclusion on the economically optimal school building configuration or on the hierarchy of energy saving measures are formulated.

1.4 Research scope

With a research domain being as wide as "*the evaluation of the accuracy of the quasi-steady-state calculation approach used for schools*", some boundaries have to be set:

- The aim of this research study is to evaluate and suggest some refinement the *quasi-steady-state* method used to objectively rate building design variants in the context of the EPBD [18]. The changes proposed along this dissertation intent to assess the energy use more realistically and to fit the energy calculations better to the specific use and typology of school buildings. Other causes of uncertainty of the calculation model such as the calculation of the heat transfer to the soil, the calculation of solar heat gains, the long-wave radiation to the sky, the choice of the calculation time step, ignoring the thermal coupling between various building zones, etc. which are also important for the accuracy of the outcome of the calculations though are not specifically linked to the use of schools, are not addressed throughout this research.

- This dissertation focuses on the energy performance evaluation. The improvement of the overall environmental quality in schools is not considered as a specific research topic. Minimum indoor air quality, and thermal and visual comfort conditions are maintained and considered as important boundary conditions. Thermal comfort conditions are evaluated in all building design variants used along this work. Due to the restrictions of the use of the dynamic simulation tool TRNSYS and the application of a zonal calculation approach, thermal comfort is however

assessed on a zonal level only. Local discomfort might occur but is not studied in particular.

- The inaccuracy of the calculation model is only one of the causes for unrealistic energy assessment results. While using the *EPR* tool as a predictive tool for energy savings, Deurinck [50] denotes the rebound effect[2], and occurring technical issues and shortcomings as additional causes for unrealistic energy use assessments. As this research focuses however specifically on the evaluation of the accuracy of tools that are used for energy rating, these causes are not further addressed in this research study.

- The focus of this research study is put mainly on the calculation of the energy use for heating and ventilation. Regarding cooling, the suggested changes are restricted to the method used for energy demand calculation. The use of equipment and lighting is only considered as a boundary condition (*i.e.* part of the considered internal heat gains). Calculation approaches that are used to calculate the energy use associated with equipment and lighting is not addressed. Likewise, the calculation of the energy use linked to the production of hot tap water is not considered.

- A large variety of schools is found depending on the age of the students and the type of the educational activities taught. As it is unfeasible to cover the whole range of schools, the scope of this research is limited to general elementary and secondary schools. Schools providing (atypical) technical education, and tertiary and special education facilities are not included in the study.

- Due to the work load related to the performance of integrated building and HVAC simulations, the study of the interaction of building and systems is restricted to the currently, most commonly used HVAC systems in schools. More innovative systems are hence not included.

[2]When energy saving measures are implemented in a building, space heating gets more affordable. Influenced by the energy cost savings, habitants tend to increase their comfort level, hereby neutralising part of the theoretically savings. This phenomenon is denoted as the rebound effect.

2

Representing the contemporary Flemish school building stock

*School buildings have typical architectural and operational characteristics which differ significantly from other building typologies. Occupancy rates, ventilation rates and internal heat gains are generally high. Daily school opening hours are limited and frequent holiday periods occur. Furthermore, a large variety of school buildings is found based on the educational activities and target age of the students. This chapter gives an elaborate overview of these typical school characteristics. First, a description is given of the contemporary Flemish school building stock: representative building sizes, geometries, shapes and room type profiles are defined based on a literature review and an exhaustive statistical survey of recently built or renovated school projects. Furthermore, an overview is given of the typical characteristics related to **(i)** the use and operational profile, **(ii)** construction and building envelope and **(iii)** HVAC systems and lighting concepts.*

The information gathered in this chapter will then be combined into reference school building models which are used along the rest of this dissertation or can be used outside the scope of this specific study for amongst others policy makers to evaluate the impact of energy-efficiency measures or different building energy policies for the contemporary Flemish school building stock.

2.1 Introduction

School buildings have typical, resembling characteristics which distinguish educational buildings from residential or other non-residential buildings. For example, schools have a strongly discontinuous users' profile and high occupant density rates causing high internal heat gains and ventilation rates in turn. These characteristics significantly affect the design, use and energy performance of the building. Furthermore, a large variety of school building (types) can be found [4] (see *Figure 2.1*).

Figure 2.1: Two examples of contemporary, elementary passive school buildings in Flanders. On the left, an example is given of a school with a simple building shape and traditional room type profile (B-Architecten, Kalmthout). On the right, a more complex building is shown with a more contemporary zone partition (*i.e.* lots of open spaces for group activities are foreseen) (Lava Architecten, Bocholt).

Depending on the educational form (from general to vocational education - see *Appendix A*) and the age of the students (from nursery to secondary education) specific space requirements for class rooms, corridors, sanitary and technical rooms are valid. This diversity on a small scale complicates energy performance evaluation of school buildings on a larger scale. Therefore, in the first part of this chapter (*§ 2.2*), a limited number of reference school buildings are defined, which are representative for the contemporary school building stock. Typical school building sizes, geometries, shapes and room type profiles are analysed based on literature review. Furthermore, a statistical survey of recently built or renovated school projects in Flanders is performed. Subsequently, this information is combined into four reference school building models. In the second part of this chapter, an overview is given of **(i)** the use and operational profile (*§ 2.3.1*), **(ii)** construction and building envelope (*§ 2.3.2*) and **(iii)** HVAC systems and lighting concepts (*§ 2.4*) in schools to get insight into typical school buildings' characteristics and design.

The reference school buildings as defined in *§ 2.2* will be used along the rest of this dissertation. In doing so, the models will be combined with the range of building and operational characteristics as set in *§ 2.3* and will be - if applicable - coupled with an HVAC system selected from the results as described in *§ 2.4*.

2.2 Development of reference school buildings

According to Annex III of the EPBD recast [18], reference buildings must be characterised by and be representative of their functionality and location, including indoor and outdoor climatical conditions. Various projects can be found, either focusing on the methodology used to develop reference buildings [51, 52, 53] or presenting the results of the development of reference buildings for dwellings [54, 55, 56, 57, 58], multi-family buildings [59], offices [60, 39, 52, 61] or commercial buildings [62, 63]. Some studies use reference buildings for the evaluation of energy saving measures [63]. Others create them in order to develop benchmark energy consumption [64, 55]. Among all researches found, only few reference buildings for schools [65, 25, 62, 66] are defined. Moreover, the available information is often not applicable for the outline of this dissertation as it is either only adequate for the specific project scope [65] for which the models were developed, or not representative for the Flemish school building stock [67, 68, 69, 70, 62, 66]. Therefore, throughout this section, a limited number of representative reference buildings for schools are developed, based on a comprehensive analysis of the typical architectural characteristics.

In *§ 2.2.1*, the modelling approach used to define the school reference buildings is discussed. In *§ 2.2.2*, the plan type and building geometry, and the room type profile for the reference school building models for elementary and secondary education are set.

2.2.1 Method and assumptions

The TABULA project [51] uses two different modelling approaches to develop reference buildings: the **representative** and the **typical type model** approach. The first approach models the entire building stock using a set of fictional but realistic, reference buildings based on average values.

The latter composes a set of typical buildings closely related to existing buildings and building components which are chosen for their reference value compared to the examined stock. Brandão de Vasconcelos et al. [53] describe the strength and weaknesses of both the modelling approaches. Based hereupon, they propose the representative modelling approach to be applied, using both expertise knowledge and elaborate statistical data to develop the final reference buildings. Considering the scope of this research, a similar approach is adopted. Furthermore, the modelling procedures as used for the definition of reference dwellings [59], multi-family buildings [59] and offices [60, 71, 52] are used as a reference (see *Figure 2.2*).

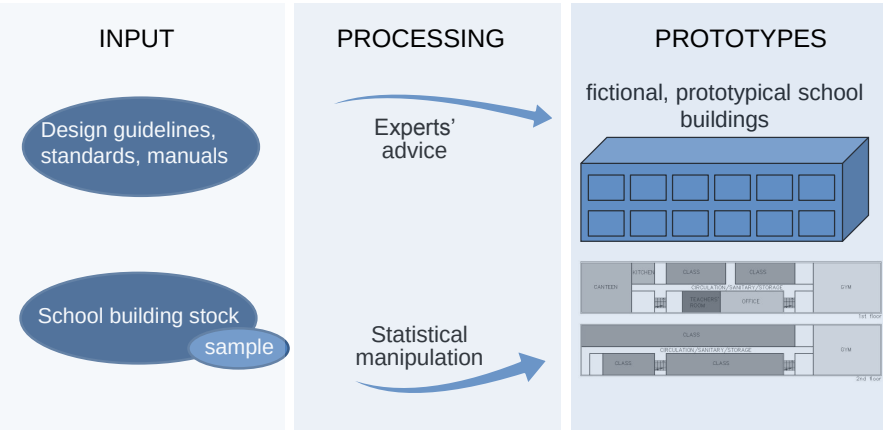

Figure 2.2: General method used to develop the reference school buildings [52, 53].

First, the required level of detailing is determined. Even though an increased number of differentiated reference models does not necessarily lead to a more accurate representation of the building stock [72], the combination of all school building types into one single model would be inadequate and would result in a large spread of requested additional input data (*e.g.* operational schedules, internal heat gains, ventilation rates) afterwards [73]. Hence, four different reference models are defined, two for elementary and two for secondary education. In a second step, the necessary architectural input data are gathered. Many literature on school architecture and infrastructure can be found. Van Bogaert [74] and more recently, Chatel et al. [75], studied school architecture and design. Leemans [3] published the results of a large-scale survey on the quality of the current Flemish school building stock. In addition, multiple guidelines and manuals on sustainable school architecture [76, 77, 78, 79, 67, 80] and various case study surveys on exemplary educational buildings [81, 82, 75] can be found. Extensive databases on specific architectural characteristics of the Flemish school building stock are however - at the moment of writing - nonexistent and exemplary energy efficient educational buildings are rare [66, 25]. Therefore, the specific geometrical building information such as averaged floor surface areas, typical heights, dimensions and rooms type profiles needed to construct the reference buildings is gathered by both literature review and a large-scale survey. For the statistical survey, the As-Built plans of 70 newly built or renovated schools in different regions in Flanders are investigated. The selection of schools is chosen from the extensive database of Flemish school characteristics of the Agency for School infrastructure (AGIOn). The selected buildings are spread over the Flemish region and all educational forms are equally covered. To incorporate current trends and changes such as the evolution towards 'Open school' concept [36]

or the more stringent energy performance requirements (EPBD), the selection is however restricted to current building practice (constructed after *2005*) only. First, the building shapes are set. Next, the related building size and dimensions are determined in line with the procedure used by Van den Dobbelsteen [60] to determine reference office buildings in the Netherlands. Finally, representative room type profiles are developed for both elementary and secondary schools. Combining all this gathered information, the reference buildings are composed.

2.2.2 Results

Overall, mandatory education in Flanders comprises three main levels: nursery, primary and secondary education. A detailed overview of the Flemish educational system is given in *Appendix A*. As there are not many physical and operational differences between the nursery and primary schools, one reference school building is set for both school types, which will be from now on referred to as elementary schools. In contrast, the organisation of secondary education is more complex and thus creates the need for more differentiation. Consequently, secondary schools are divided into two categories: general or semi-technical (ASO, TSO/STK[1], KSO), and technical (TSO/TTK, BSO) schools. This division is based on the type of classes taught and, more in particular based on the presence of one or more workshops (*i.e.* atypical spaces for specific training activities (*e.g.* wood work, food preparation) often with extraordinary heat generation or electricity use). Due to the atypical characteristics of the technical schools, they are too complex to generalise and are therefore not further studied throughout this dissertation. For the same reason, tertiary and special education facilities are omitted.

Plan type and building geometry

The building shape is an important element to be considered in the development of a reference building due to its significant impact on the energy performance of the building [71]. To ensure all-round usability of the reference buildings, the geometries must be kept simple (*i.e.* attached features and balconies are to be ignored and the general shape is kept simple [83] and easy to be reproduced [72]. Based on the architectural plans of the investigated schools however, a large variety of (complex) building shapes is found (see *Figure 2.1*). According to Steijns et al. [84], the typological evolution of school building architecture can be outlined by three basic shapes: the corridor type -the most basic school building shape designed to improve the efficiency of school buildings-, the hall type and the pavilion type. To enable the possibility to assess the impact of the building shape, two buildings shapes are retained for the final reference buildings: a rectangular building with a middle corridor and a U-shaped building.

The building size of the reference buildings can be based either on the average gross surface area or on the average occupancy (p = number of students). As school infrastructure in Flanders is subsidised and the subsidising procedure links the available gross surface area to the number of students [85], both assumptions approximately result in the same building size. Due to the strict budgetary limitations of schools, the real built gross surface area of school buildings is in most

[1]Technical secondary education (TSO) is divided into two groups of education: the TTK fraction which focuses more on technical aspects, and the STK fraction that focuses more on practical matters.

cases equal to the maximum subsidised area as set in the *'Physical and Financial Standard of the Flemish Government'* [85]. Therefore, this standard is used as a reference (see *Eq. 2.1*).

$$A = \begin{cases} 1495m^2 + 6,9(p-165) & \text{for elementary schools} \\ 6000m^2 + 7(p-500) & \text{for secondary schools} \end{cases} \tag{2.1}$$

This equation calculates the subsidised, basic gross surface area for general educational activities in elementary and secondary schools. For the final school surface, some additional (subsidised) spaces may be added depending on the organised educational activities (*e.g.* gymnastics, lab work, etc.) and the related room type profile (see *§ 2.2.2*).

To determine the average occupancy, statistics on the number of students in Flemish schools are collected. The results for the various educational forms are shown in *Table 2.1*.

Table 2.1: Average number of students in Flemish schools.

Average number of students	**nursery**	**primary**	**elementary**	**secondary**
Ministry of Education and Training (2009−2010)	263	179	280	525
Flemish Agency for Educational Service (2011)	180	265	283	–
Flemish government (2010−2011)	115	174	265	415

Based on *Table 2.1*, an average occupancy of 250 and 450 students is assumed for the reference elementary and secondary school buildings, respectively. According to *Eq. 2.1*, this results in a total maximum gross surface area of 2081.5 m^2 for the elementary school and 5625 m^2 for the secondary school. To verify, the calculated results are compared to comparable survey results as found in literature [3, 86, 87] using the subsidised (gross) surface area per student as a reference (*Table 2.2*).

Table 2.2: Comparative literature study: gross surface area per student for elementary/secondary schools. The data used for the reference buildings are marked in grey.

Average gross surface area per student, m^2/pers	**survey**	**NWF (*1986*)** [86]	**DIGO (*1998*)** [87]	**Leemans (*2009*)** [3]
Elementary schools	8.3	7-9	7	7-8
Secondary schools	12.5	10-14	16	18-29

Regarding the average gross surface areas per person for the elementary schools, the literature review shows slightly lower results (± 7 to 8 m^2/pers compared to 8.3 m^2/pers) though the difference is limited to 1.3 m^2/pers maximum, or less than 15%. Although no large changes are found between the oldest [86, 87] and the more recent survey results, a change is to be expected. The results of a large-scale questioning of school building's users by AGIOn in 2009 [3] and 2014 [88] revealed an over-all demand for more space in schools. As most rooms in schools are either fully occupied or even overcrowded [88], a future increase of the gross surface area per student is reasonable to be expected. The calculated gross surface area of 8.3 m^2/pers for the reference model is therefore concluded to be a good assumption. For the secondary models, a larger spread of the survey results is found. While comparing the assumed value to the results of the literature studies, more significant differences are found, especially compared to the results of the study of Leemans [3]. This

difference is mostly related to the exclusion of technical secondary schools in our research. These schools - which are included in the other survey studies - have larger surface areas compared to the surface areas as calculated by *Eq. 2.1* due to the need for extra space for atypical educational activities such as food preparation or lab work. Moreover, as the investment budgets of schools are tight and the amount of subsidised areas is restricted [85], the gross surface area is remained as calculated (= 12.5 m^2/pers).

According to Smet et al. [89], class rooms are sized at least 6 m by 6 m. The guidelines for sustainable school design suggests to restrict the width to 7.2 m [77] to profit maximally from the natural daylight (a). To assure good circulation, corridors must be at least 1.5 m [77] with an additional 30 cm for each hat rack provided [77, 74]. Assuming a single-sided hat rack, the corridor width used for the reference school buildings is 1.8 m. This results for example for the rectangular reference elementary school building in a total building depth of 14.6 m (see *Figure 2.6*). Due to the Flemish building fire safety legislation, the façade length is restricted to maximum 90 m. Hence, the maximum gross floor area per building layer is 1314 m^2, resulting in a two storey building model for elementary schools and a three to four storey building for the secondary school reference buildings. The net free floor height is set to 2.8 m, equal to the average survey results.
According to the *'Physical and Financial Standard of the Flemish Government'* [85], additional space may be added to the school building for sports activities and physical education. For the elementary school prototypes which include a gym (*§ 2.2.2*), an extra 485m^2 is added, resulting in a total maximum gross surface area of 2567 m^2.

To finalise the design of the reference buildings, the (theoretically obtained) dimensions are measured against the 'Statement of Requirements' as set for sustainable school building designs [77] and adjusted wherever necessary. The resulting general building and architectural data information for the 'theoretical' and 'adjusted' building models are depicted in *Table 2.3* and *Table 2.4*.
As the final energy use is influenced by the net usable more than the gross floor area, all models are given equal net floor area (*i.e.* 2057 m^2 for the elementary and 4464 m^2 for the secondary model). Resulting differences in gross floor area are then due to a slightly different amount of internal walls and circulation area (see *Table 2.4*).

Room type profile

The architectural design of a school building can be very complex. Often the building consists of zones with different comfort requirements or system configurations: class rooms, offices, laboratories, workshops, libraries, music rooms, cafeteria, etc. These differences must be dealt with when modelling the building. Lumping the room types with different functions together into more general categories would lead to averaging and blurring of the input data of the model. Introducing more elaborate room types profiles on contrary, results in greater flexibility in terms of distribution of equipment and related internal heat loads and thus in a more accurate representation of actual school buildings [66, 29]. To determine a representative room type profile, 70 As-Built plans of elementary and secondary schools are investigated. The type of the rooms, the occurring number of each type of room and the surface area of more than 2000 rooms are measured and listed. To

Table 2.3: Sizing procedure for the reference school buildings: from theoretical assumptions to final form of the references buildings for elementary and secondary school buildings.

Elementary reference school building		
	Rectangular	**U-shaped**
Theoretical size		
Number of people (p)	250	250
Max available gross surface area (A)	2567 m^2	2567 m^2
Total façade length (L)	176 m	
	L_{max}=90 m	
Number of floors	2	2
Needed area building layer	1283 m^2	
Building length	88 m	
Adjusted size based on SoR [77]		
Max available gross surface area (A_{adj})	2477 m^2	2494 m^2
Total façade length (L_{adj})	170 m	
	L_{max}=90 m	
Number of floors	2	2
Needed area building layer	1238.5 m^2	1247 m^2
Building length	85 m	
Secondary reference school building		
	Rectangular	**U-shaped**
Theoretical size		
Number of people	450	450
Max available gross surface area	5625 m^2	5625 m^2
Total façade length	339 m	
	L_{max}=90 m	
Number of floors	4	
Needed area building layer	1406 m^2	
Building length	84.7 m	
Adjusted size based on SoR [77]		
Max available gross surface area	4741.5 m^2	4778 m^2
Total façade length	285.6 m	
	L_{max}=90 m	
Number of floors	4	3
Needed area building layer	1185.4 m^2	1595.6 m^2
Building length	71.4 m	78.3 m

Table 2.4: Architectural data information of the reference school buildings.

Elementary reference school building		
General building data	**Rectangular**	**U-shape**
Gross floor area	2477 m^2	2495 m^2
Useable floor area	2057 m^2	2057 m^2
Building volume	6570 m^3	6569 m^3
Number of floors	2	2
Envelope surface area		
Roof	1212 m^2	1216 m^2
Floor	1212 m^2	1216 m^2
External wall	1271 m^2	1522 m^2
Sum envelope surface area	3694 m^2	3954 m^2
Level of compactness	1.78 m	1.66 m
Secondary reference school building		
General building data	**Rectangular**	**U-shape**
Gross floor area	4741 m^2	4778 m^2
Useable floor area	4464 m^2	4464 m^2
Building volume	12500.6 m^3	12500.6 m^3
Number of floors	4	3
Envelope surface area		
Roof	1185 m^2	1596 m^2
Floor	1185 m^2	1596 m^2
External wall	2344 m^2	2746 m^2
Sum envelope surface area	4715 m^2	5938 m^2
Level of compactness	2.65	2.11

limit the complexity of the reference buildings however, only those rooms are included which occur in more than *50%* of the investigated schools [66] (*i.e.* circulation areas, class rooms, canteen and kitchen, gym, lab, offices, sanitary, storages and teachers' room). While designing the reference school buildings, following assumptions are made:

- the kitchen is always next to the canteen,
- the canteen and gym (which is two stories high) are situated on the ground floor level,
- sanitary and storage are available on each floor and
- storage is available next to the canteen/kitchen and gym.
- as gyms are often used as polyvalent rooms and vice versa, these rooms are grouped into the same category.

The results for the prototypes defined for the elementary and secondary schools are summarised hereafter.

Elementary schools

The results of the statistical survey of the elementary schools can be found in the Appendix (see *Table B.1* to *Table B.4*). A summary of these results is depicted in *Figure 2.3*.

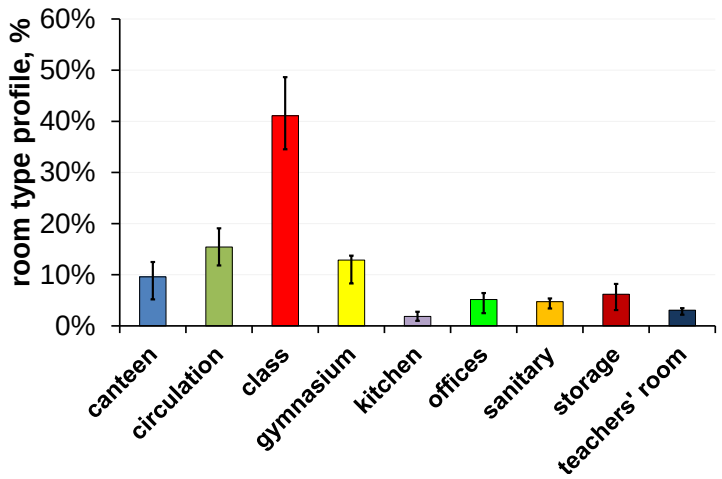

Figure 2.3: Representative room type profile of elementary schools: the mean, and the 25 - 75 percentile of the surface area per room type, normalised to the whole building floor area (%).

First, the selection of room types that is included in the reference buildings is defined. Based on the results of the statistical survey (see *Table B.5*) the following selection is made: a canteen (which occurs in 80% of the investigated cases), circulation area (97.1%), class rooms (100%), a gymnasium (65.7%), offices (80%), sanitary room (100%), a teachers' room (62.9%) and technical and storage rooms (100%). Changing rooms/showers (42.9%), laboratories (0%), libraries (11.4%), polyvalent rooms (20%), sports halls (2.9%) and workshops (2.9%) are excluded. Due to the atypical characteristics, an exception is made for kitchens. Although kitchens appear in only *48.6%* of the investigated projects, this specific room type will be included in the reference building for elementary schools.

Next, representative surface areas are coupled to each of the selected rooms (see *Table B.5*): class rooms (cover 41.1% of the total net surface area of the reference building or 845.9 m^2), a teachers' room (*i.e.* meeting/seminar room) (3.1% or 63.3 m^2), offices (5.2% or 106.4 m^2), a gym (13% or

264.8 m^2), a canteen and kitchen (11.5% or 235.5 m^2), and a combined area for circulation, sanitary and storage rooms (26.4% or 542.5 m^2). To verify the final result, the (relative) surface areas (%) are compared to the outcome of similar research studies [7, 65, 3] (see *Table 2.5* and *Figure 2.4* (a)).

Table 2.5: Comparison of the reference room type profile for **elementary** school buildings to survey results found in literature.

	canteen,kitchen	**circulation,...**	**class**	**gym**	**offices**	**teachers'room**	**Other rooms**
De Deene et al. (1998) [7]	7%	16%	56%	7%	–	–	14%
Coolen et al. (2007) [65]	20%	20%	33%	20%	5%	–	3%
Leemans (2008) [3] – actual	7%	20%	53%	11%	5%	3%	1%
Leemans (2008) [3] – ideal	8%	22%	45%	10%	5%	5%	5%
Survey – elementary schools	11.4%	26.4%	41.1%	12.9%	5.2%	3.1%	–

De Deene et al. [7] studied typical school building characteristics such as the surface area per student or the room type profile for each of the educational school types in 1998 based on survey results (360 elementary and 240 secondary schools were contacted, 16% responded). Coolen et al. [65] defined a representative room type profile for schools in the context of setting energy performance requirements, based on the analysis of a municipal database and experts advice. The exact data set used to define these specific room type profiles is however not specified. Finally, Leemans [3] collected building characteristics from 60% of all schools (3618 schools) built in Flanders and categorised the rooms into an 'actual' (= room type profiles as current found in schools based on averaged available data) and an 'ideal' (= room type profile as desirable by the users and thus giving an indication of the expected school building trends in the future) room type profile.

Comparing the average research results as found in literature to the reference room type profile (see *Figure 2.4* (a)), overall a good agreement is found: the deviations vary between 2% (canteen, kitchen) minimum and 30% (teachers' room) maximum. Some small differences between the presence of the rooms occur. As only the most commonly occurring space types (*i.e.* occur in more than *50%* of the investigated cases) are included, some of the rooms which are included in other researches are excluded from the reference building and vice versa. Furthermore, the survey results show slightly higher values for circulation, sanitary and storage/technical rooms. This is in line with the increasing need for technical rooms in more recent school buildings as they include often more advanced HVAC systems. Finally, when comparing the research results mutually (see *Table 2.5*), a tendency towards more differentiation of the room type profiles is noticed over the years: as shown in the more recently built schools (*i.e.* presented by the results of Coolen et al. [65]) or based on the expected trends for the future (*i.e.* expressed ideal situation of Leemans et al. [3]), it may be assumed that the number of traditional class rooms is decreasing compared to the older school building stock (*i.e.* presented by the actual situation by [3] and the results of De Deene et al. [7]). This is due to the fact that more support areas such as libraries or multi-media centres, relaxation spaces, staff rooms and multi-functional halls are needed [3] which is in line with the current educational trends [3] and the evolution towards the *'Open School'* concept [36]. This trend explains the rather low assumed

relative surface area for class room (41.1%) in the reference building.

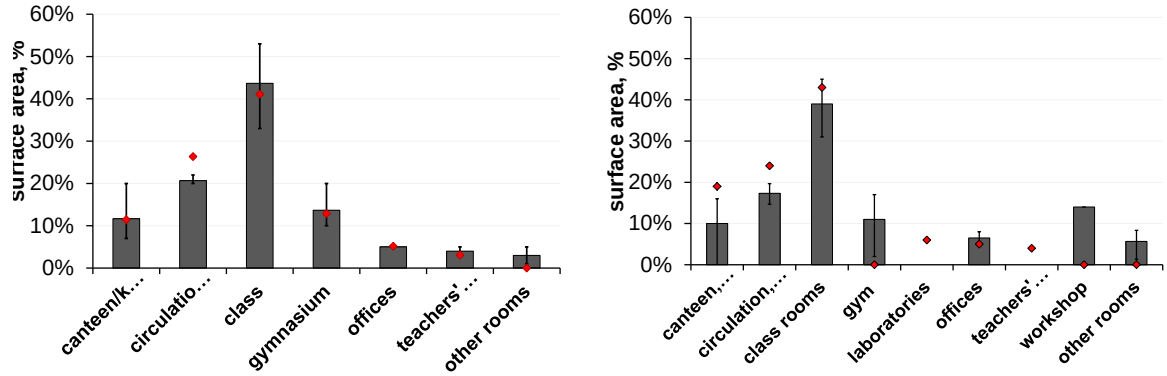

(a) Elementary (b) Secondary

Figure 2.4: Verification of the reference room type profiles for school buildings: the results of the reference building (marked in red) are compared to the average (grey column), minimum and maximum (error bars) of the results found in literature [7, 65, 3].

Secondary schools

The results of the statistical survey of the secondary schools can be found in the Appendix (see *Table B.6* to *Table B.7*). A summary of these results is depicted in *Figure 2.5*.

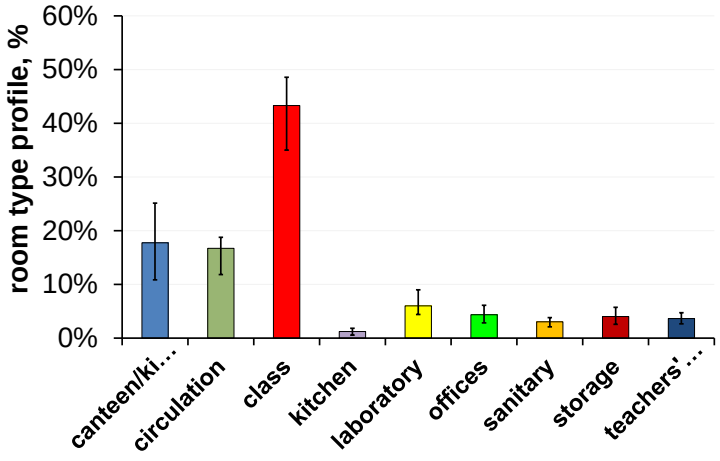

Figure 2.5: Representative room type profile of secondary schools: the mean, and the 25 - 75 percentile of the area per room type, normalised to the whole building floor area (%).

The following room types are selected to be included in the reference secondary school building: a canteen (which occurs in 91% of the investigated cases) and kitchen (54.6%), circulation area (100%), class rooms (90.9%), offices (81.8%), sanitary room (100%), a teachers' room (54.6%) and technical and storage rooms (100%). Changing rooms/showers (36.4%), a gym (36.4%), a library (9.1%) and kitchens for teaching purposes (9.1%) are excluded. Due to the atypical characteristics, laboratories are included in the reference buildings although they appear in only 36.4% of the investigated projects. The resulting room type profile consists of a canteen and kitchen (19% or 846.9 m^2), classrooms (43.3% or 1934.8 m^2), laboratories (6% or 268.5 m^2), offices (4.4% or 194.6 m^2), a teachers' room (3.6% or 162.1 m^2), and a combined area for circulation, sanitary and storage rooms

(23.8% or 1061.9 m^2). In general, the results show strong resemblances with the reference room type profile of elementary schools. The fraction of class rooms, administrative rooms (*i.e.* offices and teachers' rooms) and circulation, sanitary and story are more or less equal (< ±3%). The canteen and kitchen area are however slightly larger and no gym or sports hall are included as, due to the requested size, the gyms in secondary schools are generally built as separate building units.

To verify, the (relative) survey results are compared to the outcome of similar researches [7, 65, 3] (see *Table 2.6* and *Figure 2.4* (b)).

Table 2.6: Comparison of the reference room type profile for **secondary** school buildings to survey results found in literature.

	canteen, kitchen	**circulation,...**	**class rooms**	**gym**	**laboratories**	**offices**	**teachers' room**	**workshops**	**other rooms**
De Deene et al. (1998) [7]	6%	15%	47%	8%	–	–	–	14%	10%
Coolen et al. (2007) [65]	20%	20%	33%	5%	–	5%	–	–	3%
Leemans (2008) [3] –actual	4%	17%	37%	20%	–	8%	4%	–	4%
Survey - secondary schools	19%	24%	43%	–	6%	5%	4%	–	–

The results of the survey (see *Figure 2.4* (b) - marked in grey) show much higher surface areas for canteens compared to the results of the survey of De Deene et al. [7] and Leemans [3] though are comparable to the results of Coolen et al. [65]. This can be explained by the fact that in some of the surveyed schools the polyvalent rooms are equally identified as canteens whereas in the other surveys these rooms are categorised separately (*i.e.* other rooms). For the other rooms, a reasonably good agreement is found.

The resulting floor plans of the elementary and secondary schools are given in *Figure 2.6*, and *Figure 2.7* and *Figure 2.8*, respectively.

Note that the generic geometry of the reference school buildings is not absolute and does not cover all school building variants. Yet, as the sample of reference school building models cover various room type profiles, building shapes, sizes and numbers of floors, a broad variety of school building characteristics is covered. Hence, the amount of detailing and differentiation may be assumed sufficient for this specific research objective.

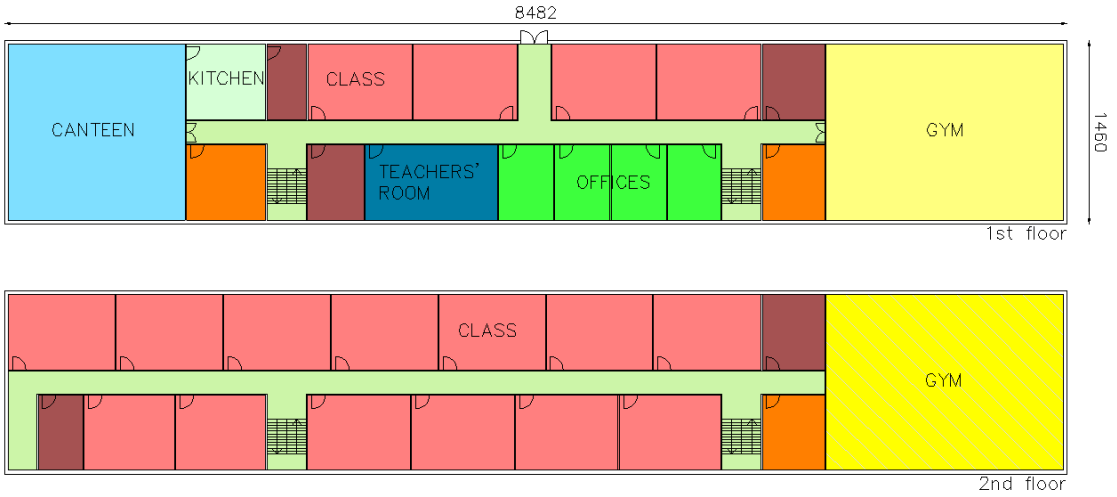

(a) Rectangular shaped building, with middle corridor.

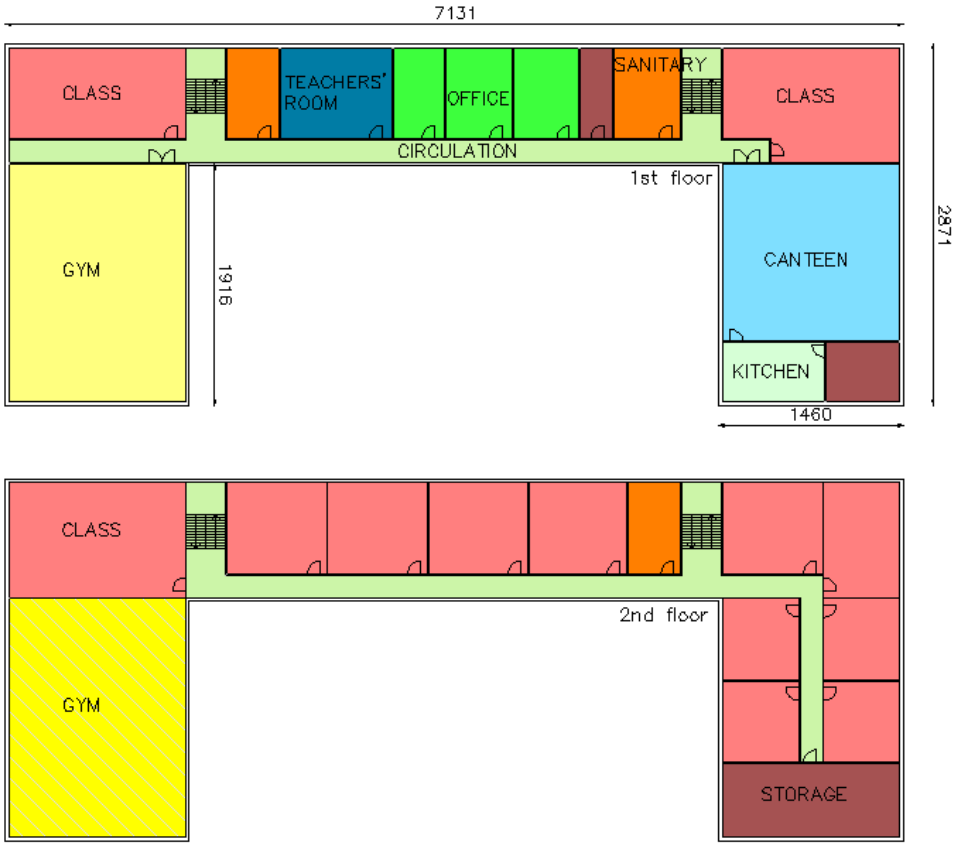

(b) U-shaped building.

Figure 2.6: Floor plan of elementary school model.

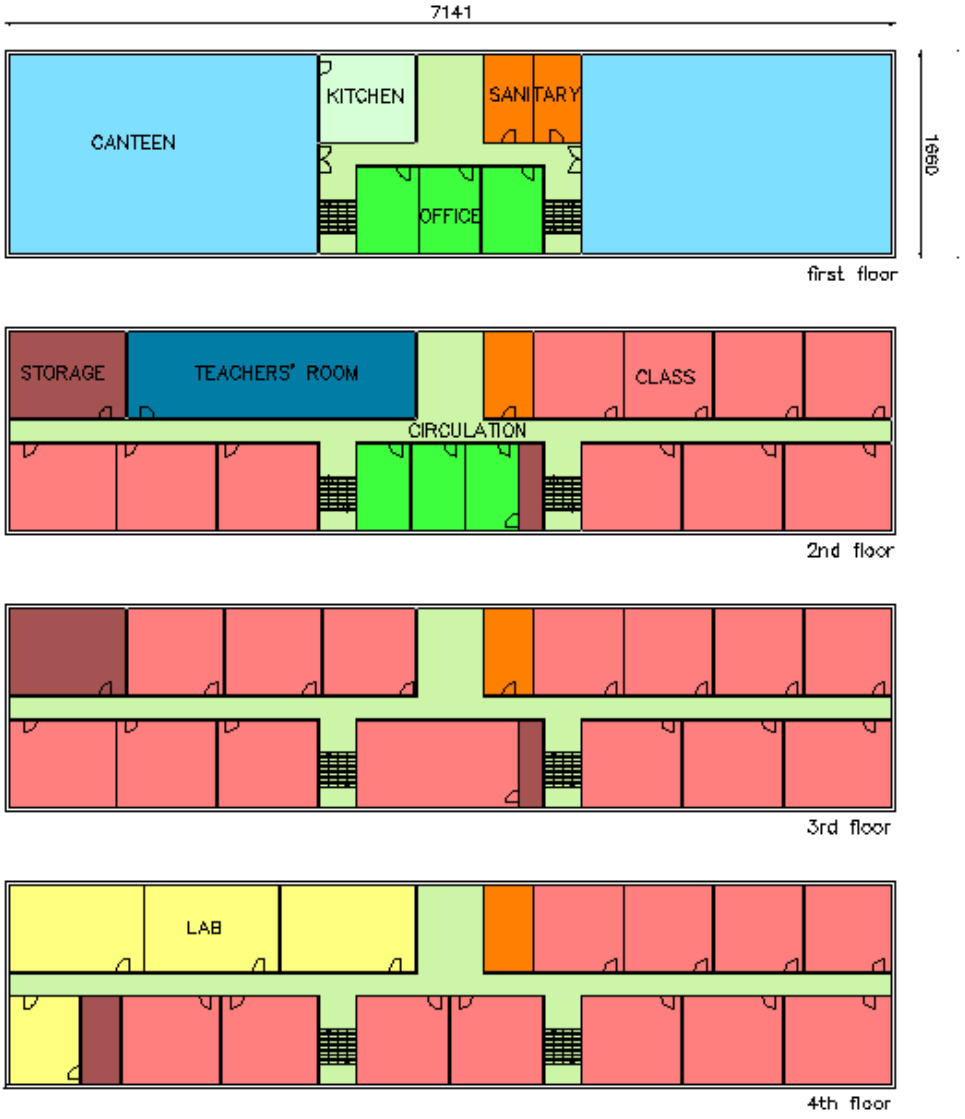

Figure 2.7: Rectangular shaped secondary school building, with middle corridor.

Figure 2.8: U-shaped secondary school building.

2.3 Typical characteristics of (contemporary) school buildings

Along this section, an elaborate overview of the typical school building's characteristics related to **(i)** the use and activities (*§ 2.3.1*) and **(ii)** the construction and the building envelope (*§ 2.3.2*) is given. This information will serve as a reference to define the ranges in which investigated parameters and boundary conditions for the investigated school buildings will be varied along the rest of this dissertation.

2.3.1 Operation and activity related characteristics

School buildings have some (a)typical characteristics which affect the design, use and energy performance of the building to a great extent. Therefore, representative values and ranges are set for amongst others operational characteristics such as heating set-points, ventilation rates, occupant density and internal heat gains are set based on guidelines, manual and (design) standards.

Room temperature,°C: specific requirements for thermal comfort and (desired) room temperatures are set in (inter)national standards and technical reports. Some standards focus on the design criteria and sizing of the heating and, if present, the cooling systems (*e.g. EN 15251* [47], *EN 12831* [90]). Others are used for energy calculation purposes (*e.g. EN ISO 13790* [37], *DIN V 18599* [43], *NEN 7120* [44]). Different standards (*ISO 7730* [48], ASHRAE standard 55-2013 [91]), regulations (*e.g.* Royal Decree dd.04/06/2012, Art.5§1 [92], BS 19.X.04 [93]) and guidelines formulate general requirements for thermal comfort and temperature settings. Other focus on schools in particular [94, 95, 96]. A summary of the values found in the aforementioned literature for the various type of rooms in schools is depicted in *Table 2.7*.

Occupant density, m^2/pers: various standards can be found specifying occupant density rates for specific room types. Some are used in the framework of energy calculations (*NEN 7120* [44], *DIN V 18599* [43], *EPR* [22]), others to calculate the ventilation rates necessary to assure the required indoor air quality (*EN 13779* [13], *EPR* [22]). A summary of the aforementioned literature review is depicted in *Table 2.8* for the different types of rooms.

Ventilation rates, m^3/(h.pers): many literature on the importance of good indoor air quality in schools can be found [100, 101, 102, 103, 104, 105]. Standards, technical reports and guidelines are published setting minimum required air exchange rates. Some provide guidance on the design and the performance of ventilation systems (*EN 13779* [13]). Others are used for energy calculation purposes (*EN ISO 13790* [37], *DIN V 18599* [43], *NEN 7120* [44]). In addition, standards (*EN 15251* [47]) and regulations (*EPR* [22], *ARAB* art.53§1/3 [106], BS 19.X.04 [93]) set minimum legal requirements and criteria for indoor air quality. Finally, guidelines can be found setting target values for good building practice in schools buildings [94, 95, 96, 107] or in specific (atypical) rooms such as kitchens or lab's [107, 108] in particular. A summary of the aforementioned literature review for the various rooms is given in *Table 2.9*.

Table 2.7: Room temperature set-point as prescribed by (inter)national standards, regulations and guidelines for various room types in schools.

Type of space	category	min. temperature, °C	max. temperature, °C
Royal Decree, 04/06/2012, Art.5 §1 *[92]*			
class rooms, offices, teachers' rooms		16	29
gymnasium		14	26
Binnenmilieudecreet (BS 19.X.04) *[93]*			
general		20	26
ISO 7730 [48]			
class rooms, offices, cafeteria	A	22±1	24.5±1.0
	B	22±2	24.5±1.5
	C	22±3	24.5±2.5
EN 15251 [47]			
class rooms, offices, cafeteria	I	21-23	23.5-25.5
	II	20-24	23-26
	III	19-25	22-27
kitchen	I	18-25	
	II	16-25	
	III	14-25	
DBFM *[95]*			
class rooms, offices, teachers' rooms, cafeteria, science lab's		21	26
gymnasium		16	
storage		10	-
circulation area, sanitary		18	-
Senternovem Eisen Frisse scholen *[96]*			
class rooms	A	21-23	22°C at θ_e <20°C max. θ_e + 2°C at θ_e >20°C
	B	20-24	23°C at θ_e <20°C max. θ_e + 3°C at θ_e >20°C
	C	19-25	24°Cat θ_e <20°C max. θ_e + 4°Cat θ_e >20°C
Building Bulletin 87 - Guidelines for Environmental Design in Schools *[97]*			
class rooms, offices		18	
gymnasium, sanitary, circulation area		15	
Bloso *[98]*			
gymnasium		16-20	
changing rooms		20-24	

Table 2.8: Occupant density rates as defined in (inter)national standards, regulations and guidelines for various room types in schools.

Type of space	category	range, m^2/pers	default, m^2/pers
***EPR* [22]**			
class room			4.0
office			15.0
meeting rooms (≈ teachers' room)			3.5
cafeteria			1.5
gymnasium			3.5
***EN 13779* [13]**			
class room		2.0 - 5.0	2.5
office		8.0 - 12.0	10.0
meeting rooms (≈ teachers' room)		2.0 - 5.0	3.0
cafeteria		1.2 - 7.0	3.5
***DIN V 18599* [43]**			
class rooms	low dense		3.5 2.5
office	low dense	18.0 10.0	
meeting room	low dense		4.0 2.0
cafeteria	low dense		1.4 0.8
gymnasium	low dense		30.0 10.0
kitchen			10.0
***NEN 2916* [99]**			
class rooms	B2	1.3 - 3.3	2.0
office	B1 - B4	0.5 - 20.0	0.8 - 12.0
meeting rooms (≈ teachers' room)	B2	1.3 - 3.3	2.0
sports hall	B5	> 20.0	30.0
***ASHRAE* [91]**			
class rooms		2.8 - 4.0	
laboratories		4.0	

Table 2.9: Ventilation rates as defined in (Inter)national standards, regulations and guidelines for various room types in schools.

Type of space	category	range, $m^3/(h.pers)$	default, $m^3/(h.pers)$	range, $m^3/(m^2.h)$	default, $m^3/(m^2.h)$	default, ACH
***Royal Decree, 04/06/2012, Art.5 §1** [92]*						
general			30.0			
EN 15251 [47]						
class room	I II III				20.0 15.0 8.0	
offices	I II III			4.3 - 5.4 2.9 - 3.6 0.7 - 2.2		
cafeteria	I II III				27.0 18.7 8.0	
EN 13779 [13]						
rooms designed for human occupancy	IDA1 IDA2 IDA3	>54 36 - 54 22 - 36	72 45 29			
rooms not designed for human occupancy	IDA1 IDA2 IDA3			- > 2.5 1.3 - 2.5	- 3 2	- 3 2
***DIN V 18599** [43]*						
class rooms			30			
offices		40 - 60		4 - 6		2 - 3
sports hall			60			6
cafeteria			30		18	
sanitary					15	
kitchen (non-residential)					90	
***DBFM** [95]*						
class rooms, offices, teachers' room			50		3.6	
science lab's						10
sports hall						3
cafeteria						6
circulation area						1
***Senternovem 'Frisse Scholen'** [96]*						
class room	A B C				22 17.5 12.5	
offices	A B C		60 45 30			
***Tashenhandbuch Recknagel** [108]*						
kitchen (industrial)					80	
science lab's						8 - 12
***Building Bulletin 101 - Ventilation in School Buildings** [107]*						
class rooms						2.5
changing rooms, showers						10
gym			29			2.5
science lab's						5
NPR 1090 [109]						
class rooms		19.8				
lab, workshops		36[1]				
offices		36 - 54				
sports hall				3.6		
kitchen (non-residential)				7.5		

[1] *In case a fume hood is present, at least 720 m^3/h of air should be extracted per m^2 hood surface area.*

Internal heat gains, W/m^2 or W/pers: the main sources of internal heat gains are occupants, the use of electronic equipment and artificial lighting. As schools are assumed to be non-dehumidified, latent heat gains are less important so only the sensible heat gains are considered throughout this dissertation.

(i) *Occupants, W/pers*: the heat production and thus internal heat gains due to occupants depend on the metabolic heat production which is in turn affected by the level of activity and the age of the person. Class room activities can be categorised as light to moderate work, mostly executed while seated. The activity level in science lab's and gymnasia is considered slightly higher. Specific values can be found in national and international standards and regulations (*EPR* [22], *PHPP* [110], *DIN V 18599* [43], *NEN 7120* [44]) and guidelines for good school building practice [95].

(ii) *Equipment, W/m^2*: the heat gains due to equipment are due to receptacles or electrical plug loads or due to heat producing activities such as cooking or lab tests. In literature, either averaged values of the internal heat load due the equipment for the whole school building (*EPR* [22], *NEN 2916* [99]) or specific values depending on the type of the various rooms (*DIN V 18599* [43], [108]) are found. In addition, several sources can be found defining the heat load of various electronic devices which occur in schools [111]. Values for different room types are summarised in *Table 2.10*. Detailed information on the availability and the use of the specific electronic equipment is however rare.

Table 2.10: Internal heat gains q_{IHG} due to occupants and equipment as defined in (inter)national standards, regulations and guidelines for various room types in schools.

	$q_{IHG,occ}$		$q_{IHG,eq}$
Type of space	**W/pers**	**W/m^2**	**W/m^2**
EPR [22]			
class room	100		3
office	100		3
PHPP [110]			
class room, cafeteria	60 - 100[1]		
office	80		
gym	70 - 280[1]		
DIN V 18599 [43]			
class room	60	17 - 24	2 - 6
office	70	4 - 7	3 - 15
meeting room (≈ teachers' room)	70	18 - 35	1 - 3
canteen	70	50 - 88	1 - 3
gym	125	4 - 13	0
NEN 2916 [99]			
class rooms		10	1
office		3 - 15	3
meeting rooms (≈ teachers' room)		10	1
gym		1 - 3	1
DBFM [95]			
class rooms, offices	75		
laboratories	85		

[1] *Values vary depending on the age of the person and the type of activity.*

(iii) ***Lighting, W/m^2***: all electrical energy supplied to light fixtures is assumed to be converted into heat. Internal heat gains due to lighting are generally calculated as the product of the normalised power density, W/(m^2.lux), and the illuminance, lux. The values of the illuminance depend on the requested visual comfort level as defined in standards (*EN 12464-1* [46]) or set in building guidelines [95, 96, 112] (see *Table 2.11*).

Table 2.11: Visual comfort in schools: required level of illuminance for various room types, lux.

Room type	**illuminance, lux**
class rooms, canteen, gymnasium	300
lab, kitchen	500
sanitary	200
circulation area	100

2.3.2 Building envelope characteristics

This section specifies the commonly used building envelopes and interior constructions and their related building physical characteristics in passive schools to define the state-of-the-art of the high performance school building practice. A database of exemplary school buildings with their typical characteristics is currently non-existing. Therefore, representative values and ranges for thermal mass, insulation level, air tightness level and glazing surface are set based on an elaborate analysis of a sample of (passive) school projects in Flanders and abroad. All schools that are included in the survey are either in use, in construction or in the final phase of design. School building projects at the preliminary draft stage are not included as not enough specific information on the building or HVAC systems is available. For the survey, 13 Flemish passive schools projects[2] are selected. To enlarge the data sample, data of 29 passive school buildings built in surrounding countries are added.

A similar approach for the data collection is applied as used by Flodberg [113] for setting the state-at-the-art of low energy office buildings. Considering the sample of Flemish school buildings in particular, general (*i.e.* educational type, designer/architect) as well as more specific building information (building size, building envelope, materials, U-values, air tightness, and glazing) is collected mostly during on-site visits. The information for the remaining international passive projects is found in the database of the 'Passiv Haus Institut' [114].

The final results are described along this section, parameter by parameter. Wherever relevant, the collected data are measured against recommendations as found in design guidelines and standards.

Thermal capacity: the cooling load and summer comfort depend on the accessibility and usability of the thermal mass [115, 116]. As schools are unoccupied during the night, they are appropriate for cooling by night ventilation and therefore an exposed thermal capacity is generally recommended [117, 77]. According to the overall survey results, masonry (heavy) structures are most commonly used (*i.e.* found in *56.8%* of the investigated cases). Mixed (medium - 21%) and timber

[2] In 2008, the Flemish government selected 24 school designs which will be used as a reference for contemporary (and future) high performance school building practice. These 'pilot' schools receive additional subsidising and guidance throughout the design phase. For the survey included in this research study, 13 of these 'pilot' projects are selected.

(light - 24%) structures are slightly less popular. Focusing on the school in Flanders in particular, the trend to use heavy structures is even more pronounced. Except for some exceptional cases, (very) light structures are rarely used. Masonry structures and mixed structures are the most common (± 60% and ± 40%, respectively).
The variations of the thermal capacity of the reference school building is obtained by varying the materials used for wall and roof constructions as shown in *Table 2.12*.

Table 2.12: Variations of the thermal mass of the structure. The average heat capacity, normalised to the building floor area, for the reference elementary school building is plotted as an example, calculated according to EN 13786 [118].

	Heat capacity C_m, Wh/(m^{2}K)	**construction**
heavy	95.2	heavy external and internal walls, heavy roof and floors
medium	56.3	heavy (intermediate) floors & external walls, light roof and internal walls
light	43.3	heavy (intermediate) floor, light roof, external & internal wall,
very light	28.7	light roof, intermediate floors, external & internal walls, heavy ground level floor

Insulation level, W/(m^2.K): the survey results for the insulation level of the building envelope parts are depicted in *Figure 2.9*. The minimum, mean and maximum U-values for (a) opaque and (b) transparent building parts are plotted. For comparison, the legal required limits applicable on the date of the start of this research (dd. 2010) [119] are added to the figure (light grey).
All results fit well the range as set by the 'Passive standard' design guidelines [117] (*i.e.* $U_{opaque} \leq$ 0.10 to 0.15 W/(m^{2}K), $U_{glazing} \leq 0.6$ W/(m^{2}K) - see *Figure 2.9* marked by dashed lines). The survey results represent the current best practice and thus set a reference for the lower limit of the insulation level (= minimum values for thermal transmittance).

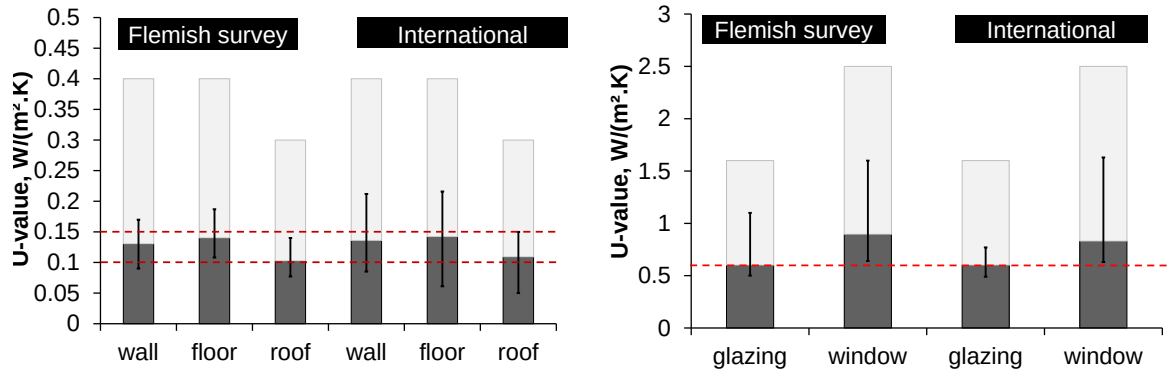

(a) Opaque building parts

(b) Transparent building parts

Figure 2.9: Survey of passive schools in Flanders and abroad: the minimum, mean (grey column) and maximum insulation level of various building parts.

Air tightness level, n_{50}: various requirements on the air tightness level of the building envelope (*i.e.* expressed by the n_{50}- value) can be found in literature. *NBN−D50−001−1* [120] requires n_{50}

$\leq$ 3 ACH for buildings that use a balanced mechanical ventilation system. When combining the balanced ventilation system with a heat recovery device, n_{50}-values $\leq$ 1 ACH are required. For passive buildings, criteria are even more strict: $n_{50} \leq 0.6$ ACH [117]. As information on the air tightness of Flemish (passive) schools based on the results of a pressurisation test is rare, only the results of the international survey are shown (see *Figure 2.10*). These results are clearly in line with the design guidelines and certification criteria for passive buildings [21]. All n_{50} - values found in the survey remain (substantially) below the required 0.6 ACH. Nine schools in 29 have a n_{50}-value of 0.3 ACH or less showing that low values for air tightness are technically well feasible.

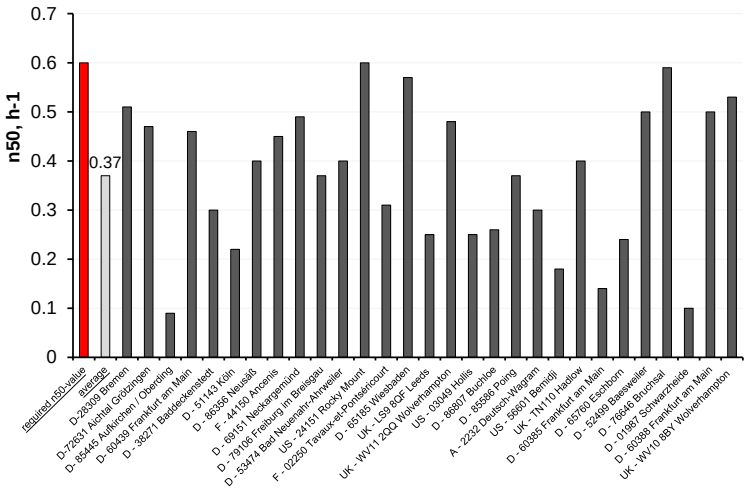

Figure 2.10: Variations of the air tightness of the building envelope in international passive schools. The required n_{50}-value = 0.6 ACH by the 'Passive House standard' is marked in red. The average survey result (n_{50} = 0.37 ACH) is shown in light grey.

Window-to-wall ratio (WWR) and shading devices: along this dissertation, the total window surface is defined by the total window to gross wall area ratio (WWR) which is the percentage resulting from dividing the total vertical fenestration area, including the frame and other non-glazed window components, by the gross exterior wall area. The results of the Flemish survey are depicted in *Figure 2.11 (a)* (average WWR = 28%), and are in line with the requirements as set for the use of day-lighting and visual comfort: to fully optimise daylight penetration and to assure a proper view-out but to avoid glare, the WWR must be at least 20% [97] but should not exceed *40%* [66, 121, 97]. For the reference buildings, all windows are assumed to be equally spread over all external walls and have all equal configuration (see *Figure 2.11 (b)*). The window surface area is varied by changing the length of the fixed middle window. The height and the dimensions of the other two window parts are kept constant. This is done for all rooms expect for the circulation, sanitary and storage areas where the WWR is fixed at 30%.

In all the investigated passive schools, external solar shading is provided: 7% uses fixed external solar shading (*e.g.* trees, overhang), 43% has movable shading devices. The rest of the analysed schools combines both techniques. In only 5 schools, an internal shading device is foreseen which is moreover mostly used for visual comfort reasons (*i.e.* possibility to darken the rooms in dorms or while projecting).

The average g-value for the glazing found in the survey is 0.5 which is in line with the recommenda-

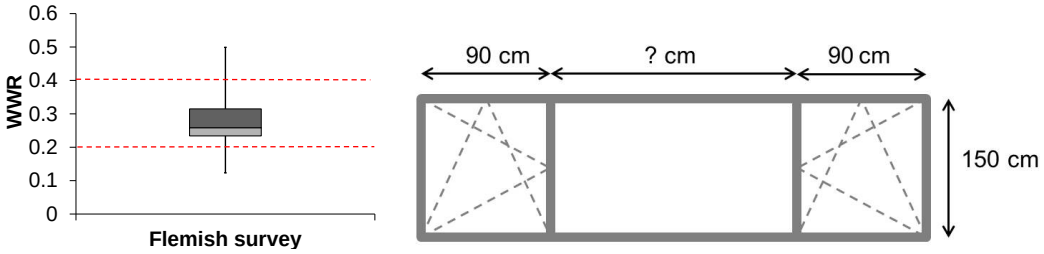

(a) window to wall ratio of Flemish schools

(b) reference window configuration

Figure 2.11: Information on windows for the reference school buildings.

tions as found for passive buildings (g > 50% and g * 1.6≥ $U_{glazing}$) [117].

2.4 Trends in HVAC system design and lighting concepts in contemporary Flemish schools

The last section aims to identify the current trends and evolutions in HVAC system design in schools. To that end, the most frequently-used HVAC system types and lighting concepts in high performance, contemporary school buildings in Flanders are studied, based on survey results. The same sample of passive school buildings (13 schools) is used as described in *§ 2.3*. In addition, 9 randomly selected, high performance (but not passive) Flemish school buildings are analysed. All extra case studies - from now on referred to as EESBs (*i.e.* energy efficient school buildings) - have an energy performance level < E70 (*i.e.* primary energy performance calculated according to EPR [22]), have a mechanical ventilation system and are all recently built or highly renovated (in use since 2010 or later). Additionally, the survey data are measured against the recommendations as found in design guidelines and standards. Multiple guidelines and manuals on sustainable system design [108, 122, 123] are published. As school building and HVAC operation differ in many ways from (other non)residential buildings, specific guidelines and standards that focus on (passive) school design are developed and used as a reference [79, 94, 117, 77, 70, 112].
This section starts by defining the used HVAC terminology in *§ 2.4.1* followed by an overview of the results of the survey on the heating, cooling and ventilation systems in schools (*§ 2.4.2*). Although the dissertation focuses on HVAC systems mainly, lighting systems are shortly discussed in *§ 2.4.3* as these influence significantly the internal heat load of the building.

2.4.1 Terminology

An HVAC system comprises all components and subsystems to fulfill both the need for good indoor air quality (*i.e.* ventilation, humidification) and thermal comfort (heating, cooling). HVAC systems can be classified in many different ways such as centralised or local systems, primary or secondary systems, active or passive systems or based on the medium used for heat transfer such as all-air, air-and-water or hydronic systems.
In **centralised** systems, heating and/or cooling is generated centrally and then distributed to the conditioned zones through the secondary system (see *Figure 2.12*). The **local** systems on the other

hand generate heating and/or cooling zonally [94].
The **primary system** - also referred to as plant - consist of boilers, chillers, storages tanks, etc. **Secondary HVAC system** components can be further classified as air handling equipment and heat distribution components between the systems and the building. Examples of the secondary HVAC system components are pumps, fans, values, ducts, pipes, etc. [124].
HVAC systems are called **passive** when heat in a building is controlled and dissipated with low or nil energy use while for the **active** systems a significant amount of energy is used.

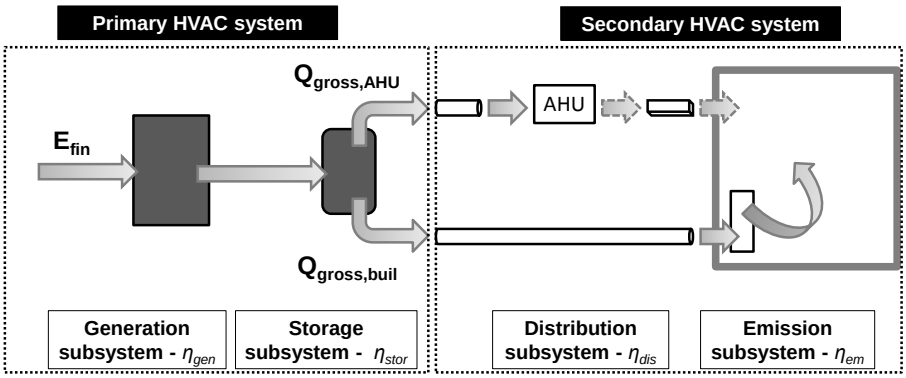

Figure 2.12: Conceptual scheme of subsystems and energy flows in a commonly used HVAC system [125].

2.4.2 HVAC systems in schools

HVAC system design in schools differs in many ways from (other non-)residential buildings. The following typical users' characteristics of schools affect significantly the HVAC system design options:

- Typically a large variability in time and space of the use and overall occupancy rates occurs. The usage of a room is frequently interrupted by play or lunch breaks and frequent holiday periods occur. Furthermore, a large variety of room types such as canteens, class rooms, gym, etc. occurs which are not commonly found in other building types. All these phenomena favour a flexible and intermittent use of the HVAC systems which complicates accurate and efficient control of the systems.
- The class rooms are characterised by a high occupancy rate. This results on the one hand in locally dense internal heat gains which in turn affect significantly the performance of the HVAC system (see *§ 6.4*). On the other hand, high ventilation rates are needed which create opportunities as the use of an all-air heating systems is benefitted and extra cooling potential for passive night or free cooling is offered.
- Budgetary limitations considering both the investment and the operational and maintenance costs are often an important issue [126] in schools and limit the HVAC design options.
- Finally, recent educational trends towards *'Open schools'* [36] and the related flexibility demand affect significantly the system design and operation.

A global summary of the HVAC systems found in the surveyed school buildings is depicted in *Table 2.13*.

Table 2.13: Results of the survey: overview of the HVAC systems found in recently built schools.

	emission system of heating/cooling							heat source				cooling source				ventilation			
case study	radiators/convectors	floor heating	chilled ceilings	(ventilation) air	air heaters	fan coil units	fossil fuels	ground	(ground)water	biomass	(outdoor) air	active cooling: compression cooling	ground	(ground)water	(outdoor) air	natural supply, mechanical exhaust	balanced mechanical	heat recovery	air conditioning
PS_1	■	■		■			■								p		■	1	■
PS_2				■			■								p		■	1	■
PS_3	■			■			■								p		■	1/2	■
PS_4				■			■	EAHX					EAHX		p		■	1	EAHX
PS_5	■			■			■								p		■	1	■
PS_6				■				EAHX	GSHP				EAHX	GSHP	n(+a)		■	1	EAHX
PS_7	■						■								p		■	2	
PS_8				■							ASHP				p		■	1/2	■
PS_9						■			GSHP					GSHP	p(+a)		■	2	■
PS_10				■			■								p		■	2	■
PS_11	■					■	■								p		■	1	
PS_12	■			■	■		■		GSHP	■				GSHX	n		■	2	■
PS_13	■		■	■			■					■			p		■	1/2	■
EESB_1		■					■									*	■	1	
EESB_2		■		■			■								p	*	■	2	■
EESB_3	■			■			■									*	■	2	■
EESB_4	■	■			■		■										■	■	
EESB_5	■						■									■			
EESB_6		■					■								p		■	1	
EESB_7	■			■			■								p		■	1	■
EESB_8	■						■									■			
EESB_9	■						■								p		■	2	

1) energy wheel 2) plate heat exchanger
** mechanical extraction without heat recovery in sanitary*
EAHX = earth-air heat exchanger, GSHP = (reversible) ground source heat pump, ASHP = air source heat pump, GSHX = ground source heat exchanger
p = passive cooling, n = natural cooling, a = active cooling

Heating

In general, central heating plants are most commonly used in schools, with one or more heat generators working on fossil fuels such as gas or oil [94]. This trend is confirmed by the survey results: 20 of the investigated case studies have a central heating plant while only two use decentralised heat generators. Most often a modulating, condensing boiler is installed (*i.e.* in all nine investigated EEBSs and 60% of the passive schools). For the passive school building sample however, slightly more variation of the heat generation systems is found (see *Figure 2.13*). A small shift, mostly towards the introduction of heat pumps, is noticed in conformity with the current trend and policy towards the implementation of more energy efficient equipment and the use of renewable energy [18]. A single case study is found which combines multiple heat generation systems (a pellet boiler, a condensing boiler and a heat pump). However, overall, the number of installed heat pumps in schools remains limited due to the high investment costs which is in great contrast with the limited (investment) budgets of schools. In addition, the cooling loads in schools remain small, hence the potential of reversible heat pumps can not be fully benefitted which makes it therefore a less attractive alternative for schools compared to for example office buildings [25].

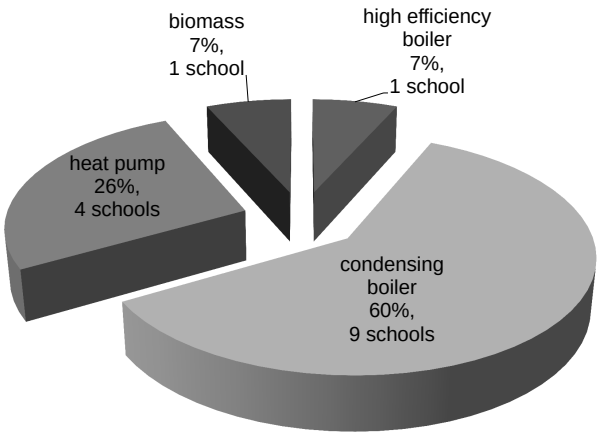

Figure 2.13: Survey results of the passive schools: occurrence heat production systems, %.

In most of the investigated school buildings, only one heat generator is foreseen. Only two (passive schools) use multiple heat generator systems cascading either 2 condensing gas boilers or 2 ground source heat pumps.

Hydronic or water-based heat distribution systems are most commonly used in school buildings although a slight change towards (basic) air heating is noticed. The combination of both strongly improved energy performance of the buildings and high required hygienic ventilation rates makes all-air heating systems become feasible in schools: a combined air/water heating system occurs in 33% of the EESBs and 46% of the passive schools. In 40% or five of the passive schools an all-air heating system is applied. Considering the all-air heating systems both the constant air volume system (CAV - 60%) and the variable air volume system (VAV - 40%) occur. The first system provides a constant air flow rate to the conditioned zone, modulating the heat supply by changing the temperature of the supply air. Survey results show a variety of CAV system configurations: the supply air is either heated centrally or locally, using either hot water or electrical (re-)heating coils. The latter system varies the airflow to meet the thermal comfort requirements of the conditioned zone using VAV-boxes. Due to the high installation, operating and maintenance costs and the difficulties related to the control, it is recommendable to limit the size of the air handling units to the required hygienic ventilation capacity. Survey results confirm as all-air heating systems are only found in the passive school building sample.

The final choice of the heat emission system depends on the size and function of the room. Generally, radiators are the most common heat emitters used in schools [70, 97]. Survey results confirm that in class rooms and offices, radiators (± 45 to 50%) and convectors (± 10%) are most frequently used. However, as aforementioned, a shift towards all-air heating (40% or 5 passive schools) is noticed or to low temperature floor heating (40% or 4 schools of the EESBs). As large (intermittently/irregularly) used spaces such as canteens and gymnasia can benefit from a faster response system, air heating (either by heating of the ventilation air or by the use of air heaters) is often implemented.

The control of the centralised heating systems is generally located on three different levels: (**i**) control

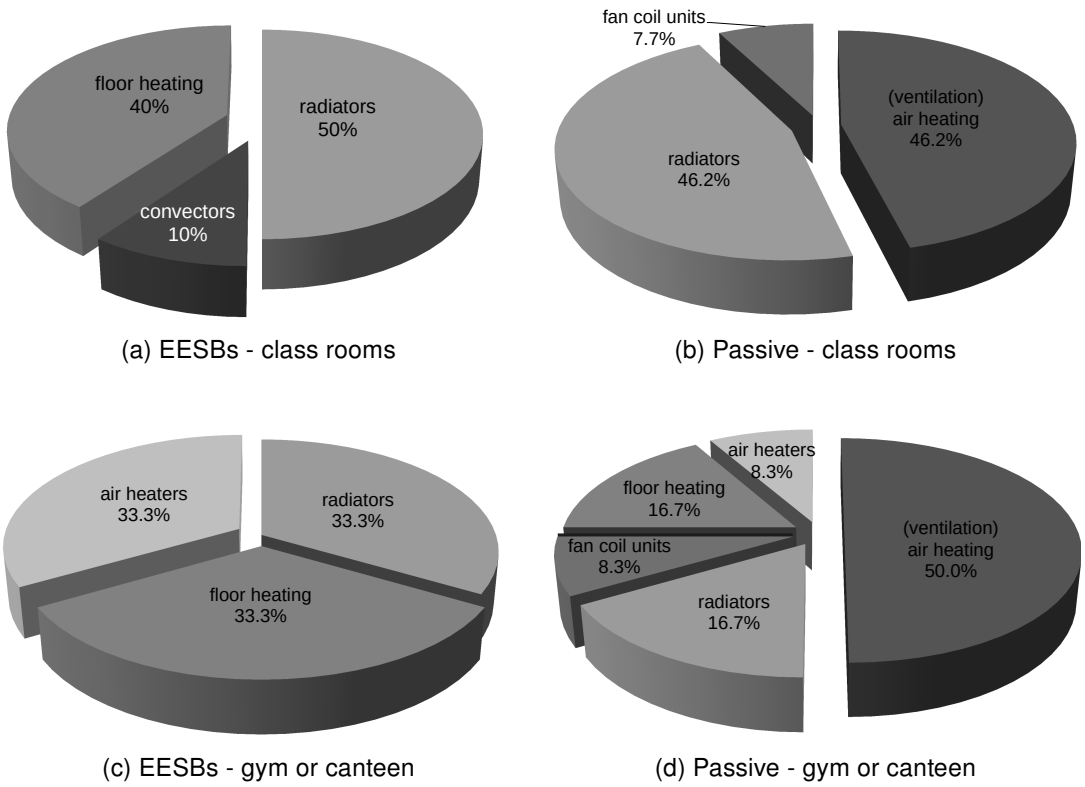

(a) EESBs - class rooms

(b) Passive - class rooms

(c) EESBs - gym or canteen

(d) Passive - gym or canteen

Figure 2.14: Overview of the most common heat emission systems in contemporary school buildings in relation to the energy performance level of the building envelope and the type of the room.

of the primary system (*i.e.* temperature of the heat generator), (**ii**) control of the secondary heating circuits and (**iii**) local control (see *Figure 2.15*). Considering the first level, the strongly discontinuous users' pattern of schools favours an energetically and economically interesting intermittent, time-controlled use of the heating system according to the operational schedule. All investigated schools either turn down (*i.e.* implement a setback of the set-point temperature for heating) or switch off the heating system during nights, weekends and holidays. To avoid discomfort at the start of a school day, often a setback temperature is maintained (*i.e.* 15°C on average). Morning recovery times prior to the school opening hours are used: 25% of the investigated schools use an optimal start-stop control. Furthermore, all case studies use an outdoor temperature reset control to adapt the hot water supply temperature to the outdoor weather conditions, and, in some cases, to the heat load pattern. For the latter control level, the survey results show that in 90% of the cases, a local temperature control is used: thermostatic radiator valves (TRVs) in case of radiators and wall thermostats in case of air or floor heating. For the 10% remaining cases, only a central temperature control is implemented using a temperature sensor in a suitable reference room (one per building or one per heating circuit). When thermal comfort is controlled by variable supply flow rates (*e.g.* TRV or throttling two-way valves), the distribution pumps are generally fitted with variable speed drives (VSD). Finally, accounting for the occasional after hours use of schools, in 50% of the investigated cases, time control override facilities are provided.

The use of domestic hot water in school is limited. Survey results found in literature [7] reveal that the gas consumption in schools related to domestic water heating is less than 10% (see *Table 6.1*). The

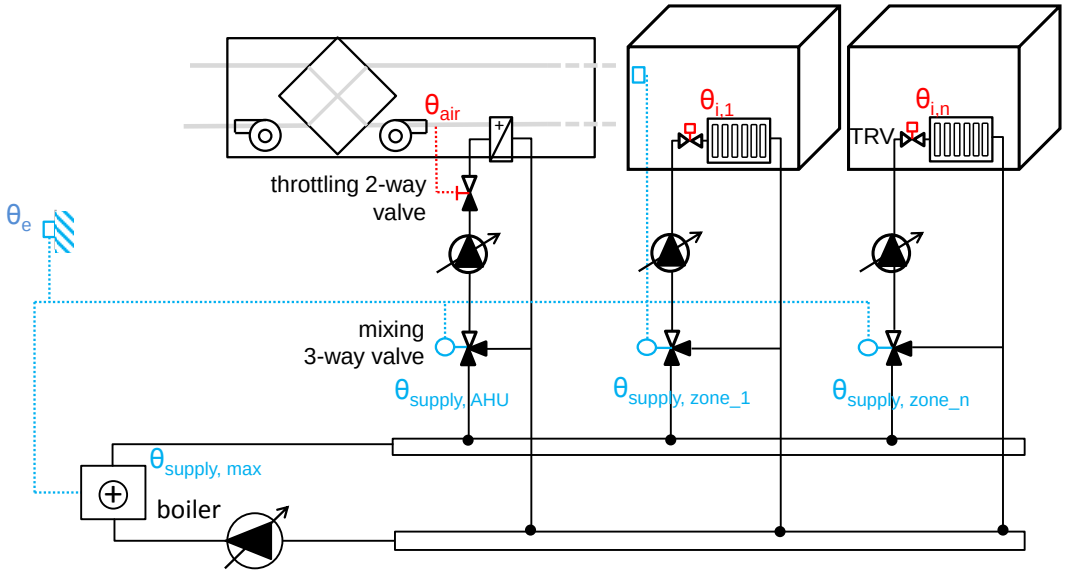

Figure 2.15: Conceptual scheme of a regular heating systems as found in the investigated school buildings. Control of the heating system is located on three levels: on the level of (i) the primary system, (ii) the secondary system and (iii) locally.

hot water is used for cleaning, in the kitchens or for occasional showers. The latter is mostly related to sport activities. In some of the investigated nursery schools however, showers are foreseen nearby the class rooms. These are however rare, and if present, they are rarely used. Hot water supply is in most cases (> 90%) foreseen by local boiler units, using either gas (40%) or electricity (56%) to heat the water. One school has installed a solar boiler.

Cooling

Schools in Flanders rarely have an (active) cooling system. In some exceptional cases, active cooling is provided in restricted zones with extremely high internal heat loads such as server rooms or computer labs. Due to better performing building envelopes and an increasing trend to use electronic devices, the cooling demand is growing. Measurements in 15 schools done by AEE INTEC [127] show that the need for cooling demand and the number of overheating discomfort situations rise in relation to an increasing building envelope performance. Nevertheless, as daily operating hours are limited (school closes around 15h30 - 16h) and schools are commonly closed during summer (July and August), the annual need for cooling remains low, even in high performance schools. Dynamic simulations of a sample of 100 fictive elementary school building design variants with a WWR of 20% and a heavy construction, and varying efficiency level of the building envelope (U_{max} = 0.37 W/(m^{2}K), U_{max} = 0.13 W/(m^{2}K)) and users' characteristics show that the average annual cooling demand remains ≤ 15 kWh/(m^2.a) for all cases (see *Figure 2.16*).

Considering the survey results, only one of the investigated schools has installed an active cooling system. A compression chiller in combination with a chilled ceiling is used to cool exclusively a densely populated computer lab. In some other schools, either the ground coupled heat exchanger which is coupled to a heat pump during the heating season or an earth tube are used to pre-cool

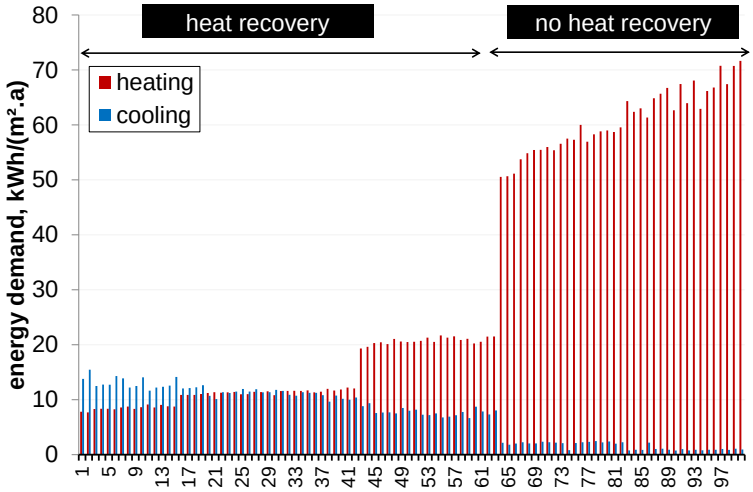

Figure 2.16: Dynamic simulation of the annual energy demand for heating and cooling (kWh/(m^2.a)) of a sample of 100 fictive elementary school building design variants with varying energy performance level of the building envelope and users' characteristics, and a WWR of 20% and a heavy structure.

the ventilation air before entering the building to enlarge the cooling capacity of the night (or free) ventilation. In most of the investigated cases however, good thermal (summer) comfort is provided by implementing cooling load reducing measures (*e.g.* external shading, thermal capacity) and free- and/or night cooling. Due to the nocturnal unoccupancy of school buildings and the moderate, dry outdoor climate with large diurnal temperature differences, Flemish schools are suitable for cooling of the building's thermal mass by night ventilation. 17 of the surveyed schools implement the possibility to ventilate during night time as a passive cooling strategy. In most of the surveyed schools, night ventilation is supplied fully mechanically (16 schools). Hybrid ventilation where fresh air is naturally supplied and mechanically extracted is foreseen in one school. None of the investigated schools applies a fully natural night ventilation strategy. Fully mechanical night ventilation is preferred in the investigated schools instead of hybrid or fully natural night ventilation despite the additional auxiliary energy use of the fans due to (**i**) the unreliability of the performance, (**ii**) the specific design and operational requirements (*e.g.* large openings, preferable openings on both sides), and (**iii**) related safety measures and installation costs of an automatic control system for the windows.
As the hygienic supply ventilation rates are generally high, thermal comfort can in most cases be guaranteed using the hygienic ventilation rates. In four of the surveyed schools however, the ventilation system is dimensioned slightly larger (4 to 5 ACH instead of 3 ACH on average in class rooms) to enlarge the (night or free-) cooling capacities. In all other cases, the ventilation capacity is restricted to the required hygienic ventilation rates.

Ventilation

EN 13779 [13] categorises ventilation systems into four main categories varying from fully natural to balanced mechanical ventilation systems. A detailed overview of pros and cons of natural versus mechanical ventilation can be found in the work of Emmerich et al. [128] and Versteeg et al. [129]. Generally, in schools built before the implementation of the EPBD, natural ventilation by occasional

(a) (b)

Figure 2.17: Measure taken to guarantee sufficient accessibility of the thermal mass in schools and enlarge the cooling capacity of night ventilation.

window airing and uncontrolled infiltration is provided [70]. Due to recently imposed requirements regarding indoor air quality, comfort related problems (*e.g.* draught, noise, dust) [129] and unreliable quality of window airing [130], mechanical ventilation becomes preferable [94, 15]. Consequently, a consistent increase of the implementation of mechanical ventilation systems is noticed [19]. More than 50% of the residential buildings built between 2006 and 2010 implemented a mechanical exhaust ventilation system. The number of fully balanced mechanical ventilation systems raised from 25% to 44% [19]. The survey results show a similar trend for educational buildings. All passive schools[3] implement a mechanical, balanced ventilation system (in combination with a heat recovery).

Ventilation systems can additionally be categorised into centralised and decentralised ventilation systems. For the first category, only one or a limited number of air handling units serves the building whereas for the latter category each air handling unit serves one or a limited number of rooms. The main advantages of using individual, decentralised units in schools are the reduced floor space requirements, and the absence of ducts and recirculation air between rooms [130, 94]. In contrast, the main advantages of central air handling units are the lower risk for noise disturbance, the lower risk for air leakage as the amount of supply and exhaust openings through the building envelope are limited and the easier maintenance due to fewer units and the accessability without interfering with class activities [130, 94]. In general, central ventilation systems are most common in schools and mostly used in newly built schools while decentralised systems are mainly applied in renovation projects [130]. This trend is confirmed by the survey results. Only two of the investigated schools implement a fully decentralised ventilation system where each air handling unit serves one or two class rooms at most. In contrast, 20 schools use a centralised air handling unit. For the latter category, the final number of installed air handling units is determined in relation to the users' profile and related need for flexibility. According to the REHVA design guidelines for schools [94], separate air handling units for gymnasia or polyvalent rooms are recommended due to their atypical, after school hours use. Accordingly, the survey results reveal that 7 of the 20 schools with a centralised ventilation system have installed multiple air handling units varying from two to four units depending

[3]The results for the EESBs can - for this particular topic - not be used as a reference as the presence of a mechanical ventilation system is used as one of the decisive selection criteria.

on the need for flexibility.

Ventilation is mandatory. According to the *EPBD*, a minimum indoor air quality (*EN 13779* - IDA3 [13]) must be guaranteed in schools. These minimum required ventilation rates go hand in hand with a significant energy use of the fans and link the indoor air quality requirements directly to the energy performance of the building. To limit the related energy use and the operational energy costs, the ventilation demand and supply must be matched as accurately as possible (*e.g.* by implementing a high performance control system) and the related (thermal) energy losses must be minimised by *e.g.* implementing a heat recovery device (HRV) or by considering the minimum ventilation requirements as a maximum design recommendation [131]. In line with these design recommendations, survey results show that in most of the investigated schools, the ventilation plants and related duct works are sized to meet exactly the minimum fresh air requirements (IDA3 = 500 to 600 $m^3/(h.class)$). Only some of the schools imply ventilation rates higher than restrictively needed to enlarge the night and free cooling capacity, as aforementioned. These schools use however an adequate control system that links the additional ventilation to the cooling demand.

Regarding the ventilation control systems, all the investigated schools apply at least a time control system relating the ventilation schedule to the school opening hours. In 52.4% of the schools, time control is extended with a demand control system that adapts the air change rates in relation to the thermal comfort (DCV-temperature) or to the required indoor air quality (DCV - CO_2). The first system is used in schools that apply an all-air heating system or have additional ventilation capacity installed to enlarge the ventilative cooling capacity. The latter system is mostly used in rooms with highly varying occupant densities and operational schedules such as canteens or gymnasia. In class rooms however, time schedules are most common as operational schedules and occupancy are generally well predictable and rather stable throughout the school year. Occupancy detection systems (DCV-IR) are commonly found in sanitary rooms or rooms which are often unoccupied such as study rooms or attics.

To reduce energy use, air-to-air heat recovery devices (HRV) are frequently used. In all of the investigated school buildings with a balanced mechanical ventilation system, a heat recovery is integrated. Energy wheels (found in 13 schools) are slightly more popular compared to plate heat exchangers (found in 11 schools, 50% is a counter flow HRV, 50% a cross flow). The efficiencies of the installed heat recovery systems η_{HR} are shown in *Figure 2.18* (a). All efficiencies - based on the information of the manufacturer - vary between 75% and 90% (= error bars) with an average of approximately 85% . In all of the case studies, the chosen heat recovery efficiency is at least equal or higher than the minimum required efficiency (75%) as found in the design guidelines [130, 117] (see *Figure 2.18* (a) - marked in dashed line) or set by the *EPR* system efficiency requirements [132]. In order to limit risks of overheating and related cooling demand, all the heat recovery devices found in the investigated schools are bypassed for summer operation.

Finally, to limit the electrical energy use of the fans, limits are set to the specific fan power (SFP) which indicates the demand on power efficiency of all supply air and extract air fans in a building. AIVC technical note 65 [133] summarises some examples of SFP-values as used in building codes in the UK (2010), Sweden (2008) and Norway (2007). Different values are found depending on the type of ventilation and the presence of a heat recovery system: SFP-values vary between 1000 and 2000 Ws/m^3 for balanced ventilation systems with heat recovery. For exhaust ventilation systems

SFP-value are set equal to 600 Ws/m^3. For comparison, the default values as defined in the *EPR* calculation method are set equal to 1200 Ws/m^3 for exhaust ventilation systems and 2000 Ws/m^3 for balanced mechanical ventilation systems. According to *EN 13779* [13], at least a class 3 is required (SFP3 = 750 - 1250 Ws/m^3). Results of the survey (see *Figure 2.18* (b)) show that the specific fan power is mostly higher than the targeted value of *EN 13779* [13].

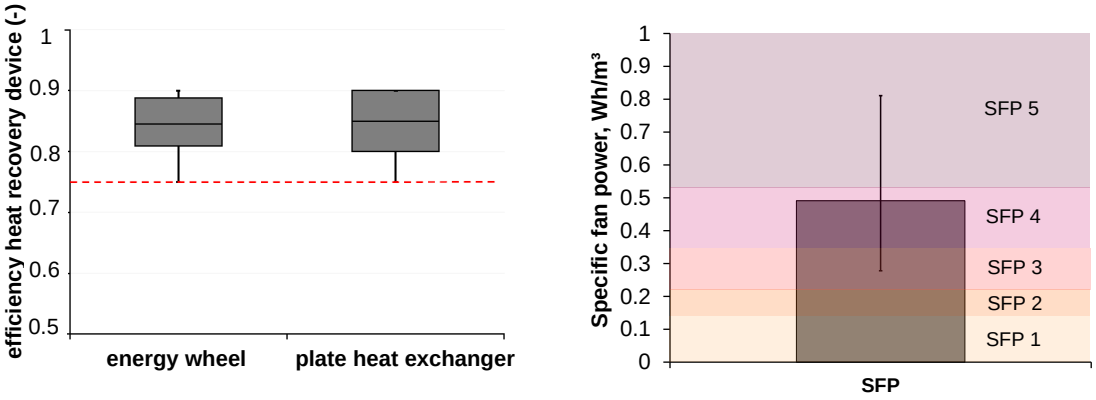

(a) Energy efficiency of heat recovery devices

(b) Specific fan power of the fans

Figure 2.18: Energy saving measures of the ventilation systems commonly applied in contemporary Flemish schools.

Humidification

Due to the implementation of mechanical ventilation systems, a slight decrease of the relative humidity (±10%) in schools is to be expected [134, 135] during the heating season compared to naturally ventilated schools. Measurements show however that, due to the dense class room occupancy rates and related high internal moist production, indoor humidity levels are rarely critically low (< 30%), even in winter [136, 134, 129]. According to measurements by Rosbach et al. [134], humidity levels in mechanically ventilated class rooms vary between 30% and 40%. Versteeg [129] obtained similar results with the lower limit varying between 28% and 42%. Moreover, as humidification systems are very expensive and delicate to maintain, humidifiers are seldom seen in schools. In none of the investigated buildings humidification is provided. Alternatively, to obtain a minimum control over the humidity ratio, a hygroscopic energy wheel, recovering both sensible (heat) and latent (moisture) energy is sometimes used. Energy wheels are mostly found in the air handling units that serve the class rooms. As some cross-contamination due to mixing of the two air streams might occur by carryover or leakage, thermal wheels are not appropriate in case exhaust air from sanitary, kitchens or science lab's is included [122] as confirmed by the survey results.

Overall, the on-site visits and interviews revealed that the users are satisfied. In most cases, the indoor climate conditions are experienced better compared to the (often bad) original situation (*i.e.* before renovation or in older school buildings). In some cases however, the complexity of the installed HVAC system and (automatic) control, and lack of sufficient knowledge of the users and operational staff have lead to improper use of the systems and likely loss of comfort and energy savings. For example, in some of the visited schools trickle vents in the windows or supply open-

ings for the ventilation air were closed to avoid draft problems. In another school, the ventilation system was switched off completely during classes and only peak ventilation during play and lunch break was provided due to acoustic problems. Furthermore, some problems were mentioned using automatically controlled external solar shading devices. In conclusion, to assure appropriate use of the systems and to maximise the related energy savings and comfort conditions in schools, it is recommended to keep the HVAC systems and their control simple and easy to maintain. Moreover, sufficient training of the operational staff and users is recommendable.

2.4.3 Lighting

The electrical power load of a lighting installation, expressed as the normalised power density (NPD),W/(m^2.100 lux), is a significant measure for the energy use. The normalised power density of the lighting installations of the surveyed buildings varies between 2 and 2.5 W/(m^2.100 lux) in class rooms, 4 to 5.5 W/(m^2.100 lux) in sanitary and storages rooms, and up to 9 W/(m^2.100 lux) in some circulation areas due to the high ceilings. For comparison, the maximum NPD value to receive grants for relighting in offices in Flanders is 2 W/(m^2.100 lux) [137].
In addition to the installed lighting power, the energy consumption of a lighting installation is strongly dependent on the lighting control system. Various control options for lightings are found in the surveyed schools, mostly differing in relation to the type of the room in which the lighting is installed. The results mentioned hereafter are mostly based on the survey results of the passive school as most of the information of the EESB sample is incomplete and therefore not representative. Absence detection where the lighting systems are switched on manually and deactivated in case no motion is detected, and presence detection where lighting systems are switched on and off in relation to real occupancy detection, are most commonly used lighting control systems in classes and offices. In $\pm$ 50% of the class rooms, an absence detection system is used. In $\pm$ 33%, a presence detection control system is installed. For the remaining cases, lighting is controlled manually. More or less similar results are found for administrative rooms though manual control systems are slightly more common in individual offices. For canteens, gym, etc. mostly presence detection is used while in sanitary, storage and circulation rooms motion detectors are generally installed. In the majority of the passive school buildings (> 90%), a (dimming) daylight control system is used.
In case daylight dimming is applied, specific requirements can found on the daylight factors, expressed as the ratio of internal light level to the external light level in [138, 77, 139]. As daylight control systems are not further investigated along this study, no data on the daylight factor was however collected in the survey.

2.5 Discussion and conclusion

School buildings have typical operational and architectural characteristics which distinguish educational buildings from other (non-residential) buildings. Occupancy density, ventilation rates and internal heat gains are generally high. Daily school opening hours are limited and frequent holiday periods occur. Furthermore, educational activities imply certain requirements to the architecture and facilities resulting in a large variety of school buildings with different building sizes, geometries, shapes and room type profiles. This diversity on a small scale complicates energy performance eval-

uation on a larger scale. To generalise the diversity, four different reference models are developed, two for elementary and two for secondary schools, based on the results of a literature review and a survey of recently built or highly renovated school buildings. Two building shapes are considered, a rectangular and U-shape, for both the reference buildings for elementary and secondary schools. The size of the reference models is based on the average number of students and dimensions are set in line with the school building subsidising procedures. For each school type, a representative room type profile is set including class rooms, offices, a teachers' room, a canteen and kitchen, sanitary, storage rooms and circulation areas. For the elementary schools, a gym is added to the school building model while for the secondary schools laboratories are included instead.
To represent the actual variety of schools along the rest of the research study, the reference buildings developed in this chapter are subsequently combined with a representative range of building (*i.e.* thermal mass, insulation level, air tightness, glazing surface, etc.), HVAC and users' related (*i.e.* heating set-points, ventilation rates, HVAC control and operation) characteristics. The state-of-the-art of the school building practice defined in this chapter serves as a reference for the current best school building practice. The specific details on the resulting school models used to elaborate each of the research objectives are however described in each of the related chapters.
To conclude, some restrictions and limitations of this chapter are summarised.

- The review of the school building characteristics presented in this chapter focuses on contemporary school building design and current trends mainly. As older school buildings often do not meet the energy performance and comfort requirements, only recently built or renovated school buildings are included for the review.
- Despite the effort made to guarantee representability of the selected survey sample, this study is not fully comprehensive as the number of analysed school buildings is limited as the number of passive school buildings in use in Flanders is currently still low (10 'pilot' schools[4]). Second, a large part of the passive school projects in Flanders are still in the design phase and are therefore not included in the survey.
- A large part of the buildings used for the study are 'pilot projects'. This means that, generally, they set a good example, however, some of the design decisions can still be optimised and are therefore not completely representative for current best building practice. Moreover, some of the exemplary passive schools were not originally designed according to the passive house standard which results occasionally in some architectural flaws such as failing compactness or large window surfaces irrespective of the orientation of the façade which are afterwards compensated by amongst others excessive amounts of insulation or by implementing oversized HVAC systems.

[4]This number is the situation on 27/04/2015, based on the information obtained by AGIOn.

3

Building energy performance assessment methods

Supporting the building energy policy (EPBD), extensive international research has been carried out to elaborate and adopt standards containing common methodologies that are used for energy labelling and certification of buildings. Overall, the CEN standards offer two main options for the energy calculation: the quasi-steady-state (seasonal or monthly) or the dynamic calculation method. Both methods attempt to simplify the complex, underlaying thermal processes by using a limited set of equations while weighing accuracy, complexity and work load in relation to the application and use of the calculation results. This chapter discusses the basic principles of both methods. First, the monthly, quasi-steady-state method as described in the European calculation standard EN ISO 13790 is analysed and compared to the national implementation of this standard as used in Belgium (EPR), in the Netherlands (NEN 7120) and in Germany (DIN V 18599) for energy rating of (non-residential) building designs. Focusing on school buildings in particular, the comparative analysis of the calculation standards concentrates mainly on the general calculation procedures and hypotheses to cope with the typical intermittent (system) use of schools. Second, a short summary of the calculation procedure for energy use for heating as described in EN 15316 (European) and EPR (Belgium) is given. The specific calculation algorithms and tabulated input values used for the calculations of each part of the heating system are discussed. Third, the algorithm for dynamic simulations as applied in the simulation tool TRNSYS is described. Fourth and last, an overview is given of the measures taken to guarantee comparability and consistency of the results of both methods.

3.1 Introduction

The Energy performance of Buildings Directive (EPBD) came into force on 4 January 2003 and had to be implemented by the EU Member States at the latest on 4 January 2006. To accelerate the adoption of the EPBD regulation in practice and improve the effectiveness, a common European framework was set out by the European Committee of Standardisation (CEN) containing a series of calculation standards. An overview of the specific standards related to the energy performance assessment methods is given in *Figure 3.1*. An overview of the whole set of developed CEN/EPB standards can be found in CEN/TR 15615 [140].

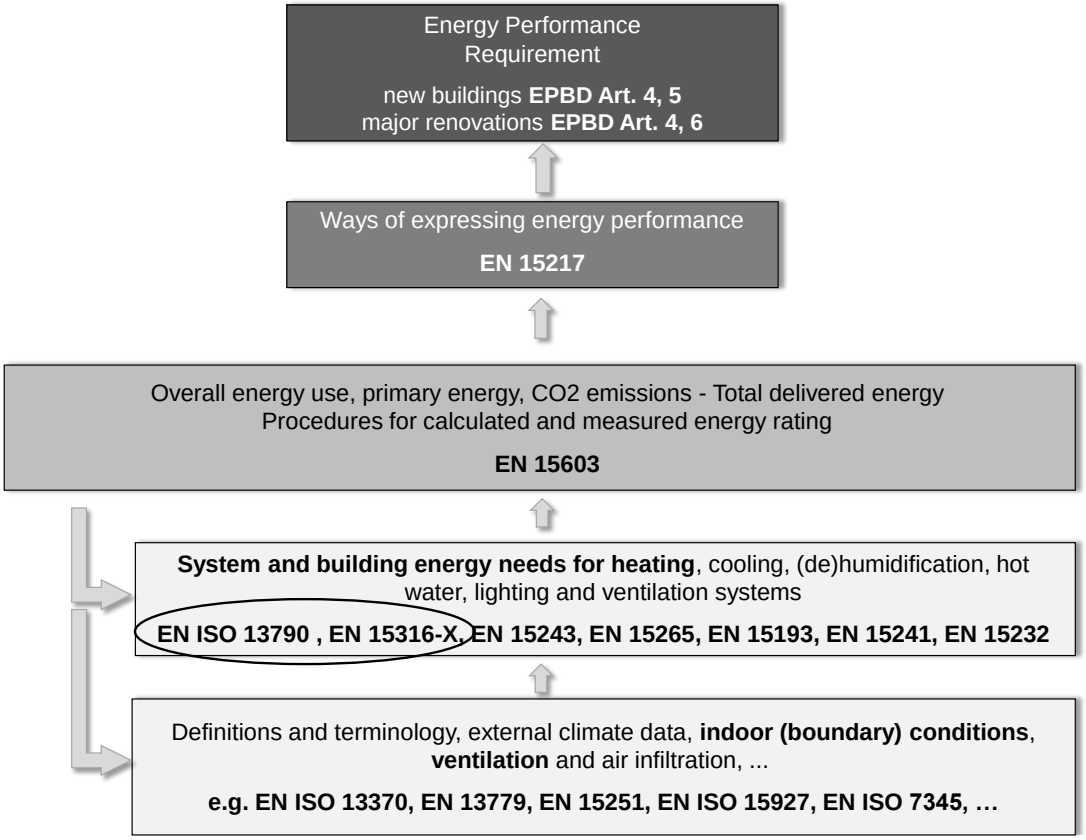

Figure 3.1: General overview of the CEN/EPB standards for energy performance assessment [141].

Overall, two methods are set forward by CEN for the energy performance assessment of building designs in the regulatory context (EPBD): **(i)** the *quasi-steady-state* calculation method which calculates the heat balance in steady-state conditions over a sufficiently long time (*i.e.* generally one month) and **(ii)** the *dynamic* method that calculates the heat balances with shorter time steps (typically 1 h) [37]. Particularly in the context of building energy regulations, the simplicity of the input, the transparency of the calculation rules, the intuitive correlation between input and output, the robustness and reproducibility of the *quasi-steady-state* method are considered as a great advantage compared to the more complex *dynamic* simulation tools [28, 142]. On the other hand, dynamic effects such as climatic conditions, user behaviour or time schedules are taken into consideration in a simplified way by time weighted averaged values and dynamic factors whereas the *dynamic* method considers accumulation, dynamic phenomena and variations of users' data in a more realistic way.

This chapter discusses the basic principles of both the *quasi-steady-state* and *dynamic* calculation method.
First, a description is given of the *quasi-steady-state* calculation approach. To do so, the European CEN/EPB standards for the calculation of the **energy demand** (EN ISO 13790 - see *§ 3.2.1*) and for the calculation of the **final energy use for heating** (EN 15316 - see *§ 3.2.2*) are analysed. As aforementioned, these CEN/EPB standards serve as a reference for the elaboration of (harmonised) energy certification procedures. They are however not obligatory hence each Member States can freely decide if and how the suggested calculation approaches are used for the (national or regional) energy performance assessment of buildings. Moreover, these standards include a range of default choices, boundary conditions and input data (*e.g.* primary energy factors, climatic data but also the classification of space categories and related users' conditions) for which representative values are to be defined by each Member State. Consequently, a large variety of practical applications of the CEN/EPB standards is found in Europe. As these national applications might offer interesting, alternative calculation approaches, a comparative analysis is made with the calculation standards as applied in Belgium (*EPR* [22]), Germany (*DIN V 18599* [43]) and The Netherlands (*NEN 7120* [44]). The German and Dutch standard are incorporated as they are both referred to as good examples of practical use of the CEN/EPB standards [143]. Moreover, the calculation tool used to evaluate and certify passive buildings in Flanders (*PHPP*[1] [110]) is mainly based on the *DIN V 18599* standard [43].
Next, in *§ 3.3*, the algorithm for *dynamic* simulations as applied in the simulation tool `TRNSYS` is discussed, followed by an overview of measures taken to guarantee comparability and consistency of the results of both the *static* and *dynamic* methods (*§ 3.4*).

3.2 Quasi-steady-state calculation method for energy performance

Despite the set-up of a general calculation framework within the context of the EPBD regulation, a large variety of *quasi-steady-state* standards is found in Europe. Basically, all these standards apply the same calculation principle: the heat balances are calculated in steady-state conditions, over a sufficiently long time. The selected time-base (*i.e.* seasonal or monthly) differs however depending on the standard that is applied. Furthermore, different calculation approaches are used to cope with dynamic effects and the thermal transient behaviour of the building, the occurrence (and interaction) of multiple building zones, the interaction between building and HVAC systems, the heat transfer to the soil and/or the calculation of the solar radiation.

In Flanders, the obligatory *quasi-steady-state EPR* calculation tool [22] applies a **monthly time-based** calculation approach. Buildings are modelled as multi-zonal buildings however the **thermal coupling** between all building zones is **neglected**. Moreover, the **interaction between the building and HVAC systems** is taken into account in a **simplified way** using tabulated subsystem efficiencies to calculate the HVAC system performance. As the overall aim of this dissertation is to evaluate the currently applied calculation method used in Flanders (*EPR* [22]), the comparative analysis of

[1] The PHPP method [110] is used parallel to the *EPR* calculation for certification of passive buildings. It is a similar, *quasi-steady-state* , monthly calculation method however some of the calculation assumptions and input data differ slightly from the *EPR* calculation [144].

quasi-steady-state calculation standards performed in this section is restricted to similar calculation approaches only. Other calculation approaches such as the holistic approach (*i.e.* the effects of recoverable heat losses of the HVAC systems are iteratively calculated in the energy demand), seasonal or simple hourly calculations or methods accounting for the thermal coupling of the building zones are not addressed here. Moreover, within the main objective of this research (*i.e.* the evaluation of the energy calculation results for school buildings in particular), the comparative analysis is restricted to the analysis of different calculation approaches and hypotheses used to take account of the typical characteristics - and more in particular the intermittent (system) use - of schools. The **empirically determined correction factors** for heat gains/losses, indoor temperatures or energy demands used in the various standards **to account for the transient thermal behaviour of the building and (system) intermittency**, are studied. Likely differences between the standards regarding the calculation of the heat transfer to the soil, the incoming solar radiation, the long-wave radiation to the sky, etc. which are also important for the accuracy of the outcome of the calculation though independent of the use and typology of the building are not addressed here.

3.2.1 Energy demand for heating and cooling

EN ISO 13790

All (national) standards analysed in this chapter are generally based on the European CEN/EPB standard *EN ISO 13790* [37]. Therefore, the monthly, *quasi-steady-state* calculation method as described in this standard is used as a keynote along this section. Wherever necessary, the relevant differences with the other standards are described.

Overall, the following basic calculation principles are valid:

- The energy demand for heating $Q_{H,nd}$ is calculated as the difference between the heat losses $Q_{H,ht}$ and the (utilised) heat gains $Q_{H,gn}$. Likewise, the energy demand for cooling $Q_{C,nd}$ is calculated by the difference between the heat gains $Q_{C,gn}$ and the (utilised) heat losses $Q_{C,ht}$.
- The heat 'gains' contain all heat flows (positive or negative) that are not or only restrictively dependent on the indoor temperature, such as the internal and solar gains. The heat transfer concerns all heat flows (positive or negative) that are (strongly) dependent on the internal temperature, such as the transmission and ventilation heat losses.
- The heat losses and gains are all calculated in steady-state conditions, over a monthly timebase. The ways to implement intermittent phenomena (*i.e.* occupancy schedules, system intermittency) are however different between the various standards.
- An ideal system operation (*i.e.* a perfect control and responsiveness, infinite system output capacity and a uniform building zone temperature distribution) is assumed for the energy demand calculations maintaining exactly the required temperatures during the time of usage. Non-ideally controlled operation of the systems is taken into account afterwards by the emission and control efficiency.

The *quasi-steady-state* method as currently described in *EN ISO 13790* [37], is originally developed in the PASSYS project [145, 146] as a correlation-based calculation method for simplified assess-

ment of energy performance of dwellings. The method calculates the heating demand by subtracting the *useful* heat gains from the heat losses (see *Eq. 3.1*). Likewise, the cooling demand is calculated as the subtraction of the heat gains and *useful* heat losses (see *Eq. 3.2*).

$$Q_{H,nd} = Q_{H,ht} - \eta_{H,gn} Q_{H,gn} \tag{3.1}$$

$$Q_{C,nd} = Q_{C,gn} - \eta_{C,ht} Q_{C,ht} \tag{3.2}$$

where $Q_{H/C,nd}$ is the statically calculated building energy demand for heating/cooling (kWh), $Q_{H/C,ht}$ are the statically calculated total heat losses (kWh), $Q_{H/C,gn}$ are the statically calculated total heat gains (kWh) and $\eta_{H,gn/C,ht}$ is the dimensionless gain/loss utilisation factor.

The total heat transfer $Q_{H,ht}$ is calculated according to *Eq. 3.3*.

$$Q_{H/C,ht} = (H_{tr} + H_{ve})(\theta_{i,H/C} - \theta_e)t \tag{3.3}$$

where H_{tr} and H_{ve} are the heat transfer coefficients by transmission and ventilation (W/K), $\theta_{i,H/C}$ is the set-point temperature for heating/cooling (°C), θ_e is the monthly averaged outdoor temperature (°C) and t is the duration of the calculation step.

The total heat gains $Q_{H/C,gn}$ are calculated using *Eq. 3.4*:

$$Q_{H/C,gn} = Q_{IHG} + Q_{sol} \tag{3.4}$$

where Q_{IHG} is the sum of internal heat gains over the given period (kWh) and Q_{sol} is the sum of solar heat gains over the given period (kWh).

The heat gains due to the internal heat sources are calculated as:

$$Q_{int} = (\phi_{IHG,occ} + \phi_{IHG,eq} + \phi_{IHG,light})t \tag{3.5}$$

where $\phi_{IHG,occ}$ is the internal heat flow from occupants (W), $\phi_{IHG,eq}$ is the internal heat gain from appliances (W) and $\phi_{IHG,light}$ is the internal heat flow from lighting (W).

Regarding the solar heat gains, in reality, they are collected through both transparent and opaque building parts. The *quasi-steady-state* calculation method discussed in this chapter however considers the solar radiation through the transparent building parts only[2]. The net solar heat gains of opaque elements - which are often only a small portion of the total solar heat gains - are omitted from the heat balance. To compensate, at the same time radiation losses from the building to clear skies are omitted from the energy balance.

In *EN ISO 13790* [37], the physical process of heat accumulation, dynamic phenomena, (system)

[2]This assumption is in line with the calculation assumptions of the Flemish EPR standard where long-wave radiation exchanges to the sky are not taken into account though counter-balanced by the fact that solar heat gains are only considered through transparent building parts. Hence, the method assumes that both cancel each other out.

intermittency and variations of input data in time or space are taking into account by:

- the empirically determined gain/loss utilisation factor $\eta_{H,gn/C,ht}$,
- an adjustment of the set-point temperature or the introduction of an intermittency factor $a_{H/C,red}$ to factor in the intermittent heating/cooling patterns or switch offs.

The utilisation factor is calculated using *Eq. 3.6* (heating) or *Eq. 3.7* (cooling).

$$\eta_{H,gn} = \begin{cases} (1-\gamma_H^{(a_{H,0}+\tau/\tau_{H,0})})(1-\gamma_H^{(a_{H,0}+\tau/\tau_{H,0}+1)})^{-1} & \text{if } \gamma_H \neq 1 \\ (a_{H,0}+\tau/\tau_{H,0})(a_{H,0}+\tau/\tau_{H,0}+1)^{-1} & \text{if } \gamma_H = 1 \\ 1/\gamma_H & \text{if } \gamma_H < 0 \end{cases} \tag{3.6}$$

$$\eta_{C,ht} = \begin{cases} (1-\gamma_C^{(a_{C,0}+\tau/\tau_{C,0})})(1-\gamma_C^{(a_{C,0}+\tau/\tau_{C,0}+1)})^{-1} & \text{if } \gamma_C \neq 1 \\ (a_{C,0}+\tau/\tau_{C,0})(a_{C,0}+\tau/\tau_{C,0}+1)^{-1} & \text{if } \gamma_C = 1 \\ 1/\gamma_C & \text{if } \gamma_C < 0 \end{cases} \tag{3.7}$$

with

$$\gamma_H = \frac{Q_{H,gn}}{Q_{H,ht}} \tag{3.8}$$

and

$$\gamma_C = \frac{Q_{C,ht}}{Q_{C,gn}} \tag{3.9}$$

where γ_H is the dimensionless heat-balance ratio for the heating mode, γ_C is the dimensionless loss-gain ratio for the cooling mode, a_0 is a dimensionless reference numerical parameter, τ_0 is a reference time constant. Values for a_0 and τ_0 are empirically set to be 1 and 15, independent of the type or the use of the considered building.

τ is the time constant of the building which is defined as

$$\tau = \frac{C_m}{H_{tr}+H_{ve}} \tag{3.10}$$

where C_m is the accessible internal heat capacity of the building or building zone (J/K).

The internal heat capacity of the building C_m is then calculated using the simplified method as described in *EN ISO 13786 annex A* [118], suitable for the determination of dynamic thermal properties required for the estimation of energy use.

$$C_m = \sum A_j k_j \tag{3.11}$$

where k_j is the internal heat capacity per surface area of the building element j (J/(m^{2}K)) and A_j is the surface area of element j (m^2).

$$k_j = \sum \rho_i c_i d_i \tag{3.12}$$

where ρ_i is the density of material i (kg/m^3), c_i is the specific heat capacity of material i (J/(kg K)) and d_i is the effective thickness of the material i (m).

For the heating mode, the gain utilisation factor for the combined internal and solar heat gains $\eta_{H,gn}$ is introduced to take into account that only part of the gains is effectively used to decrease $Q_{H,nd}$. In other words, $\eta_{H,gn}$ expresses the amount of overheating. In case $\eta_{H,gn}$ = 1, no overheating occurs while in case $\eta_{H,gn}$ = 0 all heat gains are unused and therefore lead to an undesirable increase of the internal temperature above the set-point. These unused heat gains are omitted from the quasi-steady-state heat balance. To adjust however the heat balance equation, at the same time the extra transmission and ventilation heat transfer resulting from the increase of the internal temperature above the set-point are neglected.
For the cooling mode, the loss utilisation factor for the combined transmission and ventilation losses $\eta_{C,ls}$ is introduced to take into account that only part of the heat transfer is utilised to decrease the cooling demand. The other, 'non-utilised' part of the transmission and ventilation heat transfers, which are assumed to occur during periods (*e.g.* nights) when they have no effect on the cooling demands, are omitted from the energy balance. This is counterbalanced by the fact that the calculation method ignores the fact that the cooling set-point is not always reached.

The values for the gain utilisation factor $\eta_{H,gn}$ depend on the heat-balance ratio γ_H and the time constant τ of the building. *Figure 3.2* shows the gain utilisation factor for the averaged values of the time constant τ for the rectangular reference elementary school building with a heavy (τ = 140 h) and a light structure (τ = 65 h) (see *Table 2.12*).

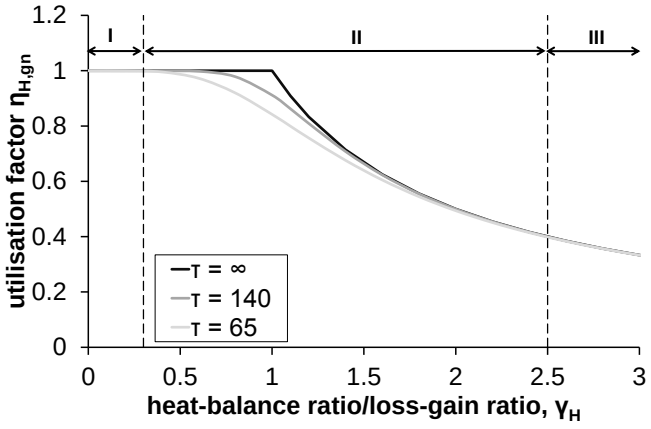

Figure 3.2: Utilisation factor $\eta_{H,gn}$ as a function of the heat-balance/loss-gain ratio γ_H for two time constants τ (h) of the rectangular reference school building for elementary education using the dynamic parameters a_0 and τ_0 in accordance with *EN ISO 13790* [37].

In case of very low heat-balance ratios (part I in *Figure 3.2*), all heat gains can effectively be used to compensate the heat losses and thus the gain utilisation factor equals one. If the energy demand for heating is zero (γ_H very large, part III) then the gain utilisation factor equals the reciprocal number of γ_H. In the intermediate zone (part II), in the case where $\tau = \infty$, all gains are fully utilised until the heat gains exceed the heat losses ($\gamma_H > 1$). In reality however, the utilisation factor decreases gradually if the time constant of the building τ decreases [147].

Corrections for reduced set-point or switch off at night or weekends

The method as described above calculates the energy demand of buildings assuming a continuous system use. Schools however typically have a strongly intermittent users' profile. The daily operating time of schools is limited to ± 8 hours and Wednesday afternoon and weekends are free. In addition, schools are closed during the school holidays (99 days). Consequently, schools are commonly intermittently heated and cooled. To account for this system intermittency, two operation modes and related calculation approaches are defined in *EN ISO 13790* [37]:

- night-time and weekend reduced set-point or switch off
- unoccupied periods (*e.g.* holidays)

In *EN ISO 13790* [37], system intermittency is taken into account by either **(i) the adjusted temperature approach** or **(ii)** the **intermittency factor approach**. The use of the adjusted temperature approach is restricted to quasi-continuously heated/cooled buildings with a setback of the set-point temperature < 3 K and/or τ < 0.2 times the duration of the shortest reduced heating/cooling period or in other words, to buildings where the expected impact of system intermittency is limited. If τ > 3 times the duration of the longest reduced heating period, the setback temperature is set equal to the normal set-point for heating. For other cases, *EN ISO 13790* [37] prescribes the use of the intermittency factor approach.

$$Q_{H,nd,interm} = \begin{cases} H_{ht}(\theta_{i,H,adj} - \theta_e)t - \eta_{H,gn}Q_{H,gn} & \text{(i)} \\ \quad with\ \theta_{i,H,adj} = \theta_{i,H,set,occ}f_{H,occ} + \theta_{i,H,set,nocc}f_{H,nocc} & \\ \textbf{or} & \\ a_{H,red}Q_{H,nd,cont} & \text{(ii)} \end{cases} \tag{3.13}$$

$$Q_{C,nd,interm} = \begin{cases} Q_{C,gn} - \eta_{C,ls}H_{ht}(\theta_{i,C,adj} - \theta_e)t & \text{(i)} \\ \quad with\ \theta_{i,C,adj} = \theta_{i,C,set,occ}f_{C,occ} + \theta_{i,C,set,nocc}f_{C,nocc} & \\ \textbf{or} & \\ a_{C,red}Q_{C,nd,cont} & \text{(ii)} \end{cases} \tag{3.14}$$

where $Q_{H/C,nd,interm}$ is the energy demand for intermittent heating/cooling (kWh), $Q_{H/C,nd,cont}$ is the energy demand for continuous heating/cooling (kWh), $\theta_{i,H/C,adj}$ is the adjusted temperature of the building for the calculation of intermittent heating/cooling (°C), $a_{H/C,red}$ is the dimensionless reduction factor for intermittent heating/cooling (-), $\theta_{i,H/C,set,occ}$ is the set-point temperature in normal heating/cooling mode (°C), $\theta_{i,H/C,set,nocc}$ is the set-point temperature in reduced heating/cooling mode (°C), $f_{H/C,occ}$ is the fraction of the time step that the building is normally heated/cooled and $f_{H/C,nocc}$ is the fraction of the time step with a reduced/increased set-point.

The **adjusted temperature approach** considers the building to be continuously conditioned though at a fictive equivalent indoor temperature which leads to the same heat losses than the one obtained with an intermittent system operation. In this approach, the reduced usability of the heat gains due to mismatch of the gains and heat demands in intermittently heated buildings is factored in implicitly. By reducing the indoor temperature, lower heat losses occur which in turn leads to a shift towards higher

values of γ_H and consequently to a lower value of $\eta_{H,gn}$ (*Figure 3.2*) [146]. The main difficulty of applying the adjusted temperature approach is the uncertainty of the definition of the appropriate fictive monthly mean indoor temperature. The adjusted temperature can not be set equal to the actual (measured or simulated) monthly averaged indoor temperature as these temperatures are strongly affected by overheating, intermittency, inertia and/or imperfect control. These effects are however already explicitly taken into account in the calculation method itself (*e.g.* overheating in the utilisation factor, imperfect control in the emission efficiency of the system). So, by implementing the actual temperatures, these effects would be accounted twice. As shown in *Eq. 3.13* and *Eq. 3.14*, the adjusted set-point temperature according to *EN ISO 13790* [37] is calculated as the time-weighted average of the set-point temperatures. Specific building, system and activity related characteristics are hence not taken into account. When assuming a set-point temperature for heating of 20°C and a setback temperature of 3°C, this results in an adjusted, monthly averaged indoor temperature of ±17.6°C for a typical operational profile of Flemish schools (see *§ 2.3.1*).

The **intermittency factor approach** considers the energy demand for intermittently conditioned buildings as a fraction of the energy demand obtained at continuous heating/cooling operation. The dimensionless reduction factor $a_{H/C,red}$ is calculated as:

$$a_{H/C,red} = 1 - b_{H/C,red}\left(\frac{\tau_{H/C,0}}{\tau}\right)\gamma_{H/C}(1 - f_{H/C}) \qquad with\ \ f_{H/C} \leq a_{H/C,red} \leq 1 \tag{3.15}$$

where f_H is the fraction of the number of hours in a week with a normal heating set-point (= ± 0.2 (*i.e.* Monday - Friday: 8h30 - 16h, Wednesday: 8h30 - 11h45)), f_C is the fraction of the number of days in a week with - at least during daytime - a normal cooling set-point (*i.e.* 5 days per week = 0.71) and $b_{H/C,red}$ is an empirical correlation factor equal to 3.

In the intermittency approach, all effects of intermittent heating or cooling are included in the applied intermittency factor. *Figure 3.3* shows the intermittency factors $a_{H/C,red}$ for various time constants of the rectangular reference elementary school building (τ = 140 h which is the averaged value of the time constant of a range of design variants for the reference school building with a high thermal capacity), τ = 85 h (medium), τ = 65 h (light), and τ = 45 h (very light)).

Corrections for (long) unoccupied periods

When a certain month contains holidays, the calculations are performed separately for the holiday period and for a normal week:

$$Q_{H/C,nd} = (1 - f_{H/C,nocc,hol})\,Q_{H/C,nd,occ} + f_{H/C,nocc,hol}\,Q_{H/C,nd,nocc,hol} \tag{3.16}$$

where $Q_{H/C,nd,occ}$ is the statically calculated energy demand for heating/cooling assuming for all days of the month the control and thermostat settings of the occupied period (kWh), $Q_{H/C,nd,nocc}$ is the statically calculated energy demand for heating/cooling assuming for all days of the month the control and thermostat settings of the unoccupied period (kWh) and $f_{H/C,nocc,hol}$ is the fraction of the month which is a holiday period.

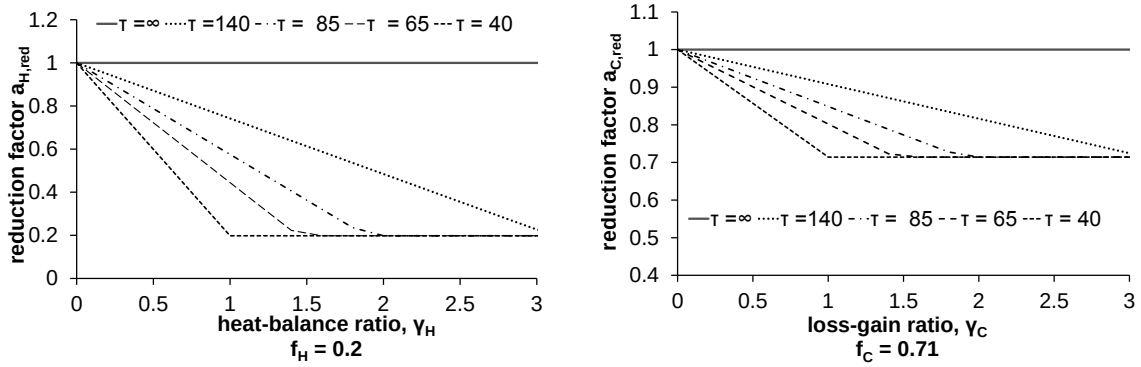

(a) Intermittent heating (b) Intermittent cooling

Figure 3.3: Heat reduction factor for intermittent heating $a_{H/C,red}$ for different time constants τ (h) of the rectangular reference elementary school building.

EPR - Belgium

In Belgium, a monthly,*quasi-steady-state* calculation tool is used for energy performance compliance checking (*EPR*). To support the calculation process, the methodology is implemented in the form of a (compulsory) software tool. The applied calculation method consists of two main parts: the calculation method to be used for **(i)** residential [23] and for **(ii)** non-residential buildings [22]. As this research study focuses on school buildings, only the latter calculation method is discussed hereafter. Overall, a similar though slightly more simplified calculation procedure to account for system intermittency is used as adopted in *EN ISO 13790* [37]. No distinction is made between quasi-continuously or intermittently conditioned buildings and a **fixed value for the adjusted temperature** $\theta_{i,H,adj}$ is used for all non-residential building types, irrespective of the heating plant operation patterns (*i.e.* setback/switch off, duration of the reduced heating period) or building typologies and characteristics.
$Q_{H,nd}$ and $Q_{C,nd}$ are calculated using the following equations:

$$Q_{H,nd} = H_{ht}(\theta_{i,H,adj} - \theta_e)t - \eta_{H,gn}Q_{H,gn} \qquad with\ \theta_{i,H,adj} = \mathbf{19}^\circ C \tag{3.17}$$

$$Q_{C,nd} = 1.1 \cdot p_c(Q_{C,gn} - \eta_{C,ls}H_{ht}(\theta_{i,C,adj} - \theta_e)t) \qquad with\ \theta_{i,C,adj} = \mathbf{23}^\circ C \tag{3.18}$$

where p_C is the (conventionally determined) probability of occurrence of an active cooling system.

Holiday periods are not taking into account explicitly but are taken into consideration implicitly by using reduction factors for the ventilation heat transfer coefficients and the calculation of the heat gains.

DIN V 18599 - Germany

The standard *DIN V 18599* [43] is a holistic performance assessment standard developed for the German energy compliance checking of non-residential buildings. Overall, a similar approach as described in *EN ISO 13790* [37] is used to calculate $Q_{H,nd}$ and $Q_{C,nd}$. To account for reduced heating operation, the *DIN V 18599* [43] standard applies the **adjusted temperature approach**. In contrast to *EN ISO 13790* [37], **a distinction** is made between **a set-back** and **switch-off heating**

mode. Consequently, two different calculation methods are used to calculate the related adjusted temperatures. Moreover, these temperatures are not calculated as a time-weighted average of the set-point temperatures as in *EN ISO 13790* [37] but are set in relation to the outdoor temperature. Finally, different adjusted temperatures are determined **(i)** for days with normal usage and **(ii)** for those days on which the usage of the building and thus the activity and users' behaviour related parameters differ considerably from normal usage days (*i.e.* weekends and holidays):

$$\theta_{i,H,adj,occ} = max(\theta_{i,H,set,occ} - f_{nocc}(\theta_{i,H,set,occ} - \theta_e), \theta_{i,H,set,occ} - \frac{\triangle\theta_{i,H,set}t_{nocc}}{24}) \quad (3.19)$$

$$\theta_{i,H,adj,nocc,we} = max(\theta_{i,H,set,occ} - f_{nocc,we}(\theta_{i,H,set,occ} - \theta_e), \theta_{i,H,set,occ} - \triangle\theta_{i,H,set}) \quad (3.20)$$

with

$$f_{nocc} = \begin{cases} 0.13\frac{t_{nocc}}{24}exp(-\frac{\tau}{250}) & \text{in case of setback mode} \\ 0.26\frac{t_{nocc}}{24}exp(-\frac{\tau}{250}) & \text{in case of switch off mode} \end{cases} \quad (3.21)$$

and

$$f_{nocc,we} = \begin{cases} 0.2(1 - 0.4\frac{\tau}{250}) & \text{in case of setback mode} \\ 0.3(1 - 0.2\frac{\tau}{250}) & \text{in case of switch off mode} \end{cases} \quad (3.22)$$

where f_{nocc} is the correction factor for reduced night-time heating operation, $f_{nocc,we}$ is the correction factor for reduced heating operation over a period of more than one day, $\triangle\theta_{i,H,set}$ is the permitted reduction of the internal temperature (= 4 K) and t_{nocc} is the daily reduced heating time, the boost heating period being counted as part of the operating time.

The total heating demand is then calculated as the time-weighted average:

$$Q_{H,nd} = Q_{H,nd,occ}d_{occ} + Q_{H,nd,nocc,we}d_{we} \quad (3.23)$$

where d_{occ} is the number of days in the month on which the building zone is in normal usage and $d_{nocc,we}$ is the number of days in the month with no or with reduced usage.

When assuming $\theta_{i,H,set,occ}$ = 20°C and $\theta_{i,H,set,nocc}$ = 17°C, the adjusted indoor temperatures for regular school days used in *DIN V 18599* [43] vary from 18.1°C to 19.2°C depending on the outdoor climate, energy efficiency level of the building envelope and the thermal capacity of the rectangular reference building for elementary schools as shown in *Figure 3.4*. Results are shown for five different energy efficiency levels (U_{mean} varying from 0.45 to 0.23 W/(m^{2}K)) and two thermal capacities of the structure (very light (square mark) to heavy (diamond mark)). As shown, these temperatures are much higher than the one that is prescribed by *EN ISO 13790* [37] and generally lower than the monthly mean temperature used in *EPR* [22].

For the cooling mode on the other hand, a different calculation approach is adopted. The cooling demand is considered as the energy needed to avoid overheating and thus to avoid an undesirable increase of the indoor temperature caused by excessive heat gains. Heat gains are considered

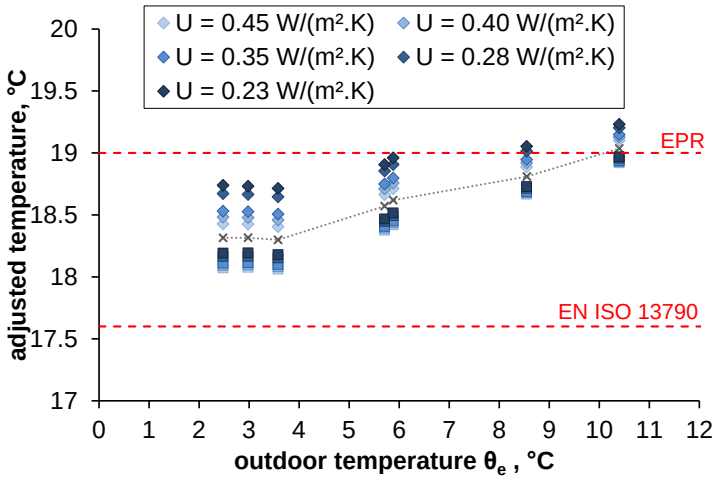

Figure 3.4: The adjusted temperatures for calculating the heat balance in function of the energy efficiency level and thermal capacity (heavy = diamond mark, very light = square mark) of the building envelope and the outdoor temperature.

hereby as useful as long as the difference between the indoor temperature and the set-point temperature for cooling remains < 2 K.

$$Q_{C,nd} = (1 - \eta_{C,gn}) Q_{C,gn} \tag{3.24}$$

A final difference found between *EN ISO 13790* [37] and *DIN V 18599* [43] is the calculation of the utilisation factor. The adopted numerical parameters $a_{H/C,0}$ = 1 and $\tau_{H/C,0}$ = 16 differ slightly from the ones that are used in *EN ISO 13790* [37].

NEN 7120 - The Netherlands

The *NEN 7120* [44] standard provides a calculation code for the energy performance assessment of both residential and non-residential buildings in the Netherlands. For the heating demand calculations, unlike *EN ISO 13790* [37], the *NEN 7210* [44] accounts for intermittent heating by an **adjustment approach** instead of the **adjustment temperature approach**. Moreover, separate correction factors are set to account for **(i)** night time setback and **(ii)** absence during weekends. Both are calculated as a function of the length of the period of reduced heating and of the thermal capacity of the building τ.

$$Q_{H,ht} = (H_{H,tr} + H_{H,ve}) a_{H,red,night} a_{H,red,we} (\theta_{i,H,set} - \theta_e) t \tag{3.25}$$

with

$$a_{H,red,night} = \begin{cases} \frac{(24 - t_{H,h,low}) + t_{H,h,low}(c_{H,red,1} - (\frac{c_{H,red,2}^2}{4 c_{H,red,3}}))}{24} & if \ \frac{t_{H,h,low}}{\tau} > \frac{c_{H,red,2}}{2 c_{H,red,3}} \\ \frac{(24 - t_{H,h,low}) + t_{H,h,low}(c_{H,red,1} - c_{H,red,2}(\frac{t_{H,low}}{\tau}) + c_{H,red,3}(\frac{t_{H,h,low}}{\tau})^2)}{24} & if \ \frac{t_{H,h,low}}{\tau} \leq \frac{c_{H,red,2}}{2 c_{H,red,3}} \end{cases} \tag{3.26}$$

$$a_{H,red,we} = \begin{cases} \frac{(7-t_{H,day,low})+t_{H,day,low}(c_{H,red,1}-(\frac{c_{H,red,2}^2}{4c_{H,red,3}}))}{7} & if\ \frac{24t_{H,day,low}}{\tau} > \frac{c_{H,red,2}}{2c_{H,red,3}} \\ \frac{(7-t_{H,day,low})+t_{H,day,low}(c_{H,red,1}-c_{H,red,2}(\frac{24t_{H,h,low}}{\tau})+c_{H,red,3}(\frac{24t_{H,day,low}}{\tau})^2)}{7} & if\ \frac{24t_{H,day,low}}{\tau} \leq \frac{c_{H,red,2}}{2c_{H,red,3}} \end{cases} \quad (3.27)$$

where $c_{H,red,i}$ are dimensionless, empirically set correlation factors ($c_{H,red,1}$ = 1; $c_{H,red,2}$ = 0.5; $c_{H,red,3}$ = 0.075), $t_{H,h,low}$ and $t_{H,day,low}$ are the number of hours per (working) day ($t_{H,h,low}$ = 14 h for school buildings) respectively number of weekend days per week ($t_{H,day,low}$ = 2 days for school buildings) with a reduced set-point temperature or switch off.

For the cooling mode, the intermittency factor approach is used, similar as described in *EN ISO 13790* [37] (see *Eq. 3.14*), but the reduction factor $a_{C,red}$ is calculated slightly differently:

$$a_{C,red} = \frac{(7 - t_{C,red}) + b_{C,red}t_{C,red}}{7} \quad (3.28)$$

where $b_{C,red}$ is an empirical correlation factor equal to 0.3 and $t_{C,red}$ is the number of days in a week with a reduced set-point or switch off (= 2 days for school buildings).

To conclude the comparative analysis of the standards used for the energy demand calculations, a short summary of all the *quasi-steady-state* calculation procedures is given in *Table 3.1*, focusing on the applied corrections for dynamic effects and system intermittency in particular. The overall adopted calculation approaches and the related calculation procedures for the monthly mean indoor temperatures are depicted. Furthermore, the values for the numerical parameters $a_{H/C,0}$ and $\tau_{H/C,0}$ used for the calculation of $\gamma_{H/C}$ are shown.

3.2.2 Energy use for space heating

The assessment of a building's energy performance includes the energy use for heating, cooling, ventilation, humidification, dehumidification, hot water and lighting. As in schools heating is the most dominant energy flow [148, 149], and active cooling and (de)humidification are rare (see *§ 2.4*), this section focuses on *quasi-steady-state* calculation methods for the energy use for heating only.

In Flanders, the obligatory *quasi-steady-state EPR* calculation tool [22] applies a **simplified, sequential HVAC subsystem calculation approach** for the final energy use of heating. Hereby, the building is decoupled from the HVAC system (see *Figure 3.5* (a)). The additional losses related to each of the subsystem processes (*i.e.* energy conversion, storage, distribution and emission) are calculated separately using **tabulated subsystem efficiencies**. The recoverable part of these thermal losses are hereby directly subtracted from the loss of each system and are thus accounted for by an increase of the related subsystems' efficiencies (see *Figure 3.5* (b)) instead of (iteratively) integrated in the energy demand calculations.
The European CEN/EPB *EN 15316* [45] offers different methods for the calculation of heating system energy requirements and related efficiencies. The included calculation approaches vary from rather simple to more complex. As the overall aim of this dissertation is however to refine the

Table 3.1: Restricted overview of the *quasi-steady-state* standards used for energy demand calculations.

Standard	Calculation approach	Temperature	Intermittency factor	Numerical parameters
EN ISO 13790				
Continuously	$Q_{H,nd} = H_{ht}\,(\theta_{i,H} - \theta_e)\,t - \eta_{H,gn}Q_{H,gn}$			
	$Q_{C,nd} = Q_{C,gn} - \eta_{C,ls}\,H_{ht}\,(\theta_{i,C} - \theta_e)\,t$	$\theta_{i,H/C,\mathbf{set}}$	-	$a_{H/C,0} = 1$, $\tau_{H/C,0} = 15$
Intermittently	**Adjusted temperature approach**			
	$Q_{H,nd} = H_{ht}\,(\theta_{i,H} - \theta_e)\,t - \eta_{H,gn}Q_{H,gn}$			
	$Q_{C,nd} = Q_{C,gn} - \eta_{C,ls}\,H_{ht}\,(\theta_{i,C} - \theta_e)\,t$	$\theta_{i,H/C,\mathbf{adj}} = f(f_{H/C,nocc};\triangle\theta_{i,H/C})$	-	$a_{H/C,0} = 1$, $\tau_{H/C,0} = 15$
	Intermittency factor approach			
	$Q_{H,nd} = a_{H,red}\,(H_{ht}(\theta_{i,H} - \theta_e)\,t - \eta_{H,gn}Q_{H,gn})$			
	$Q_{C,nd} = a_{C,red}\,(Q_{C,gn} - \eta_{C,ls}\,H_{ht}(\theta_{i,C} - \theta_e)\,t)$	$\theta_{i,H/C,\mathbf{set}}$	$a_{H/C,red} = f(b_{H/C,red};\tau_{H/C,0};\tau;f_{H/C})$	$a_{H/C,0} = 1$, $\tau_{H/C,0} = 15$, $b_{H/C,red} = 3$
EPR	**Adjusted temperature approach**			
Intermittently	$Q_{H,nd} = H_{ht}\,(\theta_{i,H} - \theta_e)\,t - \eta_{H,gn}Q_{H,gn}$			
	$Q_{C,nd} = Q_{C,gn} - \eta_{C,ls}\,H_{ht}\,(\theta_{i,C} - \theta_e)\,t$	$\theta_{i,H/C,\mathbf{adj}} = 19°C$	-	$a_{H/C,0} = 1$, $\tau_{H/C,0} = 15$
DIN V 18599	**Adjusted temperature approach**			
Intermittently	$Q_{H,nd} = H_{ht}\,(\theta_{i,H} - \theta_e)\,t - \eta_{H,gn}Q_{H,gn}$	$\theta_{i,H,\mathbf{adj}} = f(t;\triangle\theta_{i,H};\theta_e;\tau)$	-	
	$Q_{C,nd} = \eta_{C,ls}\,H_{ht}\,(\theta_{i,C} - \theta_e)\,t$	$\theta_{i,C,\mathbf{adj}} = \theta_{i,C,set} - 2K$	-	$a_{H/C,0} = 1$, $\tau_{H/C,0} = 16$
NEN 7120	**Adjustment approach**			
Intermittently	$Q_{H,ht}=(H_{H,tr}+H_{H,ve})a_{H,red,night}\,a_{H,red,we}\,(\theta_{i,H,set}-\theta_e)\,t$	$\theta_{i,H,\mathbf{set}}$	$a_{H,red} = f(t_{H,h/day,low};\tau;c_{H,red,i};f_{H/C})$	$c_{H,red,1} = 1$, $c_{H,red,2} = 0.5$, $c_{H,red,1} = 0.075$
	$Q_{C,nd} = a_{C,red}\,(Q_{C,gn} - \eta_{C,ls}\,H_{ht}(\theta_{i,C} - \theta_e)\,t)$	$\theta_{i,H/C,\mathbf{set}}$	$a_{C,red} = f(b_{C,red};t_{C,red})$	$a_{H/C,0} = 1$, $\tau_{H/C,0} = 15$, $b_{C,red} = 0.3$

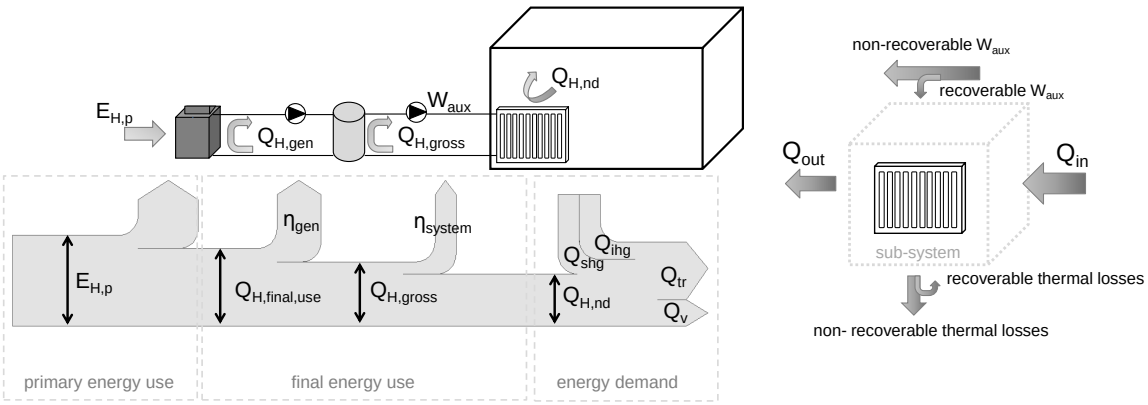

(a) Sankey diagram heating energy flows (b) Sub-system energy flow [150]

Figure 3.5: Conceptual scheme of the simplified calculation procedure as currently applied in the EPR calculation tool [22].

currently applied method for energy performance compliance checking in Flanders, the analysis focuses on those calculation approaches similar to *EPR* [22] only and thus on those methods that apply a rather **simplified approach**. Other possible, more detailed calculation approaches are not addressed here.

EPR

According to the *EPR* calculation approach [22], the final energy use for heating $Q_{H,final,use}$ is calculated in two steps. First, the gross energy demand $Q_{H,gross}$ is calculated which is the energy needed to be delivered by the generation system or plant to the secondary HVAC system (see *Figure 3.5* (a)). Next, the total energy delivered to the heating system $Q_{H,final,use}$ is calculated by dividing the gross energy demand $Q_{H,gross}$ by the generation efficiency η_{gen}.

Calculation of the gross energy demand

The calculation of the gross energy demand $Q_{H,gross}$ depends on the yearly averaged efficiency of the secondary HVAC system η_{system} which covers both the waste of energy that occurs when a building is simultaneously heated and cooled, and the overall occurring thermal energy losses of the secondary HVAC system. General system efficiencies are calculated using *Eq. 3.29*:

$$\eta_{system} = \frac{1}{1 + a_{heat} + f_{annih}/f_{heat,net}} \tag{3.29}$$

where a_{heat} is a factor representing the heat losses due to distribution of heat and imperfect control of the heating system, f_{annih} is a factor accounting for the amount of wasted energy due to simultaneous heating and cooling, $f_{heat,net}$ is the ratio of $Q_{H,nd}$ and the sum of $Q_{H,nd}$ and $Q_{C,nd}$.

An overview of all standard tabulated values for the aforementioned factors based on the type of the heat distribution medium and the applied control system can be found in the EPR calculation manual Table 8 [22].

Calculation of the final energy demand

The total energy input to the heat generation system $Q_{H,final,use}$ needed for the requested heating of the building is calculated using *Eq. 3.30*.

$$Q_{H,final,use} = \frac{Q_{H,gross}}{\eta_{gen}} \tag{3.30}$$

As boilers are by far the most frequently used heat generation system in schools (see *§ 2.4.2*), only the calculation of η_{gen} for a condensing boiler is included in this section. η_{gen} for other heat generation systems can be found in the *EPR* calculation manual [23].

The yearly averaged η_{gen} is calculated based on the 30% part load ratio of the heating system and corrected for the design return water temperature using *Eq. 3.31*:

$$\eta_{gen} = f_{H_i/H_s}(\eta_{30\%} + 0.003 \cdot (\theta_{30\%} - \theta_{mean,boiler})) \tag{3.31}$$

with

$$\theta_{mean,boiler} = 6.4 + 0.63 \cdot \theta_{return,design} \tag{3.32}$$

where f_{H_i/H_s} is the net-to-gross conversion factor (*e.g.* f_{H_i/H_s} = 0.9 for natural gas), $\eta_{30\%,boiler}$ is the 30% part load boiler efficiency based on the manufacturer's data, $\theta_{30\%}$ is the boiler supply flow temperature at which $\eta_{30\%,boiler}$ is determined (°C) and $\theta_{return,design}$ is the design return flow temperature of the heating system (°C).

EN 15316

The calculation method as described in *EN 15316* applies a similar sequential analysis assessing the thermal losses related to the emission (*EN 15316-2-1* [49]), the distribution (*EN 15316-2-3* [151]), the storage and the generation (*EN 15316-4* [152]) of heat.

$Q_{H,final,use}$ is calculated using *Eq. 3.33*:

$$Q_{H,final,use} = \frac{Q_{H,nd}}{\eta_{overall}} \tag{3.33}$$

where $\eta_{overall}$ is the overall system efficiency for the heating system, including all subsystems efficiencies as described hereafter.

Heat emission efficiency (EN 15316-2-1)

According to *EN 15316-2-1* [49], emission losses are the thermal losses of the heat emission system due to **(i)** a non-uniform temperature distribution in the heated space, **(ii)** losses to the outside from heating devices embedded in the structure, and **(iii)** losses due to imperfect control of the indoor temperature. The standard includes two methods to calculate these emission losses: **(i)** a method using the efficiencies of the emission system and **(ii)** a method using an equivalent increase in the internal temperature. As in *EPR* [22], the first method is used, only this method is included in this section. The energy delivered to the emission subsystem $Q_{H,em}$ is then calculated based on the

emission efficiency η_{em} using *Eq. 3.35*:

$$Q_{H,em} = \left(\frac{f_{hydr} f_{int} f_{rad}}{\eta_{em}} - 1\right) Q_{H,nd} \tag{3.34}$$

with

$$\eta_{em} = \frac{1}{4 - (\eta_{str} + \eta_{ctr} + \eta_{emb})} \tag{3.35}$$

where f_{hydr} is the factor for the hydraulic equilibrium, f_{int} is the factor for intermittent heating operation, f_{rad} is the factor for the radiation effect (*i.e.* only relevant for radiant heating systems), η_{str} is the partial efficiency level for the vertical air temperature profile, η_{ctr} is the partial efficiency level for room temperature control regulation and η_{emb} is the partial efficiency level for specific losses of the external components (embedded systems).

An overview of all standardised tabulated values for the efficiencies for different types of heat emission systems (*e.g.* radiator, floor or air heating systems) can be found in the standard's *EN 15316-2-1* Annex A [49].

The calculation approach described in *EN 15316-2-1* [49] is more detailed compared to the calculation method as used in *EPR* [22]. Partial subsystem efficiencies (η_{str}, η_{ctr}, η_{emb}) are included that cover each a specific part of the emission system's thermal losses. Moreover, the standardised, tabulated values for these partial efficiencies depend on several parameters: the height of the served room, the typology of the building (residential or non-residential), the heating operation mode (continuous or intermittent), and the type and the position of the heat emitters in the room. In contrast, in *EPR*, the values for η_{system} are set for emission and distribution losses simultaneously and the values for η_{system} depend only on the type of the heat distribution medium (water, air or combination of air and water) and a limited set of control options.

Heat distribution efficiency (EN 15316-2-3)

According to *EN 15316-2-3* [151], the heat losses of a distribution system depend on the average temperature of the heating medium, the temperature of the surrounding ambient and the length and insulation of the distribution pipes. The energy delivered to the distribution subsystem - also referred to as the gross energy demand - $Q_{H,gross}$ is calculated according to *Eq. 3.37*:

$$Q_{H,gross} = \frac{Q_{H,em}}{\eta_{dis}} \tag{3.36}$$

The distribution efficiency η_{dis} depends in turn on the thermal losses of the heat distribution system $Q_{H,dis,ls}$.

$$Q_{H,dis,ls} = \sum \psi_L (\theta_m - \theta_{i,H}) \cdot L_{pipes} \cdot t_{H,op} \tag{3.37}$$

with

$$\theta_m = \Delta\theta_{des} \cdot \beta_{dis}{}^{\frac{1}{n}} + \theta_{i,H} \tag{3.38}$$

with

$$\beta_{dis} = \frac{Q_{H,em}}{\phi_{H,em} t_{H,op}} \tag{3.39}$$

and

$$\Delta\theta_{des} = \frac{\theta_{s,des} + \theta_{r,des}}{2} - \theta_{i,H} \tag{3.40}$$

where ψ_L is the linear heat transfer coefficient (W/(m.K)), θ_m is the average heat transferring medium temperature (°C), L_{pipes} is the length of the pipes, $\Delta\theta_{des}$ is the temperature difference between the mean emission system design temperature and $\theta_{i,H}$ (°C), β_{dis} is the part load ratio of the heat distribution system, n is the exponent of the heat emission system, $\phi_{H,em}$ is the nominal power of the installed heat emitters (kW) and $t_{H,op}$ is the number of heating hours in the considered calculation time step (month).

The standard contains a detailed, a tabulated and a simplified method to calculate the distribution thermal losses. As in the *EPR* standard for non-residential buildings [22] the additional thermal losses of the heat distribution system are included in a global value for η_{system}, the analysis of *EN 15316-2-3* [151] is restricted to the simplified approach only.

For the simplified calculation method, approximations are made of L_{pipes} and of the ψ-values. The L_{pipes} is based on the length L_l and width L_w of the considered building or building zone, the floor height h_{floor} and the number of floors n_{floor}. A difference is made between pipes connecting the generator and vertical shafts (part V), the pipes in (vertical) shafts (part L) and connection pipes (part A) . The length of each of these pipes is then calculated according to the following equations:

$$L_V = 2 \cdot L_l + 0.0325 \cdot L_l \cdot L_w + 6 \tag{3.41}$$

$$L_S = 0.025 \cdot L_l \cdot L_w \cdot h_{floor} \cdot n_{floor} \tag{3.42}$$

$$L_A = 0.55 L_l \cdot L_w \cdot n_{floor} \tag{3.43}$$

The default values of ψ vary based on the age or class of the building and the type of the pipe. For buildings built after 1995, ψ_V = 0.2 W/(m.K), and ψ_S and ψ_A = 0.3 W/(m.K).

Heat generation efficiency (EN 15316-4-1)

According to *EN 15316*, heat generation losses are caused by **(i)** heat losses to the chimney (or flue gas exhaust) and **(ii)** heat losses through the generator(s) envelope. These thermal losses depend in turn on the type of the installed heat generator(s), the location of heat generator(s), the part load ratio of the generation system, the operation conditions and the control strategy. Due to the complexity and variety of the calculation procedures, different substandard are developed based on the type

of the heat generation system used: *EN 15316-4-1* for combustion systems [152], *EN 15316-4-2* for heat pumps [153], *EN 15316-4-3* for thermal solar systems [154].

EN 15316-4-1 [152] contains three different approaches varying in complexity from rather simple to complex: **(i)** the seasonal boiler performance or typology method, **(ii)** the case specific boiler efficiency method and **(iii)** the boiler cycling method.

The **typology method** calculates a seasonal averaged generation subsystem efficiency η_{gen} for modulating boilers according to *Eq. 3.44*:

$$\eta_{gen} = \left(\frac{(\eta_{100\%,boiler} + \eta_{30\%,boiler}) f_{H_i/H_s}}{2} - 2 - 4 \cdot f_{plt}\right) \tag{3.44}$$

where $\eta_{100\%/30\%}$ is the temperature corrected full-load/part-load net efficiency of the boiler and f_{plt} is a factor depending on the presence of a permanent pilot light.

This method is most similar to the method used in the *EPR* method [22] though even more simple as the additional generation system's thermal losses and related calculated efficiencies depend on the boiler's characteristics only. The data are not additionally corrected according to the applied heating curves while in *EPR* [22] such a correction is incorporated as η_{gen} - aside from the boiler's characteristics - is based on the design return flow temperature.

The alternative **boiler efficiency method** on the other hand, calculates the thermal losses of the boiler for three different (part) load ratios: at 100%, at intermediate load 30% and at 0%. The final boiler losses are then calculated by linear interpolation between these three calculated values.

The boiler thermal losses at full load $\Phi_{H,ls,gen,100\%}$, intermediate load $\Phi_{H,ls,gen,30\%}$ and stand-by losses $\Phi_{H,ls,gen,0\%}$ are calculated using *Eq. 3.45*, *Eq. 3.46* and *Eq. 3.47*, respectively:

$$\Phi_{H,ls,gen,100\%} = \frac{(1 - \eta_{100\%,boiler,corr})}{\eta_{100\%,boiler,corr}} \cdot \Phi_{H,boiler} \tag{3.45}$$

$$\Phi_{H,ls,gen,30\%} = \frac{(1 - \eta_{30\%,boiler,corr})}{\eta_{30\%,boiler,corr}} \cdot 0.3 \cdot \Phi_{H,boiler} \tag{3.46}$$

$$\Phi_{H,ls,gen,0\%} = 1000 \cdot \Phi_{H,boiler} \cdot \frac{c_5}{100} \cdot \Phi_{H,boiler}^{c_6} \cdot \left(\frac{\theta_{return,w} - \theta_{i,boilerroom}}{\Delta\theta_{boiler,test,0\%}}\right) \tag{3.47}$$

where $\eta_{100\%/30\%,boiler}$ is the boiler efficiency at full/intermediate load, $\Phi_{H,boiler}$ is the nominal power output of the boiler (kW), $\theta_{return,w}$ is the return water temperature as a function of the specific operating conditions, $\theta_{i,boilerroom}$ is the indoor temperature of the boiler room (= 13°C) and default values are set for $\Delta\theta_{gen,test,0\%}$ = 50°C, c_5 = 4 and c_5 = -0.4.

with

$$\eta_{100\%,boiler,corr} = f_{H_i/H_s}(\eta_{100\%,boiler} + f_{corr}(\theta_{boiler,w,100\%,test} + \theta_{boiler,w})) \tag{3.48}$$

and

$$\eta_{30\%,boiler,corr} = f_{H_i/H_s}(\eta_{30\%,boiler} + f_{corr}(\theta_{boiler,w,30\%,test} + \theta_{return,w})) \tag{3.49}$$

where f_{corr} is a correction factor taken into account variations of the efficiencies as a function of the average boiler water temperature (default value is 0.2%/°C), $\theta_{boiler,w,100\%,test}$ is the average water temperature at test conditions for full load (default value is 70°C) , $\theta_{boiler,w,30\%,test}$ is the return water temperature at test conditions for intermediate load (default value is 30°C) and $\theta_{boiler,w}$ is the average water temperature of the boiler as a function of the specific operating conditions.

The boiler efficiencies at full load $\eta_{100\%,boiler}$ and intermediate load $\eta_{30\%,boiler}$ are calculated as a function of the boiler output capacity $\phi_{H,boiler}$ according to *Eq. 3.50* and *Eq. 3.51*:

$$\eta_{100\%,boiler} = \frac{c_1 + c_2 \cdot log\phi_{H,boiler}}{100} \tag{3.50}$$

and

$$\eta_{30\%,boiler} = \frac{c_3 + c_4 \cdot log\phi_{H,boiler}}{100} \tag{3.51}$$

where default values for condensing boilers are set for c_1 = 94, c_2 = 1, c_3 = 103 and c_4 = 1.

The boiler average water temperature as a function of the specific operating conditions $\theta_{boiler,w}$ is then calculated as the average of the supply flow $\theta_{supply,w}$ and return flow $\theta_{return,w}$ temperature. The latter is calculated - in case a bypass is installed and the boiler flow rate is larger than the distribution flow rate - using *Eq. 3.52*:

$$\theta_{return,w} = \theta_{supply,w} + \frac{Q_{H,gross}}{\rho_w c_w \dot{V}_{boiler}} \tag{3.52}$$

3.3 Dynamic calculation of the energy performance

Dynamic simulations typically calculate the energy balances with a short time step (*i.e.* one hour or less). Consequently, compared to the *quasi-steady-state* calculation methods, temperature variations and energy flows in the building are calculated in a more realistic way accounting for heat accumulation, dynamic phenomena and variations in time of the use of the building. Along this dissertation, *dynamic* simulations will be used for both the calculation of the energy demand $Q_{H/C,nd}$ and for the calculation of the energy use for heating $Q_{H,final,use}$. For the first series of calculations only the building is included in the simulation model while for the latter both the building and HVAC systems are simulated. The obtained dynamic calculation results will then serve as a reference to evaluate the accuracy of the various *quasi-steady-state* calculation methods (EN ISO 13790 [37], EPR [22], NEN 7120 [44], DIN V 18599 [43]) and to determine refinements and changes to the *quasi-steady-state* calculation method. There are numerous methods to perform dynamic calculations, ranging in complexity from simple to very detailed: several studies can be found that calculate the heat demand $Q_{H,nd}$ or the final energy use $Q_{H,final,use}$ of a building using different simulation

programs such as TRNSYS [155], ESP-r [156] or EnergyPlus [157, 156]. Based on the results of a comprehensive comparison of existing dynamic simulation tools, Crawley et al. [158, 159] indicated TRNSYS as one of the best options for HVAC system simulations as it provides a large data-base of features for HVAC systems (components) which are validated against experimental data. Consequently,TRNSYS is used often for studies on energy performance assessment [155] or for integrated building and HVAC system simulation studies [160, 42]. Hence, TRNSYS is chosen as the simulation tool for all *dynamic* simulations which are performed in the context of this research study.

TRNSYS

TRNSYS is a **TR**a**N**sient **SY**stem **S**imulation program with a modular structure that is originally designed to solve the transient performance of thermal energy systems. TRNSYS is a differential equation solver in which individual components - also referred to as 'Types' - are graphically assembled in a visual interface known as the TRNSYS Simulation Studio [158]. Each 'Type' contains a code for a specific task, usually representing a component of the HVAC system (*e.g.* pumps, fans, etc.) or a specific part of the simulation model (*e.g.* ventilation schedules, weather files, etc.). The included 'Types' can vary from simple (*e.g.* pipes, mixing values, etc.) to more complex (*e.g.* Type56 which represents the whole building). All Types are compiled similarly and communicate through a set of inputs, outputs and parameters. Input data specifically related to the building (Type56) are entered through a dedicated visual interface (TRNBuild). Along this dissertation, the most recent software update TRNSYS 17 [161] is used. The general applied algorithm and calculation hypotheses of TRNSYS are described in the next subsections.

Building model

TRNBuild models the building as a multi-zone nodal model. The building is divided by the modeler into several building zones based on the different users' characteristics and heat load patterns of the included rooms. As an iterative approach is used in TRNSYS to solve the energy balances, the number of zones included in the building model has a large influence on the calculation time. As a result, the final number of zones included in the simulation model results from balancing the accuracy of the model and the related calculation time [125]. All included building zones are bounded by several construction parts such as walls or roofs and coupled to either the outdoor environment or another included building zone. Each zone is represented by a single node. At each simulation time step, the nodal air temperature and the surface temperatures of the construction elements of each of the included zones are calculated by solving the convective heat flow balance of each zone and the heat balances of each of the internal surfaces. An artificial temperature node (T_{star}) as shown in *Figure 3.6* is introduced to solve the energy balances more efficiently.

Applying the star network approach, the convective heat flow balance of zone 'i' is given by *Eq. 3.53*.

$$\phi_{gn,conv,i} + \phi_{ve,i} + \phi_{inf,i} + \phi_{cplg,i} + \frac{(T_{star,i} - T_{a,i})}{R_{star}} = C_{air}\frac{dT_{a,i}}{dt} \tag{3.53}$$

where $\phi_{gn,conv,i}$ represents the convective (internal and solar) heat flux (W), $\phi_{ve,i}$ are the ventilation heat losses (W), $\phi_{inf,i}$ are the infiltration heat losses (W), $\phi_{cplg,i}$ represents convective heat/gains

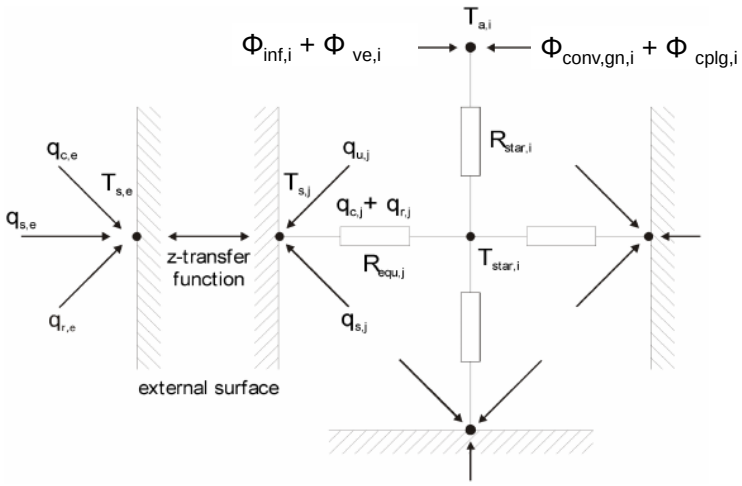

Figure 3.6: Internal heat transfer by convection and radiation are calculated in TRNSYS by an artificial star network [27].

due through coupled air flows with other included building zones (J), $T_{star,i}$ is the star temperature of zone 'i' (K), R_{star} is the resistance of the star node (K/W) and C_{air} represents the internal heat capacity (J/K) which is set equal to five times the heat capacity of the internal air volume, to account for both the air capacity and the capacity of the furniture in the zone.

The heat balance of the internal surface 'j' is then given by *Eq. 3.54*.

$$\frac{(T_{star,i} - T_{a,i})}{R_{star}} = \sum_{j} \frac{(T_{s,j} - T_{star,i})}{R_{equ,j}} \tag{3.54}$$

where $T_{s,j}$ is the surface temperature of surface 'j' (K) and $R_{equ,j}$ is the equivalent resistance of surface 'j' (K/W).

Every time step, the equations *Eq. 3.53* and *Eq. 3.54* are solved for each zone 'i'. Additionally, the heat balance for each surface temperature 'j' is solved using *Eq. 3.55*.

$$\frac{(T_{s,j} - T_{star,i})}{R_{equ,j}} = (q_{\lambda,j} + q_{s,j} + q_{r,j}) A_{s,j} \tag{3.55}$$

where $q_{\lambda,j}$ is the conduction heat flow density at the inside of surface 'j' (W/m^2), $q_{s,j}$ is the solar radiation to surface 'j' (W/m^2) and $q_{r,j}$ represents the radiative heat gains to surface 'j' (W/m^2).

To account for the thermal mass of the building components, $q_{\lambda,j}$ is calculated using the transfer function relations of Mitalas and Arsenault [162].

Each of the outer walls included in the simulation model is subject to **(i)** convective heat transfer with the outside air (modelled by means of a (fixed) convective heat transfer coefficient), **(ii)** shortwave solar radiation and **(iii)** long-wave radiation exchange with the sky and the ground (modelled by

means of view factors). The transmission of solar radiation via external windows is calculated using a detailed window model. The incoming diffuse solar radiation is distributed homogenously over the various surfaces of the envelope (absorption coefficient α is set equal to 0.6 for all surfaces, no differentiation is made based on the type of material) while the entering solar beam radiation is controlled by explicit distribution factors. These factors can be determined using either a detailed view factor algorithm or a simplified procedure using GEOSURF values. As the differences between the surface temperatures and thermal balances using both methods are negligible [163], the latter method is used. In doing so, the GEOSURF values for the floor are set equal to 1, assuming that all entering direct solar radiation is captured by the floor surface, as suggested by Judkoff and Neymark [164]. The incident solar beam radiation is then partially absorbed in accordance with its absorption coefficient α and partially reflected as diffuse radiation (see *Figure 3.10*).
Long-wave radiation exchanges to the sky are calculated depending on the geometry - or view factor to the sky - of the building elements, the temperature of the sky and the emissivity of the considered surfaces (in TRNSYS ε_L = 0.9 for all surfaces).

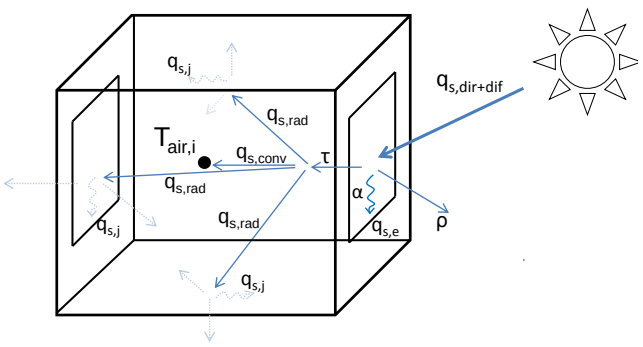

Figure 3.7: Simplified physical model for internal distribution of solar radiation in TRNSYS.

The internal radiative heat gains (*i.e.* due to people, equipment etc.) are distributed according to simple area ratios.

A more elaborate explanation on the included energy balances, the implemented star network, the transfer functions used and the internal and external radiation modes can be found in the according TRNSYS manual [161].

Despite the overall higher level of detail of the *dynamic* simulation method compared to the *quasi-steady-state* calculation method, some assumptions and simplifications are made[3] or are inherent to the use of the *dynamic* simulation tool TRNSYS leading to some restrictions and drawbacks of the simulation results [165, 125]:

- Each of the building zones is represented by a single air node. A perfectly mixed air with a uniform air temperature is assumed. Consequently, additional heat losses of the heat emitters or comfort problems due to stratification of the room air (*i.e.* a temperature gradient between

[3] In conformity with *EN ISO 13790* [37], some simplifications are introduced in the *dynamic* simulation method in order to guarantee compatibility with the *quasi-steady-state* calculation methods and to allow mutual comparison of the obtained *dynamic* and *quasi-steady-state* calculation results (see *§ 3.4*).

the air at floor level and the air at ceiling height caused by warm air rising) can not be assessed by the simulation model.
- All surfaces are assumed to be isothermal and fixed surface-averaged convective heat transfer coefficients are used. Furthermore, the heat conduction through the building elements is assumed to be one-dimensional. Additional thermal losses due to higher local surface temperatures (*e.g.* behind radiators) can hence not be calculated.
- The thermo-physical properties (*e.g.* thermal conductivity, solar absorptance, heat emissivity) of the materials composing the building elements are time-independent and isotropic.
- Finally, transfer functions are used to model heat exchange in the building elements which complicates the modelling in case of highly capacitive building elements.

HVAC system model

In *Chapter 6*, the results are discussed of a series of *dynamic*, integrated building and HVAC system simulations. This section gives an overview of the general assumptions made for the development of these HVAC system simulation models. Each simulation model consists of different connected HVAC model components (called 'Types' in TRNSYS), among which calculation data are exchanged at every simulation time step (see *e.g. Figure 6.6* and *Figure 6.7*). The entire simulation model is sequentially solved at every time step, iterating until convergence is reached [125]. The specific 'Types' used to model each of the HVAC components are not described here but can be found in *Chapter 6*.

Overall, a similar simulation approach is used and equal modelling assumptions are made as described in Parys et al. [125]. For the sake of clarity, a short summary is given hereafter.

- For the integrated building and HVAC system simulations performed throughout this dissertation, the hydraulic system is assumed to be perfectly balanced and well designed. For the modelling of the HVAC systems, heat flows between components are simulated while hydraulic calculations to assess the impact of hydraulic imbalances or improper design on the efficiency of the HVAC system cannot be not performed. The effect of deviating fluid flows or the impact of the time that is needed for the HVAC system to achieve a new equilibrium state after likely changes in the pressure can thus not be included in the simulations.
- To control heating and cooling of a building zone, the operative temperature calculated as the weighted average of the air temperature of the conditioned zone and the mean radiant temperature of all building parts enclosing the zone is maintained at the required set-point temperature. As in the TRNSYS calculation procedure, the air temperature is used to control heating or cooling, a simple equation is implemented manipulating the air temperature so that the operative temperature fits the set-point requirements.

3.4 Compatibility and consistency of (quasi-steady-state and dynamic) energy performance calculation methods

In the previous sections, a descriptive analysis is given of various (*quasi-steady-state* and *dynamic*) calculation standards/tools to be used for energy rating and certification of building designs. In the following chapters, simulation based comparisons - either comparing the various *quasi-steady-state* calculation standards mutually or comparing the quasi-steady-state calculation results to the results of *dynamic* simulations - are performed to determine to what extent the implementation of different calculation approaches or input data might lead to more accurate calculation results. To allow for a useful comparison, compatibility between the compared calculation approaches must be guaranteed. The calculation methods must be aligned and discrepancies due to differing modelling assumptions (*e.g.* implementation of (external) boundary conditions such as outdoor temperature or incident solar radiation, the effect of thermal bridges or the ground-floor heat transfer) must be limited. To do so, the procedure to harmonise different calculation methods as described in *EN ISO 13790* [37] is applied. Moreover, equal assumptions regarding building (*e.g.* composition of the building envelope, insulation thicknesses), HVAC (*e.g.* ventilation rates, set-points) and user's characteristics (*e.g.* heating schedules, occupancy rates) are implemented in all calculation methods.

Along this section, an overview is given of those specific parameters which are synchronised. The input data of the *dynamic* simulations are compared to and wherever necessary fit to the standardised input data as used in the *quasi-steady-state* methods, and vice versa.

3.4.1 Weather data and related boundary conditions

A first step to fit the calculation methods is the harmonisation of **the outdoor temperature**. For all energy calculations performed along this dissertation, a typical weather data set for Uccle, Belgium, derived from measured meteorological data between 1961 and 1990 by Meteonorm v5 [166] is used. In doing so, (hourly) outdoor air temperature data are exported from `TRNSYS` and used as monthly averaged input values in the monthly, *quasi-steady-state* methods.

3.4.2 Heat transfer coefficients and internal boundary conditions

For the **heat transfer by transmission**, the same surface areas, materials and layers are used for the included building parts. The thickness and the conductivity of every surface layer are set equal.

Although more detailed calculation approaches are possible, fixed **convective heat transfer coefficients** are used in `TRNSYS`, equal to the fixed values as used for the *quasi-steady-state* calculations: $h_{c,e}$ = 19 W/(m^{2}K) for external surfaces (except for the slab-on-ground floors where $h_{c,e}$ = 0 W/(m^{2}K)), and $h_{c,i}$ = 3.5 W/(m^{2}K) for upward and horizontal flow and $h_{c,i}$ = 1.2 W/(m^{2}K) for downward flow on the internal side [167]. As the real convective heat transfer depends however strongly on the surface temperature and thus may vary drastically under different HVAC conditions, an exception throughout this dissertation is made for the *dynamic*, integrated building HVAC system simulations

of floor heating systems. For these simulations, the internal heat transfer coefficient $h_{c,i}$ of the floor is calculated in function of the floor temperature using the internal calculation approach of TRNSYS.

As concerns the *dynamic* simulations in TRNSYS, the **heat transfer coefficients** used to calculate the **long-wave radiation** at surfaces can not be adjusted and can therefore not be aligned with the coefficients used in the *quasi-steady-state* calculations. Therefore, the internal long-wave radiation heat transfer coefficients $h_{r,i}$ used for the *quasi-steady-state* calculations are calculated using *Eq. 3.56*.

$$h_{r,i} = 5.67 \varepsilon_L F_T \tag{3.56}$$

where ε_L is the emissivity for long-wave radiation of internal surfaces and F_T is the temperature factor for radiation ($\approx$ 0.95 at internal conditions) [168].
As in TRNSYS ε_L is assumed to be 0.9 for all surfaces, this results in $h_{r,i}$ = 4.93 W/(m^{2}K) for internal surfaces.

Regarding the heat **transmission to the ground** in particular, the dynamic heat transfer through the ground floor in TRNSYS is calculated according to the method described in Annex D of *ISO DIS 13370* [169] for slab-on-ground floors. This method assumes the inclusion of a ground layer (= 0.5 m) and a virtual layer with specific thermo-physical properties (= 0.1 m) below the floor construction with a varying ground temperature below as a boundary condition. For the *quasi-steady-state* calculation on the other hand, in line with the calculation procedure as described in the *EPR* standard [22], a simple reduction factor is applied to the floor slab U-value calculated according to the 'Transmission reference document' [170].

Considering the **infiltration losses** in the *dynamic* simulations, a simplified approach is used to account for the infiltration through the envelope. A constant rule of thumb value, irrespective of the weather conditions, equal to 4% of the air flow rate measured during an air tightness test with a pressure difference between indoor and outdoor of 50 Pa is implemented [168]. Induced pressure variations due to wind and thermal stack are consequently not taken into account. Since only relatively air tight buildings are included ($n_{50} \leq 3$ ACH), the influence of this modelling simplification is expected to be rather limited [125]. Equal infiltration rates are implemented in the *quasi-steady-state* calculation methods.

3.4.3 Internal Heat gains

Both the simplified and the *dynamic* methods consider the same amount of internal heat gains due to occupants, equipment and lighting, either implemented on a monthly time-base (*quasi-steady-state*) or using realistic users' profiles (dynamic). To guarantee equivalence between the *dynamic* and *quasi-steady-state* calculation methods, *EN ISO 13790* [37] prescribes a fifty-fifty partition for the radiative and convective heat gains in the *dynamic* simulations.

3.4.4 Discussion

Despite the efforts done to align the boundary conditions and input data of *quasi-steady-state* and *dynamic* calculation methods, differences may be found between the input (*i.e.* heat losses $Q_{H/C,ht}$ or the heat gains $Q_{H/C,gn}$) or the output (energy demand $Q_{H/C,nd}$ and final energy use for heating $Q_{H,final,use}$) of the calculation methods.

While comparing the monthly, *quasi-static* and *dynamic*[4] thermal losses $Q_{H,ht}$ and gains $Q_{H,gn}$, some (small) discrepancies are found for both the heat losses and heat gains as shown in *Figure 3.8* and *Figure 3.9*.

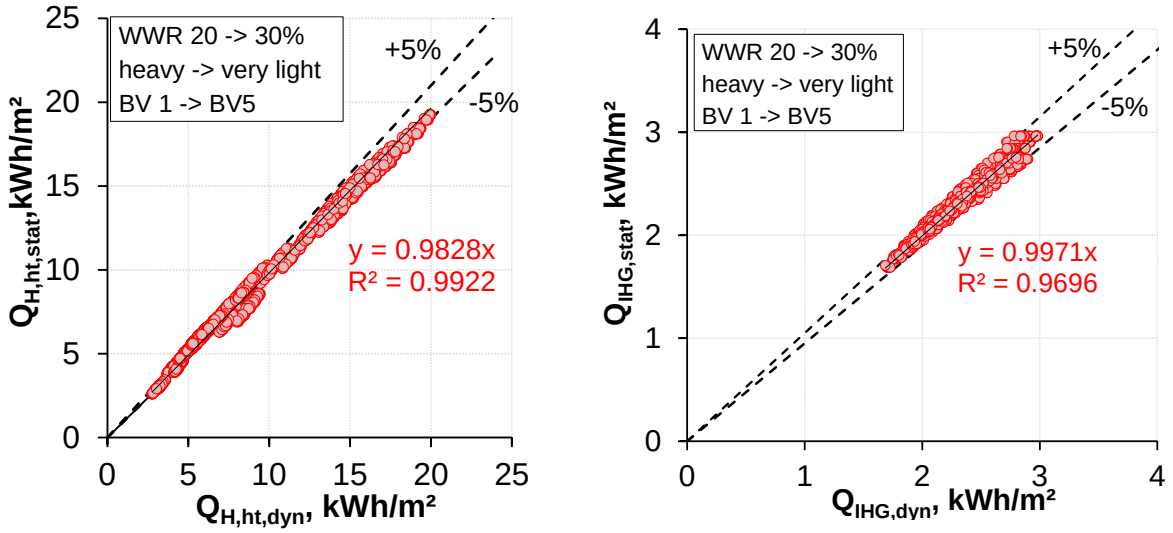

(a) $Q_{H,ht}$ (b) Q_{IHG}

Figure 3.8: Comparison of the monthly heat losses and internal heat gains, normalised to the building floor area (kWh/m^2), calculated using either dynamic simulations ($Q_{H,ht,dyn}$ and $Q_{IHG,dyn}$) or the calculation method as described in *EN ISO 13790* ($Q_{H,ht,dyn}$ and $Q_{IHG,dyn}$). Information on the building sample used for these calculations can be found in *Table 5.3* (elementary school building, see floor plan - *Figure 2.6* (a)).

The monthly *dynamic* and *quasi-steady-state* heat losses are compared for a selection of building variants with varying thermal capacity, energy performance level of the building envelope and WWR (*i.e.* the same building sample as described in *§ 5.3.1* is used). Overall, a good fit (R^2 = 0.99) is found: the relative monthly error, averaged over all building variants, is limited to 3.8%, with a maximum of < 15% found for the spring months (May). For winter months, the maximum error remains below 6%. Furthermore, no significant impact of the WWR (*i.e.* average relative error is 4.1% and 3.8% for WWR = 30% and WWR = 20%, respectively) and the thermal capacity (*i.e.* average relative error is 4.0% and 3.8% for heavy building and very light buildings, respectively) on the relative error of the heat loss calculations is found. A slight impact of the energy performance level of the building is however revealed, though the overall impact is limited as the differences between the average relative errors found for the various building variants (variant 1 to 5 - see *Table 5.3*) remain < 2.5%.

[4]To obtain the 'static' output data by the dynamic simulation tool TRNSYS, the black box approach of *EN 13790* is used as elaborately described in *§ 5.2.2*.

Similar results are found in a more comprehensive comparative analysis of the *dynamic* and *quasi-static* heat losses performed by Pernigotto [26]: for well insulated buildings which apply an operative set-point temperature for heating - as generally assumed throughout this dissertation - the differences between the heat loss calculations remain limited ($\triangle$ $Q_{H,ht}$ < 6%). Hence, one may conclude that when the models are harmonised (see *§ 3.4*), a good compatibility of the heat loss calculations is found for the investigated building sample. Hence, the impact of the differences in *e.g.* the applied method to account for ground heat losses remains limited for the investigated building sample.
The same building sample is used to evaluate the differences between the dynamically and statically calculated internal heat gains (Q_{IHG}). Again, overall a good fit (R^2 = 0.97) is found: the relative monthly error, averaged over all building variants, is limited to 1.4%, with a maximum of < 7% found. The impact of the WWR, the thermal capacity and the energy performance level of the building is negligible: the differences between the errors, averaged over the considered building variants, remain 1.5% or smaller. Hence, one may conclude that, a good compatibility of the internal heat gain calculations is found for the investigated building sample. Similar results are found in the work of Pernigotto [26].

An elaborate comparison between the *quasi-static* (*EPR*) and *dynamic* (TRNSYS) transmitted solar heat gains Q_{sol} through the transparent building parts is performed by Parys [171], for dwellings and non-residential buildings. Overall, it is shown that a good fit between the transmitted solar heat gains calculated according to *EPR* [22] and TRNSYS is found for unshaded windows, provided that similar boundary conditions are applied in both methods (*i.e.* similar glazing-to-window ratio implemented in both methods, no shading due to external obstacles assumed[5] (see *Figure 3.9*)).

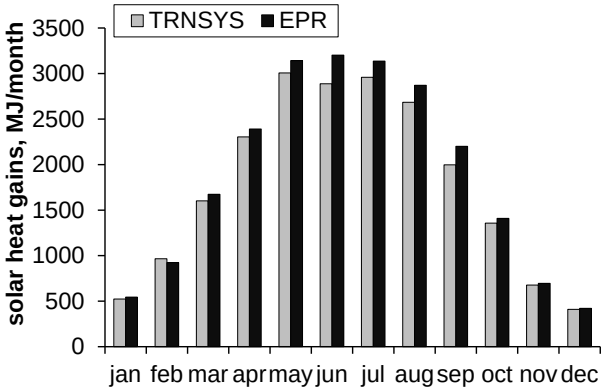

Figure 3.9: Comparison of the monthly solar heat gains calculated by the *EPR* calculation tool and in TRNSYS, for an office with a WWR = 30%, assuming no shading and applying the same glazing-to-window ratios [171].

The small differences in solar heat gain calculations are due to the fact that aside from the equivalence of the input data, the harmonisation of the solar heat gains depends on the consistency of

[5] Although in reality it is hardly the case, no shading due to external obstacles is included in this study to limit the complexity of the model. This pragmatic approach can be applied when fictional buildings are calculated, as it is the case along this research study. However, when a real school building project is rated, obviously shading due to external object must be taken into account.

the calculation approach used to calculate the incident solar radiation and the effective heat flow through windows. In TRNSYS, the calculation of the heat gains through transparent building parts is very detailed and depends on the angle of incidence, and the temperature and properties of each glass layer and cavity whereas in the *quasi-steady-state* calculation method the complex underlaying processes are simplified and summarised in the g-value of the glazing and some additional correction factors (*e.g.* correction for angle of incidence) [171, 26].
However, when taking into account (external) shading devices, especially in case of movable, automatically controlled shading, more significant differences are found [171]. In the *EPR* calculation tool [22], a simplified approach is used applying tabulated values for the movable shading reduction factor a_c. The values for these reduction factors depend on the calculated energy balance (*i.e.* different values are used for the heating and cooling balance) and the selected shading control system (*i.e.* a reduction factor is set for manually and automatically controlled shading). As shown however by dynamic simulation results performed by Parys [171] (see *Figure 3.10*), the use of automatically controlled shading, and thus the related movable shading reduction factor a_c, depends additionally on the orientation and the considered calculation month [171]. Simultaneously, Parys [171] showed that the reduction factor for movable shading as currently applied for the heat balance calculations in *EPR* [22] (*i.e.* a_c = 0.4 for non-residential buildings) is overall too high, except for South oriented windows.

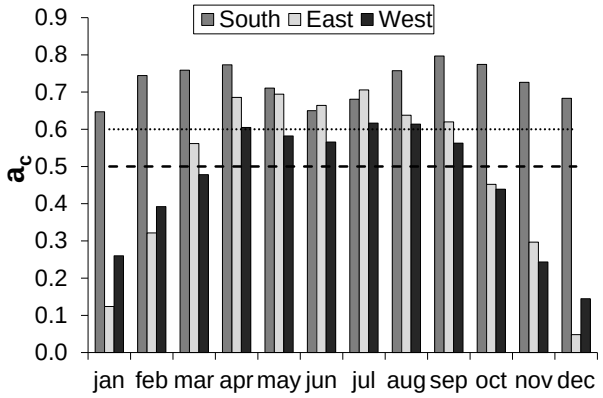

Figure 3.10: Dynamically calculated movable shading reduction factors for automatically controlled screens (see *§ 4.3.1* for the applied control strategy), expressed as a function of the orientation, for an office with a WWR = 30% and normal internal heat gains [171]. The values for a_c for automatically controlled shading, used for the heating (dashed line) and cooling balance (dotted line) in EPR [22] are marked in the figure.

To avoid any influences of these differences on the conclusions of this study and as a detailed calculation of the static solar heat gains (*i.e.* not using the default values) requires extensive building information and hence a substantial effort of the modeler, it is opt for a more pragmatic approach. The static solar heat gains are calculated as an output of TRNSYS in accordance with the general calculation assumptions of the *quasi-steady-state* method: monthly averaged solar heat gains are calculated as the short and long wave solar radiation entering the zone through all transparent building parts. To do so, the total shortwave (direct + diffuse) solar radiation transmitted through all external windows and the secondary heat flux of all external windows of each zone are summed and

used as an input for the *quasi-steady-state* calculation method.

Once the input data are aligned, the results of the *quasi-static* and *dynamic* energy demand calculations can be compared. *Figure 3.11* (a) shows the differences between the dynamically and statically calculated annual heat demand $Q_{H,nd}$, normalised to the building floor area, according to the calculation approaches described in *EN ISO 13790* [37], *EPR* [22], *DIN V 18599* [43] and *NEN 7120* [44].
Figure 3.11 (b) focuses in particular on the calculation results of *EPR* [22] and shows the impact of the thermal capacities.

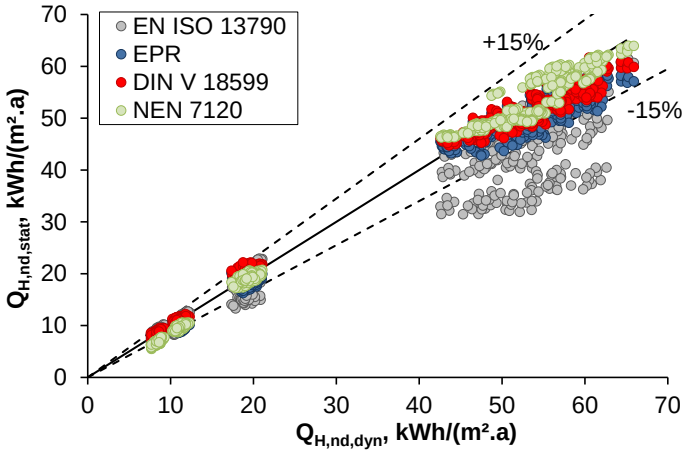

(a) selection of quasi-steady-state calculation standards

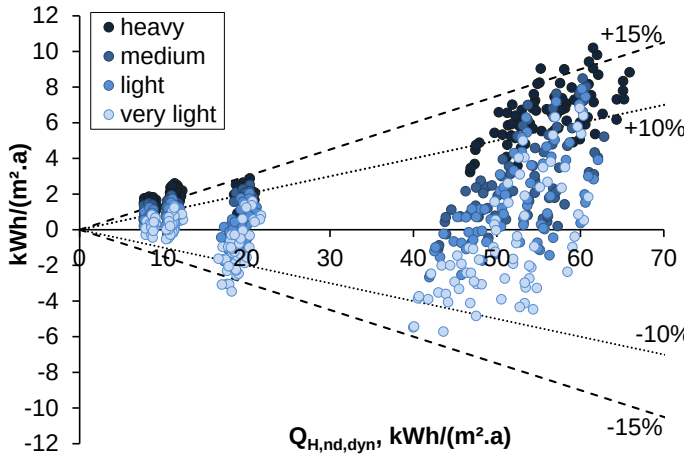

(b) EPR

Figure 3.11: Differences between the dynamic and *quasi-steady-state* calculation results of the annual heat demand, normalised to the building floor area (kWh/(m^2.a)), for a range of intermittently heated building variants of the elementary, rectangular reference school building. The results are plotted for various energy efficiency levels (see *Table 5.3*), thermal capacities (heavy to very light) and boundary conditions (see *Table 4.3*).

As shown in *Figure 3.11* (a) and (b), significant differences are found: the output of the *quasi-steady-state* standards generally tend to underestimate the heat demand. The differences between dynam-

ically $Q_{H,nd,dyn}$ and statically calculated heat demands $Q_{H,nd,stat}$ vary from ± 5% up to more than 20% depending on the applied calculation standards and on the building's characteristics (*i.e.* the thermal capacity of the building and energy efficiency level of the building envelope). The higher the thermal capacity, the larger differences are found.

3.5 Conclusion

This chapter discusses the basic principles of *quasi-steady-state* and *dynamic* calculation methods which are commonly used for building certification and energy rating of buildings in the context of EPBD. Regarding the *quasi-steady-state* calculation approach, a comparative analysis is performed between the European CEN/EPB standards (EN ISO 13790, EN 15316) and the practical implementation of the energy calculation standards to comply with EPBD in Flanders (EPR - energy demand/use), Germany (DIN V 18599 - energy demand) and The Netherlands (NEN 7120 - energy demand). Within the overall objective of the dissertation, the comparative analysis is restricted to monthly calculation methods that use a simplified approach to account for the interaction between the building and HVAC systems and apply a multi-zonal approach while the thermal coupling between all building zones is neglected. Other calculation approaches such as the holistic calculation approach for the interaction between building and system, simple hourly or seasonal calculations, or methods accounting for the thermal coupling of the building zones are not discussed. Moreover, the review is limited to the analysis of the empirically determined correction factors for heat gains/losses, for indoor temperatures or for energy demands used in the various standards to account for the transient thermal behaviour of the building and (system) intermittency. Likely differences between the standards regarding the calculation of the *e.g.* heat transfer to the soil, the incoming solar radiation, the long-wave radiation to the sky, etc. are not addressed.
Regarding the *dynamic* calculation approach, the algorithm for *dynamic* simulations as applied in the simulation tool TRNSYS is discussed. Finally, an overview of measures is given which are taken to guarantee compatibility and consistency of the results of various calculation methods.
Despite the efforts done to align the input data and boundary conditions, significant differences remain between the output of the *quasi-steady-state* and *dynamic* calculation methods varying from ± 5% up to more than 25% depending on the applied calculation standard and on the building's characteristics. Therefore, in the next chapters, the results of an elaborate study on the simplifications included in the *quasi-steady-state* calculation methods are discussed:

- In *Chapter 4*, an accurate set of representative input parameters and boundary conditions for schools is defined, which can be used directly for *dynamic* simulations or can be converted into monthly averaged input data for the simplified, *quasi-steady-state* calculation methods.
- In *Chapter 5*, the accuracy of the energy demand calculation itself is analysed. The values for the utilisation factors (*§ 5.4*) and the calculation methods used to account for system intermittency are analysed and refined (*§ 5.5*).
- In *Chapter 6*, the calculation method used to transform the heat demand to the (primary) energy use for heating is evaluated addressing in particular the impact of the dynamic interaction between buildings and the coupled HVAC systems.

4

Model simplification for energy assessment: setting deterministic boundary conditions

[Wauman et al., 2015]

Striving towards a more energy efficient building stock, ambitious energy performance objectives are set for all building types. The Belgian building energy calculation code (EPR) used to check these pre-set energy performance levels imposes a standardised calculation procedure and uses standardised boundary conditions and input data allowing for an objective evaluation and mutual comparison of various building designs. To obtain realistic and representative assessment results for the energy performance of the building designs, these standardised input data must accurately represent the typical characteristics and use of the calculated buildings. Specific boundary conditions for schools are however often unavailable or inaccurate which affects the outcome of the calculations. Therefore, throughout this chapter, typical input data for schools and their ranges as currently applied in different calculation standards are studied. The impact of the variations of the input on the energy demand calculations is demonstrated in an uncertainty analysis (UA) using the Monte Carlo analysis method (MCA) combined with the Latin Hypercube Sampling technique (LHS). Afterwards, a sensitivity analysis (SA) is done, using the method of Morris, to determine the relative importance of each investigated boundary condition and to depict the predominant input parameters. Once the most dominant boundary conditions are determined, surveys are performed in a large sample of Flemish schools to obtain exact information on typical Flemish school's use which is then used as a reference, wherever necessary, to set new, more realistic boundary conditions to be used in the context of building energy regulation.

4.1 Introduction

Building energy assessment methods used in a regulatory context impose a calculation procedure under restricted and predefined conditions to check preset energy performance levels. To guarantee objective, unambiguous and comparative performance evaluation results, a range of standardised boundary conditions and input data are used for the calculation. Deterministic values for amongst others operational schedules, ventilation characteristics and internal heat gains are found in the related calculation procedure's manuals. These values are however not always accurate as some of the semi-empirical data that are used are outdated due to current changes and trends (*i.e.* occupant density rates vary in time, user's schedules may changes due to the shift towards 'Open schools' [36]). Furthermore, the values that are currently used might not be realistic as they are based on information in international standards [37] while real boundary conditions often depend strongly on national or regional customs (*i.e.* school opening hours differ strongly between various countries or regions). Finally, the data might be too general as some values are set for a general category of buildings (*i.e.* non-residential buildings) instead of for a specific building typology (*i.e.* offices, schools, etc.).
The aforementioned inaccuracies of the input data and boundary conditions jeopardize the reliability of the outcome of the calculation results as investigated in various research studies [172, 173, 174, 175]. Dewit [172] and Macdonald [173] designate default (semi-)empirical parameters and abstractions as a significant factor of uncertainty of the energy performance assessment results. Hereby, they refer mostly to the inability of the (simplified) methods to represent accurately the occupancy and activity related boundary conditions [173] and the exact implementation of the use of the building and the underlying physical processes [172, 173]. Likewise, Kim et al. [174] indicated non-realistic model simplifications and assumptions regarding HVAC systems and control strategies as a plausible reason for inaccuracy of the energy performance assessment. Clevenger and Haymaker [175] estimated that due to the oversimplification of the modelling input data the uncertainty on the energy performance of non-residential buildings ranges from 10 to *40%*.

To achieve the goals of the EPB Directives however, accuracy and reliability of the energy performance assessment results are crucial. In addition, since the calculation methods are used for cost-optimal studies performed in the context of EPBD [24, 25], the results should be as accurately as possible to avoid inaccurate cost-optimal solutions and inefficient hierarchies of energy efficiency measures which affect in turn the evolutions and trends on the building market [26]. To that end, well-considered deterministic default values and standardised input data, specifically adapted to the typology and use of the building, are needed. Several researches on (the impact of) boundary conditions in residential buildings [176, 177, 178, 179, 180], offices [181, 182, 183, 184] or commercial buildings [176] can be found. Research on boundary conditions specifically for (Flemish) schools [185, 175] is however rare. Therefore, a set of representative boundary conditions specifically for schools is determined in this chapter. Values for (heating) schedules, control systems, use of artificial lighting and equipment, ventilation characteristics and internal heat gains are studied. Overall uncertainties related to material properties, construction characteristics and weather data are however not addressed in this research study as they are not specifically linked to the use of schools and are therefore beyond the scope of this study.

First, the methodology used for the uncertainty and sensitivity analysis performed along this chapter is described in *§ 4.2*. Second, the building simulation models used for this study are presented in *§ 4.3*. Third, the boundary conditions which are studied are summarised and scrutinized in *§ 4.3.3*. Likely variations are defined by setting the probability distribution functions and ranges based on data found in different calculation standards and similar research studies. Subsequently, these probability functions are assigned to the building models and the responses of the buildings to the input data perturbations are studied. In doing so, an uncertainty analysis through a Monte Carlo analysis is performed in *§ 4.4.1*. Afterwards, a sensitivity analysis is done, using the method of Morris, to determine the relative importance of each investigated boundary condition and to reveal the predominant parameters (*§ 4.4.2*). Once the most dominant boundary conditions are determined, surveys are performed to gather representative on-site data on which the set of new, representative, deterministic boundary conditions are based (*§ 4.5*).

The results presented in this chapter are the results of the participation in a research study '*Development of the specific boundary conditions for schools built by the passive house standard*' by Flemish government order, *i.e.* Agency for School infrastructure (AGIOn) [186]. Note that the deterministic boundary conditions as set throughout this chapter are determined to be (strictly) used in a regulatory context and are therefore chosen to be representative for the whole (school) building stock. The use of these boundary conditions will not automatically lead to a better agreement between the predicted and real energy use of a specific case study. Moreover, as this work focuses on schools in Flanders in particular, the deterministic boundary conditions which are presented are only valid for Flemish schools.

4.2 Uncertainty and sensitivity analysis techniques

Uncertainty analysis (UA) and sensitivity analysis (SA) are frequently used for building energy analysis purposes. They are used for parameter uncertainty assessment in building simulations [173, 187, 179, 188], are commonly used for decision support [189, 190] or are necessary tools for building design optimisation [191, 125].
Various uncertainty and sensitivity analysis techniques can be found. Among all these techniques, one must be chosen which is specifically appropriate for this research purpose (= parameter identification and factor prioritisation). Saltelli [192] distinguishes two overall classes of sensitivity analysis: the local and the global analysis methods. For the local analysis methods, the variables or parameters are varied one at a time by a small amount around some fixed point and the effect on the output for each of the parameters is calculated separately. For the global sensitivity method on the contrary, the global effect of all input parameters is studied. Previous (more or less) similar research studies show that both the local [181, 179, 172, 178, 177] and the global method [189, 180, 182, 172, 178, 177] are commonly used for uncertainty and factor prioritisation purposes. For the UA performed along this chapter, the global method is selected as it is the purpose to assess the global effect of all investigated boundary conditions. From the global methods, the Monte Carlo Analysis method (MCA) is chosen as it estimates the overall uncertainty in the energy demand calculations due to all the uncertainties in the input parameters regardless of the interactions and quantity

of the included parameters [173]. The MCA is performed by carrying out the following consecutive steps: **(i)** selection of a range and distribution for each input parameter, **(ii)** sample generation from these distributions, **(iii)** performance of an energy calculation for each element of this sample and **(iv)** assessment of the uncertainty of the output. For the sample generation the Latin Hypercube sampling (LHS) technique is used. This sampling technique is more effective compared to random sampling as it ensures full coverage of the whole range of each variable [192]. To that end, the range of each variable is divided in equally probable intervals and one value is randomly selected from each of these intervals [192]. The sampling is done using the SimLab tool [193].
Although the MCA method can also be used for SA purposes, the local SA technique of Morris [194] is preferred for the SA purposes as the indicators for sensitivity used in the MCA method assume near-linearity of the model. Variable independency and linearity of our model can however not be guaranteed, hence the screening method of Morris, also referred to as the one-variable-at-a-time (OAT) method [194], is chosen as the alternative. The Morris method can be characterised as a screening method with global characteristics [192]. The global sensitivity is considered as the influence of the whole range of variation of the input parameters X which is described by a probability distribution F_i . By varying the input parameter set, the 'effect' of each 'element' is then calculated using *Eq. 4.1*.

$$EE_i = \frac{Y(X_1, X_2, ..., X_{i+\triangle}, ..., X_k) - Y(X_1, X_2, ..., X_k)}{\triangle} \tag{4.1}$$

Two sensitivity measures μ and σ which are respectively the estimates of the mean and the standard deviation of the distribution F_i of the elementary effects, are used to assess the sensitivity of each investigated parameter [195]. Campolongo et al. [196] proposed adding the use of μ^*, which is defined as the estimate of the mean of the distribution of the absolute values of the elementary effects. The regular mean μ has the drawback that if the distribution F_i contains negative elements, some effects may cancel each other out.

When assessing the uncertainty and sensitivity of energy demand calculations, Furbringer and Roulet [197] and Macdonald [173] state that the number of calculations that must be performed to obtain reliable results of the uncertainty analysis is independent of the number of input parameters. According to the same researchers [197, 173], 80 simulations suffice for each building model to assess to impact of the investigated parameters.

4.3 Building Simulation Model

4.3.1 Building description

The reference school buildings as set in *Chapter 2* are used for the UA and SA. Detailed information on the size or shape of the buildings can be found in *§ 2.2.1*. As the results of this study need to be representative for all educational forms, both the reference school buildings for the elementary and secondary education are used. Furthermore, both built forms (*i.e.* rectangular and U-shape) are included. The four selected school buildings are subsequently combined with a range of construction and building envelope related characteristics. As the building properties themselves however are not

the subject of the study but are considered only to guarantee robustness of the results of the UA and SA, a pragmatic approach is used: the thermal capacity, the energy performance level (*i.e.* insulation and air tightness level) of the building envelope and the window-to-wall ratio (WWR) are discretely varied between a lower and an upper limit.

Building characteristics

In Flanders, school buildings with heavy and light structures are found (see *§ 2.3.2*) so both construction types are considered along this study. For the heavy building variants all external and internal building components are assumed heavy whereas for the light building variants light roofs and (external and internal) walls are assumed (see *Table 4.1*).

Table 4.1: Composition of the opaque structural elements (from front/inside to back/outside), based on the design of an exemplary, passive school building project at KU Leuven campus Ghent.

	material	λ, W/(m.K)	c, J/(kg.K)	ρ, kg/m^3	thickness, m
roof (light)	gypsum board	0.24	1000	750	0.012
	mineral wool (MW)	0.04	1030	50	according to energy performance level
	OSB	0.13	1700	650	0.018
	EPDM	0.25	1000	1150	0.002
roof (heavy)	plaster finish	0.52	1000	1300	0.01
	heavy concrete	1.7	1000	2400	0.15
	light concrete	0.32	1000	1050	0.1
	PUR	0.03	1400	30	according to energy performance level
	Bitumen	0.23	1000	1100	0.002
external wall (light)	gypsum board	0.24	1000	750	0.012
	OSB	0.13	1700	650	0.015
	MW	0.04	1030	50	according to energy performance level
	wood fibreboard	0.5	2100	24	0.018
external wall (heavy)	plaster finish	0.52	1000	1300	0.01
	brickwork	0.54	1000	1550	0.14
	PUR	0.03	1400	30	according to energy performance level
floor	tiles	1.2	840	2300	0.01
	light concrete	0.32	1000	1050	0.1
	PUR	0.03	1400	30	according to energy performance level
	heavy concrete	1.7	1000	2400	0.15
	bitumen	0.23	1000	1100	0.002
internal wall (light)	gypsum board (2 x)	0.24	1000	750	2 x 0.012
	MW	0.04	1030	50	0.14
	gypsum board (2 x)	0.24	1000	750	2 x 0.012
internal wall (heavy)	plaster finish	0.52	1000	1300	0.01
	brickwork	0.54	1000	1250	0.14
	plaster finish	0.52	1000	1300	0.01
intermediate floor (light)	linoleum	0.623	1400	1200	0.003
	OSB	0.13	1700	650	0.018
	wood fibreboard	0.055	2100	24	0.03
	MW	0.062	1030	50	0.2
	gypsum board	0.24	1000	750	0.012
intermediate floor (heavy)	tiles	1.2	840	2300	0.02
	chape	1.35	840	1000	0.1
	PUR	0.03	1400	30	0.03
	heavy concrete	1.73	1000	2400	0.04
	hollow core concrete slab	0.92	840	1500	0.12

To study the impact of the energy performance level of the building envelope, the global insulation level and the air tightness level are varied discretely between an upper limit (= the 'base case' variant corresponding to the legal required limits applicable on the date of the start of this research

(dd.2010 [18]) and a lower limit (= the 'best practice' variant based on the design guidelines for passive school buildings [117]). As glazing with a U-value higher than 1.1 W/(m^{2}K) is rarely used in Belgium nowadays, this U-value is considered as the upper limit. The g-value of the glazing is 0.6. The upper limit for the infiltration rate n_{50} is set equal to 3 ACH, in conformity with the minimum air tightness level required by *NBN−D50−001−1* [120] for buildings using a mechanical ventilation system.
The range of the WWR is based on day-lighting and visual comfort requirements: the WWR is at least 20% [97] but does not exceed 40% [66, 121, 97], and consequently covers more than 75% of the surveyed school buildings (see *Figure 2.11*). To guarantee good summer comfort, external shading is provided by automatically controlled screens. A simplified shading device control strategy ($q_{control}$ = threshold of total solar radiation on the surface when blinds are closed or opened) is applied using an operational hysteresis (250 W/m^2 closing - 150 W/m^2 opening) to promote stability. In case the blinds are closed, 70% of the total solar radiation on the shaded surface is blocked[1]. North-facing windows are not provided with a shading device. Shading due to external obstacles like window overhangs, trees or surrounding buildings is not modelled for simplicity reasons, except for the U-shaped building where shading caused by the side wings is taking into account.

HVAC system characteristics

Heating and cooling is provided by an ideal, all-air system, controlled according to the regular school opening hours. After school, during weekends and holidays a setback temperature of 12°C and 30°C is assumed for heating and cooling, respectively. Due to the high requested ventilation rates in class rooms, all school building variants are applied with a mechanical ventilation system. As the impact of changing boundary conditions might differ however in schools with or without a heat recovery device, the UA and SA are performed for two different ventilation systems. The 'base case variants' are equipped with a simple extraction ventilation system. The 'best practice variants' have a balanced mechanical ventilation provided with an air-to-air heat exchanger with an efficiency of 75%. The air supply is provided into the constantly occupied rooms (*e.g.* class rooms, gyms, offices). The size of the ventilation systems and applied ventilation rates are determined in relation to the design occupancy rate of the building('s zones). The operation of the fans is however controlled by a time schedule according to the school opening hours, hence likely deviations of the real occupancy rates (*i.e.* due to absence of students or outdoor classes) do not affect the ventilation rates.

Combining all these building and system's characteristics, a selection of 32 building design variants is determined. Each school building design variant represents one non-specific, yet typical, Flemish school building. 16 design variants are set for the elementary (E) and for the secondary reference school building (S), respectively. An overview of all design variants is depicted in *Table 4.2*.

[1] Along this dissertation, it is opt to model the solar shading independent of the angle of incidence of the solar radiation and hence as a reduction of the g-value of the glazing, in line with the *quasi-steady-state* calculation approach.

	geometry	capacity	WWR %	U_{wall} W/(m^2.K)	U_{floor} W/(m^2.K)	U_{roof} W/(m^2.K)	$U_{glazing}$ W/(m^2.K)	n_{50} ACH
E/S_base_1	R	heavy	20	0.37	0.37	0.29	1.1	3.0
E/S_base_2	R	light	20	0.37	0.37	0.29	1.1	3.0
E/S_base_3	R	heavy	40	0.37	0.37	0.29	1.1	3.0
E/S_base_4	R	light	40	0.37	0.37	0.29	1.1	3.0
E/S_base_5	U	heavy	20	0.37	0.37	0.29	1.1	3.0
E/S_base_6	U	light	20	0.37	0.37	0.29	1.1	3.0
E/S_base_7	U	heavy	40	0.37	0.37	0.29	1.1	3.0
E/S_base_8	U	light	40	0.37	0.37	0.29	1.1	3.0
E/S_best_1	R	heavy	20	0.15	0.15	0.15	0.8	0.6
E/S_best_2	R	light	20	0.15	0.15	0.15	0.8	0.6
E/S_best_3	R	heavy	40	0.15	0.15	0.15	0.8	0.6
E/S_best_4	R	light	40	0.15	0.15	0.15	0.8	0.6
E/S_best_5	U	heavy	20	0.15	0.15	0.15	0.8	0.6
E/S_best_6	U	light	20	0.15	0.15	0.15	0.8	0.6
E/S_best_7	U	heavy	40	0.15	0.15	0.15	0.8	0.6
E/S_best_8	U	light	40	0.15	0.15	0.15	0.8	0.6

Table 4.2: Representation of the contemporary Flemish school building stock: an overview of variations of the characteristics of a sample of 32 representative school building design variants. The base and best case variants refer to the type of ventilation system coupled to the building.

4.3.2 Building energy assessment tool and building simulation model

To assess the uncertainty and sensitivity of the energy demand calculation results, monthly, *quasi-steady-state* calculation methods have some decisive restrictions. Dynamic phenomena such as users' behaviour are simplified and values for amongst others occupant density or internal heat gains are monthly averaged. Therefore, as these phenomena can be implemented in a more realistic way in a dynamic calculation tool, the UA and SA are performed in TRNSYS.
For the building modelling, the floor plans of the reference school buildings as depicted in *Figure 2.6* and *Figure 2.8* are slightly simplified (see *Figure 4.1*).

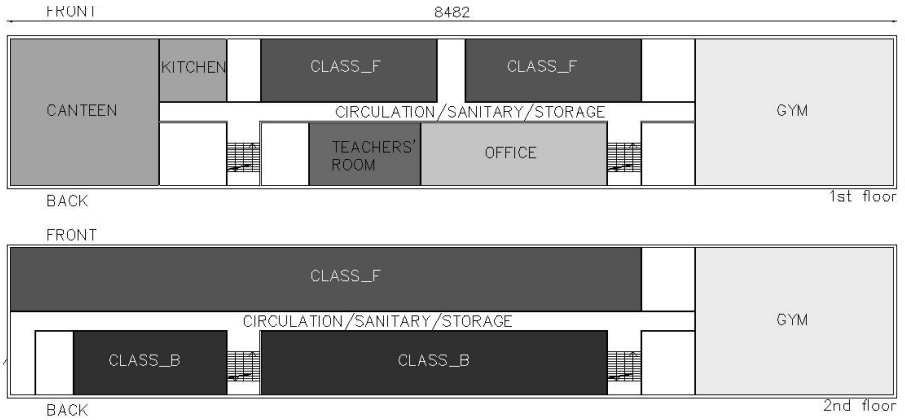

Figure 4.1: Example of the simulation model as implemented in TRNSYS used for the rectangular, reference school building for elementary education.

The building is modelled as a multi-zone building. To avoid excessive complexity of the simulation model and to limit the related calculation time, the number of included zones is limited to seven. Rooms with similar internal heat load patterns and equal schedules for heating, cooling or ventilation are united within a same zone: the class zone 1 (**F**ront) and 2 (**B**ack) (*i.e.* the zone that combines all individual class rooms is split into two separate zones depending on the orientation of the class rooms), the office zone that combines all individual offices, the teachers' room, the canteen and kitchen, the gym, and the combined zone for circulation, storage and sanitary. Although the class zones and administrative zone consists in reality of various individual class rooms and offices, no further subdivision of each of these zones is made to limit the number of zones and related simulation time. After all, it can be supposed that in schools the typical thermal behaviour of the various rooms is more or less similar. Occupancy rates and operational schedules are rather constant during the whole school year and nearly identical for all class rooms.
All considered school building models are assumed to be oriented with the main axis along the East-West direction. The thermal behaviour of the building models is simulated with a time step of 15 min. The generation of the various simulation files is done in MATLAB automatically coupling the input data to the TRNSYS tool. The output considered is the energy demand for heating (October - May) and cooling (May - October), normalised to the building floor area.

4.3.3 Activity and users' behaviour related boundary conditions

This section discusses the uncertainty interval of the input parameters specifically related to the typology and the use of school buildings. Representative distribution functions and ranges for (heating) schedules, control systems, use of artificial lighting and equipment, ventilation characteristics and internal heat gains for schools are set. Depending on the type and the source of uncertainty of each investigated input parameter, a specific but representative probability distribution function is selected.
According to Macdonald [173], normal distribution functions are mostly appropriate for expressing measured physical data (*e.g.* temperatures). Log-normal functions should be used for defining variables that exists of a combination of two or more normally distributed parameters such as infiltration rates or metabolic rates while triangular functions are more suitable to describe varying parameters with a clear minimum, maximum and most likely value such as occupant density rates [173]. For the investigated boundary conditions that cannot be classified into one of the aforementioned categories, uniform distribution functions are used as these are mostly suitable for assessing the impact of modelling simplifications (= systematic errors) [198, 173]. Overall, the ranges of the parameters included in the UA and SA are based on the values as currently applied in different (energy calculation) standards which are reviewed and described elaborately in *§ 2.3.1*.

Operational schedule: in Flanders, the school year starts on 1 September and ends on 30 June. 1 July up to and including 31 August the school is closed due to summer holiday. Lessons are evenly spread over five days from Monday to Friday. Wednesday afternoon is free. Generally, a school day starts at 8h30 and ends at 16h in nursery and primary school. In secondary school, depending on the type of education, school ends at 17h. In addition to summer holidays and weekends, schools are closed during 37 vacation days: 5 days in January, 3 at the end of February and 2 at the be-

ginning of March, 12 in April, 3 in May, 1 in June, 3 in October, 2 in November and 6 in December. This results in ± 1200 annual operating hours which is considerably less than offices which are on average about 2600 hours per year in use [199, 200].
Aside from the school opening hours, (frequently occurring) play breaks and (occasional) outdoor classes or meetings must be accounted for as these result in a change of the internal heat load pattern. To do so, correction factors are introduced expressing the part-time operation of a certain room type during a usage day. The relative absence factors (RA) for class rooms (75%), for offices (70%) and for teachers' rooms (50%) as defined in *DIN V 18599* [43] are used as a reference. As additional information on the range and distribution of the RA-factors is not available, the values are assumed to be uniformly varying within a ± 10% range [173], as depicted in *Table 4.3*.

Set-point temperature,* °*C: overall information on (set-point) temperatures for heating or cooling in schools as found in design and calculation standards is summarised in *Table 2.7*. Due to the significant differences in (heating) comfort requirements in gymnasia or sport halls compared to other room types (see *Table 2.7*), two separate temperature categories are considered for the UA: **(i)** heating set-point temperature variations for rooms with a sports function, for which the average set-point for heating is set to be 17°C and **(ii)** heating set-point temperature variations for all other rooms, for which the average set-point for heating is set to be 21°C. For cooling, the average set-point is set equal for all rooms (= 25°C) [47].
For the UA, the ranges of the set-point temperatures are based on the lower and upper limit of respectively the lowest and highest thermal comfort class as defined in standards *ISO 7730* [48], *EN 15251* [47] and in [96]. Due to the physical nature of the parameter, a normal distribution function is selected [173] as shown in *Figure 4.2*.

Although the set-point temperature ranges and the distribution functions are set equal for most of the rooms - except for the gym in case of heating - the set-point temperature variation samples used for the UA are defined for each included building zone (*i.e.* class room, office, teachers' room, canteen and kitchen and combined area for circulation, storage and sanitary) separately. This allows on the one hand the simulation of the effect of limited inter-zonal temperature control differences.

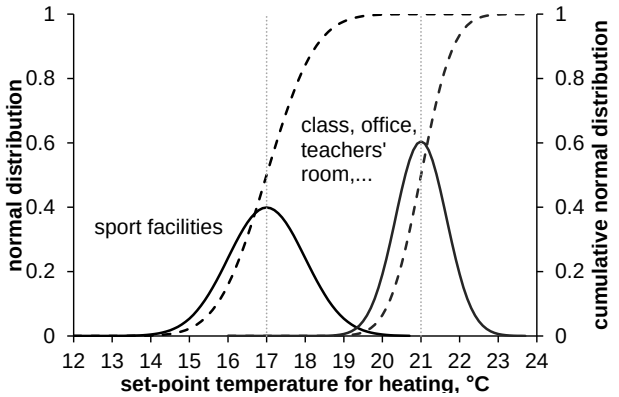

Figure 4.2: Normal distribution (full line), cumulative normal distribution (dashed line) and mean values (dotted line) of the set-point temperature for heating for different school room types as used for the UA.

On the other hand, as all other parameter variations are defined for each zone separately, potential overestimation of the impact of the set-point temperature is avoided.

Occupant density, m^2/pers: variations of the occupant density affect both the internal heat gains and the design ventilation flow rates and must therefore be taken into account in the UA and SA. According to Macdonald [173], the triangular distribution function is mostly appropriate to describe occupancy variations. The minimum, maximum and most frequent values (mode) for the various room types as used for the UA and SA are set based on the specific values as summarised in *Table 2.8*. Values used for the UA and SA are depicted in *Table 4.3*.

Ventilation rate, m^3/(pers.h): the Flemish EPBD [18] requires at least a moderate indoor air quality (IDA3 - *EN 13779*) in schools. Survey results have revealed (see *§ 2.4.2*) that these minimum IAQ requirements are generally considered as maximum design recommendations for the installed ventilation system. Consequently, the considered variations of the ventilation rates for the UA and SA fall within the IDA3 class limits with the mean value set equal to the default value for IDA3. For the determination of the ventilation rates in school buildings, it is assumed that no smoking is allowed and that the buildings are very low polluting. The mean ventilation rates for the kitchen and lab are set equal to 80 m^3/m^2 [108] and to 720 m^3/m^2 per m^2 opening of fume hood [95], respectively. For those rooms where a higher level of activity is found and consequently the CO_2 production of the users is increased, the mean ventilation rates as set according to *EN 13779* [13] are increased in relation to the activity level (*e.g.* gym = 1.8 met, lab = 1.5 met). To assess the uncertainty and sensitivity, hygienic air flow rates are uniformly varied between $\pm$ 10% of the mean values [188].
Furthermore, as intermittent ventilation is applied, each room must be pre-ventilated prior to the school start to guarantee good indoor air quality at any time of occupancy. According to *EN 15251* [47], a one-hour preliminary purge ventilation of two air volumes of the ventilated room or equivalent is required to the room before occupancy.

Internal sensible heat gains, W/pers or W/m^2: this study focuses in particular on the assessment of the uncertainty and sensitivity of the internal heat gains related to the use of schools. The uncertainty related to the sensible heat emission of people, equipment and lighting is hence beyond the scope of this research.
(i) ***Occupant, W/pers***: as the uncertainty of sensible heat emission is not studied in this chapter, the variations of the heat gains due to occupants are only related to variations of the occupant density as described previously. Values for the heat emission due to occupants as found in (inter)national standards (see *Table 2.10*) are however slightly adapted to the Flemish school system. In line with the calculation standard *DIN V 18599* [43], two separate categories of internal heat gains due to occupants are defined based on the age of the occupants: **(i)** < 12 years old = 60 W/pers (*i.e.* representative for students for the Flemish elementary schools) and **(ii)** > 12 years = 80 W/pers (*i.e.* representative for (young) adults such as students of secondary schools or teachers). Additionally, a slight increase of the heat gains is foreseen for certain (teaching) activities due to increased physical activity: $q_{IHG,occ}$ = 100 W/pers in the kitchen and lab (1.5 met) and $q_{IHG,occ}$ = 125 W/pers in the gym (1.8 met).

(ii) ***Equipment, W/m***^{2}: the source of uncertainty of load intensities is mostly related to the specifications and usage of the equipment. According to Saltelli [195], triangular probability distribution functions are mostly suitable to express these variations. The minima, maxima and modes of the triangular distribution functions used for the UA and SA are based on information found in *DIN V 18599* [43] and *NEN 2916* [99] (see *Table 2.10*). For those room types where no information is found on the range of internal heat gains due to equipment, the ranges are set to be $\pm$ 10% [173].
(iii) ***Lighting, W/m***^{2}: lighting is modelled as a function of the installed lighting power and requested illuminance. The upper limit of the variations considered for the UA and SA is set equal to the minimum required normalised power density in class rooms which is 2.5 W/(100 lux.m^2) [201]. The lower limit (= 1.5 W/(100 lux.m^2)) is based on the guidelines for low energy non-residential buildings [117] (see *Table 2.11*). A triangular distribution function is used to express the variability [173].
As most internal heat gains occur during school activities, their occurrence is linked to the school users' profile. All internal heat gains are hereby assumed constant over the time they occur. As however equipment and lighting are often only part of the occupied time in use, a partial operational time factor (POF) is introduced in line with *DIN V 18599* [43]. This factor is calculated as the fraction of the total operational time that equipment or lighting are effectively used. Reference values are found in the related standard [43] and are summarised in *Table 4.3* for the different considered school zones. As no additional information on the partial operational time factors is found in literature, the ranges are set to be $\pm$ 10% and a uniform distribution function is used to express the variability [173].

An overview of all the investigated boundary conditions including their ranges and the characteristics of their probability functions is depicted in *Table 4.3*.

Table 4.3: Overview of the uncertainty of the operational and activity related boundary conditions in school buildings.

	boundary condition	unit	pdf	range
BC1	$\Theta_{i,H,set,class}$	°C	N	μ = 20, σ = 0.66
BC2	$\Theta_{i,H,set,office}$	°C	N	μ = 20, σ = 0.66
BC3	$\Theta_{i,H,set,canteen}$	°C	N	μ = 20, σ = 0.66
BC4	$\Theta_{i,H,set,lab}$	°C	N	μ = 20, σ = 0.66
BC4	$\Theta_{i,H,set,gym}$	°C	N	μ = 17, σ = 1.00
BC5	$\Theta_{i,C,set,class}$	°C	N	μ = 25, σ = 0.66
BC6	$\Theta_{i,C,set,office}$	°C	N	μ = 25, σ = 0.66
BC7	$\Theta_{i,C,set,canteen}$	°C	N	μ = 25, σ = 0.66
BC8	$\Theta_{i,C,set,lab}$	°C	N	μ = 25, σ = 0.66
BC9	$\Theta_{i,C,set,gym}$	°C	N	μ = 25, σ = 0.66
BC10	occupant density, class	m^2/pers	T	min = 5.0, max = 2.0 , mode = 2.5
BC11	occupant density, office	m^2/pers	T	min = 20.0, max = 8.0 , mode = 14.0
BC12	occupant density, teachers' room	m^2/pers	T	min = 5.0, max = 2.0 , mode = 3.0
BC13	occupant density, canteen	m^2/pers	T	min = 3.5, max = 0.8 , mode = 1.5
BC14	occupant density, kitchen	m^2/pers	T	min = 9.0, max = 11.0 , mode = 10.0
BC15	occupant density, lab	m^2/pers	T	min = 4.6, max = 5.4 , mode = 5.0
BC16	occupant density, gym	m^2/pers	T	min = 30.0, max = 10.0 , mode = 20.0
BC17	ventilation rate	m^3/(pers.h)	U	29 ± 10%
BC18	ventilation rate, kitchen	$m^3/(m^2.h)$	U	80[1] ± 10%
BC19	ventilation rate, lab	$m^3/(m^2.h)$	U	720[2] ± 10%
BC20	IHG due to equipment, class	W/m^2	T	min = 2.0, max = 6.0 , mode = 4.0
BC21	IHG due to equipment, office	W/m^2	T	min = 3.0, max = 15.0 , mode = 10.0
BC22	IHG due to equipment, teachers' room	W/m^2	T	min = 2.3, max = 2.8 , mode = 2.5
BC23	IHG due to equipment, canteen	W/m^2	T	min = 1.0, max = 3.0 , mode = 2.0
BC24	IHG due to equipment, kitchen	W/m^2	T	min = 72.0, max = 88.0 , mode = 80.0
BC25	IHG due to equipment, lab	W/m^2	T	min = 9.0, max = 11.0 , mode = 10.0
BC26	installed lighting power density,	$W/(m^2.lux)$	T	min = 1.5, max = 2.5 , mode = 2.0
BC27	relative absence factor, class	-	U	0.25 ± 10%
BC28	relative absence factor, office	-	U	0.30 ± 10%
BC29	relative absence factor, teachers' room	-	U	0.50 ± 10%
BC30	partial operational factor, equipment class	-	U	0.70 ± 10%
BC31	partial operational factor, equipment office	-	U	0.50 ± 10%
BC32	partial operational factor, equipment teachers' room	-	U	0.35 ± 10%
BC33	partial operational factor, equipment kitchen	-	U	0.70 ± 10%
BC34	partial operational factor, equipment lab	-	U	0.80 ± 25%
BC35	partial operational factor, lighting class	-	U	0.90 ± 10%
BC36	partial operational factor, lighting office	-	U	0.70 ± 10%
BC37	partial operational factor, lighting teach	-	U	0.95 ± 10%
BC38	partial operational factor, lighting canteen	-	U	0.95 ± 10%
BC39	partial operational factor, lighting lab	-	U	0.95 ± 10%
BC40	partial operational factor, lighting gym	-	U	0.95 ± 10%

[1] *extra ventilation in the kitchen due to heat producing cooking activities is foreseen during* 50% *of the time* .

[2] *extra ventilation per surface area of the fume hood* .

4.4 Results

4.4.1 Uncertainty analysis

In this section, the results of the UA are discussed. *Figure 4.3* (a) to (f) demonstrate the impact of the uncertainty of the input data on the heating $Q_{H,nd}$ and cooling demand $Q_{C,nd}$ for the 'base case' and for the 'best practice' variants, and for the elementary and secondary school design building variants, respectively. As the cooling demand in the 'base case' design variants is practically non-existing (on average < 2 kWh/(m^2.a)), only the heating demand is discussed for these building variants. Cumulative normal distribution functions are used to show the variance of the energy demand due to the perturbations of the investigated boundary conditions as set in *Table 4.3*. The values on the y-axis indicate the likelihood that a value less than or equal to the value on the x-axis occurs. The smaller the spread on the x-axis, the more certain the result.

According to Macdonald [202], given the number of simulations performed for this study, the uncertainty of the output of the MCA can be expected to be normally distributed irrespective of the probability distributions used for the input data. To confirm this expectation, the normality plots for the heating $Q_{H,nd}$ and cooling demand $Q_{C,nd}$ of the rectangular reference elementary school building design variants are depicted in *Figure 4.4*. The figure confirms - aside from a small deviation at the low and high end of the curve of the 'base case' variant which will be explained later - a Gaussian distribution of the output results. As the plots for all other building variants show similar results, it can be guaranteed that 95% of the variations of the output are found in the confidence interval defined as the mean plus and minus two times the standard deviation as depicted in *Table 4.4*.
For the 'base case' school building design variants, this results on average in a spread of the heating demand of more than 30%. For the 'best practice' variants variations up to more than 34% and 41% are found for the heating and cooling demand, respectively. All results clearly demonstrate the impact of the boundary conditions on the energy demand calculations and emphasise the need for accurate values to be used as an input for the energy performance calculation methods.

To assess the robustness of the UA, the results for the 'base case' and 'best practice' variant of the rectangular, reference building for elementary schools with varying thermal capacity (see *Figure 4.5*

Table 4.4: Impact of varying BC's on the energy demand (95% confidence interval) for all considered building variants.

	Rectangular				**U-shape**			
	WWR=20%		**WWR=40%**		**WWR=20%**		**WWR=40%**	
kWh/(m^2.a)	**heavy**	**light**	**heavy**	**light**	**heavy**	**light**	**heavy**	**light**
$\mathbf{Q}_{H,nd,E,base}$	48.4±6.9	45.4±6.6	47.4±6.9	44.6±6.5	47.7±6.9	45.3±6.6	47.4±6.9	45.0±6.6
$\mathbf{Q}_{H,nd,S,base}$	42.4±6.7	40.1±6.3	41.4±6.7	39.3±6.3	48.6±7.9	46.0±7.5	48.2±7.9	45.7±7.4
$\mathbf{Q}_{H,nd,E,best}$	11.1±1.8	10.3±1.6	11.4±1.7	10.7±1.6	11.1±1.7	10.2±1.6	12.0±1.8	11.1±1.6
$\mathbf{Q}_{H,nd,S,best}$,	6.4±1.2	6.1±1.1	6.9±1.2	6.7±1.2	8.9±1.5	8.4±1.4	10.0±1.5	9.4±1.4
$\mathbf{Q}_{C,nd,E,best}$	5.3±1.5	5.3±1.4	11.0±1.8	11.1±1.8	7.1±1.6	6.2±1.5	12.5±1.9	11.7±1.8
$\mathbf{Q}_{C,nd,S,best}$	7.9±1.7	8.1±1.8	13.1±2.1	13.5±2.1	8.6±1.7	8.3±1.7	13.9±2.1	13.6±2.0

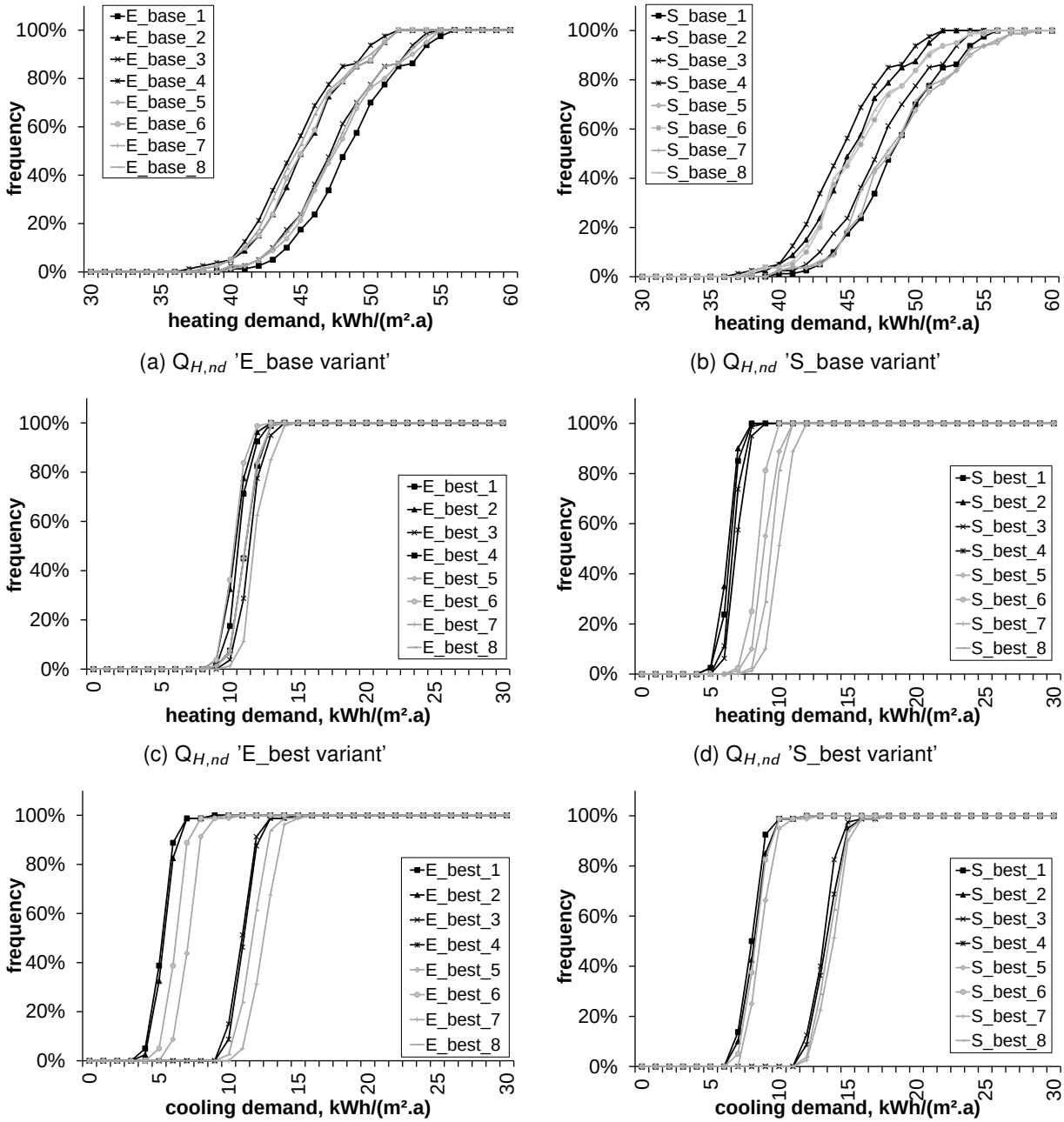

(a) $Q_{H,nd}$ 'E_base variant'

(b) $Q_{H,nd}$ 'S_base variant'

(c) $Q_{H,nd}$ 'E_best variant'

(d) $Q_{H,nd}$ 'S_best variant'

(e) $Q_{C,nd}$ 'E_best variant'

(f) $Q_{C,nd}$ 'S_best variant'

Figure 4.3: Results of the UA of the annual heating $Q_{H,nd}$ and cooling $Q_{C,nd}$ demands, all normalised to the building floor area (kWh/(m^2.a)) for 32 school building design variants expressed by cumulative normal distribution functions. The results of the rectangular building variants are marked in black, the results for the U-shaped school building are marked in grey.

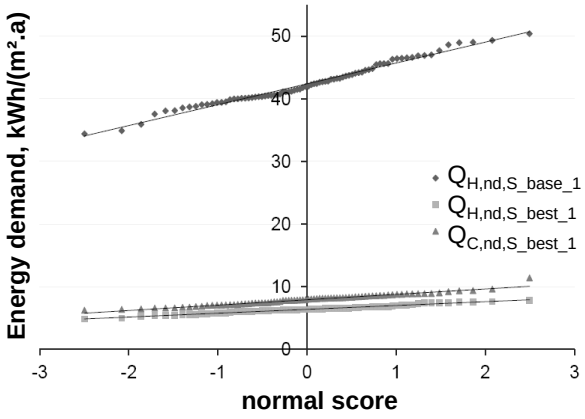

Figure 4.4: Normality plot

(a)), WWR (see *Figure 4.5 (b)*) and building geometry (see *Figure 4.5 (c)*) are shown by means of histograms and cumulative distribution functions. In conformity with the results of the normality check (see *Figure 4.4*), the plotted histograms in *Figure 4.5* (*a)* to *(f)* fit rather well to the Gauss curve. For the 'base case' variant, small deviations are found at ± 40 kWh/(m^2.a) and at ± 53 kWh/(m^2.a). This is caused by the fact that the heat demand in the 'base case' models is highly related to the transmission and ventilation losses. As a consequence, when both low ventilation rates and a low number of occupants are combined with low set-point temperatures for heating, exceptionally low heat demands occur. In the simulation sample used for this study, by chance, one such sample is generated combining a ventilation rate in class rooms of 26.8 m^3/(h.pers) with an occupant density rate of 3.8 m^2/pers and set-point temperatures for heating in all zones < 19.5°C, resulting in a (minimum) $Q_{H,nd}$ < 40 kWh/(m^2.a). On the other hand, all variants with a heat demand > 53 kWh/(m^2.a) are cases where extremely low occupant densities (< 2.3 m^2/pers) are combined with high set-point temperatures in classes (≥ 20.5°C) and high ventilation rates (> 31 m^3/(h.pers)) or high relative absence factors (> 0.8). This results in a peak at the high end of the curve, atypical for a Gauss curve. This sensitivity of the results is later in this chapter confirmed by the results of the sensitivity analysis (see *§ 4.4.2*). The results of the 'best practice' variant are less sensitive to these extremes due to the implementation of a heat recovery device and high energy efficient building envelopes, which explains the better fit to the Gauss curve.

Both the histograms in *Figure 4.5* and the values depicted in *Table 4.4* show that the spread on the results of the UA is generally not affected by the building characteristics. While varying the thermal capacity, the WWR's (affecting mostly the amount of incoming solar heat gains) or the building shape (affecting both the heat transfer due to a change of the heat loss surface and the amount of incoming solar heat gains due to extra shading caused by the side-wings in the U-shaped building) of the school models, the results of the UA remain more or less similar for all building variants (impact < 2.6%) and hence confirm robust UA results[2]. Further diversification of the building model based on construction and architectural characteristics is therefore not necessary for this specific research

[2]The orientation is not taken into account in the parameter analysis. The results of a restricted set of dynamic simulations, performed for the base (heavy structure) and best case (light structure) variant for the elementary school building model (R) with a WWR = 20 and 40%, show that the impact of the orientation on the results of the UA is restricted (impact < 0.7%).

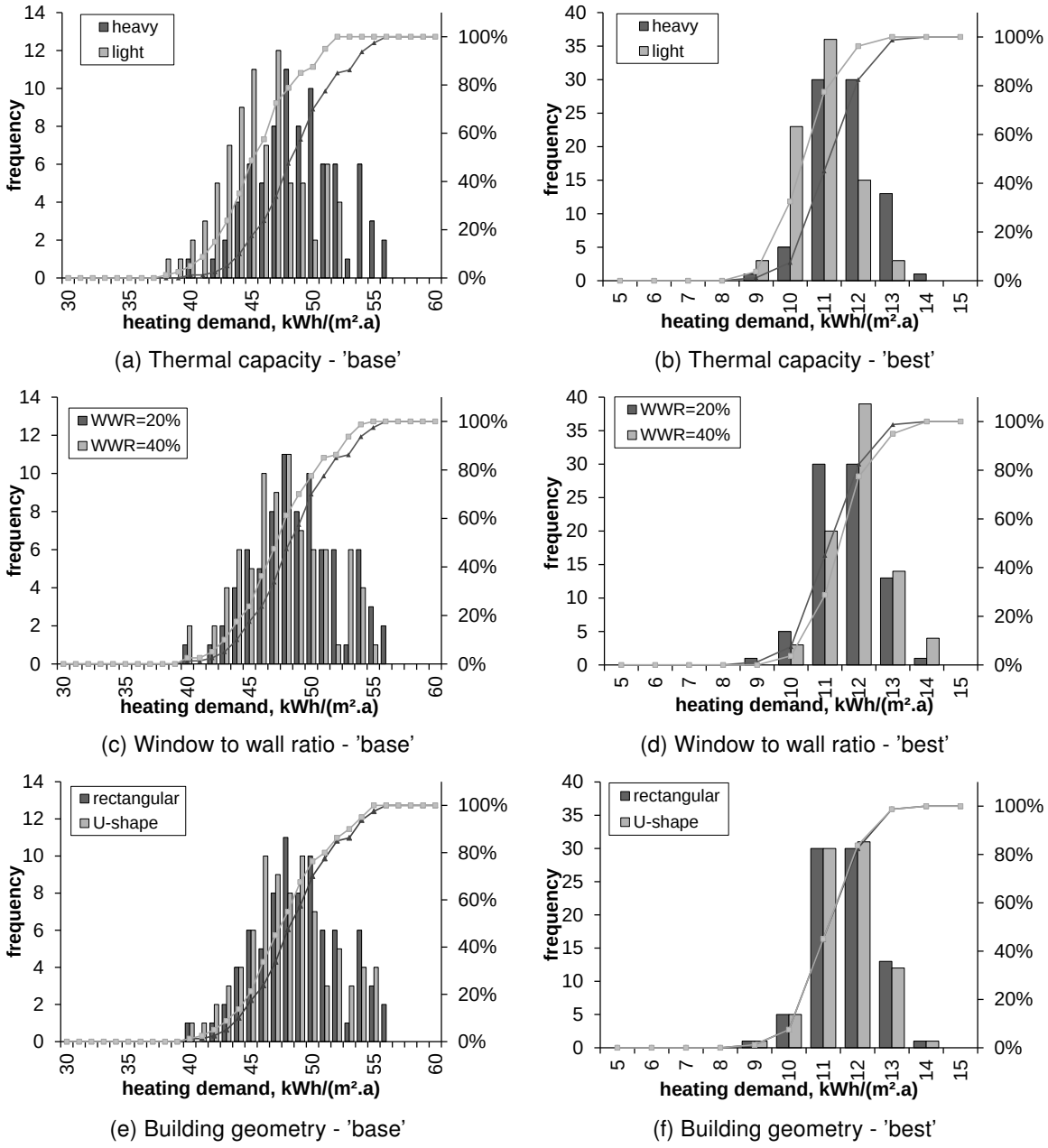

(a) Thermal capacity - 'base'

(b) Thermal capacity - 'best'

(c) Window to wall ratio - 'base'

(d) Window to wall ratio - 'best'

(e) Building geometry - 'base'

(f) Building geometry - 'best'

Figure 4.5: Assessment of the robustness of the uncertainty analysis: analysis of the impact of varying boundary conditions on the annual heat demand, normalised to the building floor area (kWh/(m^2.a)), of a rectangular elementary school building with varying building characteristics, expressed by histograms and cumulative distribution functions (%).

objective. Consequently, the results of the SA as presented in the next subsection, are discussed for the rectangular, elementary school building model only.

4.4.2 Sensitivity analysis

In this section, the results of the SA are discussed. The sensitivity of the energy demand due to each of the investigated boundary conditions is determined by the mean μ^* and the standard deviation σ of the elementary effects (see *Eq. 4.1*). A high mean μ^* indicates a large sensitivity. A high value of σ implies that the value of the elementary effect is strongly affected by the choice of the other factors' values or that the factor is nonlinear [195]. If both μ^* and σ are low, the impact of the investigated parameter is negligible.

The results of the SA are shown for the 'base case' ($Q_{H,nd}$ only, see *Figure 4.6* (a)) and the 'best practice' variants ($Q_{H,nd}$, see *Figure 4.6* (b), and $Q_{C,nd}$, see *Figure 4.6* (c)). To maintain clarity of the figure, only the five most influential parameters which cover 65 to 75% of the variations are named: the operational schedule expressed by the relative absence factor (RA_{class}), the set-point temperature for heating and cooling ($\theta_{i,H/C,set,class}$) and the use of equipment and lighting expressed by the internal heating gains (q_{IHG}) and the partial operational time factors (POF). These boundary conditions have the highest impact on the energy demand calculations and have the highest σ. Although small differences are found (see *Figure 4.6*) between the different building variants on the one hand and between the results for the heating and cooling demand on the other hand, the main trend is similar. In general, the operational schedule and related occupant attendance, and user's profiles can be considered as the most dominant parameters followed by the set-point temperature for heating/cooling. Similar results were found by Demanuele et al. [185] and Clevenger et al. [175], both stressing the substantial impact of the highly variable and unpredictable occupant behaviour on the energy performance in schools. Moreover, all the dominant boundary conditions are related to the use of class rooms. The boundary conditions related to the other school zones (*e.g.* canteen, offices) are less important. As class rooms cover more than 40% of the total surface area (*§ 2.2.2*), the use and occupancy of these specific rooms clearly dominate the energy demand of the building. An overview of the 10 predominant boundary conditions is given in *Figure 4.7*. To compare the impact of the different boundary conditions mutually, the relative mean elementary effects (%) are used, which are defined as the ratio of the mean elementary effect for the considered boundary conditions to the sum of all elementary effects of all investigated boundary conditions.

Overall, the relative absence factor for class rooms (μ^* explains 36% of the variations for the 'base case' and 29% for the 'best practice' variant) has the largest impact on the energy demand. Furthermore, when mutually comparing the results of the 'base case' and 'best practice' variants, the occupant density is much more significant for the 'base case' variant. Due to the implementation of a heat recovery device in the 'best practice' variant much lower ventilation losses occur. As ventilation rates are set in relation to the occupant density, this boundary condition is significantly less important in the 'best practice' variant. Furthermore, the overall impact of the set-point temperature for heating is slightly higher for the 'base case' variant (μ^* is 11% compared to 8.5%). Due to the lower energy performance level of the building envelope, variations of the set-point temperature lead to larger changes of the heat losses which in turn affect $Q_{H,nd}$. Conversely, for the 'best practice' variant, the impact of the internal heat gains due to lighting and equipment expressed by the partial

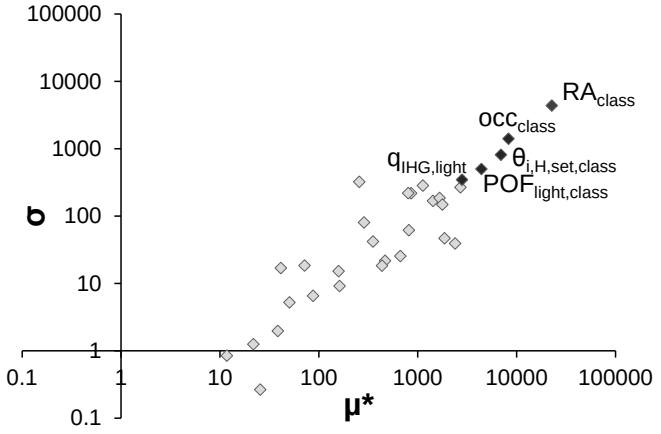

(a) $Q_{H,nd}$ 'base case'

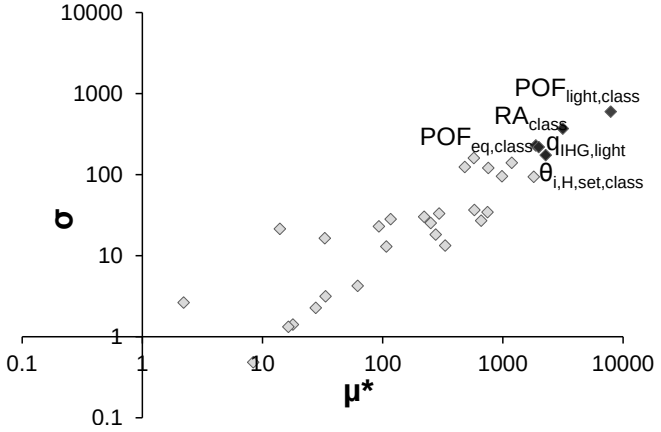

(b) $Q_{H,nd}$ 'best practice'

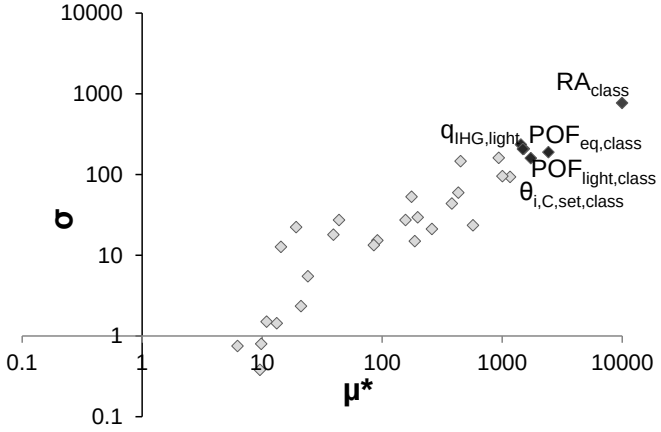

(c) $Q_{C,nd}$ 'best practice'

Figure 4.6: Morris sensitivity measures μ^* and σ of the energy demand for varying boundary conditions (logarithmic scale). Only the five most important factors are named.

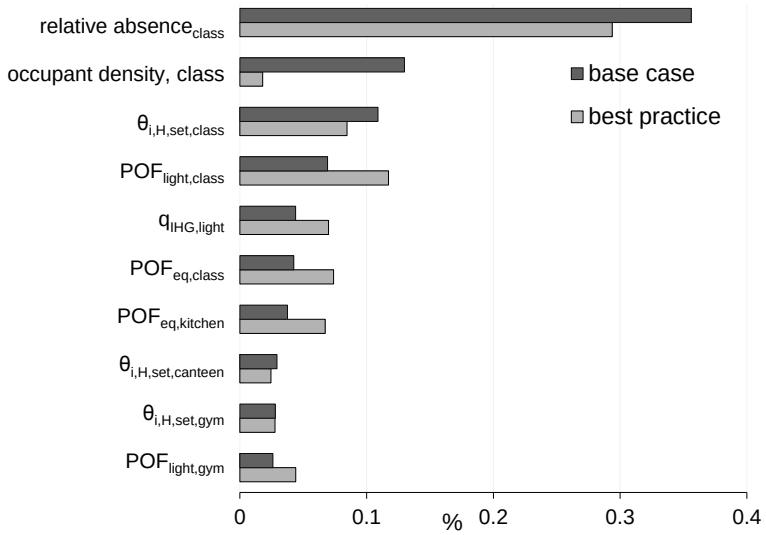

Figure 4.7: Morris sensitivity measure $\mu^*(\%)$ of the heat demand for the 10 predominant boundary conditions of the 'base case' and 'best practice' variant of the reference elementary school building model.

operation is more important. As the heat losses are generally lower, a larger part is covered by the internal heat gains. As a result, the highly insulated buildings are more sensitive to changes of the internal heat gains.

Based on the outcome of the SA, field data on operational schedules, set-point temperatures, occupant density rates and the use of equipment and lighting in class rooms are collected by surveys of Flemish schools.

4.5 Setting the deterministic boundary conditions

The objective of this particular section is to capture possible inaccuracies of the implemented boundary conditions by comparing the input data that is currently applied in the calculation standards (see *Table 4.3*) to real field data and survey results of (Flemish) schools:

- Information on **heating patterns and set-point temperatures** is mainly based on a site-visit and a detailed survey of 20 schools in Flanders. As heating patterns and set-points are strongly related to the energy performance level of the building, a sample of recently built or highly renovated schools is used to determine this information.
- Information on **user's schedules** (*i.e.* school opening hours, after school use) is based on a more general questioning of a much larger sample of schools (981 were contacted of which 8% responded) which is performed in the framework of a Master project [203].
- Data on the **occupancy and absenteeism rates** are collected by a separate questioning: 144 schools were contacted of which 12.5% responded [204]. Regarding the general user's schedules and occupancy patterns, information is based on a broader sample including both contemporary as older schools.

The questioned schools are randomly picked, are spread over the Flemish region and include elementary and secondary schools. To limit the workload and the size of the questionnaires, only

the predominant boundary conditions as revealed by the SA are included. For the less influential boundary conditions, the deterministic boundary conditions are set equal either to the average value or to the mode of the distribution functions as used for the UA and SA (see *Table 4.3*).

Operational schedule: the obtained survey results show that although schools can freely decide on the exact starting and closing time, most of the schools (*i.e.* 73 to 81%, depending on the typology of the investigated school [203]) adopt the official operational schedule as defined in *§ 4.3.3*. The other 20 to 25% of the surveyed schools start and close either 0.5 hour earlier or 0.5 hour later. As these differences are limited, no changes to the regular school opening hours as defined in *§ 4.3.3* are suggested.
Furthermore, representative values for the relative absence factor for the class rooms RA_{class} are determined accounting for the occurring outdoor classes and excursions, and for the daily play breaks. As the number of outdoor classes are limited (*e.g.* sports class - 2 hours per week) and extra excursions occur only occasionally, the RA_{class} as used in the UA and SA (= 75%) largely underestimates the real use of the class rooms. Therefore, the RA_{class} is changed to 87.5% accounting for two daily play breaks of 15 minutes and 2 hours of outdoor (gym) classes per week. Values for the relative absence factor of offices and teachers' rooms are not changed and can be found in *Table 4.3*. Due to their specific function, labs and gym are assumed to be constantly occupied. The resulting deterministic daily occupancy profiles for the various school zones are summarised in *Figure 4.9*, with the exception of Wednesday afternoon, which is free.
Considering the significant impact of the operational schedule and related occupancy on the energy demand calculations (see results of the SA in *§ 4.4.2*), the possible occurrence of after school activities is additionally investigated. The survey results show that in 70 to 80% of the questioned schools, extra classes and after school activities are organised [203]. The frequency of the after school activities (*i.e.* varying from either daily, weekly or only occasionally) and the related amount of extra school opening hours (*i.e.* varying from half an hour up to five hours) vary however substantially between schools. Moreover, after school activities and related heating and ventilation schedules are generally (in ± 65% of the questioned schools) restricted to a small part of the building (*i.e.* a single class room or gym only). One may hence conclude that the after school operation is an important aspect. However, taking in mind the highly diverse and uncertain character of the after school activities, they are hard to generalise and thus difficult to include in the set of deterministic values.

Set-point temperature, °C: the results of the study for the set-point temperatures for heating are depicted in *Figure 4.8*. The figure shows that secondary schools have a slightly more stable but somewhat lower temperature regime compared to elementary schools. Especially nursery schools which accommodate young children (< 6 years old) request slightly higher indoor temperatures (21 - 22°C). 95% of the questioned elementary schools has a set-point of 21±1°C while 85% of the questioned secondary schools has a set-point temperature of 20.5±0.5°C. Based on these survey results, the deterministic set-point temperature for heating is set equal to 21°C. As the differences in set-point temperatures remain small, no difference is made between elementary and secondary schools. For gymnasia, the survey results reveal set-point temperatures for heating varying between 12°C and 20°C, with a median of 17°C. This value is proposed as the standardised, deterministic set-point temperature for heating in gyms.

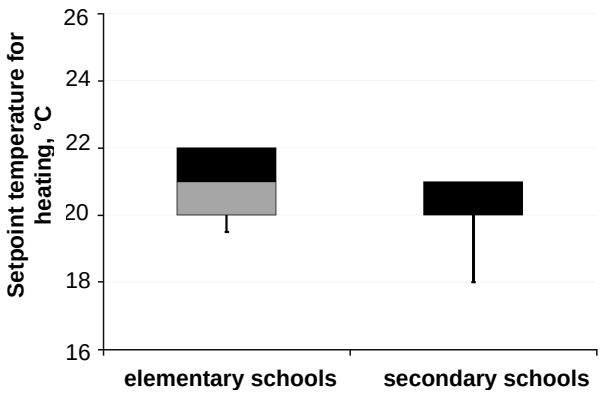

Figure 4.8: Survey results: heating set-point temperature in elementary and secondary schools.

Schools in Flanders generally do not have an (active) cooling system. Only in exceptional cases, active cooling is provided in restricted zones with extremely high internal heat loads such as server rooms or computer labs. Realistic data on set-point temperatures for cooling were therefore hard to find. Hence, the deterministic value for the set-point temperature for cooling is set equal to the mean value as used for the UA and SA, *i.e.* 25°C (see *Table 4.3*).

Occupant density, m^2/pers: the occupant density rate is calculated as the mean available surface area per student (m^2/pers). Hence, data on both the number of students and the surface area of regular class rooms are collected. The survey results reveal an average surface area of 57 m^2 for class rooms [205] and an average occupancy of 19 students per class which results in an average value for the occupant density of 3.0 m^2/pers. Similar results are found by Stranger et al. [10] based on a more recent survey of elementary schools.
In addition, information on absenteeism is gathered to account for the possible nonattendance of students due to *e.g.* illness or personal affairs. The survey results reveal an average absenteeism percentage of 6% [205]. Although the absenteeism percentage (due to illness) relates to the time of the year and differs between nursery, primary and secondary schools, a fixed absenteeism percentage is assumed as a deterministic input value for the energy calculation methods.

Internal heat gains due to equipment, W/m^2: an increasing trend in electronic equipment availability in schools is noticed the last decade [206, 207]. In class rooms mostly computers or laptops and data projectors are used although tablets, netbooks and interactive white-boards are becoming pervasive. As the latter category is however still less frequently used and the related heat gains are less significant, the survey results focus on the use of computers mainly. Information on the occurrence of computers in schools is based on the obtained survey results [203]. Additionally, available surveys on energy use and load profiles in schools [206, 207] - including detailed information on Flemish schools - are used as a reference. According to a recent study on the use and innovation of ICT in European schools [206], the number of available computers per student has been increased from one for every 20 students to one for every four students between 2000 and 2009. A similar, yet slightly less increasing trend is noticed in Flanders [207]: about 18 computers are available per 100 students or approximately 6 students per computer. Assuming a sensible heat gain of 80 W per computer [110], this leads to an average internal heat gain due to equipment $q_{IHG,eq}$ of about 5

W/m^2.
Concerning the actual use of the equipment, various exemplary schedules for equipment loads in class rooms are found in different building energy calculation standards [121, 208, 209] (see *Figure 4.9* (b) - marked in grey lines). All of these standards define a relatively high use of equipment as the computers are assumed to be used during 70 to 100% of the occupied time. In contrast, survey results on the use of ICT in Flemish schools [207] show that ICT equipment is only occasionally used: a mere 3.1% of the students uses the computer or tablets daily while 30% uses the computer only a couple of times a year. Consequently, the partial operational time factor of equipment in class room as found in the calculation standard *NEN 2916* [99] (= 15%) is considered as a more realistic estimation and hence chosen as the deterministic value (*Figure 4.9* (b) - marked in red line) to be used for the energy performance calculations.
Note that the use of ICT equipment (*i.e.* computers, smart boards, tablets) in school is developing and changing. At the same time, technology is evolving leading to more efficient applications. Both trends affect the internal heat gains due to equipment, hence the deterministic value as defined in this section might need revision over time.

Internal heat gains due to lighting, W/m^2: the internal heat gains due to lighting are calculated as the product of the requested lighting comfort requirements and the installed normalised lighting power density (NPD). In most class rooms however, board lighting is used which results in an additional required vertical luminance. Consequently, in class rooms, the target power load $P_{T,light}$, a parameter which is generally used in Flanders as a criteria for granting (re-)lighting, is more suitable to be used as a deterministic input value compared to the NPD value. Ryckaert et al. [137] developed a method to calculate this target power load in function of the number of annual usage hours (± 1200 h), the lighting system efficiency (> 90 lm/W), the efficiency of the luminaires (= 90%), the maintenance factor (= 0.85) and a surface area of the work zone of a class room equal to 42.7 m^2 as prescribed in [210]. For class rooms, this results in an installed lighting load $P_{T,light,class}$ of 10.6 W/m^2.
Concerning the use of lighting in class rooms, monitoring data are rare. Schedules for manually or automatically controlled lighting, found in similar calculation standards [121, 208] are therefore used as a reference (see *Figure 4.9* (c)). Based on these examples, a deterministic lighting profile is defined for both manually (assumed base load) and time controlled lighting (no after hour usage assumed). Both control systems assume constant use of lighting whenever the class is occupied. Results are shown in *Figure 4.9* (c). Due to the strong building case-specific characteristics, a separate calculation approach is applied in the calculation method to account for daylight controlled lighting [22]. Deterministic profiles for daylight control are hence not defined.

Finally, after hour use of equipment and lighting that is not specifically related to the school activities must be accounted for. While students' attendance and thus internal heat gains due to occupants can automatically be coupled to the occupancy schedule, the after hour use of lighting and equipment can not. Consequently, a base load is assumed for equipment use and for manually controlled lighting systems implying that part of the daily heat gains remain present during the nights and weekends. Due to lack of realistic data on base loads for equipment and lighting in Flemish schools,

the values are set equal to plausible values as found in literature: a 5% base load is assumed for equipment (NCM [209]) and lighting. Results are depicted in *Figure 4.9* (b) and *Figure 4.9* (c), respectively.

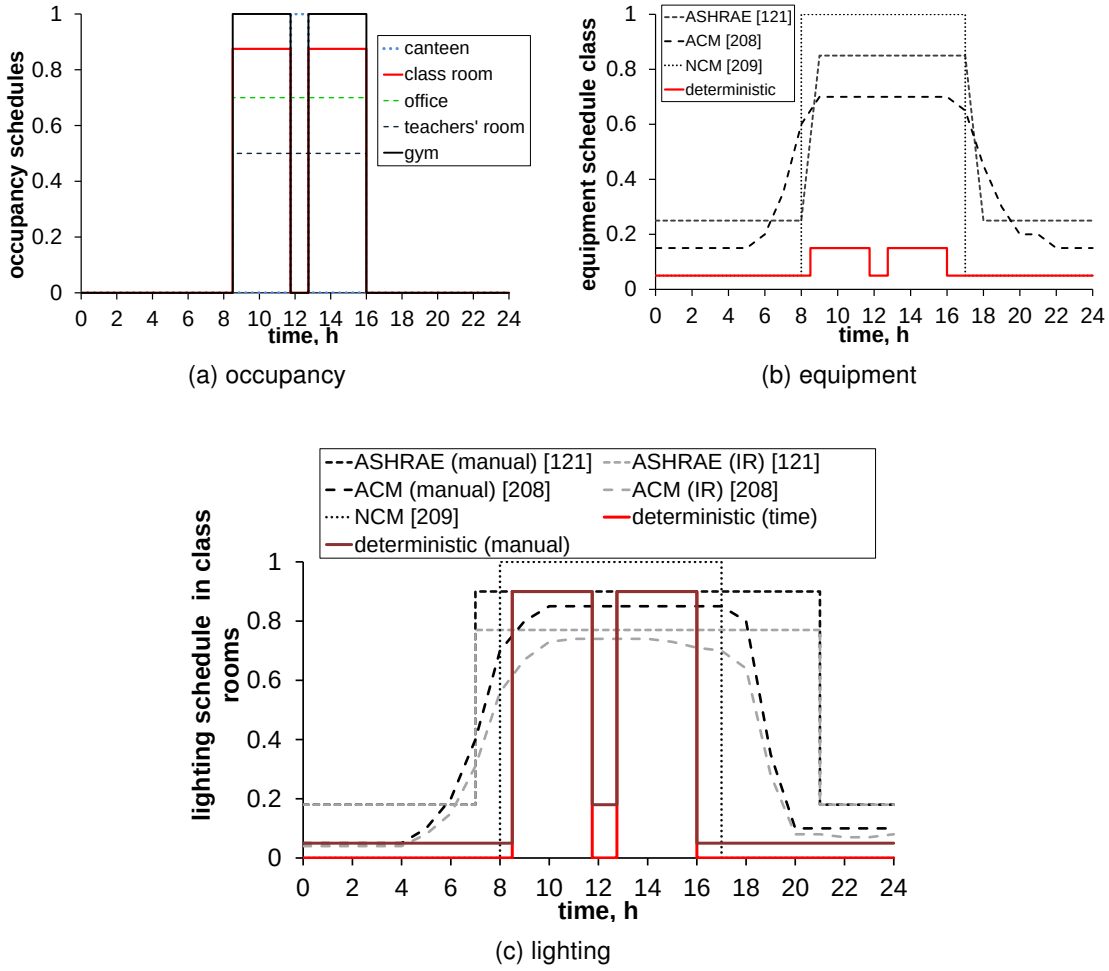

(a) occupancy

(b) equipment

(c) lighting

Figure 4.9: Comparative literature study of typical operational schedules for class rooms.

4.6 Discussion

In the previous section a proposal is defined for a more realistic set of deterministic values for the activity and operational characteristics for schools to be used for the energy performance assessment calculations. The results are summarised in *Table 4.5*.

To assess the impact of the newly defined boundary conditions on the energy demand calculations, a comparison is made between the results of the UA (box plots, see *Figure 4.10*), and the annual energy demand calculation results ($Q_{H,nd,new}$ and $Q_{C,nd,new}$) when using the newly defined deterministic boundary conditions. The result are depicted in *Figure 4.10* and summarised in *Table 4.6*. Overall, *Figure 4.10* shows an increase of the heat demand and a decrease of the cooling demand compared to the average results of the UA. The largest impact is found for the 'best practice' variants where the annual heat demand rises by 2.8 kWh/(m^2.a) or 26%, on average.

Table 4.5: *Overview of the newly defined deterministic boundary conditions typical for schools.*

	$\theta_{i,H,set}$, °C	$\theta_{i,C,set}$, °C	occupant density, m^2/pers	ventilation rate, m^3/(h.pers)	$q_{IHG,occ}$, W/pers	$q_{IHG,eq}$ (W/m^2)(1)	illuminance, lux(2)	relative absence factor, %	partial operation equipment, %	partial operation lighting,%
class room	21	25	3.0	29	60/80	5.0	300	87.5	15	90
office	21	25	14.0	29	80	10.0	500	70	50	70
teachers' room	21	25	3.0	29	80	2.5	500	50	35	95
canteen	21	25	1.5	29	60/80	2.0	300	-	100	95
kitchen	21	25	10.0	36 (+ 80(3))	100	80.0	500	-	100	95
gym	17	25	20.0	44	160/210	-	300	-	-	95
lab	21	25	5.0	36	100	-	500	-	-	95
circulation area	-	-	-	-	-	-	100	-	-	50
sanitary	-	-	-	-	-	-	200	-	-	50

(1). Equipment and lights are assumed to be switched on whenever a zone is occupied.
(2). In class rooms, $P_{T,light}$ = 10.6 W/m^2 is used. In all other rooms, NPD = 2 W/(100 lux $\cdot m^2$).
(3). Extra ventilation in the kitchen due to heat producing cooking activities is foreseen during 50% *of the time.*

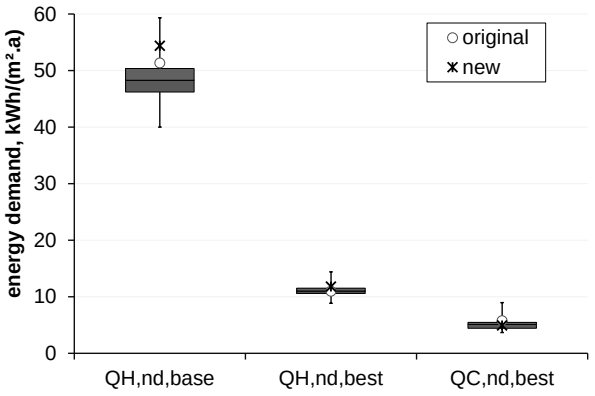

Figure 4.10: Impact of the boundary conditions on the annual heating $Q_{H,nd}$ and cooling demand $Q_{C,nd}$, normalised to the building floor area (kWh/(m^2.a)), of the sample of rectangular, elementary reference school building variants using box plots to graphically illustrate the minimum, the lower quartile, median, upper quartile and maximum energy demand.

Table 4.6: Implementation of deterministic boundary conditions: impact on the annual heating $Q_{H,nd}$ and cooling demand $Q_{C,nd}$, normalised to the building floor area (kWh/(m^2.a)), in the sample of rectangular, elementary reference school building variants.

	kWh/(m^2.a)	%
$\triangle Q_{H,nd,base}$	+3.0	+6
$\triangle Q_{H,nd,best}$	+2.8	+26
$\triangle Q_{C,nd,best}$	-0.9	-15

Furthermore, a comparison is made between the results of the EPR calculation method [22] using both the original and the adapted boundary conditions as summarised in *Table 4.7*.

Table 4.7: Overview of the boundary conditions as used in the original *EPR* calculation method [22] and as used in the method specifically adapted to the use of Flemish schools (see *§ 4.5*).

	occupant density n_{occ}, m^2/pers		**hygienic ventilation rate $\dot{V}_{vent}$, m^3/(h.pers)**		**internal heat gain people $q_{IHG,occ}$, W/pers**		**internal heat gain equipment $q_{IHG,eq}$, W/m^2**		**internal heat gain light $q_{IHG,light}$, W/m^2**		**relative absence factor RA, %**		**partial operation equipment POF_{eq}, %**	**partial operation lighting POF_{light}, %**	
	old	**new**	**old**	**new**	**old**	**new**	**old**	**new**	**old**	**new**	**old**	**new**	**new**	**old**	**new**
class room	4.0	3.0	29	29		60		5.0		6		87	15		90
office	15.0	14.0	29	29		80		10.0		10		70	50		70
teachers' room	3.5	3.0	29	29	100	80	3	2.5	20	10	30	50	35	30	95
canteen	1.5	1.5	29	29		60/80		2.0		6		100	100		95
kitchen	10.0	10.0	29	44 (+ 80*)		100		80.0		10		100	100		95
gym	3.5	20.0	29	44		160/210		-		3		100	-		95
circulation area	-	-	-	-	-	-	-	-	-	2	-	-	-	-	50
sanitary	-	-	-	-	-	-	-	-	-	4	-	-	-	-	50

** Extra ventilation in the kitchen due to heat producing cooking activities is foreseen during 50% of the time*

The introduction of the set of new boundary conditions and default input data results in a different calculation output for the ventilation heat transfer coefficients H_{ve} and for the calculation of the heat gains Q_{IHG} as shown in *Eq. 4.2* and in *Eq. 4.3*, respectively.

$$H_{ve} = \begin{cases} 0.34 \cdot [\dot{V}_{in/exf,H} + \mathbf{0.3} \cdot r_{preh,H}\ \dot{V}_{supply,H}] & (original) \\ 0.34 \cdot [\dot{V}_{in/exf,H} + \mathbf{f}_{occ} \cdot (\mathbf{RA}) \cdot r_{preh,H}\ \dot{V}_{supply,H} + \mathbf{0.5}\ \dot{V}_{\mathbf{basic}}] & (refined) \end{cases} \tag{4.2}$$

where $\dot{V}_{in/exf,H}$ represents the air flow due to infiltration/exfiltration (m^3/h), $r_{preh,H}$ is the temperature adjustment factor in case the supply temperature differs from θ_e (*i.e.* due to *e.g.* heat recovery), f_{occ} is the monthly time fraction[3] that the school is used, RA is the relative absence factor of the considered (school) zone as defined in *§ 4.5*, $\dot{V}_{supply,H}$ is the hygienic ventilation airflow rate (m^3/h) at outdoor temperature and $\dot{V}_{basic}$ is a basic ventilation flow rate (m^3/h) to guarantee good indoor air quality at any time of the day (m^3/h).

$$Q_{IHG} = \begin{cases} \mathbf{0.8} \cdot (\mathbf{0.3} \cdot RA \cdot n_{occ} \cdot q_{IHG,occ} + q_{IHG,eq} \cdot A_f + \mathbf{0.3} \cdot POF_{light} \cdot q_{IHG,light} \cdot A_f) \cdot t & (original) \\ (RA \cdot n_{occ} \cdot q_{IHG,occ} + \mathbf{POF}_{eq} \cdot q_{IHG,eq} \cdot A_f + POF_{light} \cdot q_{IHG,light} \cdot A_f)\ \mathbf{f}_{occ} \cdot t & (refined) \end{cases} \tag{4.3}$$

where n_{occ} is the number of people present in the considered (school) zone, POF_{eq} is partial operational time fraction of the equipment as defined in *§ 4.5* and POF_{light} is partial operational time

[3] In the original calculation method, this value equals **0.3** for schools. In the refined calculation approach this values is on average equal to 0.2. The actual value differs however slightly, month by month, depending on the amount of occurring weekends days and Wednesdays.

fraction of lighting as defined in *§ 4.5*.

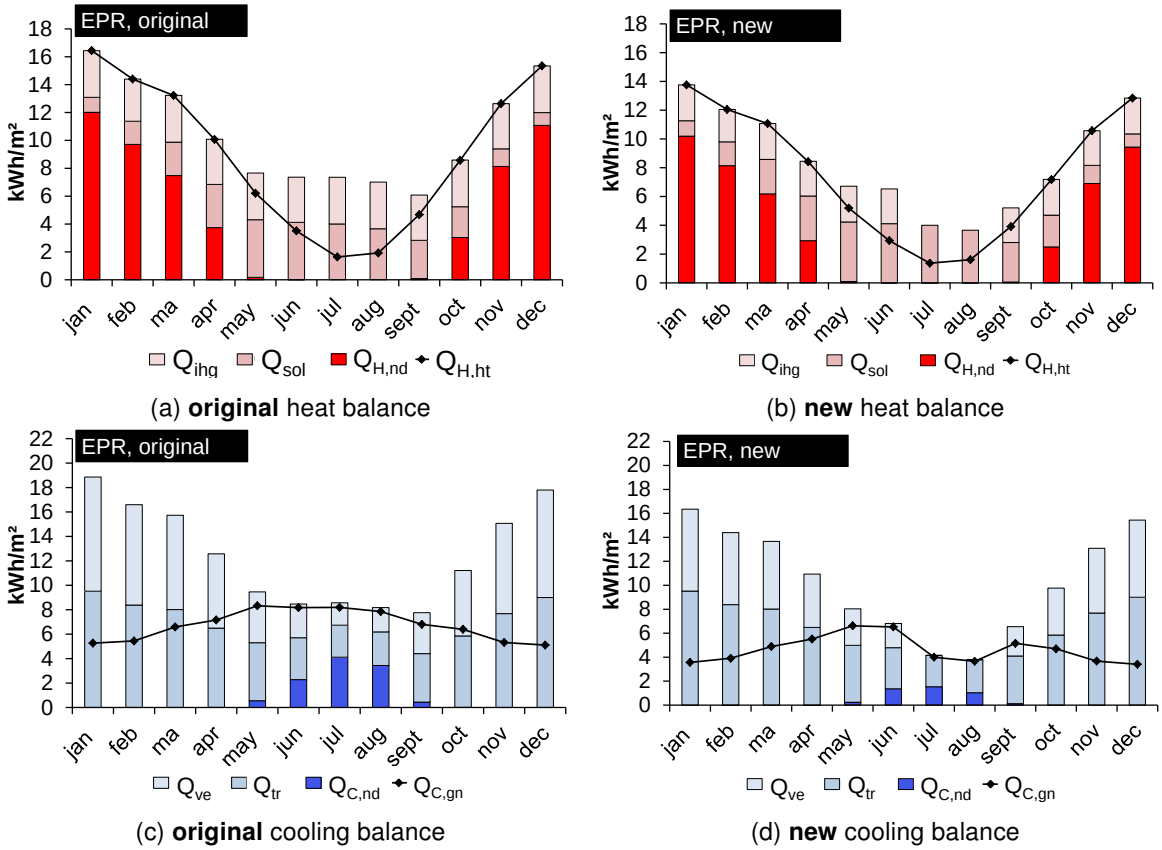

(a) **original** heat balance

(b) **new** heat balance

(c) **original** cooling balance

(d) **new** cooling balance

Figure 4.11: Impact on the monthly heating and cooling demand, both normalised to the building floor area (kWh/m^2), calculated according to the *EPR* standard for an elementary school building design variant using the original and adapted boundary conditions.

To visualise the impact of the changes of the boundary conditions, the calculation results for the heat balance (see *Figure 4.11* (a) and (b)), and for the cooling balance (see *Figure 4.11* (c) and (d)), of a randomly selected rectangular elementary reference school building design variant (heavy building structure, U_{opaque} = 0.24 W/(m^{2}K), $U_{glazing}$ = 1.1 W/(m^{2}K), U_{frame} = 1.4 W/(m^{2}K), n_{50} = 3 ACH, a WWR = 20% and a η_{HR} = 75%) are plotted. As shown in *Figure 4.11* (a) and (b), a significant decrease of the monthly internal heat gains Q_{int} of on average 30%, is found. Furthermore, an average decrease of the monthly ventilation heat losses Q_{ve} of 14% is found (see *Figure 4.11* (c) and (d)). Both effects result in an increase of the annual heat demand $Q_{H,nd}$ from 26.3 kWh/(m^2.a) to 30.2 kWh/(m^2.a) or +15%, and a drop of the annual cooling demand $Q_{C,nd}$ from 9.3 kWh/(m^2.a) to 7.7 kWh/(m^2.a) or −17%. Especially when taking in mind the strict criteria for passive school buildings (*i.e.* $Q_{H/C,nd} \leq$ 15 kWh/(m^2.a)) [21], these changes can be considered as significant. A more detailed analysis of the impact of the implementation of more realistic boundary conditions on the results of the *quasi-steady-state* calculation methods (*i.e.* EPR [22] and PHPP [110]) for passive school buildings in particular are described in previous research work [211, 144, 212].

4.7 Conclusions

Building energy assessment methods used in a regulatory context impose a calculation procedure under restricted and predefined conditions to check the compliance with the preset energy performance levels. Standardised boundary conditions and input data are implemented allowing for an objective evaluation of the building design. Tabulated values for amongst others (heating) schedules, control systems, use of artificial lighting and equipment, ventilation characteristics and internal heat gains are defined in the corresponding calculation manuals. To achieve the objectives of the EU Directives, accuracy and reliability of the assessment results are crucial. An uncertainty analysis reveals however a significant spread of about 30% of the annual heat demand $Q_{H,nd}$ and about 40% for the annual cooling demand $Q_{C,nd}$ due to realistic variations of the users' related boundary conditions in schools. Hence, as some of the currently applied data are inaccurate, unrealistic or inadequate for schools, they need to be revised, especially when these are used for the energy performance assessment of passive or net zero energy buildings which need to comply with (very) strict energy requirements. To guarantee more realistic energy assessment calculation results, boundary conditions are adapted to the use and typology of Flemish school buildings based on collected field survey data. To limit the related workload, a sensitivity analysis is performed priory through the local method of Morris, revealing the users' and load profiles, comfort settings and the occupant density rate of the class rooms as the predominant input parameters. The impact of the input data for other typical school zones is less significant. Survey results reveal amongst others a set-point temperature for heating equal to 17°C for gyms and 21°C in all other rooms, an occupant density rate of class rooms equal to 3 m^2/pers, target lighting power loads in class rooms of 10.6 W/m^2 and an after hour use of equipment and lighting of 5%.

The final result of this chapter is a comprehensive set of representative, deterministic boundary conditions to be used for energy assessment of elementary and secondary schools in particular. As the reference school building models used and implemented boundary conditions are set based on a comprehensive study of a broad range of school building characteristics, the results can be extrapolated to other school forms (*e.g.* technical or vocational schools) on the condition that the organised educational activities are more or less in line with the activities taught in the investigated school building sample. As buildings' and users' characteristics depend on local customs and the specific building typology, the results can however not simply be generalised to other building typologies or other regions. Yet, the research approach used along this dissertation can be used as a reference for similar research studies on other building types or for other regions and countries.

5

Implementation of transient thermal behaviour of a building in quasi-steady-state calculation methods

When comparing the results of quasi-steady-state and dynamic energy calculation methods often significant discrepancies are found, especially for intermittently used buildings such as schools. These differences are caused by non-realistic model simplifications inherent to the transformation of a dynamic entity into a representative, steady-state (calculation) model. The previous chapter mentions the boundary conditions and standardised input data as a cause of inaccuracy. Other researches designate however the quasi-steady-state calculation approach itself and more in particular the implementation of the transient thermal behaviour as an important source of errors. Therefore, throughout this chapter, the monthly, quasi-steady-state calculation method is evaluated and modified to the typical school buildings' characteristics. First, the ***correlation between the heat-balance or loss-gain ratio and the utilisation factor*** *is analysed and a regression analysis is performed to determine adapted values for the numerical correlation-based parameters used for the calculation of the utilisation factors. Second, the influence of* ***system intermittency*** *on the energy demand for heating and cooling is studied. The influences of the school building and system characteristics on the thermal behaviour and the related energy saving potential are analysed. Accordingly, the calculation approaches to account for system intermittency as applied by the different quasi-steady-state methods are revised based on the results of additional regression analysis.*

5.1 Introduction

Various studies can be found investigating the accuracy of the *quasi-steady-state* calculation method [27, 28, 29, 30, 31, 32, 33, 34] to be used for the energy performance assessment in a regulatory context. No clear consensus has however been reached. Some studies state that the *quasi-steady-state* calculation method is well suitable to assess accurately the energy performance of a building (design) [27, 28, 29, 30, 31] while other researches are found which reveal significant discrepancies between *quasi-steady-state* and *dynamic* energy calculation methods, especially for intermittently used buildings [28, 29, 30, 32, 33, 34, 31]. In line with the latter study results, simulation results of a broad range of design variants of the rectangular reference building for elementary schools (see floor plan - *Figure 2.6* (a)) show that the *quasi-steady-state* methods generally tend to underestimate the annual heating demand in intermittently heated school buildings (see *Figure 3.11* (a)) compared to the results of dynamic simulations. The differences vary from about 5% up to more than 25% depending on the applied calculation method and on the building's characteristics (*i.e.* the thermal capacity of the building and energy performance level of the building envelope). The higher the thermal capacity, the larger differences are found (see *Figure 3.11* (b)), concluding that the impact of the thermal capacity currently might be overestimated in the *quasi-steady-state* calculation method.

Several researches can be found which investigate the cause of the discrepancies between *quasi-steady-state* and *dynamic* energy calculation methods [31, 32, 33, 34, 213, 214]. Most of the studies analyse the impact of the building typology and users' characteristics on the accuracy of the energy calculations. Kalema et al. [31] studied the impact of the thermal mass on the *quasi-steady-state* calculation results for dwellings and multi-family buildings in the Nordic climate. While observing a high overestimation of the energy demand by the *quasi-steady-state* calculation method in very light, well-insulated buildings, Kalema et al. [31] concluded that the accuracy of the *quasi-steady-state* method is highly related to the building's characteristics. Jokisalo and Kurnitski [32] studied the applicability of the utilisation factor calculated according to *EN ISO 13790* [37] (see *Eq. 5.1*) in the Scandinavian climate for residential, multi-family and office buildings. They compared the results of dynamic simulations using the IDA-ICE software to the results of the *steady-state* calculation and found following adapted correlation between $\eta_{H,gn}$ and the heat-balance ratio γ_H for apartment buildings and dwellings (see *Eq. 5.2*), and for offices (see *Eq. 5.3*), respectively:

$$\eta_{H,gn} = \frac{1-\gamma_H^{a_H}}{1-\gamma_H^{(a_H+1)}} \tag{5.1}$$

with

$$a_H = 6 + \frac{\tau}{7} \qquad (dwelling\ and\ apartments) \tag{5.2}$$

or

$$a_H = 2 + \frac{\tau}{15} \qquad (offices) \tag{5.3}$$

Other suggestions for improvement of the *quasi-steady-state* calculation method are found in the work of Corrado and Fabrizio [33, 34]. This study focuses on the cooling demand in particular and investigates the accuracy of the utilisation factor for the Italian climate and typical Italian building typologies (*i.e.* single family, multi-family and office buildings) and users' schedules. Based on the results of a regression analysis, the window-to-floor area ξ, is added to the correlation used for the calculation of the utilisation factor $\eta_{C,ht}$ as shown in *Eq. 5.4*:

$$\eta_{C,ht} = \frac{1 - \gamma_C^{a_C}}{1 - \gamma_C^{(a_C+1)}} \tag{5.4}$$

with

$$a_C = 8.1 - 13\xi, + \frac{\tau}{17} \tag{5.5}$$

Le Dréau et al. [213] studied the influence of different building and users' characteristics on the energy demand calculation results for residential and non-residential buildings in Denmark. The following adapted equations for the utilisation factor for the calculation of the heat demand (see *Eq. 5.6*) and the cooling demand (*Eq. 5.7*) are determined for non-residential buildings:

$$a_H = 2.87 + \frac{\tau}{47} \tag{5.6}$$

$$a_C = 2.79 - 2.69\xi, + \frac{\tau}{35} \tag{5.7}$$

Panek et al. [215] determined new values for the numerical parameters $a_{H,0}$ and $\tau_{H,0}$ depending on the thermal capacity of the building for Polish residential buildings.

$$a_H = 2 + \frac{\tau}{50} \qquad (heavy) \tag{5.8}$$

$$a_H = 2 + \frac{\tau}{54} \qquad (light) \tag{5.9}$$

While using *Eq. 5.8* and *Eq. 5.9*, Panek et al. [215] showed that the average error between the *quasi-steady-state* (calculated according to *EN ISO 13790* [37]) and *dynamic* calculations in `TRNSYS` is reduced to $< 5\%$ for the annual heat demand and to $< 3\%$ for the annual cooling demand.
Finally, in the framework of the development of *NEN 2916*[1] [99], van den Ham and Linssen [214] studied the use of the utilisation factor in the *quasi-steady-state* energy demand calculations. Based on the comparative analysis of dynamic and quasi-steady-state calculation results, the following equations for the calculation of the $\eta_{H,gn}$ and $\eta_{C,ht}$ were set for intermittently heated or cooled non-residential buildings:

$$a_H = 0.81 + \frac{\tau}{76.92} \tag{5.10}$$

and

$$a_C = 1.83 + \frac{\tau}{83} \tag{5.11}$$

[1] *NEN 2916* [99] is the predecessor of the currently applied Dutch calculation standard for the energy performance assessment for non-residential buildings *NEN 7120* [44].

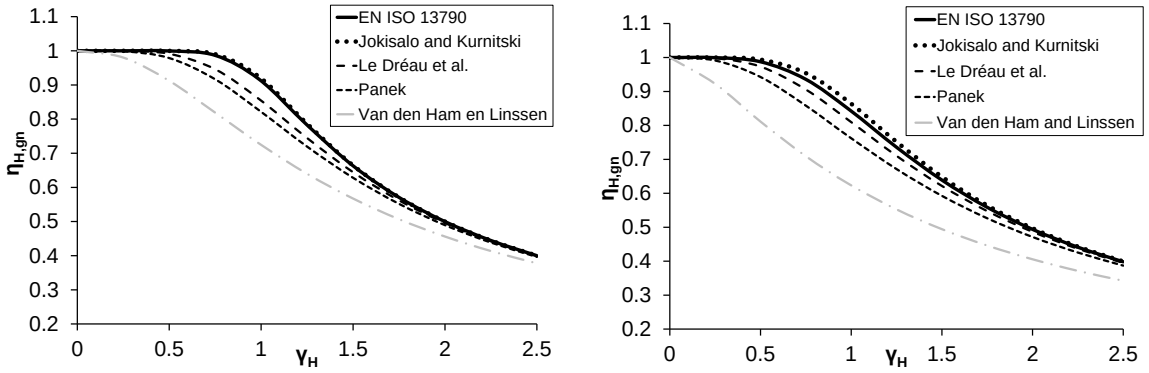

(a) $\tau = 140h$ (b) $\tau = 65h$

Figure 5.1: Utilisation factor $\eta_{H,gn}$ as a function of the heat-loss ratio γ_H for two time constants τ (h) of a building using the numerical parameters $a_{H,0}$ and $\tau_{H,0}$ according to the results of different research studies. The utilisation factor curve as determined by Van den Ham and Linssen [214] is marked in lighter grey as, in contrast to the other curves, an additional reduction of the utilisation factor due to intermittency is included.

The results of the aforementioned research studies [31, 32, 33, 34, 213, 214] differ considerably. To visualise, the various calculation options for $\eta_{H,gn}$ are shown for a non-residential building with a time constant τ = 140 h and a time constant τ = 65 h[2]. Taking in mind the general underestimation of the heat demand calculated according to *EN ISO 13790* [37] (see *Figure 3.11*), a decrease of $\eta_{H,gn}$ is expected for the optimised results. Most of the researches [213, 215, 214] show indeed a reduction of $\eta_{H,gn}$ compared to *EN ISO 13790* [37]. The results of Jokisola and Kurnitski [32] however lead to an overall though slight increase of $\eta_{H,gn}$. Furthermore, the utilisation factors determined by van den Ham and Linssen (see *Eq. 5.10* and *Eq. 5.10*)[214] are much lower compared to the other methods. This is due to the fact that an additional reduction of the utilisation factor is included to cope with the impact of system intermittency while in the other studies these effects are incorporated separately (see *Eq. 3.13* and *Eq. 3.14*).
Despite the different outcomes, all of the aforementioned studies state that in order to obtain more accurate *quasi-steady-state* calculation results, the utilisation factors $\eta_{H,gn}$ and $\eta_{C,ht}$ must be linked to the typology of the building and the related boundary conditions. Therefore, in the first part of this chapter, the currently applied equations for $\eta_{H,gn}$ (see *Eq. 3.6*) and $\eta_{C,ht}$ (see *Eq. 3.7*) according to *EN ISO 13790* [37] are studied both as a value and as a trend (see *§ 5.4*). The impact of the typical characteristics of schools on the *quasi-steady-state energy* calculation results is determined and the currently applied correlation between the heat-balance or loss-gain ratio and the utilisation factor is reevaluated.

In the second part of this chapter, the impact of system intermittency (see *Eq. 3.13* and *Eq. 3.14*) in the *quasi-steady-state* calculation method is studied as Kokogiannakis [30] demonstrated that, even after the adaptation of the utilisation factor, the monthly *quasi-steady-state* method according to *EN ISO 13790* [37] tends to underestimate the heat demand in intermittently heated buildings compared to the results obtained by the dynamic simulation tools *EnergyPlus* and *ESP-r*. In

[2] τ = 140 h and τ = 65 h are the average value of the time constant of a range of design variants of the rectangular, reference building for elementary schools with a heavy and light structure, respectively

schools where intermittent occupancy and related plant non-operation time and/or setback periods are (much) longer compared to other building typologies, a correct implementation of intermittent heating and cooling in the *quasi-steady-state* calculation method might be even more crucial. Therefore, the impact of system intermittency on the energy demand is studied (*§ 5.5*). The actual indoor temperature drop and related energy savings due to system intermittency are determined by dynamic simulations. Subsequently, a comparative analysis of the different calculation approaches used by the *quasi-steady-state* calculation method to integrate these effects of intermittency is performed (*§ 5.6.1*). Finally, with respect to the dynamic thermal behaviour of the building, some proposals are made to further refine different, currently applied *quasi-steady-state* calculation standards *§ 5.6.2*.

The results of this chapter are partially based on previous research work as described in Wauman et al. [216]. Overall, the same regression analysis techniques are used. One important difference is however made. In Wauman et al. [216], the impact of system intermittency is included in the utilisation factor in conformity with the study of van den Ham and Linssen [214]. In this research study however, in line with *EN ISO 13790* [37], the impact of system intermittency is assessed separately.

5.2 Method

In the first part of this chapter, the accuracy of the utilisation factor used in the *quasi-steady-state* standards for the calculation of the heating/cooling demand is reevaluated. According to the procedure as described in EN ISO 13790 [37], the parameter values used to determine the utilisation factors $a_{H/C,0}$ and $\tau_{H/C,0}$ are refined using regression analysis techniques. To do so, the energy demand for heating/cooling calculated according to the *quasi-steady-state* calculation approach are compared to the results of a detailed simulation method for a series of situations.

In the second part of this chapter, the influence of system intermittency on the energy demand for heating and cooling is studied. To analyse the savings due to intermittency, the heating and cooling demand of both intermittently and continuously heated or cooled schools are simulated in TRNSYS and compared mutually. Subsequently, the energy saving potential (%) due to system intermittency is calculated using *Eq. 5.12*:

$$\triangle Q_{H/C,nd} = \frac{Q_{H/C,nd,cont} - Q_{H/C,nd,interm}}{Q_{H/C,nd,cont}} \tag{5.12}$$

In the next subsections, a description is given of the Monte Carlo analysis technique (*§ 5.2.1*) used for the determination of a representative sample of school building design variants which will be used for this study. Furthermore, the calculation approach used to calculate the utilisation factors and to determine the related input data for the *quasi-steady-state* energy balances is described in *§ 5.2.2*. Last, a description of the regression analysis technique used for the revision of the correlation-based, numerical parameters is given in *§ 5.2.3*.

5.2.1 Monte Carlo analysis technique

Many characteristics of school buildings (*e.g.* occupancy, heat gains, HVAC features and control, etc.) differ significantly compared to residential buildings or offices. As all these characteristics considerably affect the dynamic behaviour and the related energy demand of the building, their impact should be acknowledged in the monthly, *quasi-steady-state* calculation method and in the determination of the numerical parameters ($a_{H/C,0}$, $\tau_{H/C,0}$, $\eta_{H,gn}$ and $\eta_{C,ht}$, $a_{H,red}$, $a_{C,red}$, etc.) in particular. As a broad range of parameters must be included, the Monte Carlo analysis method (MCA) is used combined with the Latin Hypercube (LHC) sampling technique to generate the simulation samples. Detailed information on the MCA and LHC sampling technique can be found in *§ 4.2*. Representative values and ranges for most of the typical school buildings' characteristics can be found in *§ 2.3.2* and *Table 4.3*. Considering the impact of the heat accumulating capacities of a building structure on the usability of the heat gains, the thermal capacity is not included as a parameter in the MCA but is considered separately. For each of the included building structures (heavy to very light), 200 simulations, varying all other parameters, are run.

5.2.2 Calculation of the utilisation factor

To determine realistic values for the utilisation factors, the heating $Q_{H,nd}$ and cooling demand $Q_{C,nd}$, calculated by means of dynamic simulations, are compared to the results of the simplified, monthly calculation method for a series of school building design variants. $\eta_{H,gn}$ and $\eta_{C,ht}$ can then be calculated using *Eq. 5.13* and *Eq. 5.14*, respectively:

$$\eta_{H,gn} = (Q_{H,ht,stat} - Q_{H,nd,dyn})/Q_{H,gn,stat} \tag{5.13}$$

$$\eta_{C,ht} = (Q_{C,gn,stat} - Q_{C,nd,dyn})/Q_{C,ht,stat} \tag{5.14}$$

Among all researches on the development and improvement of the *quasi-steady-state* calculation method, various methods can be found to calculate the input data of the aforementioned equations *Eq. 5.13* and *Eq. 5.14* (*i.e.* $Q_{H/C,nd}$, $Q_{H/C,ht}$ and $Q_{H/C,gn}$). Basically, they can be categorised into two groups:

- The **dependent methods** which use the output of *dynamic* simulations for the calculation of the energy demand. Thermal losses and gains on the other hand, are calculated by means of the *quasi-steady-state* calculation method. This approach is applied by Jokisalo and Kurnitski [32], by Kalema et al. [31] and Van den Ham and Linssen [214].
- The **independent methods** which calculate all input data by means of *dynamic* simulations. This approach is applied in the PASSYS project [146], by Corrado and Fabrizio [34] and is described in *EN ISO 13790* [37]. Although overall, the same basic principles are used for the different independent methods, some small differences (*e.g.* different assumptions regarding set-points) are found.

An overview of the aforementioned studies, together with the numerical parameters $a_{H/C,0}$ and $\tau_{H/C,0}$ and the methods used to determine these correlation-based parameters (*i.e.* dependent or independent) are depicted in *Table 5.1*. Additionally, information on the assumptions made regarding the use of the building and the HVAC systems (*i.e.* continuous or intermittent) is included.

Table 5.1: Literature overview of the definition of the correlation-based equations for the utilisation factors used in the *quasi-steady-state* calculation method for **non-residential buildings**.

Method	Building use	System use	Utilisation factor	Dynamic parameters	Regression method
PASSYS [145]	cont or int	cont	$a_H = a_{H,0} + \tau/\tau_{H,0}$	$a_{H,0} = 1, \tau_{H,0} = 16$	independent
EN ISO 13790 [37]	cont or int	cont	$a_H = a_{H,0} + \tau/\tau_{H,0}$	$a_{H,0} = 1, \tau_{H,0} = 15$	independent
Corrado and Fabrizio [34]	int	cont	$a_H = a_{H,0} + \tau/\tau_{H,0}$	$a_{H,0} = 1, \tau_{H,0} = 15$	
			$a_C = a_{C,0} + \xi_0\, \xi + \tau/\tau_0$	$a_{H,0} = 8.1, \tau_{H,0} = 17, \xi_{C,0} = -13$	independent
Le Dréau et al. [213]	int	cont	$a_H = a_{H,0} + \tau/\tau_{H,0}$	$a_{H,0} = 2.87, \tau_{H,0} = 47$	
			$a_C = a_{C,0} + \xi_0\, \xi + \tau/\tau_0$	$a_{C,0} = 2.79, \tau_{C,0} = 35, \xi_{C,0} = -2.69$	independent
Jokisalo and Kurnitski [217]	int	cont	$a_H = a_{H,0} + \tau/\tau_{H,0}$	$a_{H,0} = 2, \tau_{H,0} = 7$	dependent
van den Ham and Linssen [214]	int	int	$a_H = a_{H,0} + \tau/\tau_{H,0}$	$a_{H,0} = 0.81, \tau_{H,0} = 76.92$	
			$a_C = a_{C,0} + \tau/\tau_{C,0}$	$a_{C,0} = 1.83, \tau_{C,0} = 83$	dependent

As the choice of the used method (*i.e.* dependent or independent) affects the final input of the regression analysis - and thus the adapted values for the utilisation factor - the selection of the method must be well considered. Both methods have interesting advantages as well as some considerable limitations, especially considering the effect of intermittency. An overview of the pro's and con's is given in *Table 5.2*. To avoid errors based on inconsistencies between the *quasi-steady-state* and *dynamic* calculation methods (*e.g.* the considered simplified methods do not take into account solar absorbance of opaque construction parts and neglect long wave radiation to the sky, etc. - see *§ 3.4*), the independent methods using the *dynamic* calculation method to gather all input data, are preferable. Among the independent methods, the method as described in *EN ISO 13790* [37] - which is called the black box approach - is chosen.

The black box approach consists of four consecutive series of *dynamic* simulations:
Case 0: The first series of calculations comprises the determination of **the monthly $Q_{H,nd}$ and $Q_{C,nd}$** . For these simulations, a **dual set-point for heating and cooling** is assumed ($\theta_{i,H,set}$ = 20°C and $\theta_{i,C,set}$ = 25°C) allowing for realistic, free-floating indoor temperatures caused by internal and solar heat gains between both set-point temperatures.
Case 1: The second series of calculations comprises the determination of the **'static' monthly heat losses $Q_{H,ht,'stat'}$ and $Q_{C,ht,'stat'}$**. To do so, the same simulations as for 'Case 0' are performed however **all internal and solar heat gains are neglected**. Furthermore, in conformity with the *quasi-steady-state* calculation method of the heat transfer losses, **the extra heat transmission due to thermal radiation to the sky is ignored** by setting the sky temperature equal to the outdoor air temperature. This series of simulations is repeated twice. Once the set-point for heating is set equal to 20°C and once the set-point for heating is set equal to 25°C. The monthly $Q_{H,nd}$ calculated by the first series of simulations is equal to the 'static', monthly $Q_{H,ht}$. The $Q_{H,nd}$ calculated by the latter series of simulations is equal to the 'static', monthly $Q_{C,ht}$.
Case 2: The thirds series of simulations are performed **as part of the determination of the 'static' heat gains**. The same simulations as 'Case 0' are performed **though a high set-point for heating** is used to unsure that all heat gains are effectively used to lower the heat demand and thus no overheating occurs. The output obtained by these simulations is $Q_{H,nd,2}$.
Case 3: For the fourth and last series of simulations, the same simulations as 'Case 2' (thus with a **high set-point temperature for heating**) are performed however - like for 'Case 1' - **all internal and solar heat gains, and the extra heat transmission due to thermal radiation to the sky are neglected**. These extra simulations are performed to determine the total, monthly heat losses of the buildings applying a very high set-point for heating. As, by using an increased set-point temperature for heating in 'Case 2' and thus ensuring that all heat gains are used to lower the heat demand, the 'static', **monthly $Q_{H,gn,'stat'}$ and $Q_{C,gn,'stat'}$** can then be calculated as the difference between the monthly $Q_{H,nd,3}$ and $Q_{H,nd,2}$.

The black box approach calculates $Q_{H/C,gn,'stat'}$ and $Q_{H/C,ht,'stat'}$ in good accordance with the calculation assumptions as described in *EN ISO 13790* [37]. The heat transfer is calculated as the heat flow that is (strongly) dependent on the internal temperature and that is compensated by the output of the heating system or the 'usable' part of the heat gains. The heat gains contain all (solar and

Table 5.2: Determination of the static heat losses and gains used for the calculation of the utilisation factor: overview of the pro's and con's of both the independent and dependent method.

Type	PROs	CONs
independent		
PASSYS [146], EN ISO 13790 [37], Corrado and Fabrizio [34]	+ the same calculation method is used for the calculation of the static and dynamic input data, avoiding errors based on different assumptions and algorithms between methods (*e.g.* long wave radiation sky, ground heat transfer)	- the uncertainty of static output of the dynamic simulations [26] - several dynamic simulations necessary
dependent		
Jokisalo and Kurnitski, [32], Kalema et al. [31], van den Ham and Linssen [214]	+ the regression analysis includes both the gain and losses, and the utilisation factor calculated according the same method leading to a higher accuracy of the overall calculation method + limited number of dynamic simulations	- the accuracy of the correlation depends strongly on (the restrictions of) the method itself and the accuracy of the input • *accuracy of calculated monthly mean indoor temperature in intermittently heated/cooled buildings?* • *use of air or operative temperatures and the impact on the transmission and ventilation losses respectively?*

internal) heat flows that are not or only restrictively dependent on the indoor temperature.

While comparing however the monthly, *quasi-static* thermal losses and gains to the *'static'* thermal losses and gains obtained by the black box approach, some (small) discrepancies may be found. For the heat losses and internal heat gains, the differences remain limited as described in *§ 3.4.4* and demonstrated in *Figure 3.8* (a) and (b). For the solar gains however, the differences appear to be more significant. To analyse the differences in detail, the monthly solar heat gains obtained by the black box approach are compared to the *quasi-static* solar heat gains for a sample of school buildings with varying thermal capacity, energy performance level of the building envelope and WWR (for exact information on the building sample - see *§ 5.3.2*). The results are shown in *Figure 5.2*.

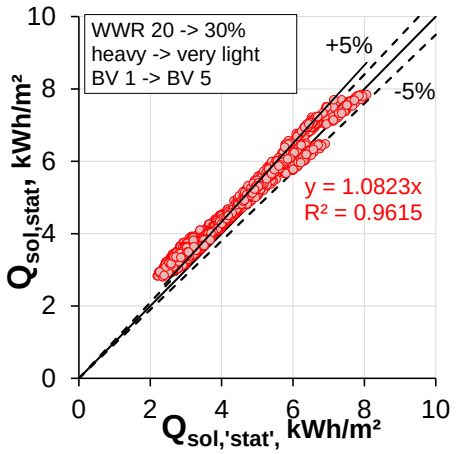

Figure 5.2: Comparison of the monthly entering solar heat gains, normalised to the building floor area (kWh/m^2), obtained by dynamic simulations (black box approach) $Q_{sol,'stat'}$ or as used for the *quasi-steady-state* calculation method $Q_{sol,stat}$.

Overall, *Figure 5.2* shows that the solar heat gains are overestimated in the *quasi-steady-state* calculation method compared to the output of the black box approach: the relative error, averaged over all investigated building variants is 9.1%, with a maximum of 24%. A restricted sensitivity analysis, analysing the impact of the WWR, occurring solar radiation, energy performance of the building envelope and thermal capacity, reveals that the calculation error for the solar heat gains depends mostly on the considered calculation period: the relative error between the solar heat gains calculations, averaged over all building variants, varies from 11.7% in January to 5.2% in April. Furthermore, a slight impact of the WWR is found as the average error between the solar heat gains is 9.8% and 8.2% for a WWR = 30% and WWR = 20%, respectively. The impact of the thermal capacity and the energy performance level of the building envelope appear to be insignificant: the differences between the relative errors, averaged over the various thermal capacities or building variants, are 0.1% or less.

For the *quasi-steady-state* calculation approach applied in Flanders, the monthly averaged solar heat gains are calculated as the short and long wave solar radiation entering the zone through all transparent building parts. Hereby, according to the hypothesis of the black box approach, the en-

tering solar radiation through the glazed surfaces is assumed to be completely absorbed by the cavity surfaces. However, in reality, a fraction of the solar irradiation is reflected outside through the windows [218]. Furthermore, another part of the heat gains is lost by transmission through the external surfaces and hence leaving the zone without affecting considerably the heat balance [26]. Consequently, a certain fraction of the entered solar gains, which depends on the building's characteristics such as the WWR [218, 26], is thus always 'unusable', irrespective of the heat-balance/loss-gain ratio of the building. This fraction is accounted for by the dynamic simulations and thus excluded for the calculation of the heat gains obtained by the black box approach. In the *quasi-steady-state* calculation method however, this fraction is neglected, which explains the over-estimation of the solar gains by the *quasi-static* methods as shown in *Figure 5.2*.

The *quasi-steady-state* calculation of the solar heat gains is hence slightly in conflict with the applied black box cavity hypothesis and may thus jeopardise the accuracy of the obtained calculation results. Research on this particular topic has been performed by Pernigotto [26], who suggested the use of correction factors for the input data (*i.e.* both heat transfer and gains) to improve the accuracy of the *quasi-steady-state* calculation method, and by Olivetti [218] who focused on the improvement of the calculation of the *quasi-static* solar heat gains in particular. As however, this dissertation focuses on school buildings specifically and the implementation of the related typical characteristics in the *quasi-steady-state* calculation methods, the calculation of the solar heat gains is not addressed here. Further research on this particular topic is however highly recommended.

5.2.3 Regression analysis

To determine new values for the correlation-based, numerical parameters, regression analyses are performed. Adapted values can be searched for by minimising the difference x between the dynamically $Q_{H/C,nd,dyn}$ and the statically $Q_{H/C,nd,'stat'}$ calculated energy demand.

$$x = \sum \left(Q_{H/C,nd,dyn} - Q_{H/C,nd,stat} \right)^2 \tag{5.15}$$

with

$$Q_{H,nd,'stat'} = Q_{H,ht,'stat'} - \eta_{H,gn} \cdot Q_{H,gn,'stat'} \tag{5.16}$$

and

$$Q_{C,nd,'stat'} = Q_{C,gn,'stat'} - \eta_{C,ht} \cdot Q_{C,ht,'stat'} \tag{5.17}$$

As the weekly school opening hours are limited and thus the time fraction of the use of schools is small ($f_{occ,monthly}$ = 20% on average, without holidays), the monthly heat gains $Q_{H,gn,'stat'}$ are generally small compared to the monthly heat losses $Q_{H,ht,'stat'}$. This jeopardises the calculation of the *quasi-steady-state* energy balances (*Eq. 5.13* and *Eq. 5.14*) as the two numerators are almost equal while the denominator is small. As a result, the outcome of the regression analysis becomes unreliable. To overcome this mathematical problem, *EN ISO 13790* [37] suggests to perform the

regression analysis on the relative overheating $dT_{R,H}$ instead.

$$dT_{R,H} = \frac{Q_{H,nd,dyn} + Q_{H,gn,'stat'}}{Q_{H,ht,'stat'}} = (1 - \eta_{H,gn})\gamma_H + 1 \tag{5.18}$$

This quantity is mathematically more robust, also for low values of the heat gains. To obtain a more accurate value for $\eta_{H,gn}$ the difference x between the original relative overheating $dT_{R,H,org}$ and the adapted relative overheating $dT_{R,H,adap}$ must be minimised by varying the dynamic parameters $a_{H,0}$ and $\tau_{H,0}$.

$$x = \sum (dT_{R,H,org} - dT_{R,H,adap})^2 \tag{5.19}$$

with

$$dT_{R,H,org} = (1 - \eta_{H,gn,org})\gamma_H + 1 \tag{5.20}$$

and

$$dT_{R,H,adap} = (1 - \eta_{H,gn,adap})\gamma_H + 1 \tag{5.21}$$

For the reevaluation of the numerical parameters for heat demand calculations, the monthly results from October till May are considered. For the numerical parameters for cooling demand calculations, data from April until October are used.

5.3 Building simulation model

This section starts with the description of the school building models used for this research study (*§ 5.3.1*). Next, representative ranges are set for the building's characteristics which possibly affect the utilisation factors: the thermal capacity, the global insulation level, the glazing properties and WWR ratios, the shading device, the air tightness level, the characteristics of the installed heating and ventilation system, and operational characteristics (*§ 5.3.2*). Third and final, this information is combined into a sample of school building design variants which is representative for the contemporary school building stock, using the LHC sampling technique.

5.3.1 Building model

Similar building simulation models as described in *§ 4.3* are used. To limit the number of calculations and the related calculation time, only one building shape is considered for the elementary schools and one for the secondary schools. To incorporate however the impact of various built forms, a rectangular shape is used for the elementary schools. For the secondary schools, the U-shaped built form is selected. Detailed information on the size, shape and room type profile of the models, and on the implementation of the building in `TRNSYS` can be found in *§ 2.2.1* and *§ 4.3.2*, respectively.

5.3.2 Building's characteristics

Thermal capacity: to evaluate the effect of the thermal inertia, the construction type used for the building simulation models is altered, in four discrete steps, between very light and heavy. The materials used for the wall and roof constructions are changed according to *Table 4.1*.

Energy performance level: to incorporate the impact of the energy performance level of the building envelope on the correlation results, the insulation and the air tightness level are varied, in 5 approximately equidistant discrete steps, between an upper limit (= the 'base case' variant corresponding to the legal required limits applicable on the date of the start of this research (dd.2010) [18]) and a lower limit (= the 'best practice' variant based on the average survey results as described in *§ 2.3.2*) in five discrete steps (variant 1 to 5 - see *Table 5.3*). g-values for the glazing are set equal to 0.6. Except for building design variant 5, the g-value is reduced to 0.5 to ensure acceptable summer comfort levels.

Window-to-wall ratio (WWR) and shading devices: The glazed surface area (WWR) is altered in two discrete steps. The lower limit is based on day-lighting and visual comfort requirements (20% [97]). The upper limit is set equal to the average WWR in schools as found in the survey of the Flemish passive schools (30% - see *Figure 2.11*). Two different external shading devices are considered for this study. The first is a system with fixed louvers[3]. When applied on a south-facing façade, they are placed horizontally, on east- and west-facing façades they are titled 30° downwards towards outdoors [125]. The width of the slats is 20 cm and the distance in between the slats is 19.5 cm. The second system is an external, automatically controlled screen. A similar control system as described in *§ 4.3.1* is used. North-facing windows are never provided with a shading device. The selection of shading device is linked to the energy performance level of the building. The higher the energy performance, the more risk for overheating, so the more attention is paid to the installation of shading devices as shown in *Table 5.3*.

HVAC system properties: In line with the general calculation assumptions of the energy demand calculations according to EN ISO 13790 [37], an ideal operation (*i.e.* a perfect control, infinite system output capacity and uniformity of the zonal air temperature) of the heating and cooling system is used for all simulations performed along this chapter. The heating/cooling patterns depend on the aim and the requested output of the performed simulations: the building models are either continuously climatised for the derivation of the utilisation factor (*§ 5.4*) or discontinuously heated or cooled to assess the impact of system intermittency on the energy demand (see *§ 5.5*)). To account for the effect of the type of ventilation and the presence of a heat recovery device on the utilisation of the heat gains, the different school building design variants are equipped either with a simple extraction ventilation system or with a balanced ventilation system with heat recovery. Given the performance level of the building envelope, building design variant one and two are combined with an extraction ventilation system. Building variants three, four and five are provided with a balanced, mechanical ventilation system. If present, an air-to-air heat exchanger with an air-to-air efficiency of 75% is used

[3] For the *dynamic* simulations in TRNSYS, simulation component Type200a for vertical shading device implemented by De Meulenaere in TRNSYS and based on the work of Safer [219] is used.

for the recovery of the ventilation heat losses. The operation of the fans is controlled by a time schedule according to the school opening hours[4], including pre-ventilation to reassure good indoor air quality at any time of occupancy [47].

The efficiency of the HVAC system links the building's energy demand to the building's energy use. As this chapter focuses on energy demand calculations in particular, the production and distribution losses are not included. The influence of the type of emission system is however investigated as it might effect the usability of the occurring (internal) heat gains. Hence, the convective fraction of the heating system is varied from fully convectional (radiative part of the heating is 0%) to a combination of both convective and radiative heating (estimated fraction of the radiative part of the heating by radiators is 40%).

Table 5.3 gives an overview of the five school building design variants included in this study. These building variants are subsequently combined with various operational characteristics (*i.e.* occupant density, ventilation rates and internal heat gains) to obtain a final selection of school buildings, representative for the Flemish school building('s use).

Table 5.3: Selection of energy performance level design variants of the school building simulation models.

	U_{wall} W/(m^{2}K)	U_{floor} W/(m^{2}K)	U_{roof} W/(m^{2}K)	$U_{glazing}$ W/(m^{2}K)	g-value glazing -	n_{50} ACH	shading device
variant 1	0.37	0.37	0.29	1.1	0.6	3.0	fixed (S)
variant 2	0.30	0.24	0.24	1.1	0.6	2.4	fixed (S)
variant 3	0.22	0.19	0.19	1.1	0.6	1.0	fixed (S), movable (E,W)
variant 4	0.15	0.15	0.15	0.8	0.6	0.6	fixed (S), movable (E,W)
variant 5	0.11	0.15	0.13	0.6	0.5	0.4	movable (E,S,W)

Operational characteristics: while assessing the overall robustness and accuracy of the *quasi-steady-state* calculation method, Le Dréau et al. [213] assigned the schedules of ventilation and internal heat loads as the most influential parameters. Hence, to derive more accurate values for the utilisation factors and obtain more accurate calculation results, these parameters must be chosen carefully, in line with the real occupancy of the building [213]. Consequently, realistically varying occupancy (*i.e.* modelled by varying occupant density of the different school rooms and variations of the relative absence factors RA), ventilation (*i.e.* modelled by varying design ventilation flow rates) and internal heat gain schedules (*i.e.* related to the varying occupancy and variations of the partial operational time factor POF) are implemented. While doing so, some extra dynamic parameters are included in the simulations in addition to the variable outdoor temperatures and solar heat gains. The variations of the operational characteristics are set based on their ranges and distribution functions as depicted in *Table 4.3*. The final values used for the *dynamic* simulations are generated from the related distribution functions using the Latin Hypercube sampling technique. For the use of equipment, the deterministic schedules as depicted in *Figure 4.9* are used. For the lighting, automatically controlled lighting schedules are assumed. Long unoccupied periods (*i.e.* holidays) are not included in the operational schedules as these are taken into account separately in the calculation method (see *Eq. 3.16*) [216].

[4] As the ventilation system is time-controlled, a constant air supply during the school opening hours is provided. The implemented ventilation rates are determined in line with the design occupancy density though are not affected by occurring absenteeism expressed by the relative absence factors.

The building is oriented with the main axis along the East-West direction[5].

As different school building variants (*i.e.* different shapes, models for elementary and secondary schools) are used for this study, the results for the energy demand calculations presented along the next sections are expressed per m^2 usable floor area to guarantee comparability of the results.

5.4 Utilisation Factor

In this section, the impact of the school buildings' characteristics on the correlation between the heat-balance/loss-gain ratio's and the utilisation factors is demonstrated. Subsequently, a regression analysis is performed to adapt the values of the numerical parameters used for the calculation of the heating ($a_{H,0}$ and $\tau_{H,0}$ - see *Eq. 5.1*) and the cooling demand ($a_{C,0}$ and $\tau_{C,0}$ - see *Eq. 5.4*) to the typical use and characteristics of schools. The regression analysis is performed in accordance with the methodology and the overall calculation approach as described in *EN ISO 13790* [37]. The 'black box approach' is used to determine the input data for the regression analysis and the utilisation factor is determined for a continuously heated/cooled though intermittently used building (*i.e.* ventilation rates and internal heat gains vary in time).

5.4.1 Calculation of the heat balance

Figure 5.3 shows the results of the calculated monthly $\eta_{H,gn}$ as a function of γ_H for the four classifications of thermal capacity of the building (*i.e.* heavy, medium, light and very light).

In case of low heat-balance ratios (γ_H < 0.3), all the heat gains are used to compensate the heat losses: the gain utilisation factors approximately equal one[6], irrespective of the thermal capacity of the building. In case of high heat-balance ratios (γ_H > 1.5), the utilisation factors equal the reciprocal number of the heat-balance ratio γ_H. In the intermediate zone, as suggested by the current expression (see *Eq. 3.6*), the utilisation factors decrease gradually in relation to the time constant τ of the building however the impact of the thermal capacity differs slightly from the original result, in relation to the U-value of the building envelope and/or the presence of a heat recovery device. To visualise the impact of the typical school buildings' characteristics on the utilisation factor, the currently applied correlation as described in *EN ISO 13790* [37] is compared to the average correlation as found for a time constant τ = 140 h (*i.e.* average value found for the heavy school building models) and a time constant τ = 40 h (*i.e.* average value found for the very light school building models) in *Figure 5.4*.
When analysing both *Figure 5.3* and *Figure 5.4*, three effects are noticed. **(i)** the new curves (see *Figure 5.4*) are slightly lower due to an overall reduction of the gain utilisation factor. As expected

[5]To assess the impact of this simulation assumption, a restricted set of additional simulations is performed on the elementary school building model with a heavy and light structure, orienting the building with the main axis along the North-South direction. As by the parameter analysis included in this chapter, a broad range of gain-loss ratios is covered, the additional simulation results confirm that a varying orientation of the building does not affect the results of the regression analysis.

[6]Due to the use of the black box approach and rounding calculation errors used to determine the 'static' input data, some of calculated values of the utilisation factor are slightly higher than one, which is physically impossible. The excesses remain however limited as all obtained values for $\eta_{H,gn}$ are smaller than 1.04.

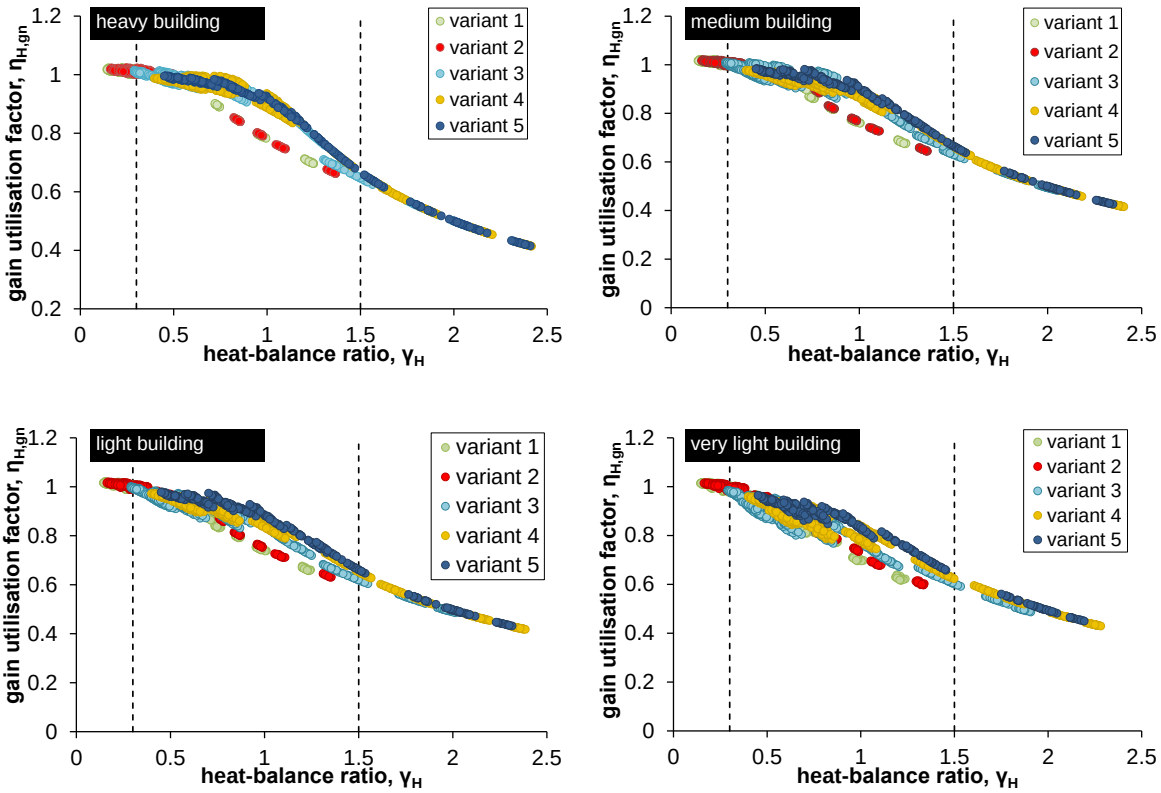

Figure 5.3: Results of the monthly gain utilisation factor $\eta_{H,gn}$ as function of heat-balance ratio γ_H for buildings with varying efficiency level of the building envelope and various thermal capacities.

(see *Figure 3.11*), the changes are slightly more pronounced for the heavy buildings although, overall, the impact of the typical school use on the utilisation factor for heating remains limited. **(ii)** The utilisation factors of the building variants one and two are significantly lower compared to the other results (see *Figure 5.3*) and **(iii)** the largest scattering of the data points is found for the buildings with a (very) low thermal capacity (see *Figure 5.3*). Hereafter, some explanations are given for the aforementioned effects.

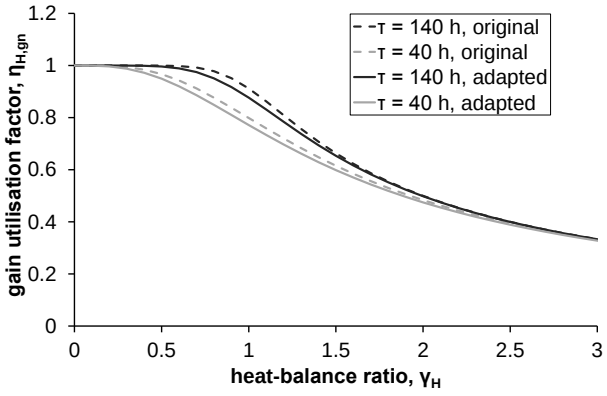

Figure 5.4: Utilisation factor $\eta_{H,gn}$ as a function of the heat-balance γ_H for two time constants (τ = 140 h and τ = 40 h) of a reference school building: impact of typical school buildings' characteristics.

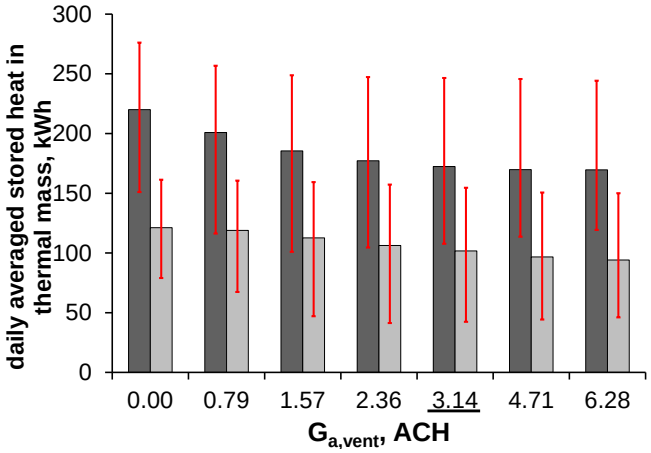

Figure 5.5: Daily averaged amount of heat stored (kWh) in the opaque building parts of the continuously heated though discontinuously occupied and ventilated school building zone 'Class N' of the rectangular elementary school building in May for varying design ventilation rates $G_{a,vent}$ (ACH), varying thermal capacity of the building (heavy - darker grey, very light - light grey) and different boundary conditions (min-max range).

In class rooms, typically, discontinuous but locally very dense occupancy occurs. This results on the one hand in temporary, very high and locally dense internal heat gains (> 35 W/m^2). On the other hand, these densely populated rooms need intense ventilation to guarantee good indoor air quality (*i.e.* in class rooms, during school opening hours, $G_{a,vent}$ = 400 - 500 m^3/h for ± 18 students or 3.14 ACH on average). These high ventilation rates have a negative impact on the heat accumulating capacity of the building structure. *Figure 5.5* shows the impact of increased ventilation rates on the daily averaged amount of heat stored in the opaque building parts of zone 'Class N' during a regular school day in May (8h30 - 15h30) for a heavy (dark grey) and very light building (light grey). The error bars mark the maximum variations due to occurring varying daily gains and loads. As shown, overall, a larger amount of heat is stored in the building mass of a heavy structure. The ventilation rate however affects this heat storage capacity and the effect is more significant in heavy buildings compared to lighter buildings: when changing the ventilation rate from 0 to 58 m^3/(m^2.h), the daily heat stored in the building mass is decreased by 27 kWh in very light and by 50 kWh in the heavy buildings. As class rooms cover about 40% of the total surface area of schools, this explains the general drop of the utilisation factor, mostly noticeable in heavy school buildings.

Furthermore, the effect of the presence of a heat recovery device on the usability of the heat gains is assessed. To do so, a series of additional *dynamic* simulations is performed: the annual heat demand is simulated with and without internal and solar heat gains for the rectangular, elementary school building model with varying energy performance of the building envelope (see *Table 5.3*), thermal capacity (heavy to very light) and heat recovery efficiency (no heat recovery, η_{HR} = 25%, η_{HR} = 75%)). To guarantee an equal amount of (solar) heat gains for all cases, all building variants apply the same shading device (fixed louvres for South-faced windows) and variant 5 is excluded as the g-value of the glazing is lower. For the users' characteristics, the deterministic boundary conditions as set in *Table 4.5* are used. *Figure 5.6* shows the reduction of the annual heat demand

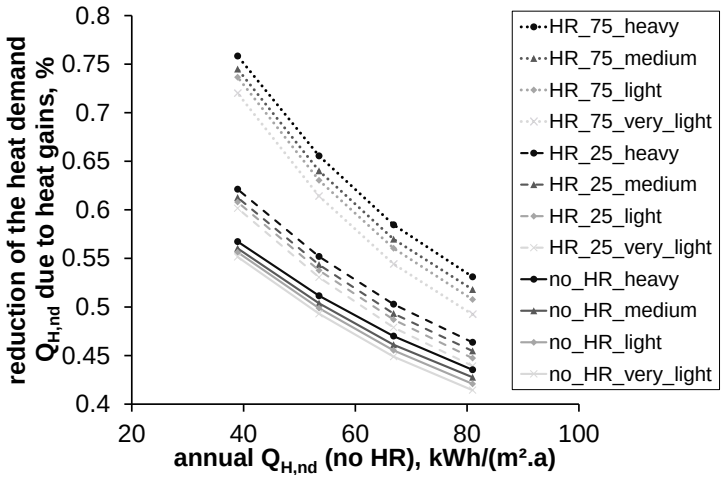

Figure 5.6: Relative impact (%) of the internal and solar heat gains on the heat demand $Q_{H,nd}$ calculations, expressed in kWh per m^2 building floor area, for various school building design variants.

due to the implementation of the solar and internal heat gains $\Delta Q_{H,nd,HG}$ as calculated by *Eq. 5.22*.

$$\Delta Q_{H,nd,HG} = \frac{Q_{H,nd,excl.heatgains} - Q_{H,nd,incl.heatgains}}{Q_{H,nd,excl.heatgains}} \tag{5.22}$$

The figure demonstrates that the impact of the heat gains on the heat demand depends, aside from the energy performance and the thermal capacity of the building envelope, on the efficiency of the heat recovery device. Whereas the implementation of the heat gains leads to a reduction of the annual heat demand of 43% and 56%, on average, for the school building variants 1 and 4 without heat recovery, respectively, the heat demand is reduced by 51% to 74% for the same building variants with heat recovery devices (η_{HR} = 75%). In addition, the figure shows the positive influence of the presence of the heat recovery device on the heat accumulating capacity of the thermal mass. Whereas the impact of the thermal capacity on the heat demand in buildings without a heat recovery device is rather insignificant (($Q_{H,nd,heavy}$ - $Q_{H,nd,verylight}$)/$\overline{Q_{H,nd}}$= ±3%) and independent of the insulation level of the building, the use of heavy structures is clearly beneficial in buildings that implement a heat recovery device. This effect increases in relation to the energy performance level of the building envelope as the annual heat demand of a heavy building is 7 (variant 1) to 15% (variant 4) lower compared to the annual heat demand of buildings with a very light structure.

Curve fitting: determination of $a_{H,0}$ and $\tau_{H,0}$

In this section, the results of the regression analysis and the determination of the adapted values for the numerical parameters $a_{H,0}$ and $\tau_{H,0}$ are described. As discussed in *§ 5.2.3*, for the heat balance, the regression analysis is performed on the relative overheating $dT_{R,H}$ instead of using $Q_{H,nd}$ (see *Eq. 5.18* to *Eq. 5.19*). Prior to the start of the regression analysis, values for the upper and the lower limits for $a_{H,0}$ and $\tau_{H,0}$ are set. In doing so, the physical meaning of the parameters is taking into account. For the current settings, where $a_{H,0}$ = 1, $\lim_{\substack{\gamma_H \to 1 \\ \tau \to 0}} \eta_{H,gn}$ = 0.5, so it is assumed that even in the case of very light weighted structures and for heat-balance ratios equal to one, still half of the

heat gains can be used to lower the heat demand. For the regression analysis, the limits for $a_{H,0}$ are set allowing for variations of utilisation of the heat gains between ± 10 ($a_{H,0}$ = 0.1) and 90% ($a_{H,0}$ = 10) for $\tau \rightarrow 0$ and $\gamma_H \rightarrow 1$. Furthermore, the lower and upper limit for $\tau_{H,0}$ are set equal to 5 and 500, respectively.

The minimum difference between $dT_{R,H,org}$ and $dT_{R,H,adap}$ is found for $a_{H,0}$ = 1.7 and $\tau_{H,0}$ = 25.7. Although monthly output data are used for the regression analysis, the impact of the use of the adapted numerical parameters on the heat demand is evaluated on an annual time basis. After all, it is the objective of the *quasi-steady-state* method to obtain a good assessment of the annual heat demand more than guaranteeing a good estimation of the monthly heat demand [37]. The differences between the annual *dynamic* $Q_{H,nd,dyn}$ and *quasi-steady-state* heat demand $Q_{H,nd,'stat'}$ are shown in *Figure 5.7*[7] using both the original and adapted values for the numerical parameters $a_{H,0}$ and $\tau_{H,0}$. As the largest relative errors are found for school building variants with the lowest heat demands, only the results of building variants 3, 4 and 5 are shown. The figure confirms an overall reduction of the calculation error. The difference between $Q_{H,nd,dyn}$ and $Q_{H,nd,stat}$, averaged over the whole simulated sample of building design variants, is reduced from 0.61 kWh/(m^2.a) to 0.38 kWh/(m^2.a), or from 4.2% to 2.0%. The maximum difference between $Q_{H,nd,dyn}$ and $Q_{H,nd,stat}$ is reduced from 21% to 13%. As shown in *Figure 5.7*, a slight difference of the results in relation to the thermal capacity however remains: the results for the heavy buildings fit slightly better to the *dynamic* calculation results compared to the very light structures. To quantify the differences between the thermal capacities, the amount of investigated cases (%) that falls within the ±5%, ±10% and ±15% confidence bounds - which represent an excellent, very good fit and acceptable fit, respectively [39] - are calculated for a heavy and a very light structure. For the heavy structures, 94.2% of the investigated cases fall within $|\triangle Q_{H,nd}| \leq 5\%$ and the differences remain smaller than 10% for all investigated cases. For buildings with a very light structure, a slightly worse fit is found as only 75.2% of the investigated cases fall within $|\triangle Q_{H,nd}| \leq 5\%$. In 6.8% of the cases, the differences remain > 10%.

Up till now, the same - either original or adapted - values for the numerical parameters $a_{H,0}$ and $\tau_{H,0}$ are used for all building construction types. Panek et al. [215] stated however in a similar research study on the revision of the utilisation factor for heating that different numerical parameters $a_{H,0}$ and $\tau_{H,0}$ should be used for the calculation of the utilisation factor based on the thermal capacity of the building (see *Eq. 5.8* and *Eq. 5.9*). When, according to the work of Panek et al. [215], the values for the numerical parameters are changed in relation to the thermal capacity, a slightly better fit for the *quasi-steady-state* and *dynamic* calculation results is found for the very light buildings: 76% of the investigated cases fall within $|\triangle Q_{H,nd}| \leq 5\%$ and in only 1.3% of the cases differences remain > 10%. For the heavy structures on the other hand, the amount of the investigated cases that falls within $|\triangle Q_{H,nd}| \leq 5\%$ is decreased to 88.5%. Hence, as the impact remains limited and to maintain uniformity among the *quasi-steady-state* calculation methods used for various building typologies,

[7] The results depicted in *Figure 5.7* represent the comparison of the *quasi-steady-state* and *dynamic* heat demand of a **continuously heated** building. Only the impact of **intermittent use** and hence discontinuous occupancy, ventilation and heat gain schedules, is assessed. Furthermore, the input data used for the *quasi-steady-state* calculation (*i.e.* $Q_{H,ht}$ and $Q_{H,gn}$) are the data obtained by the black box approach instead of being calculated according to the *quasi-steady-state* calculation standards. Results differ therefore from the results plotted in *Figure 3.11* (a).

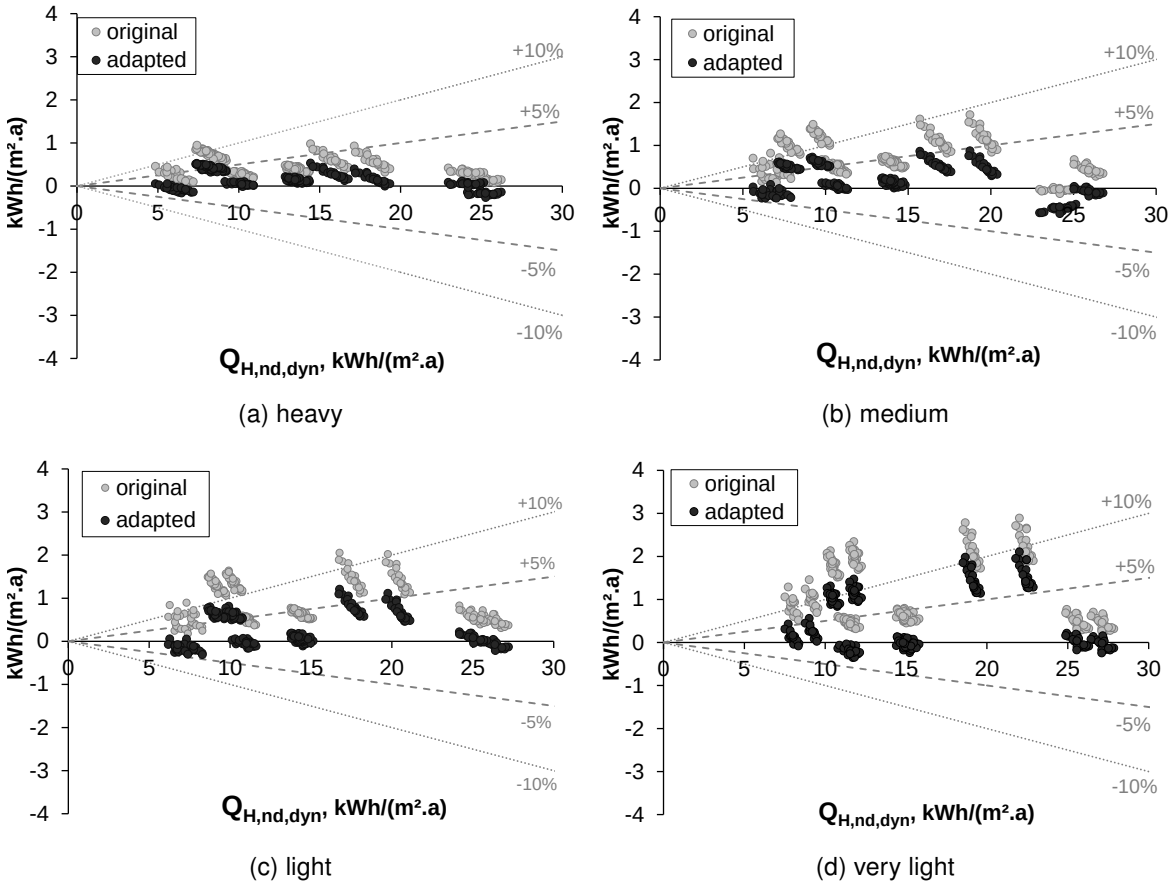

Figure 5.7: The difference between the dynamic $Q_{H,nd,dyn}$ and 'static' heat demand $Q_{H,nd,'stat'}$ in **continuously heated** reference school buildings using the output of the black box approach (*i.e.* $Q_{H,ht}$ and $Q_{H,gn}$) and both the original ($a_{H,0}$ = 1 and $\tau_{H,0}$ = 15) and the adapted numerical parameters ($a_{H,0}$ = 1.7 and $\tau_{H,0}$ = 25.7) as input data for the calculation of $Q_{H,nd,'stat'}$.

no changes to the trend as prescribed in *Eq. 3.6* are suggested.

5.4.2 Calculation of the cooling balance

Figure 5.8 demonstrates the results of the calculated monthly $\eta_{C,ht}$ as a function of the loss-gain ratio γ_C for the four classifications of thermal capacity of the building (*i.e.* heavy, medium, light and very light).

The figures show that the obtained results fit well to the general correlation as proposed by *EN ISO 13790* [37] although, generally, higher values for the $\eta_{C,ht}$ are found. The thermal capacity positively affects the usability of the losses though the impact of the time constant of the building is less significant compared to the original curves. As a result, a lower value of the numerical parameter $\tau_{C,0}$ is to be expected. Similar results are found by Corrado et al. [33].

To visualise the impact of the typical school buildings' characteristics on the utilisation factor, the currently applied correlation as described in *EN ISO 13790* [37] is compared to the average correlation as found for a time constant τ = 140 h (*i.e.* average value found for the heavy school building models) and a time constant τ = 40 h (*i.e.* average value found for the very light school building

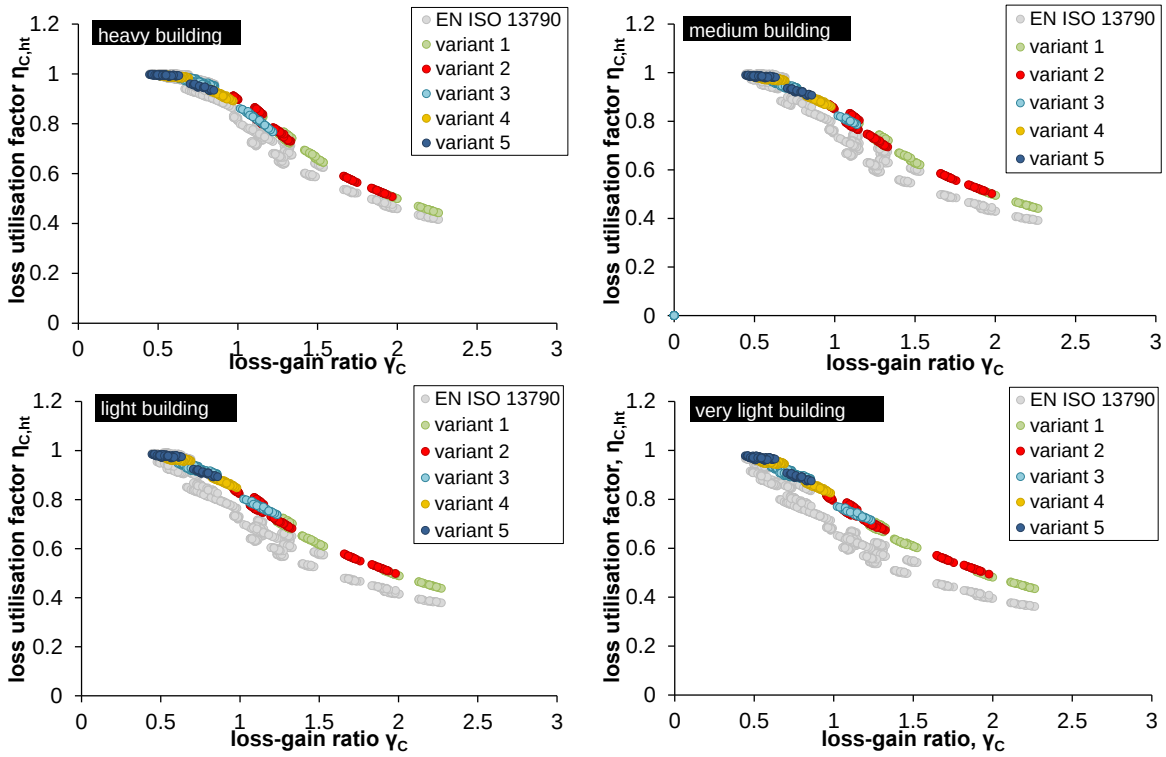

Figure 5.8: Results of the monthly loss utilisation factor $\eta_{C,ht}$ as function of loss-gain ratio γ_C for buildings with varying efficiency level of the building envelope and various thermal capacities. For comparison, the results for the utilisation factors $\eta_{C,Ht}$ calculated according to EN ISO 13790 [37] are added (marked in grey).

models) in *Figure 5.9*.

The overall increase of the loss utilisation factor $\eta_{C,ht}$ can be explained as follows. The $\eta_{C,ht}$ takes account for the unusable part of the heat transfer in lowering the cooling demand, mainly due to a mismatch in time of the occurring losses and cooling demands [37]. In class rooms however, due to the high occupancy and related ventilation rates, the occurring internal heat loads are generally coupled with (potentially) high heat losses. Moreover, as the outdoor air temperatures in Belgium -

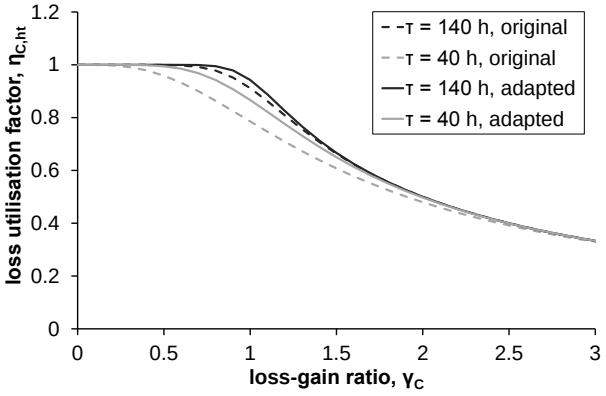

Figure 5.9: Utilisation factor $\eta_{C,ht}$ as a function of the loss-gain ratio γ_C for two time constants (τ = 140 h and τ = 40 h) of a reference school building: impact of typical school buildings' characteristics.

based on the weather data file of Uccle used for the simulations in TRNSYS [166] - are often lower than the set-point temperature for cooling ($\theta_{e,daily,air,max}$ = 24.5°C), these ventilation losses offer considerable cooling capacity. Hence, as heat gains and losses are matched in time, the usability of the losses is positively affected, which explains the increase of the utilisation factor as shown in *Figure 5.8*.

Curve fitting: determination of $a_{C,0}$ and $\tau_{C,0}$

For the regression analysis, a minimum difference between the dynamically calculated cooling demand $Q_{C,nd,dyn}$ and the statically calculated cooling demand $Q_{C,nd,stat}$ is found for the numerical parameters $a_{C,0}$ = 2.5 and $\tau_{C,0}$ = 10. The differences between the annual *dynamic* $Q_{C,nd,dyn}$ and quasi-steady-state cooling demand $Q_{C,nd,'stat'}$ calculated using both the original and adapted values for the numerical parameters $a_{C,0}$ and $\tau_{C,0}$ are shown in *Figure 5.10*.

The figure confirms a general reduction of the error between the quasi-steady-state and *dynamic* calculation results: while using the adapted values for the numerical parameters, the annual cooling demand $Q_{C,nd}$ is calculated approximately within an accuracy of 0.5 to 1 kWh/(m^2.a). Due to the small cooling demands $Q_{C,nd}$ however, the relative differences remain rather high. For the heavy

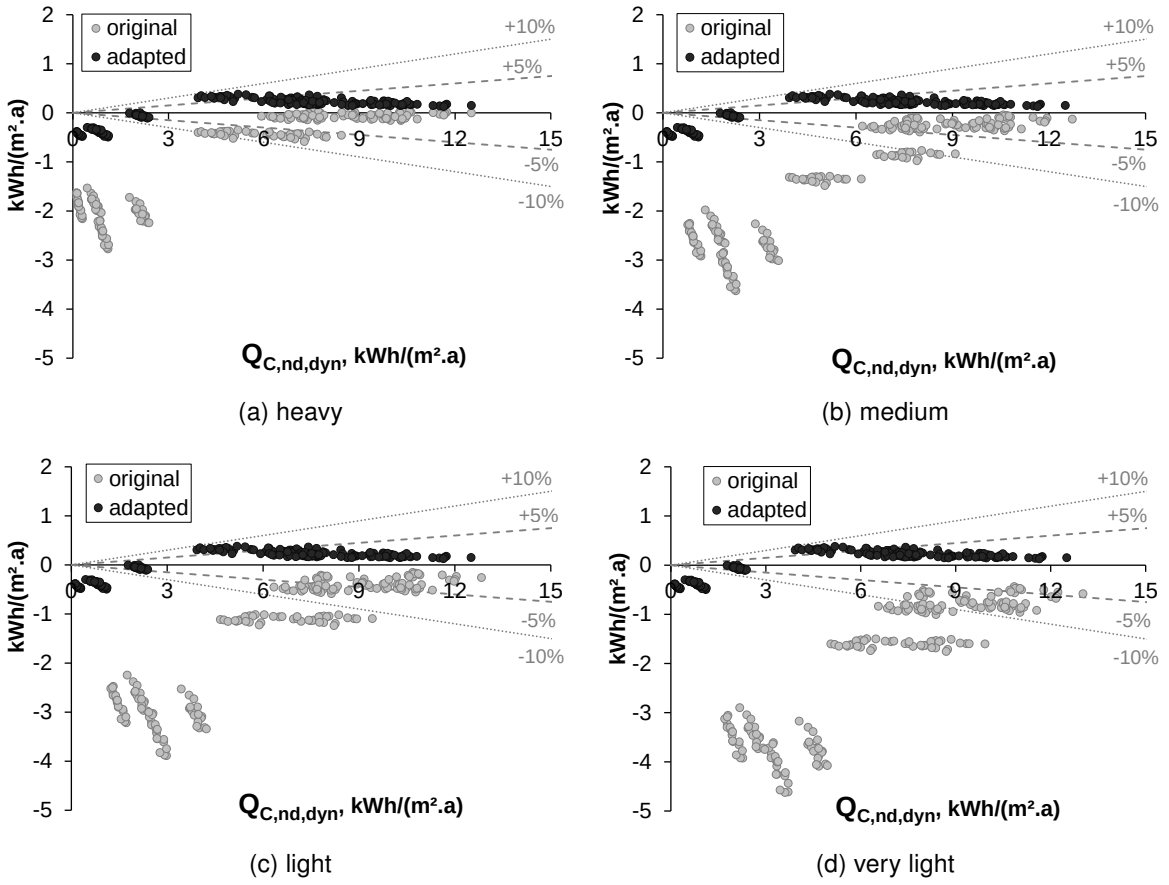

Figure 5.10: The difference between the dynamic $Q_{C,nd,dyn}$ and 'static' cooling demand $Q_{C,nd,'stat'}$ in **continuously cooled** reference school buildings using the output of the black box approach (*i.e.* $Q_{C,ht}$ and $Q_{C,gn}$) and both the original ($a_{C,0}$ = 1 and $\tau_{C,0}$ = 15) and the adapted numerical parameters ($a_{C,0}$ = 2.5 and $\tau_{C,0}$ = 10) as input data for the calculation of $Q_{C,nd,'stat'}$.

school building design variants, 62% falls within $|\triangle Q_{C,nd}| \leq 5\%$ and for 70.5% of the simulated building variants, the differences are < 10% . For the school buildings with a very light structure, a slightly better fit is found as 72.5% of the investigated cases fall within $|\triangle Q_{C,nd}| \leq 5\%$ and differences remain < 10% for all cases.

Corrado et al. [34] and Le Dréau et al. [213] added a an extra numerical parameter $\xi_{C,0}$ to the equations for the utilisation factor in addition to the time constant of the building (see *Eq. 5.5* and *Eq. 5.7*). Similarly, an extra regression analysis is performed adding $\xi_{C,0}$ to the correlation. A minimum difference between the dynamically calculated $Q_{C,nd,dyn}$ and the statically calculated cooling demand $Q_{C,nd,stat}$ is found for the numerical parameters $a_{C,0}$ = 3.0, $\tau_{C,0}$ = 10 and $\xi_{C,0}$ = 1.9. Results are shown in *Figure 5.11*.

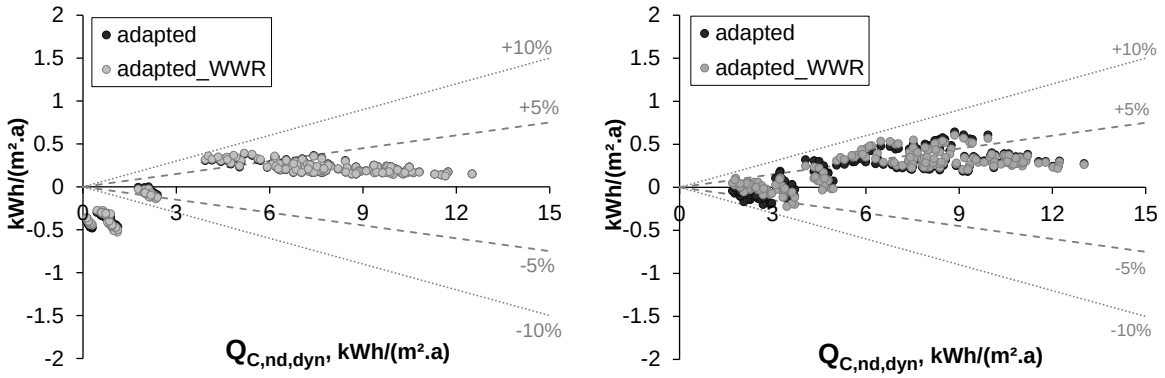

(a) heavy (b) very light

Figure 5.11: The absolute difference between $Q_{C,nd,dyn}$ and $Q_{C,nd,'stat'}$, both normalised to the building floor area (kWh/(m^2.a)) using the adapted correlation-based numerical parameters indepedent ($a_{C,0}$ = 2.5 and $\tau_{C,0}$ = 10) or dependent of the window-to-wall-ratio ($a_{C,0}$ = 3.0, $\tau_{C,0}$ = 10, $\xi_{C,0}$ = 1.9)

As for the simulations results performed in the context of this research study no significant correlation with the WWR is found, the impact of adding an extra parameter $\xi_{C,0}$ in relation to the window surface area on the accuracy of the quasi-steady-state calculation method is negligible, especially for the heavy buildings (see *Figure 5.11* (a)). For the very light buildings, a slightly better fit is found for the lowest cooling demands though overall the effect is limited (see *Figure 5.11* (b)). Therefore, in line with *§ 5.4.1*, no changes to the trend as prescribed in *Eq. 3.7* are suggested.

5.5 The effects of system intermittency on the building's energy demand

In *§ 5.4*, it is shown that more accurate results for the *quasi-steady-state* energy demand calculations in continuously heated or cooled buildings can be obtained compared to the *dynamic* calculation results when the utilisation factor is linked to the typology of the building and the related boundary conditions. For intermittently heated/cooled buildings however, as declared by Kokogiannakis [30]

and Corrado et al. [220], the accuracy of the energy calculation results is simultaneously determined by the applied calculation approach to account for system intermittency. Further revision of the *quasi-steady-state* method for strongly intermittently climatised buildings such as *e.g.* schools is therefore necessary.

To do so, the thermal behaviour (*§ 5.5.1*) and the related energy savings (*§ 5.5.2*) of a series of intermittently climatised school buildings are studied by *dynamic* simulations in TRNSYS. The same sample of school building design variants as applied for the derivation of the utilisation factor (see *§ 5.3.1*) is used. The sample is however restricted to the elementary school buildings. All building design variants are combined with an ideal heating/cooling system using a set-point temperature for heating $\theta_{i,H,set,occ}$ = 20°C and a set-point for cooling $\theta_{i,C,set,occ}$ = 25°C when the building is occupied. When the building is unoccupied, either a setback ($\Delta\theta_{i,H/C,set}$ = 3 K[8]) or a switch off pattern[9] is applied.
Subsequently, the calculation approaches as currently applied to implement these effects in different *quasi-steady-state* calculation standards are evaluated (*§ 5.6.1*). Finally, based on the results of *dynamic* simulations and additional regression analyses, the *quasi-steady-state* calculation methods are further revised and adapted to the typical school use.

5.5.1 Impact of heating system intermittency on indoor temperature variations

In intermittently climatised buildings the set-point temperature profiles coincidence with the occupancy profiles. Instead of maintaining a constant temperature, heating/cooling is reduced or completely switched off during time of absence. The related energy savings depend on the effectiveness of the temperature set-back: the real temperature decrease/increase is not necessarily (immediately) equal to the (theoretically) forced setback but fluctuates in relation to the intermittency pattern (*i.e.* number of hours of plant operation, the applied heating pattern (*i.e.* switch off or set-back) and the applied temperature reduction), the thermal capacity, outdoor climate and energy performance level of the building envelope [145].

The results of the *dynamic* simulations are depicted in *Figure 5.12* and *Figure 5.13*. The average daily mean indoor temperature $\theta_{i,daily}$ is plotted in function of the daily mean outdoor temperature $\theta_{e,daily}$ according to the assessment method of Kalamees et al. [221]. $\theta_{i,daily}$ is calculated by sorting the daily indoor temperature for each building variant according to the outdoor temperature, using intervals of 1°C. Averaging the values per interval leads to a mean value for a specific outdoor temperature. The average results are marked with the dashed lines. For comparison - and if applicable - the averaged indoor temperature for the energy calculations according to the adjusted temperature approach of *EN ISO 13790* [37] (= 17.6°C, see *§ 3.2.1*) is added in red.
Figure 5.12 shows the maximum variation of $\theta_{i,daily}$ in function of the **thermal capacity**. *Figure 5.13* shows the results for varying **energy performance levels** of the building envelope.
As shown in *Figure 5.12*, the thermal capacity has a positive influence on the indoor temperatures

[8] A setback of 3 K is selected in accordance with the requirements for quasi-continuously heated/cooled buildings and hence the adjustment temperature approach as described in EN ISO 13790 [37] (see *Eq. 3.13*)

[9] In case of switched off heating, a minimum indoor temperature of 5°C is maintained to avoid frost damage.

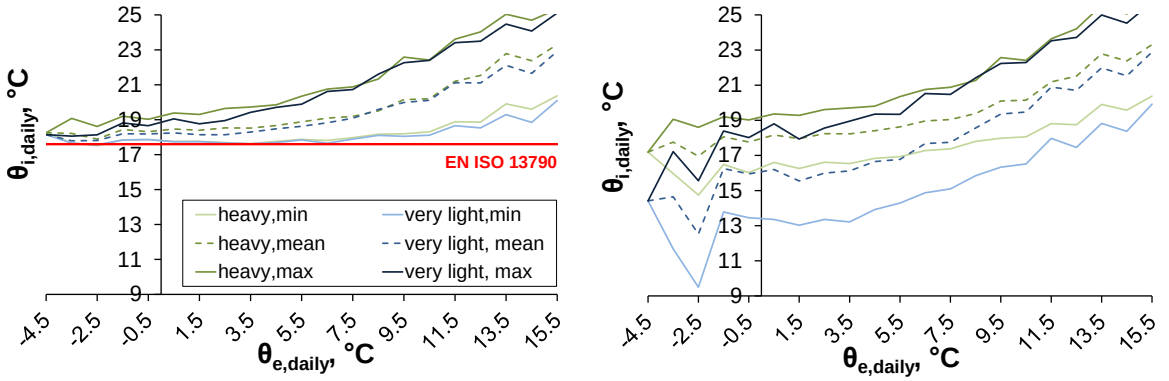

(a) setback (b) switch off

Figure 5.12: The average daily mean indoor temperatures $\theta_{i,daily}$ (°C) as a function of the daily mean outdoor temperature $\theta_{e,daily}$ (°C) for a selection of elementary school building design variants with various **thermal capacities** implementing (a) a setback temperature or (b) a switch off heating pattern - dashed line shows the mean results.

as (slightly) higher $\theta_{i,daily}$ are found in buildings with a high thermal capacity. The impact of the construction type (heavy - light) is however limited for those buildings that implement a setback temperature. Considering the heating season (*i.e.* $\theta_{e,daily}$ < 15.5°C), the average temperature difference between the heavy and light structures is smaller than 0.3°C. Moreover, approximately equal minimum mean indoor temperatures ($\theta_{i,daily,min}$ = 17.5°C) are found for the heavy and light buildings. The impact of the thermal capacity is however more pronounced in those cases that switch off heating completely while absent. The average temperature difference between the heavy and light structures is 1.6°C for the heating season. Furthermore, a larger difference between the minimum mean indoor temperatures for the various construction types is found: $\theta_{i,daily,min}$ = 14.7°C in the heavy buildings while $\theta_{i,daily,min}$ = 9.5°C for the very light buildings.

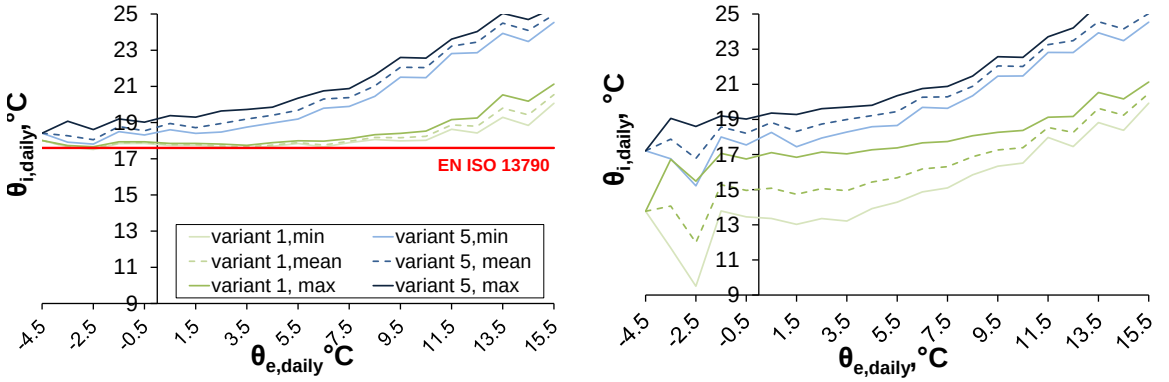

(a) setback (b) switch off

Figure 5.13: The average daily mean indoor temperatures $\theta_{i,daily}$ (°C) as a function of the daily mean outdoor temperature $\theta_{e,daily}$ (°C) for a selection of elementary school building design variants with **varying energy performance levels** of the building envelope implementing (a) a setback temperature or (b) a switch off heating pattern - dashed line shows the mean results.

The impact of the energy performance level of the building on the indoor temperatures is shown in *Figure 5.13*. The $\theta_{i,daily}$ increases significantly if the energetic quality of the building is enhanced. Considering the heating season, the $\theta_{i,daily}$ in building variant 5 is on average 2.4°C (setback) and 4.1°C (switch off) higher than the temperatures in building variant 1. Similar results are found by Deurinck et al. [222] and in previous work done by the authors [204, 223] studying the impact of boundary conditions and building's characteristics on the indoor temperatures in (terraced) dwellings and school buildings, respectively.

5.5.2 Energy saving potential of system intermittency

Energy saving potential of intermittent heating

The impact of the **thermal capacity** on the energy saving potential (calculated according to *Eq. 5.12*) due to intermittent heating is shown in *Figure 5.14*. An extra graph is added that shows the calculated average intermittency factors $a_{H,red}$ used in the calculation method to express the energy demand of intermittently heated buildings as a fraction of the energy demand of continuously heated buildings (see *Eq. 3.13*). The energy saving potential due to intermittent heating is clearly influenced by the thermal capacity of the building. Generally, the higher the thermal capacity, the lower the energy saving potential and thus the higher values are found for the reduction factor $a_{H,red}$. The impact of the thermal capacity on the energy savings differs however depending on the applied heating pattern: energy savings vary from 5.9 kWh/(m^2.a) (heavy) to 10.8 kWh/(m^2.a) (very light) on average when applying a switch off whereas the energy saving potential is 4.8 kWh/(m^2.a) (heavy) and 6.1 kWh/(m^2.a) (very light) on average in buildings that apply a setback temperature for heating. Similar results are found in the studies of Loga et al. [38] and Corrado et al. [220].
The influence of the thermal capacity is however only affecting the cool down/re-heat process. Once the setback temperature is reached (steady-state conditions), heat losses are not further influenced by the thermal capacity. This explains why the saving potential is almost equal for the medium, light and very light structures. The impact of the thermal mass is limited as relatively short cool down periods occur. Using a complete switch off, the cool down process is much larger. The indoor tem-

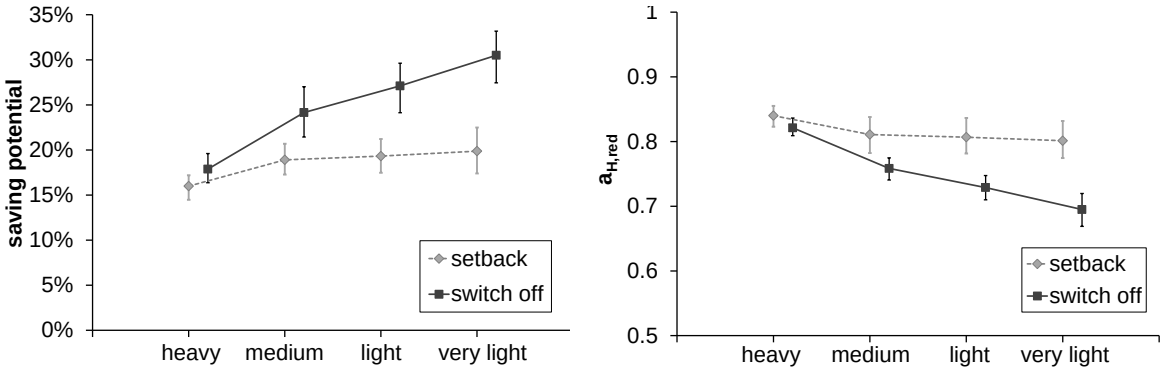

(a) average relative saving potential

(b) intermittency factor $a_{H,red}$

Figure 5.14: The average energy saving potential in **intermittently heated** schools implementing a reduced set-point temperature or a switch off heating pattern for a varying **thermal capacity**. The related confidence bounds (25 – 75%) are marked by the error bars.

perature can decrease much more so the effect of the re-heat process becomes dominant which benefits clearly the use of lighter structures.

The reduction of the energy savings in highly capacitive buildings can be explained by the fact that the effect of temporarily stored heat gains and the introduction of setback or switch off heating patterns are contra productive. In continuously heated buildings, the energy demand is positively affected by the implementation of thermal mass. Due to the extra capacity, more 'unused' heat gains can be temporarily stored and be used on a later time step when less instantaneous heat gains are available. In discontinuously heated buildings however, due to these extra stored heat gains, the indoor temperatures decrease less in buildings with a high thermal capacity (see *Figure 5.15*) which leads to higher heat transfer losses and thus lower potential energy savings.

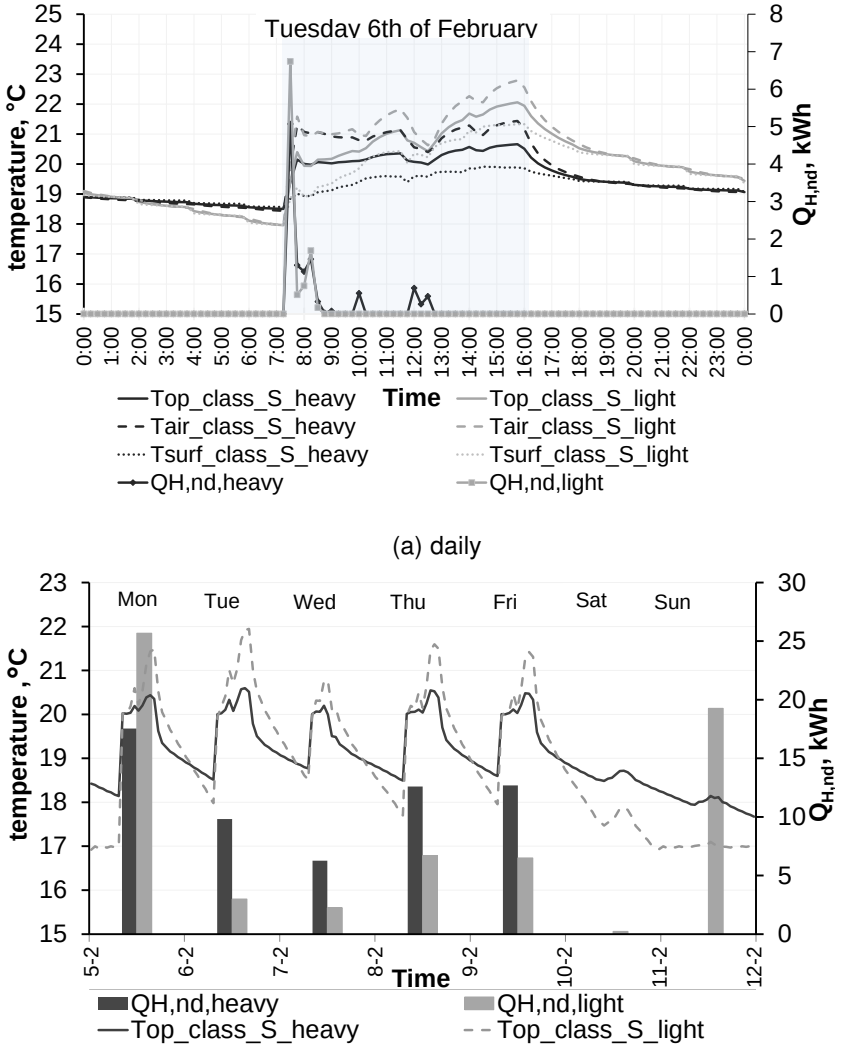

(a) daily

(b) weekly

Figure 5.15: Daily/weekly heating and temperature pattern (ideal heating assumed) on a regular school day in winter for the rectangular, reference elementary school building, oriented with the main axis along the East-West direction, a global insulation level of U = 0.17 W/(m^2K), n_{50} = 0.6 ACH and with the building structure altered between heavy and light.

To visualise, the temperature variations on a regular school day (see *Figure 5.15* (a)) and a regular school week (see *Figure 5.15* (b)) in winter are plotted for one of the included school building design variants. *Figure 5.15* (a) shows the air, operative and mean surface temperature of the class zone oriented to the South (class_B - see *Figure 4.1*) for a light and heavy elementary school building on Tuesday 6th of February. *Figure 5.15* (b) shows the operative indoor temperature and the corresponding energy demand for heating of the same school zone for a regular school week in winter (Monday 5th - Sunday 12th of February). Both figures demonstrate the damping effect of the thermal mass on the temperature drop during absence: temperatures decrease less in highly capacitive (school) buildings. The operative temperature in zone 'class S' at the beginning of the school day (see *Figure 5.15* (a)) has dropped from 21.5°C to 18°C for the light building. The temperature of the heavy building is at that moment still 18.5°C. For heavy structures, the lowered set-point temperature for heating is not reached during the whole week so no heating is required during nights (see *Figure 5.15* (a)) and weekends (see *Figure 5.15* (b)). On the other hand, during the day, the energy demand for heating of the heavy structures is mostly larger as more constructive mass needs to be heated. Both points explain why the effect of highly capacitive buildings is less positive in intermittently heated buildings compared to continuously heated buildings.

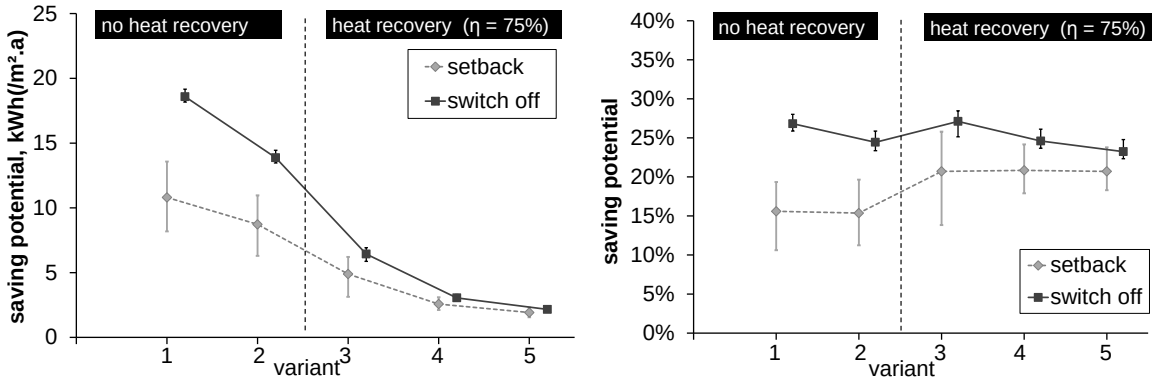

(a) average absolute saving potential

(b) average relative saving potential

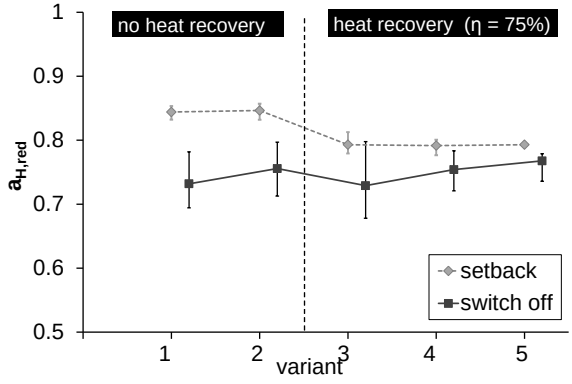

(c) intermittency factor, $a_{H,red}$

Figure 5.16: Energy saving potential in **intermittently heated** schools implementing a setback or a switch off heating pattern for various **energy performance levels** of the building envelope. The related confidence bounds ($25-75\%$) are marked by the error bars.

The energy saving potential of a building due to intermittent heating is additionally influenced by the **energy performance level** of the building (see *Figure 5.16*). The more energy efficient the building, the more slowly the indoor temperatures decrease and consequently the less effective the setback/switch off is and hence the lower the energy saving potentials are. For building variant 1 the averaged energy saved due to heating intermittency is 10.8 kWh/(m^2.a) (setback) and 18.6 kWh/(m^2.a) (switch off). For building variant 5, the averaged energy savings are limited to 1.9 kWh/(m^2.a) (setback) and 2.2 kWh/(m^2.a) (switch off). Additionally, as in more energy efficient buildings the reduction of the indoor temperature is limited and the average temperatures are less influenced by the heating pattern, the effect of introducing a larger setback temperature becomes much less effective.
The difference of the relative energy saving potential for buildings with a heat recovery device is due to a drop of the heat demand $Q_{H,nd}$ in the continuously heated buildings more than due to a drop in the savings due to intermittency.

Energy savings due to cooling intermittency

Similar *dynamic* simulations are performed to assess the energy saving potential due to intermittent cooling. Results are shown in *Figure 5.17* for varying **thermal capacities**. Similar to the results as found for intermittent heating, *Figure 5.17* shows that for higher thermal capacities, lower energy savings are obtained. The influence of the thermal capacity on the energy savings is however less influenced by the cooling settings (setback or switch off). Due to the diurnal outdoor temperature and solar radiation patterns, smaller energy savings and smaller differences between the setback and switch off cooling pattern are to be expected which is confirmed by the simulation results. In buildings using a setback, energy savings vary from 0.4 (heavy) to 1.0 kWh/(m^2.a) (very light), on average. In buildings switching off the cooling, similar results are found for heavy buildings whereas for the very light buildings slightly higher savings are found (= 1.1 kWh/(m^2.a)). The large spread (25 – 75% confidence interval) of the relative energy savings for cooling is due to an overall small cooling demand.

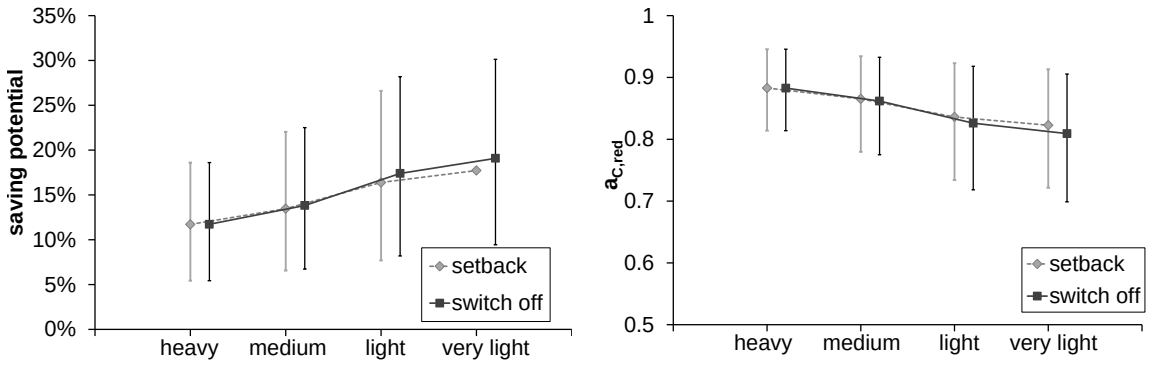

(a) average relative saving potential

(b) intermittency factor, $a_{C,red}$

Figure 5.17: Energy saving potential (%) in **intermittently cooled** schools implementing a reduced set-point temperature of 30°C or a switch off cooling pattern for varying **thermal capacity**. The related confidence bounds (25 – 75%) are marked by the error bars.

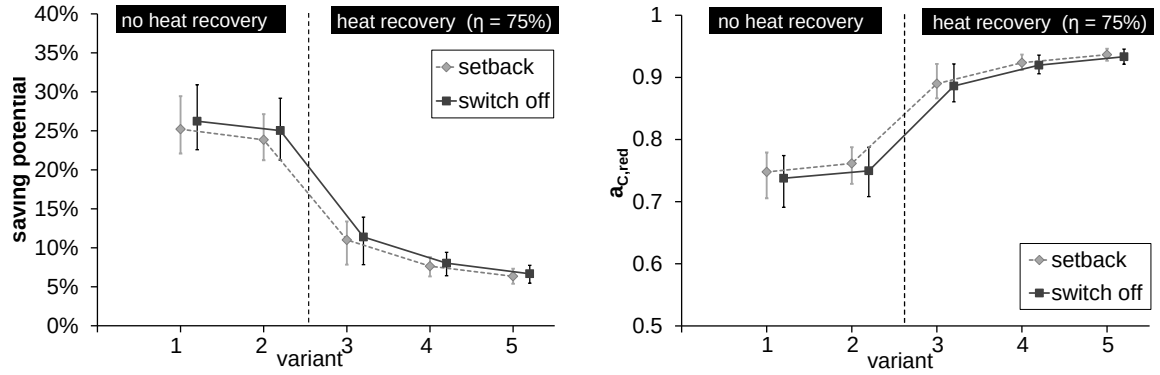

(a) average relative saving potential

(b) intermittency factor, $a_{C,red}$

Figure 5.18: Averaged energy saving potential (%) in **intermittently cooled** schools implementing a reduced set-point temperature or a switch off cooling pattern for various energy performance levels of the building envelope. The related confidence bounds (25-75%) are marked by the error bars.

To analyse the impact of the **energy performance level** of the building on the energy savings due to intermittent cooling, results are shown in *Figure 5.18*. The more energy efficient the building, the faster the indoor temperatures increase due to occurring internal and solar heat gains. Consequently, the applied cooling patterns are less effective and lower energy saving potentials are found compared to less energy efficient buildings. Similar results are found by Loga et al. [38]. For building variant 1, the cooling demand $Q_{C,nd}$ decreases by $\pm 25\%$ (setback) on average due to intermittent cooling. For building variant 5, the average reduction of the cooling demand $Q_{C,nd}$ is however limited to 6.3% for a setback and 6.7% for a switch off cooling pattern.

The simulation results clearly emphasise the impact of the thermal capacity and energy performance of the building - both combined in calculation of the time constant $\tau = C_m/(H_{tr}+H_{ve})$ - on the energy saving potential due to system intermittency. The following general conclusions are drawn:

- The energy saving potential due to system intermittency is the highest in buildings with a low time constant.
- The results show the importance of the setback temperature, especially in buildings with a lower time constant. For these buildings, switching off the heating is much more beneficial than the application of a setback heating pattern. In buildings with high time constants on the contrary, the impact of the applied heating or cooling pattern is less significant.
- The effect of system intermittency on the energy demand is more significant for heating than for the cooling season.

5.6 Implementation of heating intermittency's energy savings in the quasi-steady-state calculation method

In this section, a quantitative comparative analysis of the different *quasi-steady-state* methods used for the calculation of the energy demand as described in *§ 3.2.1* (*EN ISO 13790* [37], *EPR* [22], *DIN V 18599* [43], *NEN 7120* [44]) is made. The analysis focuses on heat demand calculations in

particular as the results of the previous section show that the effect of system intermittency is much more significant for heating than for cooling. Furthermore, as the number of daily operating hours is limited (school closes around 15h30 - 16h) and schools are commonly closed during summer (July and August), the annual cooling demand in schools remains low, even in high performance schools (see *Figure 2.16*).

5.6.1 Comparative analysis of the quasi-steady-state calculation methods for the heat demand in intermittently heated buildings

The heat demand of a series of intermittently heated school buildings is calculated according to *EN ISO 13790* [37], *EPR* [22], *DIN V 18599* [43] and *NEN 7120* [44] and is compared to the results of *dynamic* simulations in TRNSYS. As this section focuses specifically on the evaluation of the accuracy of the implementation of heating intermittency in the *quasi-steady-state* method, only this aspect of the method is reviewed here. In concrete, this means that for all of the considered *quasi-steady-state* methods, the same values for the numerical parameters are used for the calculation of the utilisation factors $\eta_{H,gn}$ ($a_{H,0}$ = 1.7, $\tau_{H,0}$ = 25.7 - see *§ 5.4.1*) and that the same deterministic boundary conditions are applied (see *Table 4.5*) in all methods. The results are shown in *Figure 5.19*[10] (a) and (b) for heavy and very light school building design variants, respectively.

The amount of investigated cases (%) that falls within the ±5%, ±10% and ±15% confidence bounds are depicted in *Table 5.4*.

Table 5.4: Amount of quasi-steady-state calculation results that show an acceptable (±15%), very good (±10%) or excellent (±5%) fit to the *dynamic* calculations.

	$Q_{H,nd,ENISO13790}$	$Q_{H,nd,EPR}$	$Q_{H,nd,DIN}$	$Q_{H,nd,NEN7120}$
$\lvert \Delta Q_{H,nd} \rvert \leq 5\%$	13.0%	44.3%	57.6%	23.9%
$\lvert \Delta Q_{H,nd} \rvert \leq 10\%$	20.5%	74.5%	86.6%	42.3%
$\lvert \Delta Q_{H,nd} \rvert \leq 15\%$	33.0%	93.8%	96.3%	55.5%

As shown in *Figure 5.19* and *Table 5.4*, the worst fit is found for *EN ISO 13790* [37], especially for very light buildings where the differences between the *dynamic* and the *quasi-steady-state* heat demand calculated according to *EN ISO 13790* [37] run up to 40 kWh/(m^2.a) or > 65%. This is mainly due to the fact that the newly derived value for the correction factor $\tau_{H,0}$ is also used to calculate the impact of system intermittency (see *Eq. 3.15*), leading to a strong overestimation of the reduction factor $a_{H/C,red}$, mostly noticeable for very light buildings. The calculation method for system intermittency - and more in particular the use of the correlation based parameters $b_{H,red}$ - as applied in *EN ISO 13790* [37] must therefore be reevaluated. Regarding the results of the other calculation standards, the differences between the *dynamic* and *quasi-steady-state* calculation results are less significant. Nevertheless, as the application of the newly derived values for the numerical parame-

[10] The differences between the results depicted in *Figure 5.19* and *Figure 3.11* (a) are due to the fact that different adapted numerical parameters are used. For *Figure 5.19*, the adapted values for the numerical parameters as set in *§ 5.4.1* (*i.e.* $a_{H,0}$ = 1.7 and $\tau_{H,0}$ = 25.7) are used while in *Figure 3.11* (a), the original values as found in *EN ISO 13790* [37] (*i.e.* $a_{H,0}$ = 1 and $\tau_{H,0}$ = 15) are used.

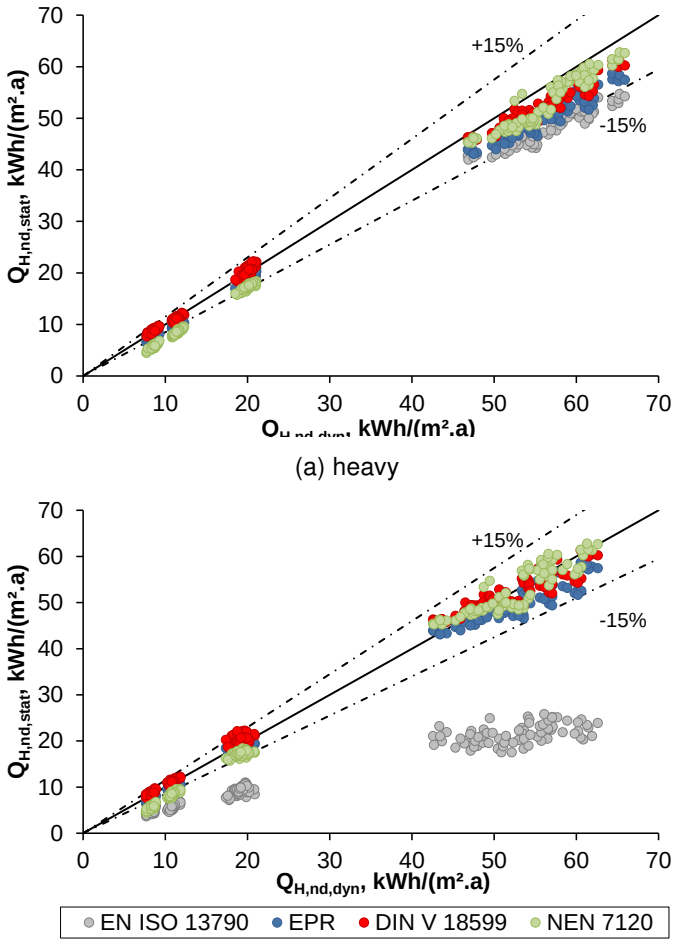

(a) heavy

(b) very light

Figure 5.19: Quantitative comparative analysis of the dynamically and statically average annual $Q_{H,nd}$, both normalised to the building floor area (kWh/(m^2.a)), for **intermittently** heated school buildings with varying thermal capacities and efficiency level of the envelope. For the quasi-steady-state calculations, the adapted numerical parameters $a_{H,0}$ = 1.7 and $\tau_{H,0}$ = 25.7 are used.

ters $a_{H,0}$ and $\tau_{H,0}$ seems insufficient to bring the inter-method match of the *quasi-steady-state* and *dynamic* calculation results to an acceptable level (*i.e.* all buildings fall within $\mid \Delta Q_{H,nd} \mid < 15\%$), it is investigated if the *quasi-steady-state* results can be further improved by modifying the applied calculation approach to account for system intermittency.

As described in *Chapter 3*, either the **adjusted temperature approach** or the **adjustment or intermittency** factor approach (*§ 3.2*) are used. It depends however more on the calculation standard than on the applied calculation approach which of the previously mentioned influencing building/system characteristics are effectively taken into account. A summary of the calculation procedures including the numerical parameters used to calculate the effects of intermittency is given in *Table 5.5*.

The following two proposals are defined to further improve the accuracy of the *quasi-steady-state* calculation method:

Table 5.5: Literature overview: different simplified calculation approaches to account for system intermittency.

Calculation standard	Calculation approach	Numerical parameters
EN ISO 13790 *[37]*	**Intermittency factor approach** $a_{H,red}$ = 1 - $b_{H,red}$ γ_H $\tau_{H,0}/\tau$ (1-$f_{H,hr}$)	$b_{H,red}$ = 3, $\tau_{H,0}$ = 25.7, $f_{H,hr}$ = 0.2
EPR *[22]*	**Adjusted temperature approach** $\theta_{i,H}$ = 19°C	
DIN V 18599 *[43]*	**Adjusted temperature approach** $\theta_{i,set,H,adj,occ} = max(\theta_{i,H,set,occ} - f_{nocc}(\theta_{i,H,set,occ} - \theta_e), \theta_{i,H,set,occ} - \frac{\triangle\theta_{i,H,set} t_{nocc}}{24})$ $\theta_{i,set,H,adj,nocc,we} = max(\theta_{i,H,set,occ} - f_{nocc,we}(\theta_{i,H,set,occ} - \theta_e), \theta_{i,H,set,occ} - \triangle\theta_{i,H,set})$	$\triangle\theta_{i,H,set} = 4K$
NEN 7120 *[44]*	**Adjustment approach** $a_{H,red,night}$ = $\frac{(24-t_{H,h,low})+t_{H,h,low}(c_{H,red,1}-(\frac{c_{H,red,2}^2}{4c_{H,red,3}}))}{24}$ if $\frac{t_{H,h,low}}{\tau} > \frac{c_{H,red,2}}{2c_{H,red,3}}$ $\frac{(24-t_{H,h,low})+t_{H,h,low}(c_{H,red,1}-c_{H,red,2}(\frac{t_{H,low}}{\tau})+c_{H,red,3}(\frac{t_{H,h,low}}{\tau})^2)}{24}$ if $\frac{t_{H,h,low}}{\tau} \leq \frac{c_{H,red,2}}{2c_{H,red,3}}$ $a_{H,red,we}$ = $\frac{(7-t_{H,day,low})+t_{H,daylow}(c_{H,red,1}-(\frac{c_{H,red,2}^2}{4c_{H,red,3}}))}{7}$ if $\frac{24t_{H,day,low}}{\tau} > \frac{c_{H,red,2}}{2c_{H,red,3}}$ $\frac{(7-t_{H,day,low})+t_{H,day,low}(c_{H,red,1}-c_{H,red,2}(\frac{24t_{H,h,low}}{\tau})+c_{H,red,3}(\frac{24t_{H,day,low}}{\tau})^2)}{7}$ if $\frac{24t_{H,day,low}}{\tau} \leq \frac{c_{H,red,2}}{2c_{H,red,3}}$	$c_{H,red,1}$ = 1, $c_{H,red,2}$ = 0.5, $c_{H,red,3}$ = 0.075 $t_{H,h,low}$ = 14 h $t_{H,day,low}$ = 2 d

- The default values used to calculate either the adjusted temperatures or the adjustment factor are matched to the typical use of Flemish school buildings. For *DIN V 18599* [43], $t_{nocc,weekday}$ is set equal to 15.5 h instead of 17 h and an extra term is added to include Wednesday afternoon $t_{nocc,wednesday}$ = 20 h. For *NEN 7120* [44], $t_{H,h,low}$ is set equal to 16.4 h instead of 14 h.
- Adapted values for the numerical, correlation based parameters $b_{H,red}$ as used in *EN ISO 13790* [37] and $c_{H,red,1/2/3}$ as used in *NEN 7120* [44] are set based on the results of additional regression analyses.

5.6.2 Determination of adapted numerical parameters

The intermittency factor approaches as described in *EN ISO 13790* [37] and *NEN 7120* [44] use a correction factor for either the heat demand or the heat transfer to include the overall effects of intermittency. The equations used to calculate the intermittency factors (see *Eq. 3.15*, and *Eq. 3.26* and *Eq. 3.27*) include (one or more) correlation-based numerical parameters. Similar to the numerical parameters as used for the calculation of the utilisation factor (*i.e.* $a_{H,0}$ and $\tau_{H,0}$), more accurate results for the *quasi-steady-state* calculations are to be expected when the parameters used to calculate the intermittency factors are linked to the specific typology of the building and the related boundary conditions.

Determination of $b_{H,red}$ (*EN ISO 13790*)

For the regression analysis, a similar methodology is used as described in *§ 5.2*: the same regression analysis technique is applied, the black box approach is used to obtain the 'static' input data using TRNSYS and the same sample of school building variants is used as described in *§ 5.3*. The monthly *dynamic* $Q_{H,nd,dyn}$ and *quasi-steady-state* heat demands $Q_{H,nd,'stat'}$ are calculated and the differences between both values are minimised by varying the value for the dynamic parameter $b_{H,red}$. Taking account for the impact of the thermal capacity on the thermal behaviour of a building (see *Figure 5.14*) and the poor *quasi-steady-state* calculation results for (very) light structures (see *Figure 5.19*), different values for $b_{H,red}$ are defined in function of the thermal capacity of the structure C_m instead of using a single value as currently applied in *EN ISO 13790* [37] ($b_{H,red}$ = 3 - see *Eq. 3.15*). A minimum difference between $Q_{H,nd,dyn}$ and $Q_{H,nd,'stat'}$ is found when $b_{H,red}$ is calculated in function of C_m according to *Eq. 5.23*:

$$b_{H,red} = -0.0002 C_m{}^2 + 0.0451 C_m + 0.0813 \tag{5.23}$$

The results of are shown in *Figure 5.20*. The differences between the *dynamic* $Q_{H,nd,dyn}$ and 'static' heat demand $Q_{H,nd,'stat'}$[11] using both the original and adapted values for the numerical parameter $b_{H,red}$ are depicted.

When applying the adapted values for $b_{H,red}$, the average difference between the 'static' and *dynamic* calculation results is lowered: $\Delta\ Q_{H,nd,dyn-'stat'}$ is decreased from 6.2 kWh/(m^2.a) to 1.4

[11] The 'static' heat demands are here calculated using the heat losses $Q_{H,ht}$ and heat gains $Q_{H,gn}$ as obtained by the black box approach, using the adapted value for the utilisation factor ($a_{H,0}$ = 1.7, $\tau_{H,0}$ = 25.7) and applying the intermittency factor approach of EN ISO 13790 (see *Eq. 3.15*)

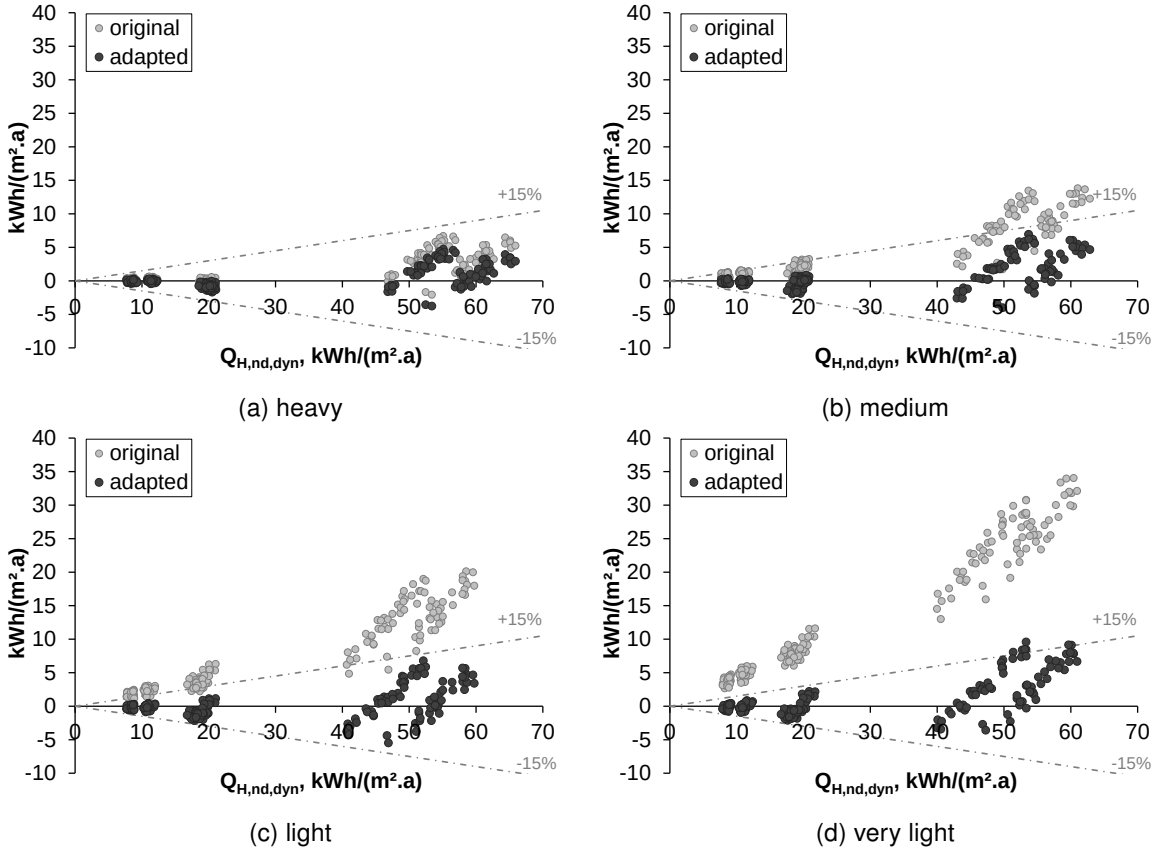

Figure 5.20: The difference between the dynamic and 'static' heat demand $Q_{H,nd,'stat'}$, normalised to the building floor area, of intermittently heated reference school buildings using respectively the original value ($b_{H,red}$ = 3) and the newly derived values for the numerical parameter $b_{H,red}$ calculated as a function of the heat capacity of the structure C_m.

kWh/(m^2.a), on average, or lowered by 17% to < 5%, on average.

Determination of $c_{H,red,1}$, $c_{H,red,2}$ and $c_{H,red,3}$ (*NEN 7120*)

The results in *Figure 5.19* show that overall a good fit between the *quasi-steady-state* $Q_{H,nd,stat}$ and *dynamic* heat demand $Q_{H,nd,dyn}$ is found when the adjustment factor approach as described in *NEN 7120* [44] is used. This section evaluates if this fit can be even further improved when the default values for $t_{H,h,low}$ and the values for the correlation-based numerical parameters $c_{H,red,1}$, $c_{H,red,2}$ and $c_{H,red,3}$ (see *Eq. 3.26* and *Eq. 3.27*) are adapted to the typical use of Flemish schools. The results of the regression analysis show that a slightly better fit is found for the comparison of the heat demands as the following numerical parameters are used: $c_{H,red,1}$ = 1.12, $c_{H,red,2}$ = 0.87, $c_{H,red,3}$ = 0.21. The results of the regression analysis are presented in *Figure 5.21*.

Applying the adapted numerical values, the average absolute difference between the annual *dynamic* $Q_{H,nd,dyn}$ and quasi-steady-state heat demand $Q_{H,nd,'stat'}$ is decreased from 1.5 kWh/(m^2.a) to 1.0 kWh/(m^2.a), on average or from 8.8% to 3.1% on average.

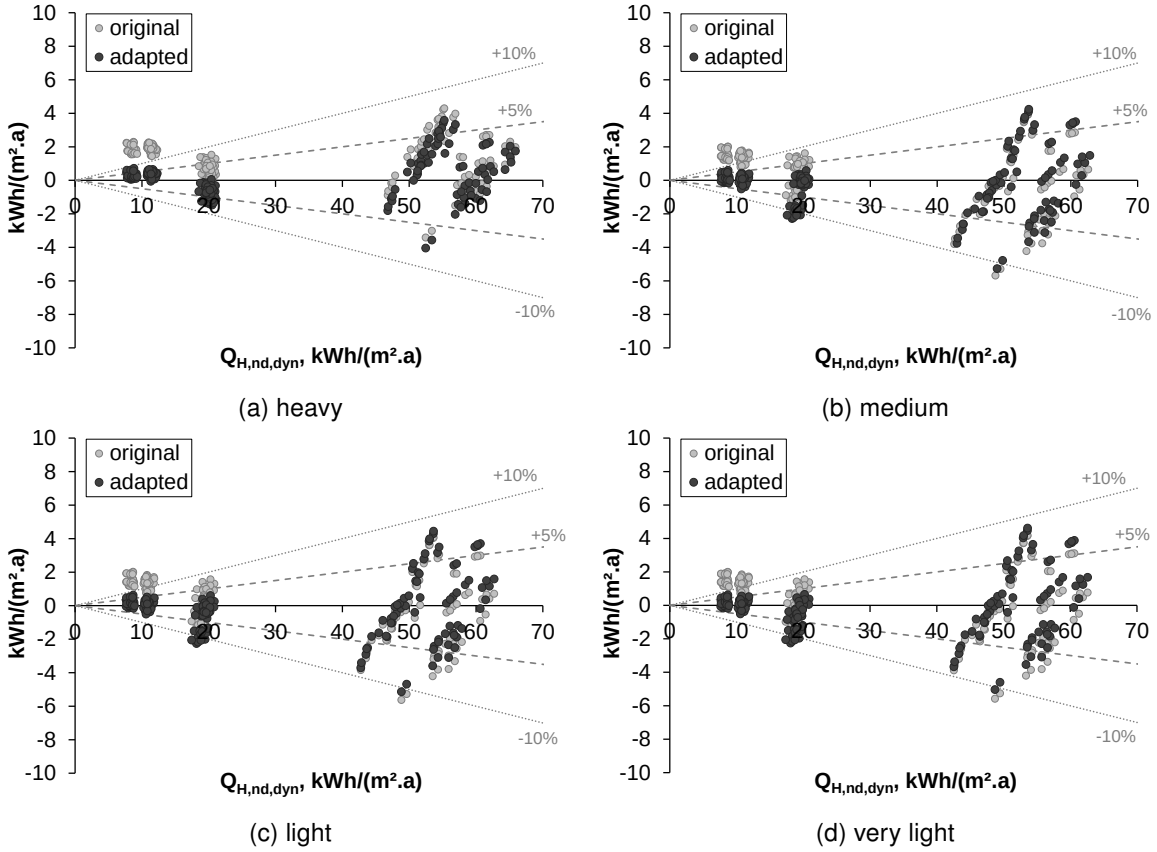

Figure 5.21: The difference between the dynamic and 'static' heat demand $Q_{H,nd,'stat'}$ of intermittently heated reference school buildings, normalised to the building floor area, using respectively the original value ($c_{H,red,1}$ = 1, $c_{H,red,2}$ = 0.5 and $c_{H,red,3}$ = 0.075) and the newly derived values for the numerical parameter $c_{H,red,1}$ = 1.12, $c_{H,red,2}$ = 0.87, $c_{H,red,3}$ = 0.21.

5.6.3 Results

The following revisions are suggested to the original EPR calculation standard in order to fit the calculation method better to the typical characteristics of school buildings.

First, for the calculation of $Q_{H/C,nd}$, new values for the correlation factors are derived to calculate the utilisation factors as shown in *Eq. 5.24* and *Eq. 5.25*.

$$\eta_{H,gn} = \begin{cases} (1-\gamma_H^{(\mathbf{1}+\tau/\mathbf{15})})(1-\gamma_H^{(\mathbf{1}+\tau/\mathbf{15}+1)})^{-1} & (original-see\ \S\ 3.2.1, Eq.\ 3.6) \\ (1-\gamma_H^{(\mathbf{1.7}+\tau/\mathbf{25.7})})(1-\gamma_H^{(\mathbf{1.7}+\tau/\mathbf{25.7}+1)})^{-1} & (refined-see\ \S\ 5.4.1) \end{cases} \quad (5.24)$$

$$\eta_{C,gn} = \begin{cases} (1-\gamma_C^{(\mathbf{1}+\tau/\mathbf{15})})(1-\gamma_C^{(\mathbf{1}+\tau/\mathbf{15}+1)})^{-1} & (original-see\ \S\ 3.2.1, Eq.\ 3.7) \\ (1-\gamma_C^{(\mathbf{2.5}+\tau/\mathbf{10.0})})(1-\gamma_C^{(\mathbf{2.5}+\tau/\mathbf{10.0}+1)})^{-1} & (refined-see\ \S\ 5.4.1) \end{cases} \quad (5.25)$$

Second, a different calculation approach is suggested to calculate the impact of heating system intermittency and more in particular to calculate the heat transfer $Q_{H,ht}$. Whereas in the original *EPR* method [22] the impact of intermittency is accounted for by an adjusted indoor temperature (see *Eq. 3.17*), the refined calculation method based on *NEN 7120* [44], calculates intermittency as a correction of the heat transfer of a continuously heated building (see *Eq. 3.25*). Furthermore, the numerical parameters and default input data used to calculate the correction factors $a_{H,red,night}$ and $a_{H,red,we}$ are adapted to the characteristics of Flemish schools.

$$Q_{H,ht} = \begin{cases} (H_{H,tr} + H_{H,ve})(\mathbf{19} - \theta_e)t & (original - see\ \S\ 3.2.1, Eq.\ 3.17) \\ \mathbf{a}_{H,red,night}\mathbf{a}_{H,red,we}(H_{H,tr} + H_{H,ve})(\mathbf{21} - \theta_e)t & (refined - see\ \S\ 5.6.2, Eq.\ 3.25) \end{cases} \quad (5.26)$$

To assess if indeed a better fit is found between the results of the dynamic simulations and the refined *quasi-steady-state* calculation results, the average annual heat demand $\overline{Q_{H,nd}}$, the relative error Δ, the standard deviation σ, the residual root mean square error (RMSE) and the coefficient of determination (R^2) of the calculation results for a heavy and very light building with varying efficiency levels of the building envelope are depicted in *Table 5.7*. Furthermore, the amount of investigated cases (%) that falls within the ±5%, ±10% and ±15% $\Delta Q_{H,nd}$ confidence bounds are depicted in *Table 5.6*.

Table 5.6: Dynamically and statically calculated annual heating demand, $Q_{H,nd}$, normalised to the building floor area (kWh/(m^2.a)).

	$\mathbf{Q}_{H,nd,ENISO13790}$	$\mathbf{Q}_{H,nd,EPR}$	$\mathbf{Q}_{H,nd,DIN}$	$\mathbf{Q}_{H,nd,NEN7120}$
$\lvert \Delta Q_{H,nd} \rvert \leq 5\%$	21.3%	43.6%	28.3%	**80.3**%
$\lvert \Delta Q_{H,nd} \rvert \leq 10\%$	51.0%	76.0%	51.6%	**97.4**%
$\lvert \Delta Q_{H,nd} \rvert \leq 15\%$	74.3%	88.1%	72.0%	**100.0**%

The results in both tables show that the best fit between the 'static' and the *dynamic* calculation results is obtained when the (adapted) calculation approach of *NEN 7120* [44] is applied. The latter standard calculates the annual heat demand within an accuracy of 2.2 kWh/(m^2.a) or $< 5\%$, irrespective of the energy performance or thermal capacity of the building. The remaining uncertainties related to the simplifications of the calculation method are thus significantly reduced and are lower than the inaccuracies due to for example the uncertainty of input data and boundary conditions as described in *Chapter 4*.

Table 5.7: Statistical analysis of the impact of the suggested modifications to the quasi-steady-state calculation approaches for intermittently heated school buildings. For the calculation results, the different calculation approaches as described in the calculation standards to account for the thermal transient behaviour of the building and systems are applied. The input data used for the calculations is obtained by the black box method. The best results are underlined and marked in bold.

		heavy					very light				
		TRNSYS	**EPR**	**EN ISO 13790**	**DIN V 18599**	**NEN 7120**	**TRNSYS**	**EPR**	**EN ISO 13790**	**DIN V 18599**	**NEN 7120**
	$Q_{H,nd}$, kWh/(m^2.a)	**60.3**	55.5	55.5	58.2	**60.2**	**57.0**	56.8	48.9	**57.7**	55.5
	Δ, %		7.9	7.8	3.4	**0.0**		0.1	14.0	**-1.4**	2.4
variant 1	**σ**		16.6	15.7	7.6	**3.5**		7.9	41.8	**7.3**	10.5
	RMSE		5.1	5.0	2.6	**1.5**		2.6	8.5	**2.7**	2.9
	R^2		0.701	0.762	0.709	**0.807**		0.366	0.377	0.370	**0.418**
	$Q_{H,nd}$, kWh/(m^2.a)	**52.3**	48.5	48.7	**51.1**	51.0	**48.8**	**49.9**	43.0	50.8	46.4
	Δ, %		7.15	6.62	**2.18**	2.35		**-2.48**	11.61	-4.21	4.62
variant 2	**σ**		11.9	11.7	4.5	**3.7**		**6.7**	32.6	8.9	13.1
	RMSE		4.1	3.9	**1.9**	2.0		**2.4**	6.4	2.9	3.3
	R^2		0.712	0.727	0.723	**0.896**		0.601	0.520	0.610	**0.735**
	$Q_{H,nd}$, kWh/(m^2.a)	**20.0**	**20.6**	22.2	22.5	21.0	**19.1**	22.2	20.6	22.8	**19.3**
	Δ, %		**-2.95**	-10.80	-12.58	-4.81		-16.19	-7.49	-19.11	**-1.14**
variant 3	**σ**		1.3	3.6	4.8	**0.8**		9.0	3.4	10.5	**0.8**
	RMSE		1.1	2.3	2.7	**1.0**		3.4	1.8	3.9	**0.8**
	R^2		0.522	0.596	0.524	**0.760**		0.048	0.154	0.050	**0.173**
	$Q_{H,nd}$, kWh/(m^2.a)	**11.4**	10.7	12.3	12.2	**11.2**	**10.9**	12.3	12.0	12.8	**10.9**
	Δ, %		6.49	-7.66	-7.15	**1.78**		-13.13	-9.99	-17.04	**0.32**
variant 4	**σ**		0.6	0.6	0.6	**0.1**		1.4	0.8	1.8	**0.1**
	RMSE		0.8	0.9	0.9	**0.3**		1.5	1.1	1.9	**0.2**
	R^2		0.443	0.550	0.461	**0.875**		0.144	0.458	0.161	**0.607**
	$Q_{H,nd}$, kWh/(m^2.a)	**8.5**	8.4	9.9	9.8	**8.4**	**8.4**	9.9	9.9	10.3	**8.4**
	Δ, %		2.04	-16.32	-14.97	**1.92**		-0.18	-0.19	-0.23	**-0.01**
variant 5	**σ**		0.2	1.0	1.0	**0.1**		1.2	1.1	1.5	**0.0**
	RMSE		0.4	1.4	1.3	**0.3**		1.6	1.6	2.0	**0.2**
	R^2		0.505	0.552	0.519	**0.817**		0.278	0.409	0.298	**0.708**

For the comparative analysis as presented in *Table 5.6* and *Table 5.7*, the input is obtained by the black box approach. The 'static' input is hence obtained by the dynamic simulation tool TRNSYS. As some small discrepancies occur (see *Figure 3.8* and *Figure 5.2*), the actual output of the *quasi-steady-state* calculation methods might deviate from the results presented in the tables. Therefore, a final comparison is made to assess the impact of the proposed changes on the actual output of the *quasi-steady-state* calculation method, using the input data generated by the *quasi-steady-state* calculation tool itself. The results are depicted in *Figure 5.22* (a) and (b).

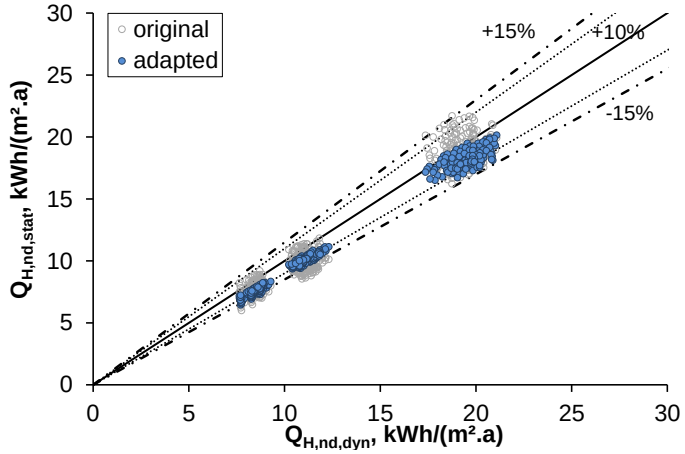

(a) impact original vs. revised method

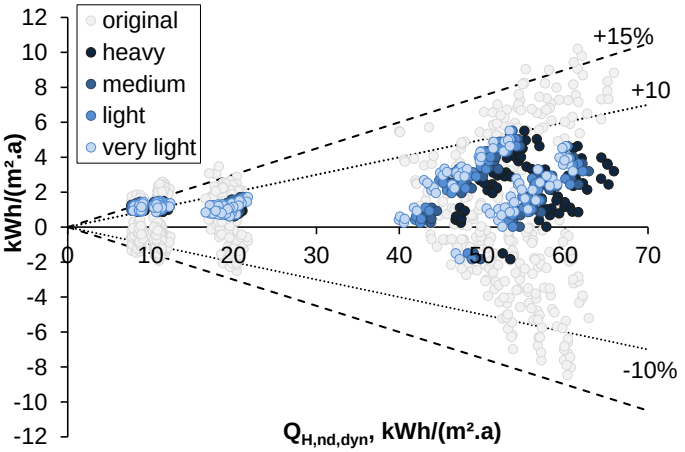

(b) impact of thermal capacity

Figure 5.22: Differences between the *quasi-steady-state* and *dynamically* calculated annual $Q_{H,nd}$, normalised to the building floor area, for a range of intermittently heated elementary school building variants.

Both figures show that when the suggested changes to the *quasi-steady-state* calculation method are applied, overall a good fit and less scattering of the data points are found. The average difference between the *quasi-steady-state* and the *dynamic* calculation results is limited to 7.3%. Furthermore, *Figure 5.22* (b) reveals that the accuracy of the *quasi-steady-state* calculation results depends less on the thermal capacity of the building compared to the original results (see *Figure 3.11*). The average difference between the *quasi-steady-state* and dynamic heat demand for the heavy, medium, light and very light building vary between 6.8 and 7.7%.

5.7 Conclusion

Simulation results and literature review show that to be able to obtain more accurate energy assessment results in the context of EPBD, the *quasi-steady-state* calculation method as currently applied needs to be adapted to the typology of the evaluated building. Consequently, throughout this chapter, various proposal are elaborated to adapt the *quasi-steady-state* calculation method to the typical use and characteristics of school buildings.

First, the impact on the dynamic behaviour of the building is studied. The accuracy of the **utilisation factor** used in the *quasi-steady-state* calculation method to account for the thermal transient behaviour of the (school) building is studied and a proposal is made to adapt this correction factor better to the use schools. To do so, the heating and cooling demand, calculated by means of *dynamic* simulations, are compared to the results of simplified, monthly calculation results for a series of school building design variants. New, **correlation-based numerical parameters** are then set using the black box approach and regression analysis techniques as described in *EN ISO 13790*: $\mathbf{a}_{H,0}$ **= 1.7** and $\tau_{H,0}$ **= 25.7** for the heat balance and $\mathbf{a}_{C,0}$ **= 2.5** and $\tau_{C,0}$ **= 10** for the cooling balance.

Next, the calculation approach used in the *quasi-steady-state* methods to account for system intermittency is analysed. The results of *dynamic* simulations performed along this chapter reveal that the energy saving potential due to intermittency depends amongst others on the time constant of the building and the applied heating or cooling pattern. Hence, these effects must be accounted for in the calculation method. Therefore, a comparative analysis of the results of different *quasi-steady-state* methods and *dynamic* simulations is performed. The results reveal that the best fit between the *quasi-steady-state* and *dynamic* results is found when the calculation approach as described in *NEN 7120* is applied. This method accounts for intermittent heating by correcting the calculated heat losses using an **adjustment factor** which depends on both the length of the period of reduced heating and on the thermal capacity of the building. Two additional proposals are then defined to further adapt this method to the typical school use:

- The default values used to calculate the adjustment factor ($\mathbf{t}_{H,h,low}$ **= 16.4 h** instead of 14 h) are matched to the typical characteristics and use of Flemish school buildings.
- New numerical, correlation-based values for the parameters $\mathbf{c}_{H,red,1}$ **= 1.12,** $\mathbf{c}_{H,red,2}$ **= 0.87,** $\mathbf{c}_{H,red,3}$ **= 0.21** are set based on the results of a regression analysis.

Due to the suggested changes to the method, the average difference between *dynamic* and *quasi-steady-state* heat demand is reduced to 7%, on average (*i.e.* calculated according to the adapted NEN 7120 standard). The maximum difference found is reduced from 22% to 16%.

Note that, aside from the adjustment and correction factors, the accuracy of the quasi-steady-state calculation method depends highly on the accuracy of the implemented input data. Especially for the solar heat gains, significant discrepancies between the quasi-static and dynamic input data are found. Further research on this particular topic is hence highly recommended.

6

Prediction of the energy use for heating

Energy demand calculations offer interesting information on the energy efficiency level of the building (components). Nevertheless, they do not necessarily reflect well the final energy use of the building as this is additionally determined by the design, the efficiency and the use of the HVAC systems. In line with the calculation methods found in CEN/TR 15615 to support the EPBD regulations, the EPR tool uses a simplified method to calculate the annual energy use of buildings applying a subsystem approach that uses tabulated values for each of the (sub)system efficiencies to assess the related subsystems' thermal losses. The efficiencies are set based on the selection of the separate HVAC system's components but are generally irrespective of the building characteristics. Moreover, it neglects the mutual interplay between the various subsystems. As a result, the currently applied method might (over)simplify the dynamic and nonlinear interaction of the building and HVAC systems. Within this context, the overall objective of this chapter is to study the impact of the building and HVAC system selection on the overall HVAC system performance. Once this impact is determined, it is evaluated if it is taken into account accurately in the simplified calculation approach (EPR). To do so, integrated dynamic building and system simulations are conducted for a series of typical heating and ventilation systems as found in contemporary school buildings. To assess the interaction between the building and systems, building models with varying building characteristics (i.e. insulation qualities, thermal capacities, WWR and orientation) are coupled to the selected HVAC system variants. The overall method used along this chapter has already successfully been applied in a similar study on office buildings by Parys [125].

6.1 Introduction

In Flanders, for the assessment of the energy use of buildings in a regulatory context, a simplified, sequential HVAC subsystem calculation approach is used that decouples the building from the HVAC

system as described in *§ 3.2.2*. Thermal losses are calculated separately for each of the included subsystems using tabulated subsystem efficiencies (see *Figure 3.5*). The recoverable part of the thermal losses are hereby directly subtracted from the loss of each system and are thus accounted for by an increase of the related subsystems' efficiencies. This method is intuitive and simple as no iterations are needed to simulate the performance of the building and its system. Hence, it is an interesting option to be used in a regulatory context.
Korolija et al. [39] demonstrated however, based on the results of a series of dynamic integrated building and system simulations of offices in the UK, that the energy efficiency of HVAC systems depends on the thermal characteristics of the building. Similar research is performed by Peeters et al. [41] and Van der Veken et al. [224] who demonstrated the relation between the insulation quality of the building envelope and the emission and distribution efficiency of heating systems in residential buildings. Simultaneously, the accuracy of the currently used tabulated data for the (sub)system efficiencies could be questioned as some of the data might be (over)simplified, are inaccurate or are simply lacking due to the fast evolution towards high performance buildings and new technologies. In concrete terms, the *EPR* method for non-residential buildings [22] uses a single system efficiency value to cover the performance of emission, distribution, storage and control systems. No differentiation between the different subsystems is made (see *§ 3.2.2*). Maivel et al. [225] showed that the emission and distribution system efficiencies as tabulated in the alternative calculation standards *EN 15316-2-1* [49] and *EN 15316-2-3* [151] cause an overestimation of the energy used by low temperature radiator heating systems compared to the results of integrated dynamic simulations. Consequently, they defined a new set of tabulated values applicable for the Central and North European climate and for nearly zero and low energy buildings [225].

The aforementioned restrictions jeopardise the use of the simplified calculation method in his current form. An integrated calculation approach that treats building and systems as a complete entity instead of separately designed subsystems could be a better alternative [125, 226, 224, 42]. Comprehensive studies which examine the HVAC system as a holistic system, taking into consideration the interaction between the building and system on the one hand and the mutual interactions of all system and control components on the other hand, are however rare [42]. Moreover, the combined building and HVAC simulations are computationally intensive and require a substantial effort of the modeler and are thus less appropriate for design performance evaluation in a regulatory context. For the sake of simplicity and reproducibility, it is better to opt for a more simple procedure.
In this context, Korolija et al. [157] studied the response of different types of (secondary) HVAC systems for offices in the UK and fitted regression models to predict the HVAC energy use based on the results of the energy demand calculations. The developed simple regression models proved to be effective and accurate. Similar work has been done by Parys [125, 40] and by Van der Veken et al. [227] who analysed the monthly efficiencies for the generation, distribution and emission subsystems for various HVAC systems in offices and dwellings, respectively. Parys [40] deduced regression models for the energy use calculations based on integrated building and HVAC system simulation results and proposed these to be used as an alternative for the default fixed system efficiencies of the EPR calculation standard.

In line with the aforementioned research studies, it is evaluated if the alternative calculation approach using regression models based on the results of dynamic simulations could offer more accurate calculation results for the final energy use for heating compared to the *EPR* calculation standard [22]. Additionally, a comparison is made with the results of the simplified calculation method as described in the CEN/EPB *EN 15316* [49] (see *§ 3.2.2*) to investigate if this standard offers a better alternative for the *EPR* calculation method as currently applied in Flanders.

Four consecutive steps are performed. First, **a selection of HVAC system variants are defined** which are representative for the current Flemish schools (*§ 6.2*). Due to the complexity of the necessary dynamic simulations, it is unfeasible to cover the whole range of HVAC systems and related control configurations found in schools. Therefore, a restricted selection of four commonly found ventilation and heating systems in contemporary schools is made, based on the survey results as described in *§ 2.4.2*. Second, dynamic, **integrated building and HVAC system simulations are performed** to analyse both the complex, dynamic and nonlinear interaction of the building and HVAC systems, and the mutual interaction between the various subsystems (*§ 6.3* and *§ 6.4*). Third, **simple energy estimation models are deduced** as a function of the heating demand using regression techniques (*§ 6.5*). In the fourth and final step, the **robustness of the regression models is evaluated** (*§ 6.5.3*).
The work done in this chapter can be seen as a continuation of the work done by Parys [125]. Overall, a similar methodology is used though it is applied on a different building typology and for a different selection of HVAC systems.

For the study, a restricted sample of contemporary school building design variants and a limited series of HVAC system (configurations) are selected. Inherent to (**i**) the building and HVAC system selection, (**ii**) the sizing procedures applied and (**iii**) the modelling approach used, several design decisions and simplifications had to be made which affect the outcome of this study. This lead to some important restrictions and limitations, as summarised in *§ 6.6*.
Moreover, the research scope is restricted to the analysis of the accuracy of the simplified calculation approach used in the *quasi-steady-state* calculation methods (*i.e.* EPR [22] or EN 15316 [49]) to determine the energy use for heating. The advantages and disadvantages of each of the chosen HVAC systems and the implemented control systems will not be discussed here. Neither are the results used to search for better design variants or optimised design solutions.

6.2 HVAC system selection

A large variety of HVAC systems can be found in schools. An overview of the currently most commonly applied systems in schools is given in *§ 2.4.2*. As system sizing and dynamic simulations of HVAC systems are very time-consuming, it is unfeasible to include all these systems in this study. Therefore, a limited selection is made. To maximise the scope and usability of the research results, the HVAC selection is focused on the most dominant energy flows. To determine these, results of various studies on energy use in schools are compared to the survey results as described in *§ 2.4*. A typical energy usage profile for Belgian elementary and secondary schools was set by De Deene

Table 6.1: Energy usage profile of Belgian (*1998*) [7] and Dutch (*2009*) [228] elementary and secondary schools in relation to the energy source.

	elementary schools - BE	**elementary schools - NL**	**secondary schools - BE**	**secondary schools - NL**
Fuel consumption				
heating	100%	99.5%	90%	98.8%
domestic hot water	-	0.5%	8%	1.2%
other	-	-	2%	-
Electricity use				
lighting	73%	49.7%	72%	47.4%
circulation pumps	10%	4.2%	12%	5.1%
domestic hot water	-	4.2%	-	0.4%
cooling systems	6%	-	6%	-
ventilation	-	-	-	1.4%
ICT	-	1.4%		25.4%
other	11%	10.5%	10%	20.3%

et al. [7] (see *Table 6.1*). As this study is based on data gathered in 1998, the results of a similar though more recent study of Dutch schools are used for comparison.

As shown in *Table 6.1*, the fuel consumption in schools is almost entirely ($> 90\%$) related to heating. Similar, recent international studies on the total energy use in schools confirm that heating is by far the most dominant energy flow in schools, accounting for 47% to about 80% of the total annual primary energy use [229, 149, 148]. Due to the more stringent building's energy policy, a decrease of the heating energy use is however to be expected over the next years. Recent measurements of the energy use of recently built schools in Luxembourg [230] confirm this expectation as the thermal energy use in passive schools is decreased by more than 50% compared to standard school buildings. The electricity usage profile is more diverse. Lighting is the most dominant factor covering about 50% of the electricity usage in schools, although a slight shift in time (1998 $\rightarrow$ 2009) is noticed towards the use of ICT. According to *Table 6.1*, cooling, (de)humidification and ventilation electricity usage are nearly non-existing. The survey results as described in *§ 2.4.2* confirm that active cooling and (de)humidification devices are seldom seen, even in contemporary and newly built schools. On contrary, as good indoor air quality is mandatory and the requested hygienic ventilation rates in class rooms are high, the use of a mechanical ventilation is highly recommendable. Consequently, at present, ventilation systems are more frequently installed in schools and a significant increase of the fan electrical use is to be expected, as confirmed by recent survey results of a sample of recently built schools in Luxembourg by Thewes et al. [230].
Therefore, this study focuses on both heating and ventilation systems. (Active) cooling is not included although passive cooling strategies are integrated in the model to guarantee good thermal comfort. Lighting and according control systems are only considered as a boundary condition (*i.e.* as a fixed part of the internal heat gains). Finally, as the need for hot water in schools is generally limited and mostly supplied by local electrical boilers (see *§ 2.4.2*), (centralised) production of domestic hot water is not included in this study.

A large variety of heating and ventilation system configurations can be found. Moreover, as for this study, each system is sized and assembled according to the school building to which it is coupled, it is an intensive and time-consuming process. As it is therefore unfeasible to cover all systems and related control configurations, a restricted selection of four commonly found ventilation and heating systems in schools is made. The final choice of the included system (components) is based on the survey results as described in *§ 2.4.2*.

Selection of the ventilation system

Due to the high required ventilation rates in school, the use of a mechanical ventilation is preferable. So, only this option is retained for this research study, including both exhaust and balanced mechanical ventilation systems. Natural ventilation systems are not studied.

Selection of the heating system

Centralised heating systems with a gas boiler are by far the most frequently used in schools (67%, see *Figure 2.13*). Given the significant predominance of (condensing) boilers in schools, they are selected as the heat generation systems. Other more innovative alternatives such as heat pumps are not included as they are rarely found in contemporary schools due to the high investment costs. In addition, as active cooling is not included in the study, the potential of reversible heat pumps can not be fully benefitted. Consequently, only the impact of variations of the secondary heating system on the energy performance is studied. As shown in *§ 2.4.2*, hydronic heat distribution systems are most common though a slight change towards air heating systems is noticed. Therefore, both hydronic and the combination of hydronic and air distribution systems are included. Regarding the heat emission subsystems, radiator heating, floor heating as well as air heating are commonly found in the investigated schools (see *Figure 2.14*) hence all these systems are included for this research study.

The resulting final selection of HVAC systems is depicted in *Table 6.2*.

	HEATING							VENTILATION		
	emission			distribution		production				
	radiators	floor heating	(ventilation) air	hydronic	combined hydronic and air	boiler	fossil fuels	natural supply, mechanical	mechanical	heat recovery
HVAC1	HT									
HVAC2	LT							*		
HVAC3			central					*		
HVAC4			local					*		

** only mechnical extraction without HR in sanitary*

Table 6.2: Final selection of commonly found HVAC system configurations in schools included in this study.

The first system (HVAC1) comprises radiator heating and an exhaust-only ventilation system without heating recovery. As no heat recovery of the ventilation air is foreseen, the specific design heat loads are rather high (± 110 to 130 W/m^2) so high temperature radiator heating is applied. For the second system (HVAC2), the exhaust ventilation system is replaced by a balanced mechanical ventilation systems with heat recovery devices, combined with low temperature radiator heating. No additional air heating is foreseen in HVAC1 or HVAC2. For the third system (HVAC3) radiator heating is changed by a floor heating system in combination with basic centralised air heating. Finally, the fourth and last considered HVAC system (HVAC4) comprises an all-air heating system using both central and local air heating coils.

The energy performance of an HVAC system depends not only on the system typology but also on the specific selected components and their characteristics, the sizing procedures applied, the settings and the control strategy used, and the assumptions made regarding the quality of workmanship [125]. General design decisions and modelling assumptions that needed to be made for this investigation are summarised hereafter:

- Each of the included systems are sized properly, according to the related design standard.
- The HVAC system is assumed to be well commissioned and is assumed to be perfectly hydraulically balanced.
- The system configuration and current good practice control systems are selected, based on the survey results of the passive and EESBs as described in *§ 2.4*.

An overview of the installed (thermal) components and their related characteristics, sizing procedures, control strategies and settings, and modelling assumptions are described along the text. Other components such as hydraulic components, filters, etc. which are equally essential for the well functioning of the system but do not affect the thermal balance of the building are not specifically described hereafter nor incorporated in the dynamic simulation models.

6.2.1 Description of the selected HVAC system configurations

In this section the properties of the investigated heating and ventilation systems and related control strategies are described. First, the common characteristics and design assumptions that are similar for each of the incorporated systems are discussed. Second, in the following subsections, specific details on the design and sizing procedure of each of the investigated HVAC systems (components) are summarised.

One of the main characteristics of school buildings is the variability of the user's schedules and the occupancy which in turn requires flexible heating and ventilation systems. Accordingly, for the investigated heating systems, multiple heating circuits are foreseen. A separate heating circuit is provided for each of the building zones characterised by similar (time) trends of thermal loads and/or occupancy: two separate heating circuits are foreseen for the class zone as this zone is additionally split into two zones based on the orientation (see *Figure 6.1* - marked in pink and red), one heating circuit for the administration zone (see *Figure 6.1* - green), one for the canteen/kitchen (*Figure 6.1* - blue) and one for the gym (see *Figure 6.1* - yellow). Furthermore, various AHU's are foreseen for the building zones characterised by similar use and occupancy: one air handling unit is foreseen for

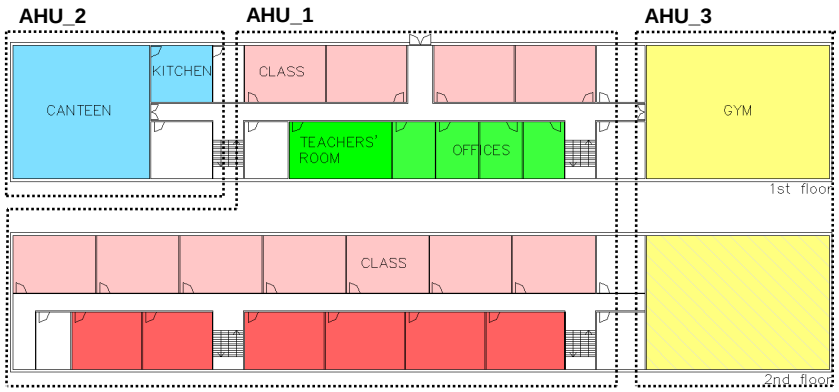

Figure 6.1: Simulation model of the reference school building used for this research study, partitioned in various heating (marked in colours) and ventilation zones (marked by dotted lines).

the class and administrative zone, one for the gym and one for the canteen.

A commonly used - though rather traditional - heat distribution system configuration is chosen using one central heating circuit (= primary system) and all secondary circuits coupled to a distribution header (see *Figure 6.2*). The primary and secondary system are decoupled using an open header that acts as a hydraulic separation between the different pump flows.
Heating is generally scheduled according to the school operational profile. After school and during weekends, the heating is switched off. To reassure good thermal comfort at the start of each school day however, the heating starts prior to the school opening hours. The exact start time depends on the type of the heating system that is installed[1]. A room set-point temperature for heating of 21°C is used in the occupied zones/rooms except for the gym where a set-point of 17°C is implemented. The unoccupied areas such as the circulation area, the storage rooms and sanitary are not heated.
The operation of the ventilation fans is controlled by a time schedule according to the zonal occupancy profiles. No demand control ventilation is installed as the effect in (elementary) schools is expected to be limited as, generally, classes are equally and more or less constantly occupied during the whole school year. Pre-ventilation prior to the school opening hours is applied to reassure good indoor air quality at any time of occupancy [47].
For the use of lighting, automatically controlled lighting schedules according to the zonal occupancy profiles are assumed (see *Figure 4.9* (c)).

6.2.2 Exhaust ventilation, high temperature radiator heating, passive (night) cooling (HVAC1)

Heating system configuration and control

The first HVAC system comprises a traditional hydronic heating system with a modulating, condensing gas boiler and radiators controlled by thermostatic radiator valves (TRV) in every occupied zone. The schematic, conceptual diagram as shown in *Figure 6.2*, presents, in a simplified way, the main

[1] It is opt for a fixed start-up time control system, applying a time setting independent of the outdoor temperature or the energy efficiency level of the other building variants. The exact start up time for each of the investigated HVAC systems is however determined by 'trial and error' simulations, checking comfort requirements for the least energy efficient building variant (variant 1 - see *Table 6.6*) in the winter months. As the range of energy performance level of the building envelope is limited, no significant differences in the start-up time are found over the various included building variants.

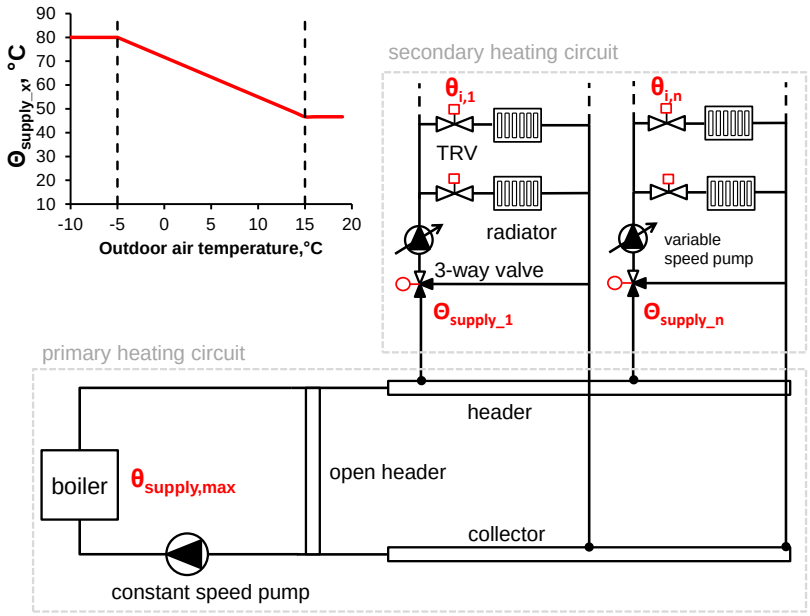

Figure 6.2: Conceptual scheme of the system configuration of HVAC1 and HVAC2 as it is implemented in TRNSYS [125]. System configurations of real HVAC system in schools might deviate. A reset temperature control curve setting the supply hot water in relation to the outdoor air temperature and the respective heat load of the zone, is calculated for each of the heating circuits separately.

heating components that are included in the simulation model of HVAC1 .

Two-plate radiators with a single convection fin element are used with a height of 90 cm and a total width depending on the required heat load. The radiators are sized according to the technical reports of the Belgian Building Research Institute [231] and the European design heat load calculation standard *EN 12831* [90]. The characteristics of the radiators are summarised in *Table 6.3*.

A radial distribution system is used for the hot water distribution. The lengths of the pipes are approximately measured on the floor plan (see *Figure 6.1*). The distribution pipes are all insulated according to the energy efficiency requirements for technical systems [132]. Pipe diameters are calculated allowing maximum friction losses of 100 Pa/m according to *EN 15316-2-3* [151]. For the secondary circuits where the supply flow rate to the radiators is controlled by thermostatic radiator valves, variable speed pumps are installed. All the pumps are sized based on both the design flow and the differential pressure for each of the served zones.

Table 6.3: Characteristic of the selected radiator type [108].

radiator exponent n	1.3
height, m	0.9
specific nominal thermal power, W/m	1961
specific water content, l/m	11.3
specific weight, kg/m	49.9
nominal radiative fraction, %	15

The boiler heat output capacity is calculated as the sum of all nominal powers of the emission systems of each zone. A design outdoor temperature of -8°C, representative for the Belgian climate, is applied and a safety margin of 10% is foreseen to cover for the occurring distribution losses [232]. The calculated boiler output capacities vary from 261 kW to 304 kW related to the energy efficiency level of the building. The final selection of the boiler depends however on the real availability of boilers. *Table 6.4* summarises the information of the boiler models which can be selected throughout this chapter based on the technical data from a leading manufacturer.

Table 6.4: Characteristics of the condensing gas (natural gas H, net heat value (NHV) = 46.3 MJ/kg) boilers used along this chapter [125].

$\Phi_{nom,max}$	$\Phi_{nom,min}$	C_{burner}	V	UA	$W_{aux,min}$	$W_{aux,max}$	$W_{aux,off}$
kW	kW	kJ/K	m^3	kJ/(K.h)	W	W	W
142	47	94.5	0.221	46.52	45	185	30
186	47	114	0.306	55.22	45	229	30
246	82	121	0.292	66.28	50	330	30
311	104	128	0.279	77.22	55	385	30

The heating is scheduled to start at 4 AM on Mondays and at 5 AM on the other school days. An outdoor temperature reset control, applied on each building zone separately, automatically adjusts the heating circuit flow temperatures in accordance to the zonal heat load and the average outdoor temperature of the 6 previous hours [125]. Depending on the heat load pattern, supply flow temperatures vary between 80°C and 50°C. The set-point temperature of the boiler is then set equal to the maximum supply temperature of all the secondary heating circuits. An on/off burner control is applied based on the required supply flow set-point temperature: the boiler and boiler pump are turned on as soon as there is heat load and the boiler outlet temperature drops below a minimum (= boiler set-point - 3 K). The boiler is switched off when there is no heat load or when the maximum boiler set-point temperature is reached (= boiler set-point + 3 K). In between, the burner power is modulated according to the heat load pattern between a maximum and minimum value (see *Table 6.4*) to reach the required set-point supply flow temperature. To avoid excessive cycling of the boiler, a minimum on/off time of 6 minutes is set [125].

Ventilation system configuration

A mechanical exhaust ventilation system is foreseen. Fresh outdoor air is supplied at a constant flow rate in the occupied rooms through trickle vents in the windows. The used air is extracted by four extraction fans which are sized according to *EN 13779* [13] (IDA 3): the first serves the classes and offices (8500 m^3/h), the second serves the canteen (6300 m^3/h) and the third serves the gym (700 m^3/h). The air is generally supplied and extracted in the same zone though part of the air from the class rooms flows through the circulation zone to the sanitary rooms (15 $m^3/(m^2.h)$) where it is extracted by a separate extractor (1800 m^3/h). In the kitchen a small additional exhaust hood is foreseen to extract polluted air due to specific cooking activities. All fans and ducts are sized according to the design flow rates but are 20% oversized to avoid lacking ventilation due to polluted filters or grilles. The installed fan power is estimated based on the nominal air flow rates and the specific

fan power. Although practice shows in some cases higher SFP-values of the fans (see *§ 2.4.2*), the values for the specific fan power used for this research are set in accordance to the requirements as set by the EPR regulation and the design guidelines for energy efficient non-residential buildings of the Passiv Haus Institut [117]: the SFP-value of the exhaust fans is set equal to the average value of the required SFP class 3 (= 1000 Ws/m^3) [13]. For the local exhaust fans (*i.e.* kitchen hood and sanitary), a lower value of 600 Ws/m^3 is used [133] as the coupled ducts are shorter and related expected pressure losses are lower.

Passive cooling strategy

To maintain summer comfort in the investigated buildings, passive night cooling by mechanical ventilation is used. Based on the results of the survey and the advice of an expert on HVAC system design in schools, it is noticed that natural night ventilation is not preferable in Flemish schools. Safety reasons, and the related high investment and maintenance costs of automatically operable windows are often referred to as the most important draw backs. The application of (additional) stack ventilation is hence restricted to those buildings where summer comfort can not be guaranteed by night ventilation using the mechanical (hygienic) ventilation. Additional free cooling by manually opening of the windows is possible but is not considered along this study.

The control of the night ventilation depends on multiple control parameters: the night ventilation schedule (0h < time < 6h), the indoor (star) temperature ($\theta_{star} > \theta_{i,H,set}$), the outdoor air temperature, and the difference between operative and outdoor air temperature ($\theta_{i,H,op}$ - θ_e > 2°C) [233]. For those building variants (*i.e.* the building variants with a light building structure or a WWR = 40%) where additional cooling is necessary by natural ventilation, a simplified calculation is performed to assess the feasible stack ventilation rates for night cooling and to determine the impact on the school building design.

6.2.3 Balanced mechanical ventilation with heat recovery, low temperature radiator heating and passive night cooling (HVAC2)

The second HVAC system is a variant of HVAC1 as only the ventilation system and hot water supply flow temperatures are changed. The overall heating system configuration is similar to the one used for HVAC1 (see *Figure 6.2*).

Heating system configuration

The heating and related control system are equal to the system used for HVAC1 though the components are sized smaller due to the lower heat demands. Furthermore, the necessary boiler heat output capacities vary from 175 kW to 130 kW and the maximum supply flow temperature is reduced to 60°C.

Ventilation system configuration

Balanced mechanical ventilation including heat recovery is foreseen instead of the exhaust ventilation system. Three AHU's, sized according to *EN 13779* [13], are installed: the first AHU serves the classes and offices (supply fan = 10300 m^3/h, extraction fan = 8500 m^3/h), the second AHU serves the canteen (supply fan = 6600 m^3/h, extraction fan = 6300 m^3/h) and the third serves the gym (sup-

ply and extraction fan = 700 m^3/h). The imbalance between some of the supplied and exhausted air flows is due to the fact that part of the air is extracted separately for hygienic reasons (*i.e.* sanitary and kitchen).

The SFP values of the fans are set in accordance with the required SFP-class in *EN 13779* [13]. As the survey results show no significant differences between the SFP-values for the exhaust and supply fans, both values are set equal to the average value of the required SFP-class 3 (= 1000 Ws/m^3). For local exhaust fans (*i.e.* kitchen hood and sanitary), a value of 600 Ws/m^3 is used [133]. The AHU's are equipped with cross flow heat exchangers. The overall heat transfer coefficients of the exchangers (UA) are sized according to the effectiveness - NTU (number of transfer units) method assuming both fluids unmixed [234]. Typical air-to-air cross flow heat exchanger efficiencies vary between 50 and 80% [122]. As the average efficiency found in the survey is 75%, this value is used in this study. All the implemented heat recovery devices can be bypassed in case of night ventilation or, during daytime, whenever the air supply temperature exceeds the maximum supply air temperature (= 22°C) and the outdoor air temperature is lower than the indoor temperature but higher than 14°C while occupied or higher than 10°C while unoccupied [233].

6.2.4 Floor heating in combination with central air heating coils, passive (night) cooling (HVAC3)

For the third HVAC system, the same balanced mechanical ventilation system as described in HVAC2 is used. Regarding the heating system, the radiators are exchanged for a floor heating system. Moreover, basic additional air heating by central heating coils in the AHU's for the class rooms, offices and teachers' room (AHU_1) and for the canteen (AHU_2) is foreseen as a feasibility study based on the design heat load calculations showed that the maximum heat load capacity of the floor heating system in the canteen (specific design heat load $q_{H,canteen}$ up to 122 W/m^2) and the class zone ($q_{H,class}$ up to 100 W/m^2) of the least insulated building design variant is insufficient to cover the occurring heat losses.

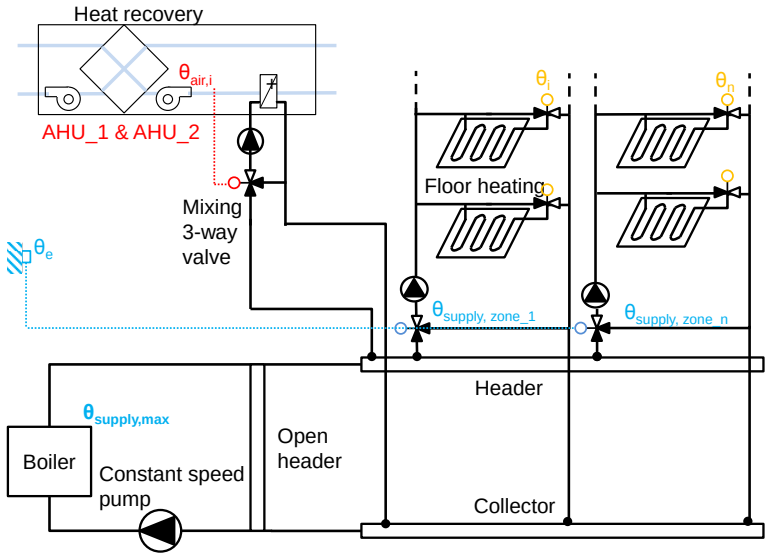

Figure 6.3: Conceptual scheme of the system configuration of HVAC3 as it is implemented in TRNSYS [125]. Real HVAC system configurations applied in schools might deviate.

Heating system configuration

PE pipes (λ = 0.40 W/(m.K)) with an external diameter of 17 mm and a thickness of 2 mm are embedded in the screed layer and spaced at a calculated distance which depends on the heat load of the served zone as calculated according to the design heat load calculation method *EN 12831* [90], though neglecting the heat losses through the heated floor. As the maximum calculated average heat load intensity is ± 80 W/m^2, the floor heating is sized for a 50/30/20[2] according to the simplified design procedure for floor heating as described in TV 181 [235].

Additional air heating is foreseen, maintaining the temperature of the supplied air at 18°C [122]. Central heating coils are installed in AHU_1 and AHU_2. The coils are designed according to the Effectiveness - NTU method [234] assuming single pass cross flow plate heat exchangers with mixed air. For the sizing of the heating coils, the same outdoor temperature as applied in the design heat load calculations is used (= -8°C), the presence of a heat recovery device with an efficiency of 75% is taken into account and the relative humidity of the outdoor air is assumed to be 89% [125].

Control strategies

For the floor heating, an on/off control system based on the zonal indoor temperature is applied to control the constant speed pumps which are used for circulating the water to and from the radiant floor. Supply flow temperatures to the air heating coils are automatically adjusted to the heat load using a PID controller and motorised three-way valves. To account for the slower reaction of the floor heating systems, the start-up time differs slightly from the one that is used for HVAC1 and HVAC2. In case of heat demand, the floor heating system is switched on at 3.5 AM on Mondays to guarantee good comfort after the weekend break.

6.2.5 All-air heating system (CAV/VAV), central and/or local post-heating coils (HVAC4)

The final HVAC system variant consists of an all-air heating system using both central and local hydronic heating coils to heat the supply air flow. To limit the size of the installed air handling units, the all-air heating system is only applied if the hygienic ventilation rates are capable of providing the required heat. As the heat capacity of air is relatively low (c_{air} = 1.008 kJ/(kg.K) versus c_{water} = 4.186 kJ/(kg.K)), the heat capacity of an all-air heating system is limited. Consequently, only the most energy efficient building design variants - building variants 3 till 5 as depicted in *Table 6.6* - with an average specific heat load lower than ±70 W/m^2 are coupled to an all-air heating system.

To guarantee the same flexibility of the heating system as the previous HVAC system selections, five separate AHU's are installed, one for each of the heated zones (see *Figure 6.4*): 2 AHU's for the class zones, 1 for the canteen/kitchen, 1 for the administration rooms and 1 for the gym. For the AHU's serving multiple rooms (*i.e.* AHU_1 to AHU_3, serving various class rooms and offices - see *Figure 6.4*), the supply air is preconditioned in the central AHU equal to the set-point temperature for

[2] Alternatively, one could opt for a 50/40/10 regime, reducing the difference between supply and return flow temperature. When applying these alternative settings for a single case, an effect is found on the distribution and generation efficiencies and on the pump energy use. As all distribution pipes are assumed to be well insulated, the impact is rather insignificant (*i.e.* differences between the average $\eta_{dis} < 2\%$). Furthermore, a slight decrease of the generation efficiency (*i.e.* differences between $\eta_{gen} < 2\%$) is found. Comparable results are shown in *Figure 6.15* (a) and (b) for the distribution and generation efficiencies, respectively. Finally, as the hot water flow rate is increased, the pump energy use is raised accordingly.

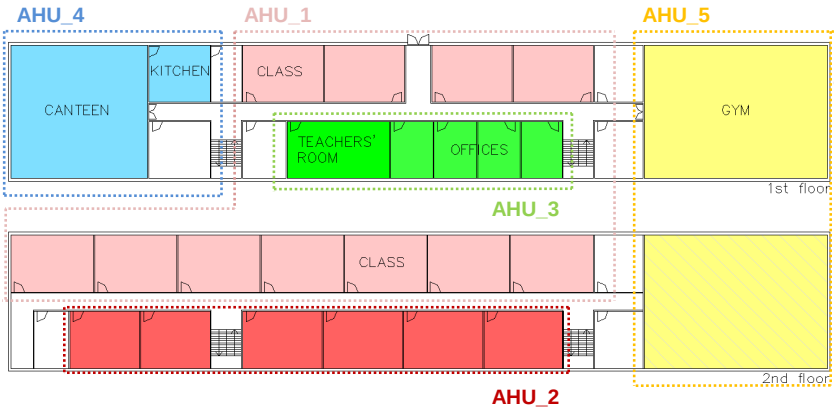

Figure 6.4: All air heating system of a prototypical rectangular, elementary school building: overview of the installed AHU's.

heating (= 21°C). Whenever necessary, the supply air is post-heated by local heating coils placed at the ventilation supplies of each of the served zones. For the AHU's serving a single room such as the canteen or the gym, the supply air is only conditioned locally. With the air flow rates set according to the indoor air quality requirements, the maximum heat load capacities can be calculated as shown in *Table 6.5*. Different maximum heat load intensities are found for occupied and unoccupied periods as the maximum allowed supply air flow temperature varies in relation to the occupancy pattern. When unoccupied, the maximum allowed supply temperature is 52°C. During occupancy however, the supply air temperature can not exceed the indoor temperature by more than 11°C to avoid excessive temperature stratification [236].

Table 6.5: Maximum heat load intensity of the hygienic ventilation air in various school zones.

		canteen	**class room**	**gym**	**office**
occupant density	m^2/pers	1.5	3	20	14
ventilation rate	m^3/(pers.h)	29	29	44	29
max. heat load intensity, occupied	**W/m^2**	**71.7**	**35.8**	**8.2**	**7.7**
max. heat load intensity, unoccupied	**W/m^2**	**202.0**	**101.0**	**26.0**	**21.6**

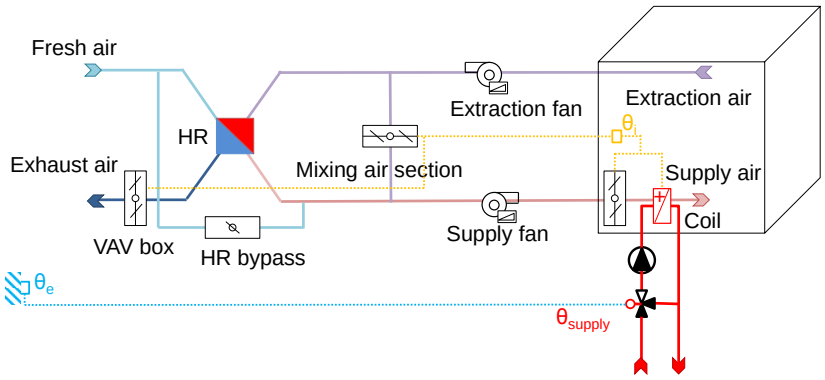

Figure 6.5: Conceptual scheme of the air handling unit used for ventilation and heating of the gym.

When the specific design heat load of the zone exceeds the maximum heat load intensity, recirculation air is needed for peak power supply. As shown in *Table 6.5*, rather high heat capacities can be reached in canteens and class rooms. In contrast, for offices and gyms, the hygienic ventilation need is much lower so extra heat capacity is created by using a mixing section (see *Figure 6.5*).
To avoid problems while commissioning, controlling and maintaining the (complex) ventilation systems, a CAV system that maintains the ventilation rate equal to the required hygienic ventilation flow is preferable in schools. Therefore, for the class rooms, a CAV system is chosen. The desired indoor set-point temperature is obtained by varying the supply air flow temperature but keeping the air volume flow rate constant. In all other school zones however, a VAV system is foreseen, as either the required air flow to heat the zone exceeds the required hygienic ventilation air flow (*i.e.* gym and administrative zone) or highly variable occupancy rates and operational schedules are to be expected (*i.e.* canteen).
The heating in the zones is managed according to the heat load pattern by - ordered based on the priority - a varying supply air temperature and variable air flow rate (VAV boxes and variable speed fans). To heat the supply air, counter flow heating coils are used which are sized according to the Effectiveness - NTU method [234] (regime 70/50/20). The supply flow temperatures to the coils are automatically adjusted using a PID controller in combination with motorised three-way valves, with the maximum supply temperature limited by an outdoor temperature reset control.
In case heating by the hygienic ventilation air is insufficient, the supply air flow is raised. The VAV boxes are controlled by P-controlers varying the ventilation rates between 20 and 100% of the maximum design air flow rates [237].
Similar to the other investigated HVAC systems, the heating system is overall on/off controlled based on a time schedule. The heating schedule of the all-air heating system is slightly delayed compared to the other systems as heating starts at 5 AM on Monday's and at 6 AM on other school days.

The cross-sections of the ducts are calculated according to *EN 13779* [13] assuming air velocities of 2.5 m/s. For the insulation of the ducts, a typical R-8 insulation level is assumed which equals an R-value of 1.41 (K·m^2)/W.

The cooling capacity of mechanical night ventilation in class rooms and canteens is high due to the required hygienic ventilation flow rates. On contrary, in the gym ($n_{vent,hyg}$ = 0.37 vol/h) and offices ($n_{vent,hyg}$ = 1 vol/h) ventilation rates are much lower. Due to the installation of VAV boxes, the ventilation and consequently the ventilative cooling capacity is increased. In case night cooling is requested, ventilation rates are varied by the VAV boxes based on the zone temperature using a P-controller between a minimum (= 20% of the maximum air flow [237]) and the maximum air flow as sized according to the design heat load calculations.

6.3 Integrated building and HVAC system simulation approach

Along this section, the simulation approach used for the integrated, dynamic simulations in TRNSYS is described (*§ 6.3.1*). Subsequently, a short description is given of the selected building design variants and the included boundary conditions (*§ 6.3.2*). Finally, an overview is given of the most impor-

tant characteristics and input parameters used for the simulation of all HVAC system components (*i.e.* fans, pumps, pipes, boilers) in TRNSYS in *§ 6.3.3*.

6.3.1 Method

The integrated simulation approach is illustrated by two simplified examples. *Figure 6.6* illustrates the conceptual diagram of a school building heated by radiators controlled by thermostatic radiator valves and supplied by a condensing gas boiler [125]. *Figure 6.7* shows an air handling unit with a heat recovery device including bypass and air heating coil controlled by a PID controller to (pre)heat the supply air flow. The considered data flow between the included system components is indicated by the arrows. The thermal behaviour of the building and system is studied with a time step of 3 minutes, which can be considered as a good balance between overall simulation time and precision [41].

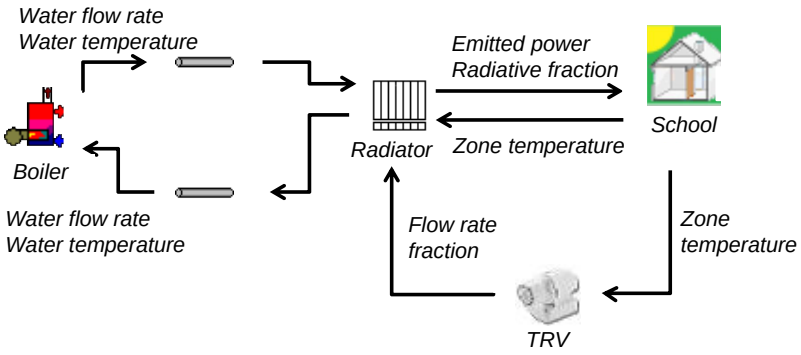

Figure 6.6: Illustration of integrated building and HVAC simulation approach in TRNSYS for radiator heating as applied in HVAC1 and HVAC2 [125].

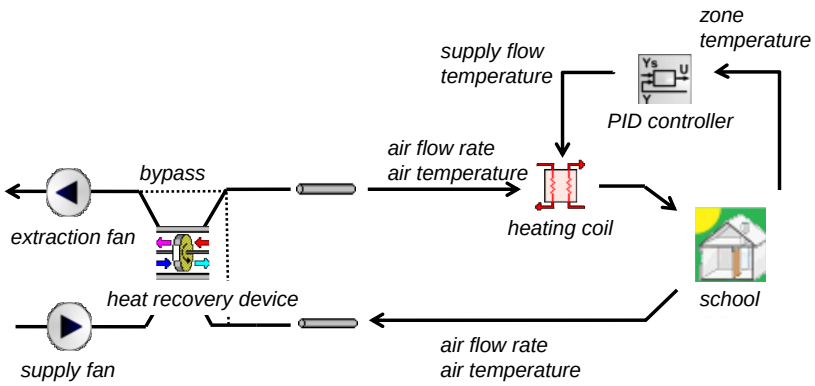

Figure 6.7: Illustration of an air handling unit including air heating coil as simulated in TRNSYS and used for HVAC3 and HVAC4.

For the simulation of radiator heating systems, the simplified simulation approach of Dolisy et al. [238] is applied. As there is only one temperature available per zone in TRNSYS (see *§ 3.3*) only one heat emitter with a total output capacity equal to the calculated design load is modelled per zone. To determine however relevant distribution losses by the simulation model, a distribution pipe is cou-

pled to the heat emitter with the length equal to the average of all distribution pipes needed to supply the real number of heat emitters. To determine the actual distribution losses, the thermal losses calculated for this pipe are then multiplied by the exact number of heat emitters that are foreseen in the considered building zone.

For each combination of building and HVAC systems, two series of dynamic simulations are performed [131, 39]. Series 1 contains the dynamic simulations of the building envelope with ideal assumptions regarding the HVAC operation to calculate the 'ideal' energy demand. Series 2 comprises the detailed simulations of both the building and the system and is executed to determine the 'real' energy demand incorporating the impact of the equipment (sizing), climatic conditions, and the implementation of operational schedules and control systems. These simulation results are then used to calculate the emission, control, distribution, generation and overall efficiencies using *Eq. 6.1* to *Eq. 6.4*.

The $\eta_{overall}$ is calculated as the ratio of the 'ideal' heating demand determined by the Series 1 simulations and the 'real' heating demand obtained by the Series 2 simulations according to *Eq. 6.1*:

$$\eta_{overall} = \frac{Q_{H,nd}}{Q_{H,final,use}} \tag{6.1}$$

The η_{em} is defined as the ratio of the heat demand and the energy delivered by the emission systems to each of the conditioned zones[3].

$$\eta_{em} = \frac{Q_{H,nd}}{Q_{H,emitted}} \tag{6.2}$$

The η_{dis} is then calculated by dividing the energy delivered by the emission systems by the gross heat demand.

$$\eta_{dis} = \frac{Q_{H,emitted}}{Q_{H,gross}} \tag{6.3}$$

Finally, the η_{gen} results from dividing the gross heating demand by the final energy use for heating or the heat output of the boiler.

$$\eta_{gen} = \frac{Q_{H,gross}}{Q_{H,boiler}} \tag{6.4}$$

In accordance with *EPR* [22], results for the subsystem efficiencies are discussed on a monthly time base. To link the HVAC system performance to the operation of the system and the building properties, the monthly averaged calculated subsystem efficiencies of each of the considered HVAC systems are expressed as a function of the monthly averaged part load ratio of the heating system β.

[3] As TRNSYS applies a single (zonal) air temperature and only one-dimensional heat transfer can be calculated, emission losses $Q_{H,em,str}$ due to amongst others non-uniform temperature distributions cannot be simulated. Therefore, specific emission losses are calculated manually according to *EN 15316-2-1* [49]. Depending on the height of the conditioned building zone, η_{str} is set equal to 0.93 ($h < 4m$ - class rooms, canteen, offices) or 0.91 ($h > 4m$ - gym). The emitted power calculated by TRNSYS is then adjusted accordingly before being coupled to the building model (TRNSYS Type56). As a result, the occurring variations of the emission efficiencies are entirely related to the performance of the applied control system.

This particular value is chosen as a reference as it incorporates the effect of the thermal insulation of the building, weather conditions and internal loads and as it is currently applied in *EN 15316* [49, 151, 152] to determine the subsystem efficiencies (see *§ 3.2.2*).
The monthly averaged part load ratio of the heating system β is calculated according to *Eq. 6.5*:

$$\beta = \frac{Q_{H,nd}}{\phi_{boiler} \cdot t_{op}} \tag{6.5}$$

where ϕ_{boiler} is the nominal power the boiler (kW) and t_{op} is the number of operational heating hours including the reheat period per month.

6.3.2 Building model and characteristics

As both the sizing procedure of the HVAC systems and the integrated simulations of building and HVAC systems are complex and time-consuming, only one reference building is used for this study. The rectangular, elementary school building is chosen for its simple though common and representative shape and room type profile. More information can be found in *§ 2.2.2*.

To assess the impact of the building's characteristics on the (sub)system efficiencies, a sample of 18 school building design variants is set ranging the thermal capacity and the energy efficiency of the building envelope, the glazing properties, the window-to-wall ratio (WWR), the shading devices and orientation of the building to represent the current school building practice.
The same sample of building design variants (variant 1 to variant 5 - see *Table 5.3*) as described in *§ 5.3.1* are used for this research study. The same U-values, glazing properties, air tightness levels and shading devices are implemented. The construction of the building is however either heavy or light. The WWR is varied between 20% [97] and 40% [66, 121, 97] and the impact of the orientation is evaluated by turning the building in two directions. All building variants are once simulated with the main axis along the North−South direction and once with the main axis along the East−West direction. Deterministic boundary conditions for amongst others user's schedule, internal heat gains and ventilation rates are used as set in *Table 4.5*.

An overview of the incorporated building design variants is depicted in *Table 6.6*. The names added in the first column refer to the considered building's characteristics. The subsequent letters and numbers refer to the thermal capacity of the building (**H**eavy - **L**ight), the considered WWR (**20** *or* **40**%), the orientation (**NS** or **EW**) and the building energy efficiency level (variant **1** to **5**) respectively. As, by applying only passive cooling strategies, the summer comfort can not be guaranteed in highly energy efficient school buildings with a light building structure, only design variant 1 to 3 are considered for the light school building models.

Table 6.6: Sample of 18 design variants of the rectangular, elementary school building model: building envelope efficiency, thermal capacity, shading, WWR and orientation are varied.

	orientation -	U_{wall} W/(m^{2}K))	U_{floor} W/(m^{2}K)	U_{roof} W/(m^{2}K)	$U_{glazing}$ W/(m^{2}K)	g-value -	n_{50} ACH	WWR %	shading device -	thermal capacity -
H20NS_1	N-S	0.37	0.37	0.29	1.12	0.57	3	20	fixed (S)	heavy
H20NS_2	N-S	0.3	0.24	0.24	1.12	0.57	2.4	20	fixed (S)	heavy
H20NS_3	N-S	0.22	0.19	0.19	1.12	0.57	1	20	fixed (S), mobile (E,W)	heavy
H20NS_4	N-S	0.15	0.15	0.15	0.78	0.55	0.6	20	fixed (S), mobile (E,W)	heavy
H20NS_5	N-S	0.11	0.15	0.13	0.6	0.47	0.4	20	mobile (E,S,W)	heavy
H40NS_1	N-S	0.37	0.37	0.29	1.12	0.57	3	**40**	**fixed (S), mobile (E,W)**	heavy
H40NS_2	N-S	0.3	0.24	0.24	1.12	0.57	2.4	**40**	**fixed (S), mobile (E,W)**	heavy
H40NS_3	N-S	0.22	0.19	0.19	1.12	0.57	1	**40**	fixed (S), mobile (E,W)	heavy
H40NS_4	N-S	0.15	0.15	0.15	0.78	0.55	0.6	**40**	fixed (S), mobile (E,W)	heavy
H40NS_5	N-S	0.11	0.15	0.13	0.6	0.47	0.4	**40**	mobile (E,S,W)	heavy
L20NS_1	N-S	0.37	0.37	0.29	1.12	0.57	3	20	**fixed (S), mobile (E,W)**	**light**
L20NS_2	N-S	0.3	0.24	0.24	1.12	0.57	2.4	20	**fixed (S), mobile (E,W)**	**light**
L20NS_3	N-S	0.22	0.19	0.19	1.12	0.57	1	20	fixed (S), mobile (E,W)	**light**
H20EW_1	**E-W**	0.37	0.37	0.29	1.12	0.57	3	20	fixed (S)	heavy
H20EW_2	**E-W**	0.3	0.24	0.24	1.12	0.57	2.4	20	fixed (S)	heavy
H20EW_3	**E-W**	0.22	0.19	0.19	1.12	0.57	1	20	fixed (S), mobile (E,W)	heavy
H20EW_4	**E-W**	0.15	0.15	0.15	0.78	0.55	0.6	20	fixed (S), mobile (E,W)	heavy
H20EW_5	**E-W**	0.11	0.15	0.13	0.6	0.47	0.4	20	mobile (E,S,W)	heavy

6.3.3 HVAC system components

The overall simulation approach and the selection of the simulation models used for all HVAC system (components) in TRNSYS, including their underlaying thermal dynamics and physical processes, are based on similar work done by Parys [125] and by Bertagnolio [239]. For the sake of clarity however, the main simulation models and related input parameters are summarised and briefly explained along this section. The detailed mathematical description and related input parameters of the models can be found in the TRNSYS manual [161].

Heat emission system

The **radiators** are modelled by the dynamic, lumped capacitance radiator model TRNSYS Type362 [240] that calculates both the emitted radiator power and the radiative fraction of the emitted power based on the water flow, the surrounding temperature and the incoming water temperature. The most important parameters to describe the radiator are the nominal flow, the nominal heat emission at 90/70/20-regime, the radiator exponent and the thermal capacity of the water content and the metal. The mathematical description can be found in Holst [240].

The **thermostatic radiator valves** on the radiators are modelled based on the IEA annex 10 'perfect thermostatic valve' model as developed by Ast [241]. It is a lumped capacitance model of the temperature sensor including the (relatively small) thermal resistance of the casing and the (larger) resistance between the sensor and the water. The valve authority is set equal to 0.7. The hysteresis is 0.5°C and the nominal and maximal temperature differences between the valve and ambient are assumed to be 2°C. All valves are assumed to have an infinite rangeability: 100% of the maximum flow rate when the valve is fully open and 0% of flow rate when fully closed.

For the modelling of a radiant **floor heating** in TRNSYS, a thermally active layer available in TRN-Build is used. A constant water flow rate at a variable supply temperature is used as the input to the active layer. Pipe length, outside diameter, pipe wall thickness and pipe wall conductivity are the most important input parameters. As the convective heat transfer coefficient between surface and zone air depends on the temperature of the active layer - unlike all other modelled cases that use a fixed preset value - convective heat transfer coefficient are calculated using the internal calculation method of TRNSYS (see *§ 3.4.2*).

Heating coils are modelled using the TRNSYS Type5 model for sensible heat exchangers (see *Figure 6.8*). The most important input parameters are the configuration mode, the overall heat transfer coefficient of the heat exchanger (UA) and the flow conditions. The calculated nominal UA-value is hereby adjusted for non-rated conditions according to the HCSIMOL model [242]. A constant hot water supply flow rate is supplied by a **constant speed pump** (TRNSYS Type110) which is switched on or off by a temperature sensor in the supply air duct. The hot water supply temperature is controlled by a **PID controller** (TRNSYS Type22) adjusting a three-way, mixing valve. The latter is modelled as a simple equation.

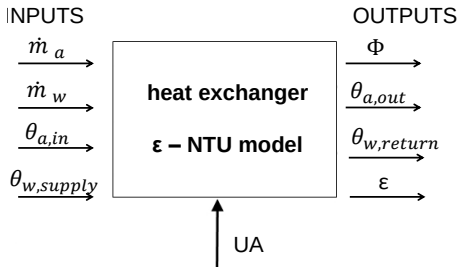

Figure 6.8: ε - NTU simulation model of a heat exchanger [243] with $\dot{m}_a$ the load side flow rate (air), $\dot{m}_w$ the source side flow rate (hot water), θ_a is the load side (air) temperature, $\theta_{w,supply}$ is the hot water supply temperature, ϕ emitted heat, $\theta_{w,return}$ is the hot water return temperature and ε the effectiveness of the heat exchanger.

The **VAV boxes** are modelled as simple equations that compute the percentage of VAV openings controlling the entering air flow rate to the served zones based on the (zonal) indoor temperatures using a PID controller (TRNSYS Type22). The maximum air flows in heating and cooling regime are determined based on the respective required heating and cooling demands.

Heat distribution system model

For the simulation of the distribution **pipes and ducts**, the 'plug-flow' pipe model (TRNSYS Type31) is used. The surrounding temperatures of the pipes and ducts are simulated by the thermal simulation model and used as an input for the pipe models. In line with the simplified calculation approach as applied in EPR [22], the distribution thermal losses which occur in heated zones are considered recoverable and are thus injected as heat gains in the zones which they serve. Possible air leakage from the ducts is neglected in the simulation model [125].

For the **pumps**, TRNSYS Type110 is used that calculates the mass flow rate of the distributed fluid, the outlet temperature and the electrical power use of the pump. The pump model does not include any transient behaviour upon start-up and shut-down processes. For the calculation of the outlet fluid temperatures, it is assumed that none of the pump power is converted into fluid thermal energy. The electric pump power $P_{el,pump}$ is calculated according to the model of Bernier and Lemire [244] as a polynomial function of the control signal χ ($0 \geq \chi \geq 1$):

$$\frac{P_{el,pump}}{P_{el,shaft,nom}} = a + b\chi + c\chi^2 + d\chi^3 \tag{6.6}$$

where $P_{el,shaft,nom}$ is the shaft power of the pump at nominal conditions.
In accordance with the work of Parys [125] and the survey results of passive schools, an 'average' pump efficiency (η_{pump} = 0.685 and a motor part load ratio of 80% (*i.e.* surveyed part load ratio's of the motor vary between 75 and 80%) are assumed for this study. The following polynomial curves are then obtained (see *Table 6.7*):

Table 6.7: Pump coefficients of the polynomials curves according the model of Bernier and Lemire [244]. An average pump efficiency (η_{pump} = 0.685) and a motor part load ratio of 80% are assumed.

Control	a	b	c	d
constant speed pump	0.1946	1.7268	-1.6080	0.7583
variable speed pump	0.1633	0.2637	-0.4485	1.1059

Heating plant model

For the dynamic simulations, the dynamic **boiler** model developed by Haller et al. [245, 246] (TRNSYS Type869) is chosen. This model uses the incoming water flow rate and temperature as inputs and calculates the hot water outlet temperature and the related energy use. Parameters are the nominal range of thermal powers (ϕ_{nom}), the thermal capacitance of the burner (C_{burner}), the water content (V_w), the UA-value of the boiler and the auxiliary electrical energy use (W_{aux} - see *Table 6.4*). More details on the calculation procedure and input parameters can be found in Haller [246] and in the work of Parys [125].

Air handling units

For the modelling of the **air-to-air heat exchangers** in TRNSYS, a combination of a zero capacitance sensible heat exchanger (TRNSYS Type5, see *Figure 6.8*) and a sensible air-to-air heat recovery device with controlled outlet conditions (TRNSYS Type760) is used. The first type is used to calculate the sensible effectiveness ε based upon the specified flow configuration and on the UA of the heat exchanger. The modelled effectiveness is then supplied as an input for TRNSYS Type760 to determine the maximum possible amount of energy that can be transferred between the two air streams given their inlet conditions. The heat exchangers are bypassed based on an on/off signal of a differential controller (TRNSYS Type2).

The air **mixing section** which is used to maintain the fresh air fraction equal to the required hygienic ventilation rate, is modelled as a simple equation in TRNSYS in combination with a mixing pipe (TRNSYS Type11) to determine the resulting supply air temperatures.

A simplified pressure independent **fan** model is used [125] as only the thermal aspects are modelled. The fan model (TRNSYS Type3) calculates the outlet mass flow rate, the outlet temperature and the power consumed by the fan. For the calculation of the air flow outlet temperature, the fraction of pump power that is converted to fluid thermal energy is assumed to be zero. To avoid detailed calculations of the pressure drops in the air ducts, the electric fan power $P_{el,fan}$ is calculated by a polynomial function of the control signal χ:

$$\frac{P_{el,fan}}{P_{el,fan,nom}} = a + b\chi + c\chi^2 + d\chi^3 + e\chi^4 \tag{6.7}$$

The polynomials used along this study are based on the AIVC technical note 65 [133], assuming a 'normal' control system [125] (see *Table 6.8*).

Table 6.8: Coefficients for the polynomials curves used to calculated the electric fan power, assuming a 'normal' control system [133].

Control	a	b	c	d	e
CAV	0	1	0	0	0
VAV	0	1.0547	-2.5576	3.6314	1.1285

Although in reality a fraction of the fan power will be converted into fluid thermal energy[4], this fraction is neglected along this study in line with the work of Parys [125]. Simultaneously, no internal heat gains or corrections of the supply air temperature due to the fans are included in the energy demand calculations.

6.4 Results and discussion

This section covers the results of the integrated building and HVAC system simulations. First, the impact of the system selection on the energy use for heating including the auxiliary energy use for pumps, boiler and fans, both expressed in terms of primary energy, $E_{H,p}$ is studied (*§ 6.4.1*). Second, the overall performance of each of the HVAC systems is discussed in *§ 6.4.2*.

Before analysing the results of the integrated simulations, both the accuracy of the simulation results and the thermal comfort are assessed for all simulated cases.

[4] In case this fraction is simulated, the final energy use of heating is reduced, though the impact is limited (*e.g.* for H20NS_1 and H20NS_3 coupled to HVAC2, the final energy use for heating is reduced by 1.5 kWh/(m^2.a) and 0.6 kWh/(m^2.a), respectively, when a conversion factor of 0.6 is assumed for the fan energy use [247]). The impact on the overall energy performance assessment of the HVAC system is also small (*i.e.* $\Delta\,\eta_{overall} < 2\%$, mostly determined by the differences of the emission efficiencies). When the energy demand calculations would be adapted accordingly by either implementing additional internal heat gains due to the fans or introducing a correction of the supply air temperature as described in EN 15241 [247], the difference of the efficiencies is expected to be reduced even more.

Table 6.9: Overview of the average and maximum simulation errors found for each of the investigated HVAC systems.

HVAC1		**HVAC2**		**HVAC3**		**HVAC4**	
average	**max**	**average**	**max**	**average**	**max**	**average**	**max**
0.9%	1.3%	2.2%	7.1%	2.3%	4.9%	4.1%	8.7%

The quality of the execution of the simulations is assessed by determining the monthly simulation error Δ:

$$\Delta = 1 - \frac{(Q_{H,emitted} + Q_{H,losses,total})}{Q_{H,boiler}} \tag{6.8}$$

The results for all HVAC system simulations are depicted in *Table 6.9*.

The lower Δ, the better the accuracy of the simulation results. Slight deviations from zero are possible, caused by the differences in the internal energy between the beginning and end state [40] or due to the restrictions related to the implemented calculation time step and the control algorithms in TRNSYS[5]. n The average simulation errors remain all 4% or lower. The maxima - found for the spring and autumn months with the lowest heat demands - are all $< 10\%$, so it is assumed that the simulations are well executed.

Subsequently, a comfort analysis is performed. In order to be able to compare the performance of the different HVAC systems mutually, the thermal comfort of each of the investigated cases must be comparable. Therefore, the thermal comfort of each of the investigated case is assessed using the Degree Hours criterion as described in method B of *EN 15251, Annex F* [47]. The temperature-weighted time fractions that the required set-point temperature is not achieved in winter and summer are depicted in *Table 6.10* and *Table 6.11*, respectively. Only the results for those school building design variants and school zones where the comfort conditions are most critical are added to the table.

Table 6.10: Weighted percentage of the time that the **heating set-point** is not met during the occupied period for all included system and building design variants.

	critical zone	**HVAC1**	**HVAC2**	**HVAC3**	**HVAC4**
H20NS_1	class (N)	4.6%	5.1%	3.7%	1.8%
H40NS_1	class (N)	5.4%	6.0%	5.8%	7.9%
L20NS_1	class (N/S)	6.2%	6.3%	7.9%	-
H20EW_1	class (E)	5.2%	6.7%	3.9%	5.1%

Overall, *Table 6.10* shows acceptable results for the winter comfort analysis. For some cases however - mostly the lighter buildings or buildings with a high WWR - the time fractions exceed the re-

[5]For the simulations in TRNSYS, a time delay between control decisions is implemented in addition to temperature dead bands to promote controller stability. To do so, TRNSYS Type 93 (Input value recall) is used to feed into the controller the outputs of other components at the previous time step instead of the current time step.

Table 6.11: Weighted percentage of the time that the **cooling set-point** is not met during the occupied period for all system and building design variants.

	critical zone	**HVAC1**	**HVAC2**	**HVAC3**	**HVAC4**
H20NS_5	gym (N/S)	0.0 %	4.7%	1.2%	0.1%
H40NS_5$^{(1)}$	class (N)	0.1%	0.3%	0.1%	5.7%$^{(2)}$
L20NS_3$^{(1)}$	class (N)	8.2%	10.0%	10.6%	-
H20EW_5	gym (E/W)	0.1%	3.7%	0.0%	0.7%

(1). Night cooling by natural stack ventilation is foreseen in addition to the mechanical night ventilation for the offices and gym as the hygienic ventilation rates only ($n_{vent,office}$ = 1 ACH, $n_{vent,gym}$ = 0.37 ACH) are insufficient to guarantee an acceptable level of summer comfort.

(2). The lowest thermal comfort level is obtained in the gym instead of the class zone (N).

quired 5%, implying that the heating systems in these buildings are more difficult to control. As however the differences remain limited (< 8%) and the failure of comfort is mostly restricted to (slightly too) low temperatures at the start of the school days, all results are retained for further analysis.
Regarding the summer comfort (see *Table 6.11*), the applied passive night ventilation is insufficient to guarantee an acceptable comfort level in lighter buildings. For building variants 1 to 3, the weighted percentage is ±10%. As time fractions up to 25% are found when variants 4 and 5 are coupled to a light structure, these building design variants are excluded for the study.

6.4.1 Assessing the impact of the HVAC system selection on the primary energy use for heating and ventilation

Figure 6.9 demonstrates the results of the dynamic simulations in terms of total annual heat demand $Q_{H,nd}$ and annual primary energy use for heating and ventilation $E_{H,p}$ for the different HVAC systems, both normalised to the building floor area.

The primary energy use $E_{H,p}$ is calculated by adding the auxiliary energy needed for all heating system components W_{aux} to the delivered energy to the heating system and converting it to primary energy. In doing so, national conversion factors are taken into account which represent the conversion step from energy source to energy carrier: 1 for fossil fuels and 2.5 for electricity [22], specifically valid for Flanders[6]. The results are summarised in *Table 6.12*.

Four general trends can be noticed. **(i)** The primary energy use of the HVAC1 is generally higher than that of the other HVAC systems. **(ii)** The results for each of the building variants coupled to HVAC2 and HVAC3 are more or less comparable. Except for the lighter building structures, slightly lower $E_{H,p}$ are found. **(iii)** Due to additional fan electrical use, the primary energy use in HVAC4 is overall slightly higher than that of HVAC2 and HVAC3. Finally, **(iv)** a strong correlation between the primary energy use and the heat demand is noticed (see *Figure 6.9*).

[6]Despite the requirement of the EPBD regulation for non-residential buildings in Flanders (*i.e.* at least 10 kWh per year per m^2gross surface area must be covered by renewable energy source), no renewable energy sources are taken into account for this study.

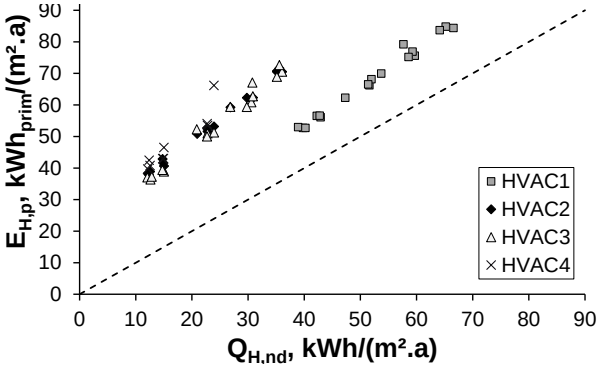

Figure 6.9: Annual primary energy use for heating and ventilation in function of the heat demands, all normalised to the building floor area (kWh/(m^2.a)), for the HVAC system variants HVAC1 to HVAC4.

The first trend noticed is entirely related to the lack of a heat recovery device in HVAC1. The lower heat demands in HVAC2 to HVAC4 consequently result in lower annual energy use for heating. The differences in $E_{H,p}$ between HVAC1 and HVAC2 to HVAC4 remain however limited as the savings due to the implementation of a heat recovery device are partially compensated by additional auxiliary energy use of the supply ventilation fans in HVAC2 to HVAC4. This trend is confirmed by the results of a recent survey of the energy use of school buildings in Luxembourg [230]. Measuring data and monitoring results reveal that the mean electrical energy use has significantly increased in new low-energy and passive schools due the amongst others the use of mechanical ventilation systems,

Table 6.12: Simulation results for $Q_{H,nd}$ and $E_{H,p}$ for varying building energy efficiency levels.

kWh/(m^2.a)	$Q_{H,nd,HVAC1}$	$Q_{H,nd,HVAC2-4}$	$E_{h,p,HVAC1}$	$E_{h,p,HVAC2}$	$E_{h,p,HVAC3}$	$E_{h,p,HVAC4}$
H20NS_1	65.2	36.0	84.8	70.5	69.0	-
H40NS_1	66.6	35.6	84.4	71.6	72.6	-
L20NS_1	57.7	30.8	79.2	70.5	67.1	-
H20EW_1	64.1	35.2	83.7	70.7	68.9	-
H20NS_2	59.7	30.6	75.6	61.7	60.0	-
H40NS_2	59.3	30.9	76.9	62.3	62.7	-
L20NS_2	53.7	26.9	69.9	59.2	59.4	-
H20EW_2	58.6	29.8	75.2	62.3	59.4	-
H20NS_3	51.6	22.7	66.2	51.6	49.8	53.5
H40NS_3	52.0	23.9	68.1	53.2	51.3	66.2
L20NS_3	47.3	20.5	62.3	50.8	50.6	-
H20EW_3	51.4	22.7	66.5	52.6	50.0	54.1
H20NS_4	42.9	14.5	56.1	41.5	39.4	43.0
H40NS_4	42.3	15.0	56.5	40.6	38.9	46.5
L20NS_4	-	-	-	-	-	-
H20EW_4	42.8	14.8	56.6	42.9	39.4	43.0
H20NS_5	39.8	11.7	52.7	38.3	35.4	39.7
H40NS_5	38.9	12.3	52.9	37.9	34.7	42.5
L20NS_5	-	-	-	-	-	-
H20EW_5	40.2	12.6	52.7	38.9	36.3	40.8

neutralising partially the thermal energy savings due to the higher energy efficiency of the building. Furthermore, while comparing the results of HVAC2 to HVAC4 mutually, it is shown that - for the investigated building sample - the deviations of $E_{H,p}$ due to the implementation of different types of emission systems (radiators, floor heating or all-air heating) are small. Similar results are found by Olesen [248] stating that in well insulated buildings the impact of the choice of the emission system on the final energy performance of the HVAC system is limited.
Second, the effect of the building's characteristics on the primary energy use remains limited. The $E_{H,p}$ found for similar building variants (*e.g.* H20NS1, H40NS1, L20NS1, H20EW1) are all of the same order of magnitude, except for the lighter buildings where slightly lower $E_{H,p}$ are found. The latter phenomenon is entirely related to the lower heat demands found in lighter buildings as the dynamically calculated subsystem efficiencies are generally lower (see *§ 6.4.2*).
Third, the highest energy use is found for HVAC4. $E_{H,p,HVAC4}$ is on average 10.5% higher compared to HVAC2 and HVAC3, with a maximum difference found of 25%. When an all-air heating system is applied, the ventilation systems are sized according to the design heat loads. In some cases this leads to 'oversized' ventilation systems (*i.e.* $G_{a,vent} > G_{a,vent,hyg}$) which in turn causes additional electrical energy use of the fans. The higher the heat demand, the more significant the differences are. Moreover, as the extra ventilation capacity of the all-air system is used to enlarge the free-cooling capacity, the fan energy use is also slightly higher in summer months.
Fourth and final, $E_{H,p}$ is strongly correlated with the annual heat demand $Q_{H,nd}$ (see *Figure 6.9*). The correlation differs however depending on the selected HVAC system. Similar results are found by Korolija [71] and by Parys [125] while performing a system performance analysis of different HVAC systems in offices.

6.4.2 Overall performance of the HVAC systems

In what follows, the overall performance of each of the HVAC systems is discussed. Variations of the final energy use for heating and the auxiliary energy use for pumps, boiler and fans are studied over all building design variants and for all included HVAC systems. Additionally, the dynamically calculated subsystem efficiencies are studied and compared to the efficiencies as used in the *quasi-steady-state* calculation standards *EPR* [22] and in *EN 15316* [49, 151, 152] (see *Table 6.13*). Regarding the evaluation of the emission efficiencies, only the impact of imperfect control can be included in the study. As TRNSYS applies a single (zonal) air temperature and only one-dimensional heat transfer is calculated, emission efficiency losses due to temperature stratification, shielding of emission devices or increased heat losses through locally heated building envelopes, cannot be simulated. Consequently, the variations of the emission efficiencies noticed along this chapter are entirely related to changes of the control efficiencies.

The differences between the various values depicted in *Table 6.13* are due to different assumptions and calculation hypotheses of the considered calculation standards. Details can be found in *§ 3.2.2* and in the related calculation standard's manuals.

Table 6.13: Overview of the subsystem efficiencies calculated according to *EPR* [22] and *EN 15316* [49]. For the generation efficiencies according to EN 15316 [152], the boiler efficiency method is used (see *§ 3.2.2*). The yearly values for the generation efficiency as depicted in the table are hence calculated based on monthly calculation results.

	EPR			**EN 15316**			
	η_{system}	η_{gen}	$\eta_{overall}$	η_{em}	η_{dis}	η_{gen}	$\eta_{overall}$
HVAC1	0.93	0.92	0.86	0.90	0.98	0.85	0.76
HVAC2	0.93	0.96	0.89	0.87	0.98	0.90	0.77
HVAC3	0.93	0.98	0.90	0.82	0.98	0.92	0.74
HVAC4	0.93	0.94	0.87	0.90	0.98	0.88	0.78

Final energy use for heating

HVAC1

Figure 6.10 shows the simulated annual final energy use for heating $Q_{H,final,use,dyn}$ in relation to the annual heat demand $Q_{H,nd}$ of the building, both normalised to the floor area of the building. For comparison, the annual final energy uses for heating according to the *EPR* [22] calculation standard $Q_{H,final,use,EPR}$ are added to the figure.

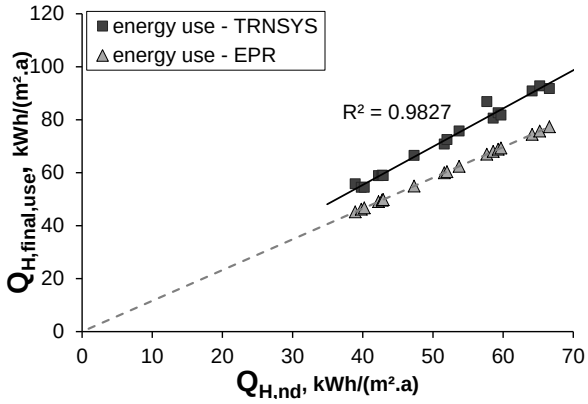

Figure 6.10: $Q_{H,final,use}$ expressed as a function of $Q_{H,nd}$, both normalised to the building floor area (kWh/(m^2.a)), for HVAC1 coupled to 18 different school building design variants, calculated in TRNSYS or using the *EPR* [22] calculation standard.

The results of the integrated dynamic simulations of HVAC1 show that the thermal losses of the heating systems add approximately 25 to 30% to the net heating demand. These additional losses are clearly underestimated by *EPR* [22] as $Q_{H,final,use,EPR}$ is on average 16% or 11.8 kWh/(m^2.a) lower than $Q_{H,final,use,dyn}$. The maximum difference of 29% is found for the light design variant with a WWR = 20% and the main axis oriented along the North−South direction (L20NS_1).

To analyse the subsystem performances in detail, the monthly averaged emission efficiency η_{em} (see *Figure 6.11* (a)), distribution efficiency η_{dis} (see *Figure 6.11* (b)) and the generation efficiency η_{gen} (see *Figure 6.11* (c)) for the 18 investigated school building design variants equipped with HVAC1 are shown in relation to the part load ratio of the heating system β. For comparison, the

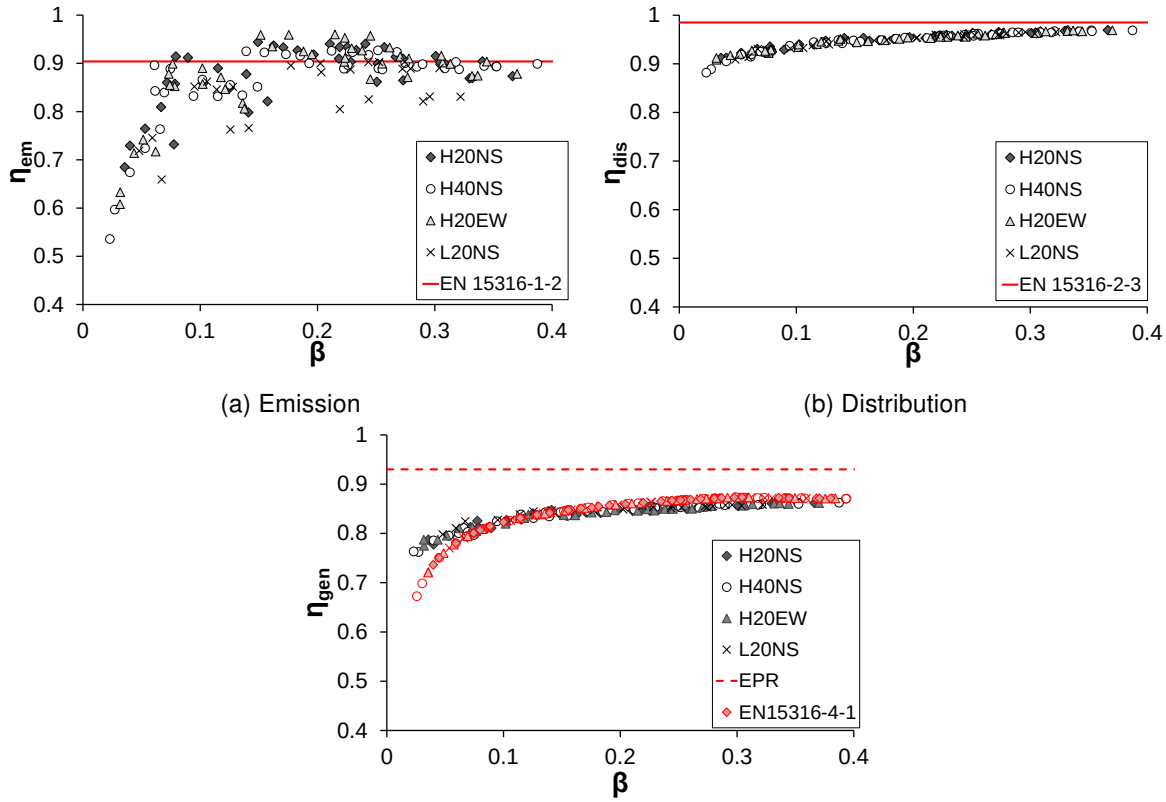

(a) Emission

(b) Distribution

(c) Generation

Figure 6.11: Monthly averaged η_{em}, η_{dis} and η_{gen} for all building design variants equipped with HVAC1 in function of the part load ratio of the heating system β.

according subsystem efficiencies as used in *EPR*[7] [22] and in *EN 15316* [49, 151, 152] are added to the figures.

Overall, three phenomena are noticed. **(i)** The dynamically calculated efficiencies decrease when part load ratios of the heating system β are lowered, especially noticeable for η_{em} (see *Figure 6.11* (a)). **(ii)** η_{em} depends on the building's characteristics while the effect of the building on η_{dis} and η_{gen} is rather negligible. **(iii)** A rather good fit is found between the calculated subsystem efficiencies calculated according to *EN 15316* [49, 151, 152] and the efficiencies obtained by the integrated dynamic simulations. The yearly averaged efficiency values as currently applied in the *EPR* method [22] however, deviate more significantly. Especially the dynamically calculated generation efficiencies η_{gen} are significantly lower than the values as currently applied in the *EPR* standard [22] (see *Figure 6.11* (c)). In what follows, the aforementioned trends are explained.

First, *Figure 6.11* (a) shows that when going towards lower part load ratios, significant decreases of the emission (and more in particular the control) efficiencies η_{em} occur. Similar results are found by Bauer [249] and Van der Veken et al. [227]. Both researchers indicate the decrease of the control efficiency at part load ratios as the most important cause of the loss of η_{em}. When highly fluctuating internal and solar heat gains occur, accurate control of the heating system becomes difficult: heat outputs of the heating system results easily in overheating and hence affect negatively the control

[7]Only the generation efficiency according to *EPR* is added to the figures as no separate values for the emission and distribution efficiencies are calculated in this standard (see *§ 3.2.2*).

efficiencies. This decreasing trend is clearly influenced by the buildings' characteristics. The lowest emission efficiencies are found for building variants with a large WWR (H40NS).
Second, *Figure 6.11* (a) to (c) demonstrate that the distribution η_{dis} and generation efficiencies η_{gen} are not influenced by the buildings' characteristics while the emission/control efficiencies η_{em} depend on the buildings' characteristics. The impact of the insulation level, the occurring heat gains (*i.e.* WWR and building orientation) and the thermal capacity of the building on the emission efficiency η_{em} is demonstrated in *Figure 6.12* (a) and (b).

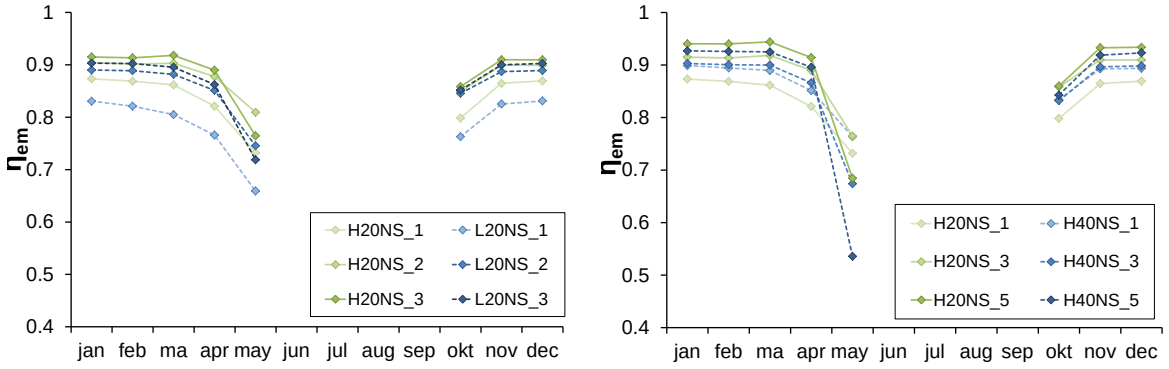

(a) impact thermal capacity

(b) impact energy efficiency level and WWR

Figure 6.12: Impact of the buildings' characteristics (*i.e.* U-value, thermal capacity, WWR, orientation) on the monthly averaged η_{em} (light structure = dashed line).

Figure 6.12 (a) shows that overall slightly lower performances of the control systems are found in lighter buildings. *Figure 6.12* (b) demonstrates that the impact of the energy efficiency of the building on the control efficiency differs in winter and in summer. In winter months, control efficiencies are slightly higher in better insulated buildings. The deviations remain however limited as the heating system and related control settings are designed in accordance to the buildings' characteristics. An opposite trend is noticed in summer and autumn months when higher solar heat gains occur and accurate control of the heating system becomes harder. As shown by *Figure 6.12* (b), this trend is more pronounced in higher energy efficient buildings.

Third and final, the differences between the dynamic and static efficiency values are discussed. Regarding the system efficiencies η_{system}, at part load ratios > 0.1, a rather good fit is found for both calculation standards, however a slightly better fit is found for *EN 15316* [49, 151]. The differences between the dynamic and static calculated system efficiencies increase however significantly at lower part load ratios ($\beta < 0.1$) as in the static calculation approaches the occurring decrease of the emission and distribution efficiencies at low part load ratios are not taken into account. Regarding the generation efficiencies η_{gen}, overall rather low, dynamically calculated values are found. This can mostly be explained by the frequently occurring part load ratios, excessive cycling, high related thermal losses of the boiler and hence lower generation efficiencies. For the design heat load calculations according to *EN 12831* [90], the boiler is sized as the sum of the design heat loads of all zones. Furthermore, the reheat capacity is included while, simultaneously, all solar and internal heat gains are neglected. Consequently, the typically high occurring internal heat gains in class rooms

result in frequent low part load ratios. Furthermore, the use of an open header in combination with a constant speed pump in the primary heating circuit negatively affects the generation efficiency: as the return water flow is mixed with the 'unused' part of the supply hot water flow, an increased return water flow temperature is found and hence lower efficiencies of the boiler are obtained. Both effects appear not to be taken into account properly in the *EPR* calculation standard [22]. As shown in *Figure 6.11* (c), the alternative, boiler efficiency method as described in *EN 15316-4-1* [152] leads to a much better fit. This can be explained by the fact that in the boiler efficiency method, more accurate thermal losses of the boiler related to the boiler operating conditions (*i.e.* expressed by the part load ratio β) and a correction of the return flow temperature for bypass operation of the boiler are calculated (see *§ 3.2.2*, *Eq. 3.52*).

HVAC2

Figure 6.13 shows the results for the annual final energy use for heating $Q_{H,final,use,dyn}$ in relation to the annual heating demand $Q_{H,nd}$ of the building, both normalised to the building floor area. For comparison, the annual final energy uses for heating calculated according to the *EPR* standard $Q_{H,final,use,EPR}$ [22] are added to the figure.

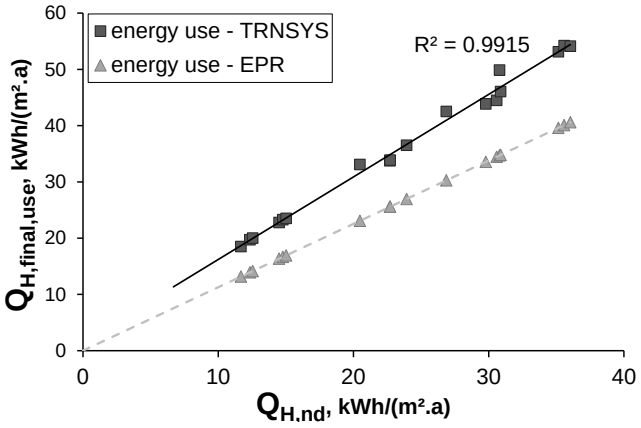

Figure 6.13: $Q_{H,final,use}$ for heating system HVAC2 coupled to 18 school different building design variants, calculated using dynamic integrated building simulations (TRNSYS) or the *EPR* calculation method [22].

Similar results as for HVAC1 are obtained. The *EPR* tool [22] significantly underestimates the heating energy use compared to the results of the dynamic simulations. The average deviation is 36.9% or - 9.60 kWh/(m^2.a), with a maximum found of 43.7% for the building variant L20NS_1. Moreover, some limited variations of $Q_{H,final,use}$ are found due to different building characteristics.

The monthly averaged system η_{system} and generation efficiencies η_{gen} for all investigated school building design variants equipped with HVAC2 are depicted in *Figure 6.14* (a) and (b), respectively, together with the subsystem efficiencies as used in the static calculation methods *EPR* [22] and *EN 15316* [152].

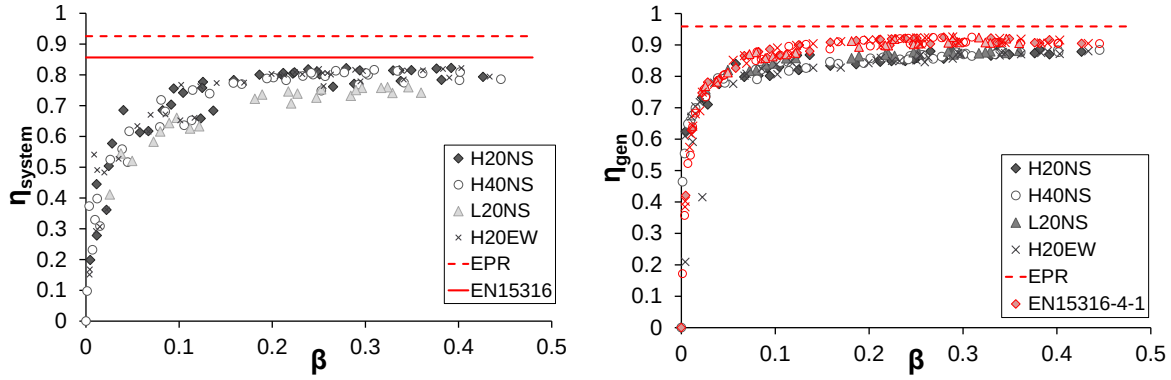

(a) System (b) Generation

Figure 6.14: Monthly averaged η_{system} and η_{gen} for all building design variants equipped with HVAC2 in function of the part load ratio of the heating system β.

Similar though even more distinct phenomena as previously described for HVAC1 are noticed. **(i)** A similar decrease of the subsystem efficiencies when going towards lower part load ratios β is noticed. **(ii)** η_{system} depends on the buildings' characteristics while the effect of the building on the generation efficiency η_{gen} is negligible and **(iii)** overall, an overestimation of η_{system} and η_{gen} is found for *EPR* [22]. For *EN 15316* [152], overall, a better fit is found between the statically and dynamically calculated generation efficiencies η_{gen}.

The curves of the monthly averaged generation efficiency η_{gen} are similar to that of HVAC1 although the efficiencies at high part load ratios are slightly higher and the decrease of the efficiency in spring months is larger (see *Figure 6.11* (c) vs. *Figure 6.14* (b)). The first effect indicates the impact of the heating curve: while lowering the temperature regime of the heating system (*i.e.* maximum supply temperature is 80°C for HVAC1 and 60°C for HVAC2), the efficiency of the boiler is increased as more condensation occurs. A similar effect is demonstrated in *Figure 6.15* where the differences in η_{gen} are shown between a heating system that applies an outdoor reset temperature control and a heating system that uses a constant supply temperature (see *Figure 6.15* (b) - heating systems at constant temperature are marked by *). The figure shows indeed a slight impact of the return water flow temperature on the boiler efficiency.
The second effect is caused by the fact that for HVAC2 lower part load ratios occur. Although lower (default) reheat capacities for HVAC2 are included compared to HVAC1, the importance of the reheat capacity in proportion to the total heat load is higher in HVAC2 ($\pm 32\%$ compared to $\pm 20\%$ in HVAC1), causing more frequent and lower part load ratios. The heat emission system is sized as such that for occupied class rooms with high internal heat gains, small heat delivery results easily in overheating which complicates the control of the system and explains the more significant decrease of $\eta_{H,system}$ compared to HVAC1.

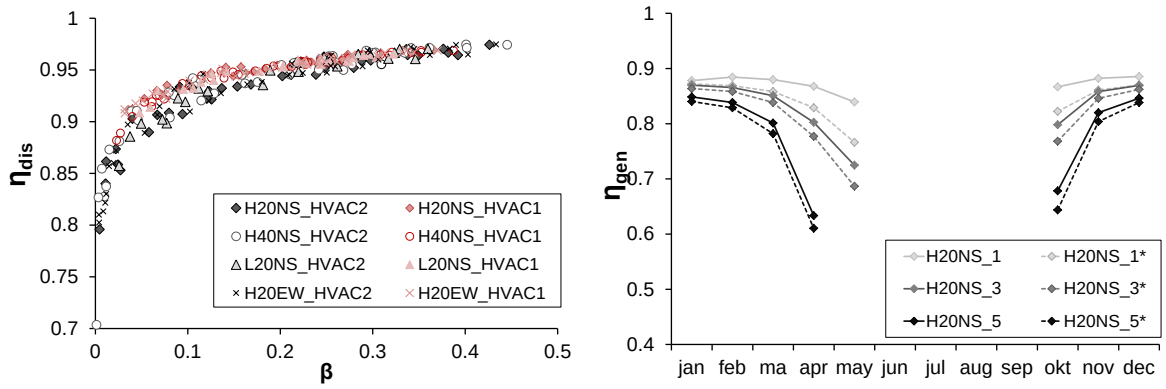

(a) distribution efficiencies (b) generation efficiencies

Figure 6.15: Impact of the applied heating curve on the monthly averaged distribution and generation efficiencies.

HVAC3

Figure 6.16 shows the results of the integrated HVAC and building simulations for HVAC3 and compares the dynamically calculated annual final energy use for heating $Q_{H,final,use}$ (kWh/(m^2.a)) to the results of the *EPR* calculation method [22].

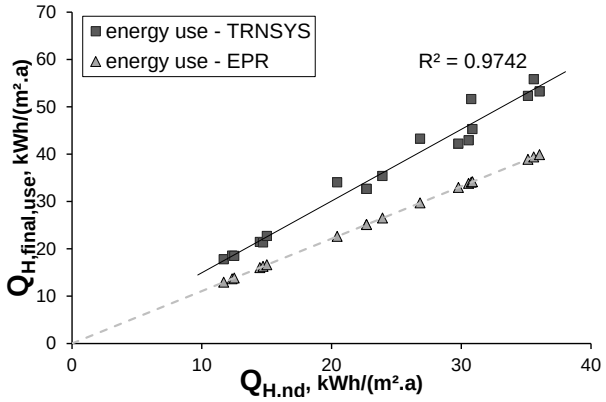

Figure 6.16: The annual $Q_{H,final,use}$ for heating systems HVAC3, normalised to the building floor area (kWh/(m^2.a)), of all investigated school building design variants, calculated by dynamic integrated building simulations (TRNSYS) or by the *EPR* calculation standard [22].

Similar as for HVAC1 and HVAC2, the heating energy use of HVAC3 is largely underestimated by *EPR* [22]: an average deviation of 35.9% or - 9.5 kWh/(m^2.a) is found, with a maximum of 51.6%. Furthermore, *Figure 6.16* shows that the impact of the buildings' characteristics on the overall performance of the HVAC system is higher for HVAC3 compared to HVAC1 and HVAC2 as the data points plotted in the figure are more scattered and a lower value for R^2 is found.

The results for the dynamically calculated, monthly averaged system η_{system} and generation efficiencies η_{gen} of the HVAC3 system variants are shown in *Figure 6.17* (a) and (b), respectively. In general, similar results are found as described for HVAC1 and HVAC2. The subsystem efficiencies decrease at low part load ratios. The system efficiencies η_{system} depend on the building's charac-

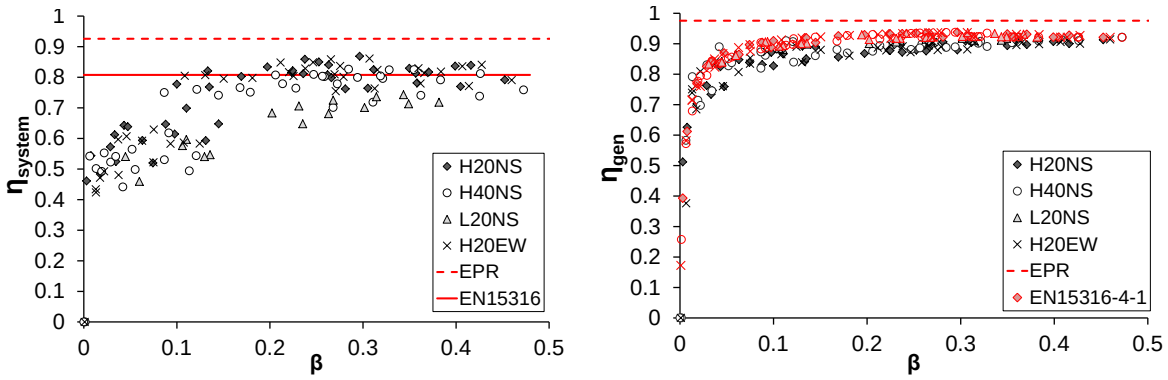

(a) System (b) Generation

Figure 6.17: Monthly averaged η_{system} and η_{gen} for all building design variants equipped with HVAC3 in function of the part load ratio β of the heating system.

teristics while the effect of the building on the generation efficiencies η_{gen} is generally insignificant. Finally, at high part load ratios, a rather good fit is found between the efficiencies calculated according to *EN 15316* [49, 151, 152] and the dynamically calculated efficiencies while the results of the *EPR* method [22] show a worse fit.

Two additional trends are however noticed. **(i)** The plotted data in *Figure 6.17* (a) are more scattered compared to the results for the radiator heating systems revealing that the control efficiencies of the highly capacitive and slower floor heating systems are more influenced by the buildings' characteristics compared to radiator heating and **(ii)** overall higher boiler efficiencies are obtained when lower temperature regimes are applied ($\eta_{gen,HVAC3} > \eta_{gen,HVAC2} > \eta_{gen,HVAC1}$).

HVAC4

Finally, the results for HVAC4 are discussed. *Figure 6.18* shows the results of the integrated building and system simulations for HVAC4 and compares the dynamically calculated annual final energy use for heating $Q_{H,final,use}$, normalised to the building floor area, to the results of the *EPR* calculation method [22]. Overall, similar results are found as those obtained for the other investigated

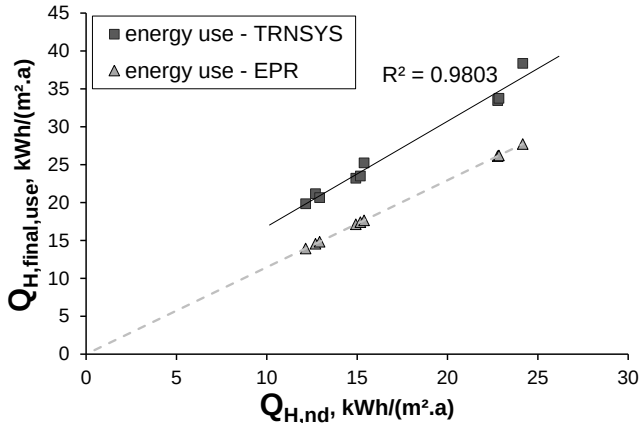

Figure 6.18: The annual $Q_{H,final,use}$ for heating systems (kWh/(m^2.a)) HVAC4 in all 9 investigated school building design variants, calculated using dynamic integrated building simulations (TRNSYS) or according to the *EPR* calculation standard.

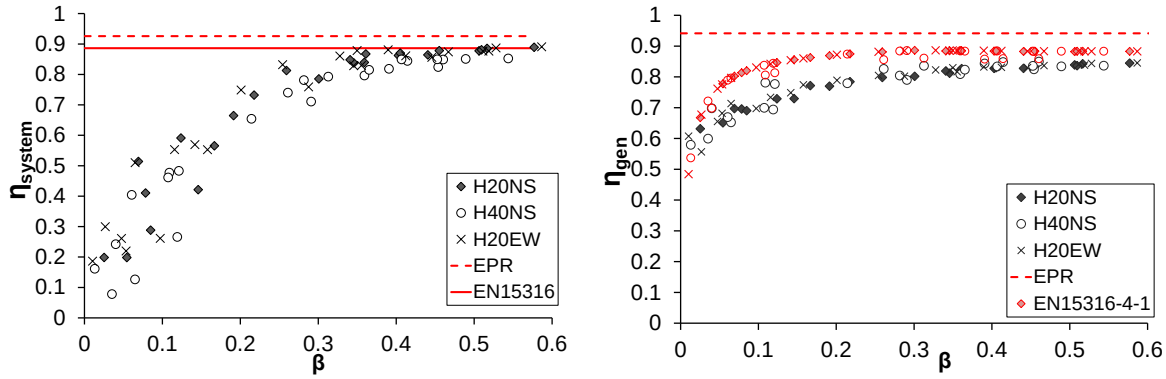

(a) System (b) Generation

Figure 6.19: Monthly averaged η_{system} and η_{gen} for all building design variants equipped with HVAC4 in function of the part load ratio β of the heating system

HVAC systems. The final energy use for heating of HVAC4 is largely underestimated by *EPR* [22]: an average deviation of 27.0% or - 7.1 kWh/(m^2.a) is found, with a maximum of 31.2%.

The dynamic, monthly averaged system η_{system} and generation efficiencies η_{gen} of the HVAC4 system variants are shown in *Figure 6.19* together with the efficiencies calculated according to *EPR* [22] and to *EN 15316* [49, 151, 152]. Overall, the results are similar to those found for HVAC1 to HVAC3. However, compared to the other investigated HVAC system variants, slightly more differences occur between the dynamically calculated generation efficiencies η_{gen} and the ones calculated by *EN 15316-4-1* [152], especially noticeable at low part load ratios.

Discussion and conclusions

The annual subsystem efficiencies of each of the investigated HVAC system variants, averaged over all building design variants are summarised in *Table 6.14*.

Table 6.14: Summary of the statically (according to *EPR* [22] and to *EN 15316* [49, 151, 152]) and dynamic calculated (TRNSYS) annual averaged subsystem efficiencies for all investigated HVAC system design variants.

	EPR			**EN 15316**				TRNSYS			
	η_{system}	η_{gen}	$\eta_{overall}$	η_{em}	η_{dis}	η_{gen}	$\eta_{overall}$	η_{em}	η_{dis}	η_{gen}	$\eta_{overall}$
HVAC1	0.93	0.92	**0.86**	0.90	0.98	0.86	**0.76**	0.89	0.96	0.85	**0.72**
HVAC2	0.93	0.96	**0.89**	0.87	0.98	0.90	**0.77**	0.80	0.95	0.85	**0.65**
HVAC3	0.93	0.98	**0.90**	0.82	0.98	0.92	**0.74**	0.80	0.96	0.87	**0.67**
HVAC4	0.93	0.94	**0.87**	0.90	0.98	0.88	**0.77**	0.89	0.89	0.80	**0.64**

The following overall conclusions can be drawn:

- The results for HVAC2 to HVAC4 show large similarities which demonstrates that, for this particular study of rather well insulated buildings, **variations of the typology of the heat emission system (*i.e.* radiator, floor or air heating) have only a slight impact on the overall HVAC system performance**.

- The subsystem **efficiencies decrease significantly when part load ratios β are low**. As the losses of the efficiency are only noticed in periods of low heat demands, it can be however expected that the overall effect on the annual energy use will be limited.
- The **control efficiency of the HVAC systems is affected by the characteristics of the building** to which the HVAC system is coupled. Especially for the lighter buildings, a lower performance of the control efficiencies is noticed. Variations over the other three building design variants (*i.e.* H20NS, H40NS and H20EW) remain however limited to $< 10\%$.
- The **final energy use** for heating is significantly **underestimated by the *EPR*** standard [22] mainly due to a high overestimation of the generation efficiencies. Dynamic simulation results show that the generation efficiencies depend highly on the hot water temperature regime (*i.e.* heating curve, return temperature) and the part load ratios of the heating systems. Based on the comparative analysis of the static and dynamic calculated efficiencies, these effects appear however to be underestimated in the currently applied *EPR* calculation method [22]. The boiler efficiency method of *EN 15316* [152] that adds supplementary data to take into account the specific boiler operation conditions of the individual installation and includes the option to calculate the impact of recirculation (*i.e.* bypass) on the return water temperature, offers a better fit and could thus be a better alternative for the *EPR* calculation standard.

In section *§ 6.5*, an attempt is made to include the aforementioned phenomena into the simplified calculation model in order to obtain more accurate prediction of the energy use for heating.

6.4.3 Auxiliary energy use

The auxiliary energy use for heating and ventilation comprises the electrical use of the fans, pumps and the boiler. *Figure 6.20* shows the results of the dynamic simulations for the total annual primary auxiliary energy use E_{aux} in relation to the annual heat demand $Q_{H,nd}$ of the building, both normalised to the building floor area.

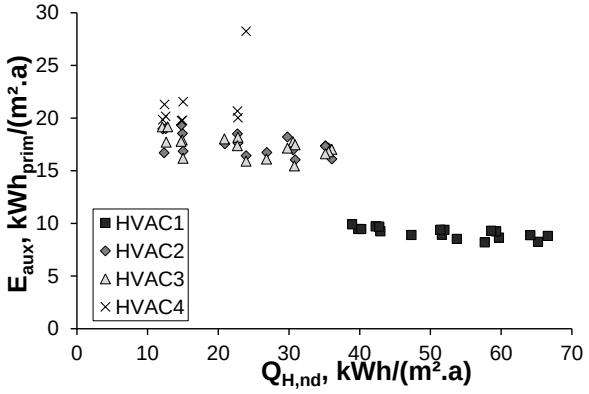

Figure 6.20: Annual primary auxiliary energy use for boiler, pumps and fans E_{aux} of all building design variants equipped with HVAC1 to HVAC4 in function of the buildings' heat demand $Q_{H,nd}$, both normalised to the building floor area (kWh/(m^2.a)).

Figure 6.20 shows a correlation for the annual primary auxiliary energy use for heating E_{aux} with the annual heat demand $Q_{H,nd}$ though the correlation is much less apparent (*e.g.* the data points

of HVAC1 are plotted almost horizontally) compared to the correlation found for $Q_{H,final,use}$ (see *Figure 6.9*). In general, a slight increase of the auxiliary energy use is noticed when $Q_{H,nd}$ decreases. Whereas pump energy use drops when going towards lower heat demands, fan energy use increases as night ventilation occurs more frequently. As the increase of the fan energy use is more significant compared to the decrease of the pump energy, an overall increase of the E_{aux} for decreasing heat demands is noticed. A single exception is found for H40NS_1 coupled to HVAC4. For this case, extra fan energy use is necessary to heat the building. Similar results are found by Koroloija [39] and by Parys [125] while performing an analysis of the auxiliary energy use of the HVAC systems in office buildings, based on integrated building and systems simulations.

An overview of the total primary energy use of the ventilation and the heating system, including the energy use for pumps and boiler $E_{H,p}$ of each of the investigated HVAC systems is given in *Figure 6.21* for 5 different building design variants (variant H20NS1 to H20NS5).

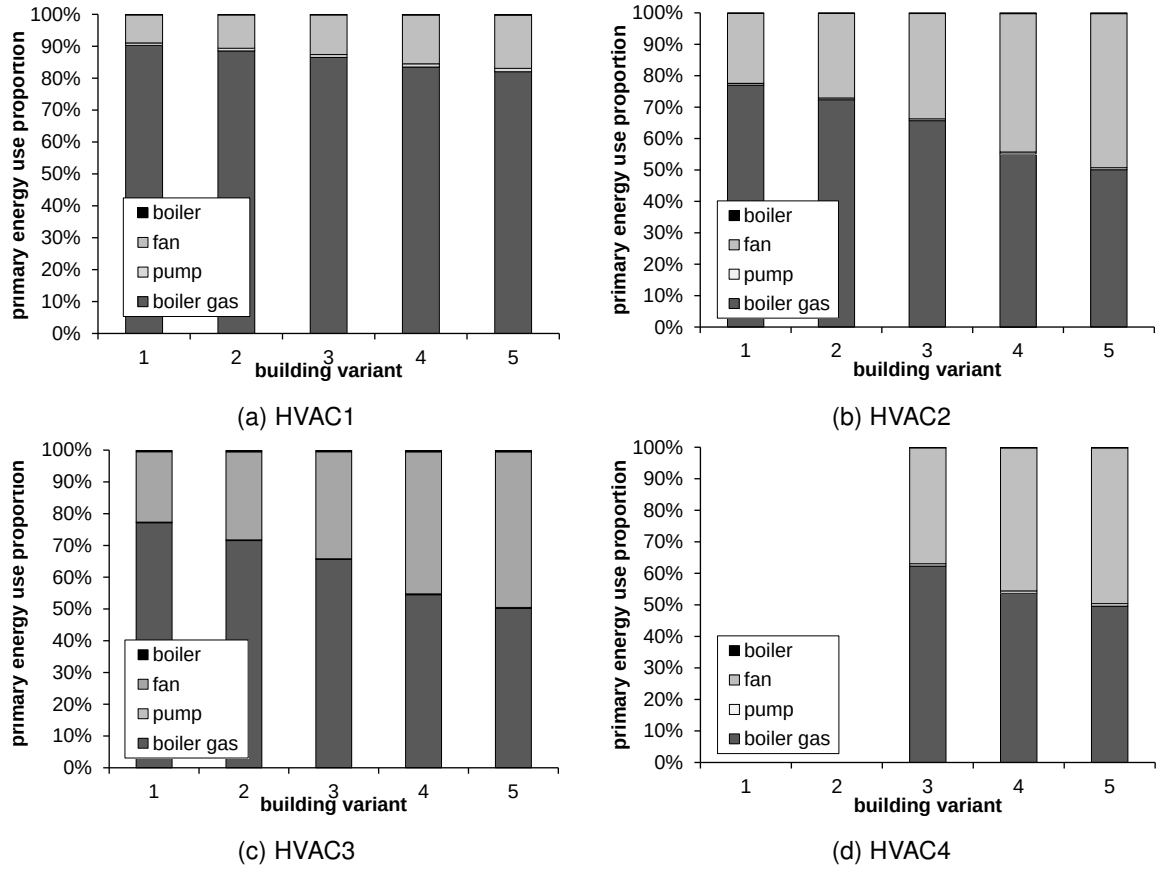

(a) HVAC1

(b) HVAC2

(c) HVAC3

(d) HVAC4

Figure 6.21: Annual total primary energy use $E_{H,p}$ for all investigated HVAC system design variants and for various building energy efficiency levels (H20NS1 - H20NS5) determined by dynamic integrated simulations.

Overall, two phenomena are noticed: **(i)** the electricity use of both the boiler and pumps are very small compared to the fan electrical use and the gas consumption for heating and **(ii)** a relatively increased share of the auxiliary energy use for buildings with lower $Q_{H,nd}$ is noticed. For HVAC1, the gas consumption covers a large part of the $E_{H,p}$, varying from 76.5 $kWh_{prim}/(m^2.a)$ to 43.0 $kWh_{prim}/(m^2.a)$ depending on the $Q_{H,nd}$ of the related building. The fan electrical use varies from

7.5 $kWh_{prim}/(m^2.a)$ to 9.3 $kWh_{prim}/(m^2.a)$, of which 6.7 $kWh_{prim}/(m^2.a)$ is used for hygienic ventilation. The occurring deviations of the fan energy use are caused by an increased need for cooling by night ventilation in better insulated buildings. Pump and boiler energy use vary in relation to the heat demand between 0.66 $kWh_{prim}/(m^2.a)$ and 0.53 $kWh_{prim}/(m^2.a)$, and 0.13 $kWh_{prim}/(m^2.a)$ and 0.11 $kWh_{prim}/(m^2.a)$, respectively.
For the other HVAC system variants HVAC2 to HVAC4, a much higher electrical fan energy use is noticed due to the use of a balanced mechanical ventilation system and the implementation of an all-air heating system. The primary energy use of the fans varies between 15.6 $kWh_{prim}/(m^2.a)$ and 27.7 $kWh_{prim}/(m^2.a)$), of which 13.8 $kWh_{prim}/(m^2.a)$ is related to hygienic ventilation. Moreover, due to the use of heat recovery devices, the gas consumption is lowered from 54.2 $kWh_{prim}/(m^2.a)$ to 19.1 $kWh_{prim}/(m^2.a)$. At the same time, the primary pump energy is lowered from 0.39 $kWh_{prim}/(m^2.a)$ to 0.17 $kWh_{prim}/(m^2.a)$ and the boiler energy use is decreased from 0.12 $kWh_{prim}/(m^2.a)$ to 0.10 $kWh_{prim}/(m^2.a)$ compared to HVAC1.

6.5 Deduction of regression models

In *§ 6.4.2*, the impact of the HVAC system selection and the buildings' characteristics on the overall HVAC system performance has been studied. Results show that the subsystem efficiencies depend highly on the part load ratios of the heating system: the lower the part load ratios, the lower the efficiencies are. Furthermore, a slight impact of the buildings' characteristics on the control efficiencies is found. As both effects affect the overall HVAC system performance, they should be accounted for properly in the *quasi-steady-state* energy assessment method. Therefore, simple prediction models based on the results of the integrated, dynamic simulations are developed to evaluate if the assessment of the final energy use for heating could be further improved by using these regression models compared to the simplified calculation method of *EPR* [22] or *EN 15316* [49].

6.5.1 Method

Several studies on the prediction of energy use in schools have been performed using different prediction models [250, 230, 149]. All these developed regression models are based on a broad range of dependent and independent variables (*i.e.* building characteristics, weather conditions, users' parameters, etc.). Within the framework of this particular study (*i.e.* energy assessment in a regulatory context) however, the energy prediction models are preferably kept simple, using a single independent variable. In accordance with the work of Korolija [71] and Parys [125], the monthly averaged heat demand, normalised to the building floor area, is suggested to be used for the regression analysis. This value can be easily calculated using the (refined) *quasi-steady-state* calculation method as described in the previous chapters. Furthermore, influences of parameters such as weather conditions, building and material properties, use, occupancy, etc. are incorporated and consequently (indirectly) included in the energy use calculations.
Different regression models can be used. A general, detailed overview can be found in Zhao and Magoulès [251]. Compared to other data driven modelling methods, the regression analysis technique is a simple though straightforward and accurate method and therefore highly appropriate to be used for this specific research purpose [71]. Based on an elaborate analysis of different regression

models, Korolija [39] selects the power law and second order polynomial functions to be the best options for the prediction of $Q_{H,final,use}$. The regression parameters are determined using the curve fitting tool in MATLAB. To evaluate the accuracy of the developed regression models, a comparative, statistical analysis is performed to determine the best model fit. Two statistical indexes are used: the root mean square error RMSE and the regression coefficient R^2.

$$RMSE = \sqrt{\sum (y_i - \hat{y_i})^2} \tag{6.9}$$

and

$$R^2 = 1 - \frac{\sum (y_i - \hat{y_i})^2}{\sum (y_i - \bar{y_i})^2} \tag{6.10}$$

where $\sum (y_i - \hat{y_i})^2$ is the sum of squares of the residuals and $\sum (y_i - \bar{y_i})^2$ is the total sum of squares. The R^2-value of a fitted model gives the percentage of variance in the simulation result that can not be accounted for by the corresponding regression model.

6.5.2 Results

Regression models for the final energy use for heating

In this section, the results of the regression analysis for the calculation of the final energy use for heating $Q_{H,final,use}$ are discussed. Quadratic and power law regression models are composed for each of the HVAC systems to predict the heating energy use as a function of the heat demand $Q_{H,nd}$ (see *Figure 6.22* (a) to (d)). As *Figure 6.22* shows an almost linear correlation between $Q_{H,final,use}$ and $Q_{H,nd}$ - except for the lowest heat demands where the decrease of the system efficiencies cause a slight increase of the $Q_{H,final,use}$ - a linear function is added additionally to assess the feasibility of the use of a single coefficient to express the energy use as a function of the heat demand (*i.e.* in conformity with *EPR* [22] and *EN 15316* [49]). All regression models are forced to go through the origin to be physically correct [125]. The related regression coefficients of the power law and quadratic models are depicted in *Table 6.15*. The results for the linear models are added to this table although the related coefficients 'a' are not obtained by the regression analysis but are set equal to the annual overall system efficiency $\eta_{overall}$ of each of the HVAC systems, averaged over all considered building design variants, as obtained by the integrated dynamic simulations.

Table 6.15: Overview of the regression coefficients for all investigated HVAC system variants.

	Power law $y = ax^b$		**Quadratic** $y = ax^2 + bx$		**Linear** $y = ax$
	a	**b**	**a**	**b**	**a =** $\eta_{overall}$
HVAC1	1.79	0.884	-0.016	1.541	0.72
HVAC2	1.814	0.864	-0.038	1.660	0.65
HVAC3	1.862	0.8351	-0.040	1.646	0.67
HVAC4	2.122	0.683	-0.0751	1.706	0.64

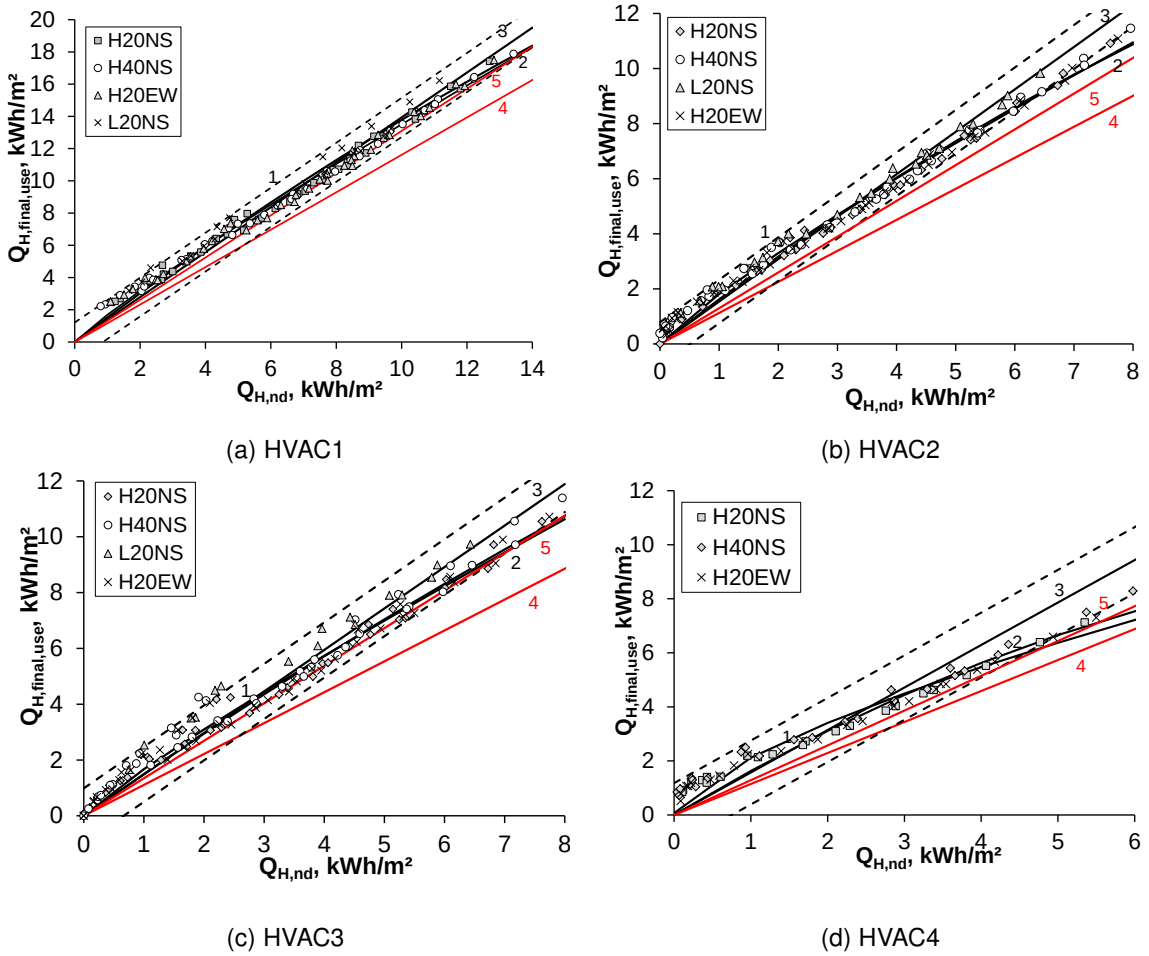

(a) HVAC1

(b) HVAC2

(c) HVAC3

(d) HVAC4

Figure 6.22: Bivariate regression models for the prediction of the monthly final energy use for heating, normalised to the building floor area (kWh/m^2), of a selection of typical heating systems in schools. A power law (1), quadratic (2) and linear (3) function are plotted, including the 95% prediction band for the linear model. For comparison, the results calculated according to the *EPR* [22] (4) and the *EN 15316* [49, 151, 152] (5) calculation standard are added.

Next, a comparative, statistical analysis of the results of the various (regression) models is performed. Although the regression models are fit on monthly calculated data points, the accuracy of the fitted models is assessed based on annual calculation results. For each HVAC system design variant the absolute and relative RMSE and the R^2-value of the annual final energy use for heating are calculated and the results are depicted in *Table 6.16*.

Overall, a good correlation between the regression model predictions and the simulation results is found: all R^2 values are $\geq$ 92%, with the lowest values found for HVAC4. Prediction errors RMSE of the power law and quadratic regression models are comparable and demonstrate overall a much better fit with the dynamic results compared to the results of the *quasi-steady-state* calculation methods according to *EPR* [22] and *EN 15316* [49, 151, 152]. The averaged RMSE's are all < 2.9 kWh/(m^2.a) or < 12%. For HVAC1, HVAC2 and HVAC3 however, the best fit is found when the linear models are used to predict the energy use: R^2 values are all > 97% and the averaged RMSE's remain below 5%. The linear model predictions for HVAC4 are slightly less accurate though the average RMSE is still limited to < 10%.

To visualise the differences between the model predictions and the results of the simulations, the

Table 6.16: Results of the statistical analysis of the (regression) models used for the prediction of the final energy use for heating using HVAC1, HVAC2, HVAC3 or HVAC4. Those statistical parameters that lead to the best model fit are underlined.

		EPR	EN15316	power	quadratic	linear
HVAC1	RMSE, kWh/(m^2.a)	12.6	5.0	2.8	2.4	2.0
	RMSE, %	16.8%	6.4%	4.2%	3.4%	2.4%
	R^2	0.981	0.981	0.982	0.982	0.981
HVAC2	RMSE,kWh/(m^2.a)	10.0	5.8	1.5	1.6	1.3
	RMSE, %	26.7%	15.6%	3.4%	3.4%	3.1%
	R^2	0.992	0.992	0.993	0.992	0.992
HVAC3	RMSE,kWh/(m^2.a)	10.2	4.5	2.7	2.6	2.1
	RMSE, %	25.7%	10.4%	8.3%	6.3%	4.9%
	R^2	0.977	0.977	0.980	0.979	0.977
HVAC4	RMSE,kWh/(m^2.a)	7.6	5.3	2.1	3.1	2.1
	RMSE, %	29.7%	21.5%	7.7%	11.7%	9.3%
	R^2	0.952	0.952	0.922	0.933	0.952

prediction errors are plotted in *Figure 6.23*.

Overall, three effects are noticed. **(i)** While the *EPR* calculation method as currently applied [22] significantly underestimates the final energy use for heating compared to the results of the dynamic simulation, the developed regression models tend to generally overestimate the energy use. For the *quasi-steady-state* calculation method, (slight) overestimation is however preferable to underestimation. **(ii)** In general, compared to the dynamic simulation results, better results for the final energy use for heating are found when the regression models are used instead of the simplified calculation approach of *EPR* [22] or *EN 15316* [49]. When comparing the results of the different regression models mutually, the use of the linear models results in the best fit. Except for some exceptional data points - mostly representing the results of the buildings with a lighter structure (see *Figure 6.23* - marked in lighter red) - the data points of the linear models are plotted within the ± 5% accuracy interval. This confirms the feasibility of the use of the currently applied simplified calculation method, using yearly averaged (sub)system efficiencies, independent of the buildings' characteristics, to calculate the final energy use as a (linear) function of the heat demand. Nevertheless, based on the results of the same comparative analysis, a revision of the yearly averaged efficiency values of *EPR* is highly recommended, either based on dynamic simulation results or on alternative simplified calculation methods. **(iii)** When comparing both the *quasi-steady-state* calculation approaches, in line with the results described in *§ 6.4.2*, significantly better results are found when the calculation standard *EN 15316* is used. Hence, considering the investigated building and HVAC sample, the *EN 15316* calculation method appear to be a better option than the *EPR* standard.

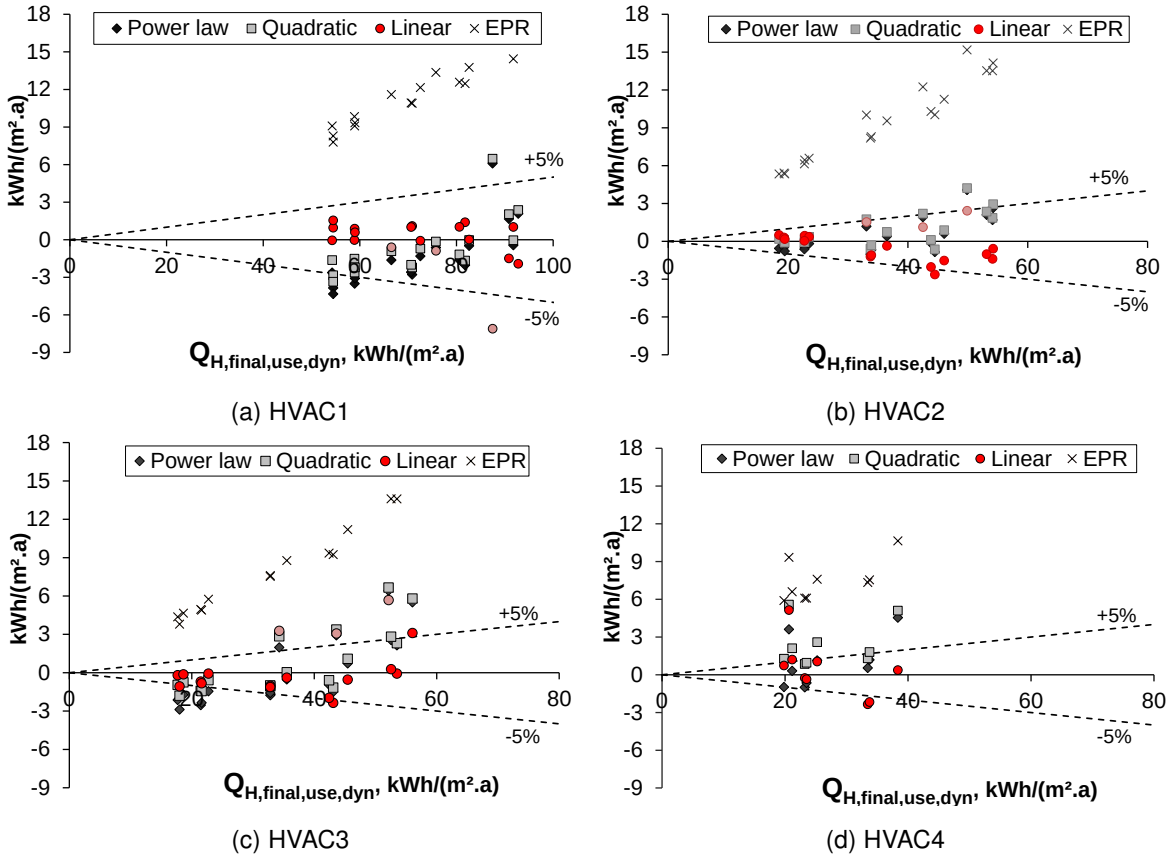

Figure 6.23: Prediction errors of the annual final energy use for heating, normalised to the building floor area (kWh/(m^2.a)), assessed by 3 bivariate regression models (*i.e.* power law, quadratic and linear). The results calculated according to the *EPR* calculation standard [22] are added for comparison. The results for the light buildings are marked in lighter red.

Regression models for the auxiliary energy use

As shown in *§ 6.4.3* and *Table 6.17*, the total auxiliary energy use consists mainly of the fan energy use.

Table 6.17: Annual averaged fraction of the auxiliary energy used (%) per HVAC system component.

	pump	boiler	fan
HVAC1	6.8%	1.4%	91.8%
HVAC2	1.8%	0.6%	97.6%
HVAC3	1.6%	0.7%	97.8%
HVAC4	1.6%	0.5%	97.9%

Due to the high ventilation rates in schools and related high fan energy use, the fraction of the auxiliary energy use assigned to the pumps and boiler remains small (< 10% for HVAC1 and < 3% for the other HVAC system variants). Furthermore, as the fan energy use is not - or only slightly in case of HVAC4 - correlated with the heat demand, it is meaningless to fit the auxiliary energy use to

the heat demand. Accordingly, the results of the regression analysis lead to very low R^2-values (R^2 = 0.2 or less) and the standard errors of the correlation coefficients found are unacceptably high. Therefore, no regression models are deduced for the auxiliary energy use.

6.5.3 Evaluation of the robustness of the regression models

As demonstrated in the previous section, simplified (regression) models can be used to predict the annual final energy use for heating $Q_{H,final,use}$ of schools. Linear models using (yearly) averaged overall system efficiencies based on the results of integrated simulations to calculate the final energy use for heating as a function of the heat demand of the building lead to good calculation results (Δ $Q_{H,final,use}$ < 10%) compared to the results of the simulations in TRNSYS. The accuracy of the determined linear functions is however still uncertain. It is necessary to evaluate the robustness of the calculated energy use for unpredictable variations of the use of the school buildings. Therefore, the results of the calculated final energy use for heating using the linear models are tested against simulation results in TRNSYS using different users' related boundary conditions and input parameters. Each of the integrated, dynamic simulations is repeated twice varying the use of the electrical equipment (*i.e.* expressed by variations of the internal heat gains due to equipment $q_{IHG,eq}$ and the partial operational time factors of the use of the equipment POF_{eq} - see *Table 4.3*) and lighting (*i.e.* expressed by variations of $q_{IHG,light}$ and POF_{light} - see *Table 4.3*), and occupancy profile's (*i.e.* expressed by variations of the relative absence factors - see *Table 4.3*) between a minimum and maximum value as determined in *§ 4.3.3*. The robustness of the regression models is then analysed by checking if the additional data points fit well within the 95% prediction band[8] of each regression model. The results of the robustness analysis are plotted in *Figure 6.24*.

As shown, the prediction bands of the HVAC3 are slightly larger compared to the other HVAC system variants due to the larger scattering of the original data (see *Figure 6.16*). Overall, the data points fit well within the 95% prediction bands.
Furthermore, the relative RMSE's are determined. A RMSE of 4.4% is calculated for HVAC1. The RMSE for HVAC2 is 12.1%. For HVAC3, a RMSE of 16.4% is found and for HVAC4, the RMSE is 10.2%. Both the scatter plots and the results for the RMSE calculations confirm a reasonable robustness of the linear model for likely variations of school buildings' use.

6.6 Uncertainties and restrictions of the study

To obtain the results presented in this chapter, many design decisions, modelling assumptions and simplifications had to be made. The most important sources for uncertainty of the output are summarised hereafter:

- The results are based on elaborate, integrated dynamic simulations including a building model and most of the thermal components of the HVAC system. Hereby, an attempt is made to include as good as possible the dynamic effects and the transient behaviour of the system components. However, despite the level of detailing of the integrated model, some realistic

[8] This range designates the 95% confidence interval for new observations and includes the uncertainty in the determination of the model parameters and the original data point scattering [125].

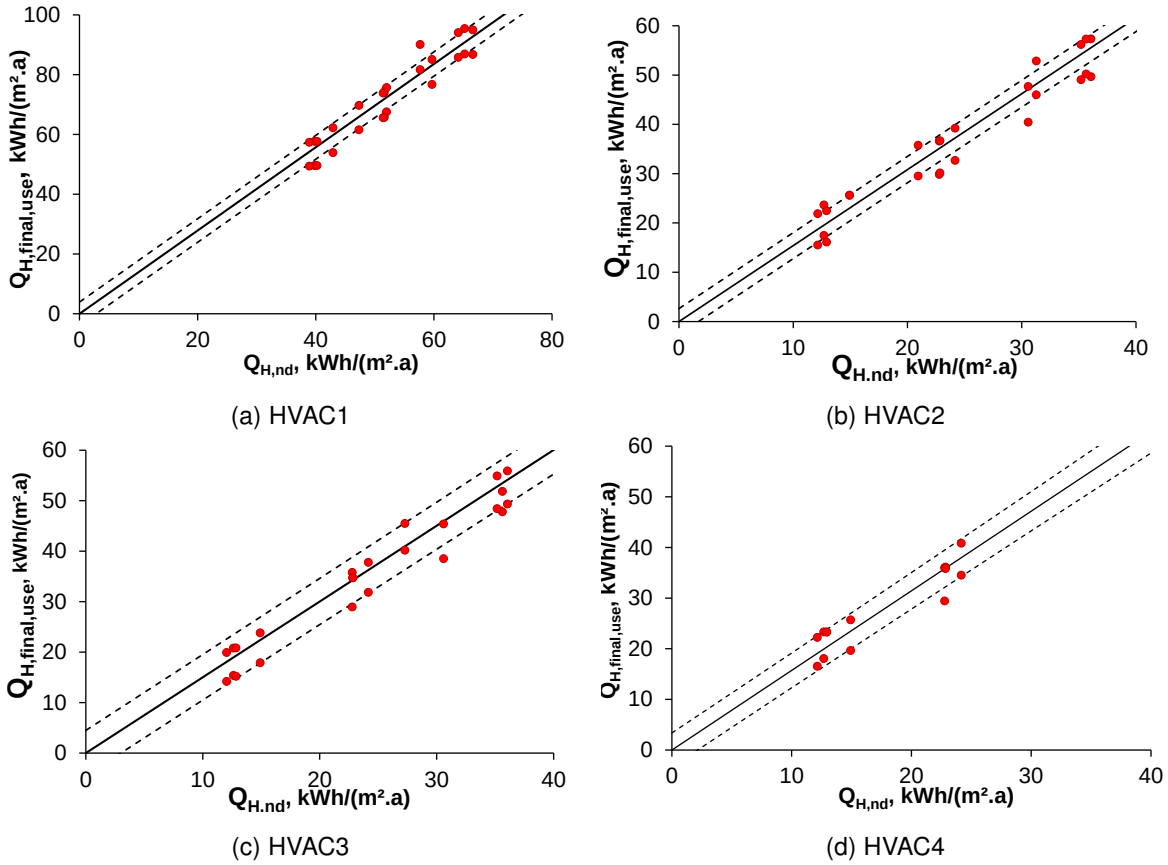

Figure 6.24: Linear model validation through fitting of the simulation data results using varying user's conditions for various building variants of the modelled school building.

effects that influence the building energy use are neglected either due to inherent restrictions of the simulation model (*e.g.* realistic variations of the emission efficiencies cannot be calculated - see *§ 3.3*) or due to the modelling assumptions made (*i.e.* all components are assumed to be correctly installed and are connected to well balanced hydraulic or air distribution circuits which is however highly unlikely in real buildings [125]).

- Several building design variants are selected ranging the energy performance level, the orientation, the WWR and the thermal capacity of the building. Moreover, the impact of the boundary conditions on the derived regression models has been studied. Other building characteristic such as the built form or the size of the building are however not included in the study. As the goodness-of-fit of the determined regression models (*i.e.* $R^2 > 0.92$) shows that the variations of the school building design are covered well by using the net energy demand as the input variable, on may assume that the impact of other building characteristics which are also incorporated in the net energy demand calculation, will be accounted for in a similar, good way [125].
- The building is modelled as a multi-zone building. For the sake of simplicity however, only different seven zones are incorporated. The implementation of a building model of higher resolution might affect the outcome. For elementary schools, where occupancy rates and operation schedules are rather constant over the whole school year and nearly identical for all class rooms, the impact is expected to be limited. Different results might however be obtained

in secondary schools where occupant densities and operational schedules of the class rooms can be more flexible and inconsistent.

Furthermore, some restrictions are specifically related to the limited scope of this study:

- As system sizing and dynamic simulations of HVAC systems are very time-consuming, the HVAC system selection is limited to four of the most commonly found heating and ventilation systems in contemporary schools. Although other alternative heat generation, distribution and emission systems are likely to be found in schools, they are not studied here. One may however assume that, as the impact of varying heating curves, part load ratios and building characteristics on the emission, distribution and generation efficiencies is assessed, the impact of the introduction of an alternative heat generation system on the overall efficiency will be limited.
- The results are restricted to newly built schools.

Overall, an indication is given of the deficiencies of the currently applied *quasi-steady-state* calculation standard *EPR* and the need for revision to obtain better results for the overall energy performance assessment is revealed. Nevertheless, before being able to present the regression models as a refinement of the method, further research is necessary to assess the impact of the modelling and design uncertainties on the regression models. Moreover, additional research is necessary to check if the results (and the use of linear models) can be extrapolated to other HVAC system (configurations), control systems, etc.

6.7 Conclusion

This chapter describes the results of integrated, dynamic building and HVAC system simulations of a selection of four traditional HVAC systems in schools. The investigated HVAC systems, for which mostly the type of heat emission system and ventilation are varied, are coupled to a representative sample of contemporary elementary school building design variants.

In the first part of this chapter, the influence of both the buildings' characteristics and the selection of the HVAC system components on the HVAC system performance is analysed. The results reveal that for the investigated, rather well insulated school building variants, the impact of the type of the heat emission system on the overall HVAC system performance is limited. Furthermore, it is shown that the control efficiency of the HVAC systems is affected by the characteristics of the building to which the HVAC system is coupled. Especially for the lighter buildings, a lower performance of the control efficiency is noticed. Variations over the other three building variants remain however limited to $< 10\%$. Finally, a decrease of the subsystem efficiencies is noticed when part load ratios decrease. Nevertheless, as the losses of efficiency are only noticed in periods of low heat demands, the overall effect on the annual final energy use for heating is limited.

In the second part, it is evaluated if these affects are accounted for accurately in the *EPR* calculation standard. Results show that the final energy use for heating is significantly underestimated by *EPR* (on average, 16% or more) compared to the dynamic results, mainly due to highly overestimated generation efficiencies. The dynamic simulation results show that the generation efficiencies depend highly on the hot water temperature regime and the part load ratios of the heating system. These effects appear to be currently underestimated in the *EPR* calculation method. While searching for

more accurate calculation results for the final energy use for heating, two alternative calculation approaches are studied: the simplified calculation method of *EN 15316* and the calculation approach using regression models based on the results of dynamic simulations. A comparative analysis of the results of regressed power law, quadratic and linear models, using the heat demand as an independent variable, reveals that the simplified calculation approach using a single coefficient to express the final energy use as a function of the heat demand offers good calculation results. A revision of the overall system efficiencies is however highly recommended, either based on dynamic simulation results or based on the CEN/EPB calculation standard *EN 15316*. Especially the boiler efficiency method of *EN 15316*, which provides more accurate calculation results by taking into account the specific boiler operational conditions and which is much easier to be implemented compared to the regression models, appears to be an interesting alternative.

For the auxiliary energy use for boilers, pumps and fans, the correlation with the heat demand is less apparent as the auxiliary energy flows consist mostly of fan energy use which is - aside from the all-air heating system - independent of the heating demand. As a result, no good regression models for the auxiliary energy use are found.

7

Impact of the changes of the quasi-steady-state calculation method on the results of a cost-optimal design

Since the implementation of the recast of EPBD in 2010, Member States are requested to set minimum energy performance criteria for buildings and HVAC systems with the aim of achieving cost-optimality. A comparative cost-benefit evaluation methodology has been set forward that enables the determination of optimised buildings and results in both an economical optimal combination of energy saving measures and in a hierarchy of energy saving investments. In 2013, a cost-optimal study is performed in Flanders commissioned by the Flemish Energy Agency (VEA) which revealed amongst others the cost-optimal levels of energy performance requirements for new and renovated school buildings. In doing so, the total cost and the total primary energy use over the life span of the building are weighed where the latter is calculated using the EPR calculation tool. In the previous chapters however it has been shown that the currently applied EPR calculation tool for schools offers considerable room for improvement. It is therefore possible that while using the current calculation tool, inaccurate cost-effective assessment results are obtained and inefficient energy saving measures are promoted on the building market. Therefore, in this chapter, an assessment of the influence of the changes of the calculation method on the results of some cost calculations is made for a limited set of energy saving measures in a reference school building. The impact of the changes of the quasi-steady-state calculation method on both the Pareto Front obtained by the cost optimal study and on the hierarchy of building measures is studied.

7.1 Introduction

Over the years, the European building regulation moved towards minimum energy performance levels for buildings based on a cost-optimal study taking into account all lifetime costs of the building [18]. Ever since, various cost-optimal studies have been conducted, differing in the choice of the considered building typology (*i.e.* dwellings [252, 253, 24, 191, 254], offices [255, 256, 125, 25, 257], schools [25, 257]), the choice of considered variables (*i.e.* optimisation of energy saving measures for building envelope only [125] or the combination of both building envelope and technical systems [25, 24]) or the applied energy calculation method to assess the total energy use (*i.e.* using *quasi-steady-state* calculation tools [125, 25, 24] or dynamic simulation tools [253]). Despite the differences, all these cost-optimal studies are performed for a more or less similar purpose: to assess costs and long-term benefits of further strengthening the energy performance regulation and to promote the introduction of the most cost-effective energy saving measures on the national building market. To guarantee a certain level of comparability and consistency of the cost-optimal study results and related building policy decisions over all European Member States, a common comparative methodology framework is established by the European Commission [258]. Additional guidelines are published describing how to perform the cost-optimal study [259] and mentioning important effects of cost calculation assumptions such as long-term energy price developments or discount rates [260]. The definition of the implemented input data (*e.g.* climate conditions, costs, etc.) and the calculation of the energy use is however done by and on the level of individual Member States [259]. In Flanders, energy use calculations in the framework of EPBD are performed using the *quasi-steady-state* calculation tool *EPR*. As discussed in previous chapters, the method as currently applied for schools offers significant room for improvement. In *Chapter 4*, the deterministic standardised input data are revised. In *Chapter 5* and *Chapter 6*, the monthly, *quasi-steady-state* calculation method itself is modified to the typical school buildings' characteristics. Consequently, it is possible that while using this revised calculation tool, different results for the cost-optimal study are obtained. Therefore, along this chapter, a limited set of cost-benefit calculations of a combination of energy saving measures are performed. Based on these cost calculations, the impact of the suggested changes of the calculation method on the results of the cost-optimal study is assessed.

First, the methodology that is used for the cost-optimal study is described in *§ 7.2*. The approach used for the *quasi-steady-state* calculation of the primary energy use for heating and ventilation is given in *§ 7.2.1*, highlighting in particular the differences between the currently applied and refined method. In *§ 7.2.2*, the cost calculation method and related calculation hypotheses and assumptions are summarised. Next, an overview is given of the included energy efficiency measures (*§ 7.3*). Information on the energy costs and data for the investment, repair and maintenance costs for the investigated energy measures are described in *§ 7.4*. Finally, the results of the cost-optimal study are discussed. The impact of the changes to the energy calculation method are studied on both the Pareto Front (*§ 7.5.1*) and the energy saving potential assessed by the return on investment of the different energy saving measures (*§ 7.5.2*). To do so, the Pareto fronts for both energy calculation approaches are determined and it is investigated if different economic optima or differences in the number or order of the Pareto solutions occur. Finally, as cost calculations are often highly uncertain, a restricted sensitivity analysis is performed (*§ 7.6*).

Note that the results of the cost-optimal study presented along this chapter do not reveal the absolute cost-optimal solution for school buildings. It is only the purpose of this study to give an indication of the impact of the changes to the calculation method on the results of a cost-optimal school design. These results can then be used as a reference to emphasise the need for revision of the currently applied *quasi-steady-state* calculation method. The number of incorporated building energy efficiency measures regarding the building envelope are limited and only three traditional HVAC systems are coupled to the investigated building variants. Moreover, only a restricted sensitivity analysis of the results is performed.

7.2 Methodology

Along this chapter, the impact of the refined *EPR* calculation method [22] is studied on the results of a restricted, bi-dimensional cost-optimal study. In doing so, two objectives, an energetic and economic one, are balanced over the whole life span of the building for a series of school building design variants. The energetic objective includes the energy use for heating and the auxiliary energy use for the ventilation fans, both expressed in terms of primary energy and normalised to the net floor area of the building (*§ 7.2.1*). The economic objective is set equal to the net present cost (NPC) (*§ 7.2.2*).

The overall approach used for this study is based on the comparative methodology framework as set in the context of the EPBD regulation [261] and related (national) guidelines [258, 262]. This methodology consists of multiple, consecutive calculation steps. **(i)** A representative school building model must be identified. As the reference school building models as defined in *Chapter 2* suit the requirements set for these building models, one of the developed reference school buildings is selected for this study. **(ii)** A set of energy efficiency measures must defined to improve the energy performance of the investigated school building model. The investigated variables in this study are restricted to the building envelope properties of which the impact is assessed for three different HVAC systems. **(iii)** The primary energy use of all building variants must be determined. To assess the impact of the suggested changes to the *EPR* calculation method [22], the primary energy use is calculated twice. Once the *EPR* tool as currently applied in Flanders [22] is used and once the refined calculation tool as obtained along this dissertation is applied. As the number of considered building design variants are limited, all possible combinations are calculated separately without using a specific optimisation algorithm. **(iv)** The costs of each of the investigated energy saving measures must be estimated and combined with the results of the energetic calculations in order to search for cost-optimal solutions. The Pareto optimality approach that considers both the economic and energetic objectives equally, is used to determine the optimal solutions, which are also referred to as non-dominated or Pareto solutions. A solution is called non-dominated if no other feasible measure can be found that improves one objective without causing simultaneous deterioration of the other objective [191]. This approach has been frequently applied in similar cost-optimal studies on residential [191, 254, 24] and non-residential buildings [125, 25]. A more elaborate description of this method is given by Verbeeck [191] and by Allacker [254]. The combination of all non-dominated solutions is called the

Pareto Front. The cost-optimum is the specific data point on the Pareto front with the lowest cost.

To guarantee fair comparison of the calculation results, the thermal comfort of each of the investigated cases must be comparable. Therefore, the thermal comfort of each building variant is assessed using the Degree Hour criterion as described in Method B of *EN 15251, Annex F* [47]. For the building variants with a WWR = 30%, 15% of the cases are excluded for the cost-optimal study as overheating occurs in more than 5% of the occupied time. For the building variants with a WWR = 20%, no cases are excluded as an acceptable summer comfort is guaranteed for all investigated cases.

7.2.1 Energy performance assessment

To assess the impact of the changes of the energy calculation methods, the energy use for heating and ventilation is calculated once by the original *EPR* calculation method [22] and once by the refined method as obtained along the previous chapters of this dissertation. Both methods calculate the energy use for heating $Q_{H,final,use}$ as the ratio of the heat demand $Q_{H,nd}$ and the overall HVAC system efficiency $\eta_{overall}$, though differences are found for both the calculation of $Q_{H,nd}$ (see *Eq. 3.13*) and $\eta_{overall}$ as summarised hereafter.

First, for the calculation of $Q_{H,nd}$, different correlation factors are used to calculate the gain utilisation factor as shown in *Eq. 5.24* and *Eq. 5.25*.
Second, different calculation approaches are found for the calculation of system intermittency and more in particular the calculation of the heat transfer $Q_{H,ht}$. Whereas in the *EPR* method [22] the impact of intermittency is accounted for by an adjusted indoor temperature (see *Eq. 3.17*), the refined calculation method based on *NEN 7120* [44], calculates intermittency as a correction of the heat transfer of a continuously heated building (see *Eq. 3.25*). Furthermore, the numerical parameters and default input data used to calculate the correction factors $a_{H,red,night}$ and $a_{H,red,we}$ are adapted to the characteristics of Flemish schools (see *Eq. 5.26*)
Third, boundary conditions are refined and adapted to the typical school's use (see *§ 4.5* and *Table 4.7*) which results in different calculation outputs for the ventilation heat transfer coefficients H_{ve} and for the heat gains Q_{IHG} as shown in *Eq. 4.2* and in *Eq. 4.3*, respectively.
Fourth, for the calculation of $\eta_{overall}$, two different approaches are used. For the original calculation, the approach as described in *EPR* is applied (*§ 3.2.2*) calculating the overall system efficiency as the combination of the system efficiency (see *Eq. 3.29*) and the generation efficiency (*Eq. 3.31*). For the refined method however, the optimised, yearly averaged values for $\eta_{overall}$ based on integrated building and system simulations, as yielded in *Chapter 6*, are used.
Fifth and final, for the calculation of the auxiliary energy use of the ventilation fans $\mathbf{W}_{aux,fan}$, the calculation approach as described in the *EPR* standard [22] is used for both methods though the boundary conditions differ depending on the method used as shown in *Eq. 7.1* and *Table 4.7*.

$$W_{aux,fan} = \begin{cases} c_{syst} \cdot \dot{V}_{supply,H} \cdot \mathbf{0.3} \cdot t & (original) \\ c_{syst} \cdot (\dot{V}_{supply,H} \cdot \mathbf{f}_{occ} + \dot{V}_{basic} \cdot \mathbf{0.5}) \cdot t & (refined) \end{cases} \tag{7.1}$$

where c_{syst} is a default value for the specific fan power (*i.e.* 0.33 Wh/m^3 for exhaust ventilation systems, 0.55 Wh/m^3 for balanced, mechanical ventilation systems), $\dot{V}_{basic}$ is a basic ventilation flow rate (m^3/h) to guarantee good indoor air quality at any time of the day (see *§ 2.3.1*) and t = 8750 h.

To convert the energy use to primary energy use, conversion factors are used. For fossil fuels, the factor equals 1. For electricity, the factor equals 2.5 [22]. Despite the requirement of the EPBD regulation for non-residential buildings in Flanders (*i.e.* at least 10 kWh per year per m^{2}gross surface area must be covered by renewable energy source), no renewable energy sources are taken into account for this study.

7.2.2 Economic performance assessment

When assessing the economic performance of a chosen combination of energy saving measures, either a macro or a microeconomic approach can be adopted [191]. In a macroeconomic analysis, the focus is put on the costs and benefits of certain energy saving measures while taking into account the changes for the society and the economy as a whole. In a microeconomic analysis, the impact of the energy saving measures is evaluated from a strictly financial viewpoint as the total costs for the building owner are assessed. As macroeconomic analyses are very complex and as decisions regarding investing in certain energy saving measures are generally made by the building owners [191], a microeconomic approach is selected within the context of this research study, in order to evaluate the real financial costs for the building owner over the period that the building is used.

Calculation of the net present cost

The net present cost of a building energy saving measure is determined by

- the investment costs I_c related to the construction of the building,
- the costs for maintenance M_c and repair R_c of the building and systems,
- the residual values of the HVAC system components V_f,
- and the energy costs E_c related to the specific energy use of the considered school building variant.

To assess the net present cost of a building design variant, the global cost calculation method as described in *EN 15459* [263] is used. This method calculates all expected costs over the whole life span t_{buil} of the building according to *Eq. 7.2*.

$$\begin{aligned} NPC(t_{buil}) &= I_c + \sum_j [\sum_{i=1}^{r} [(M_{c,i}(j)(1 + r_M)^i + R_{c,i}(j)(1 + r_R)^i \\ &+ E_{c,i}(j)(1 + r_E)^i) \cdot R_d(i)] - V_{f,t_{buil}(j)} \cdot R_d(t_{buil})] \end{aligned} \tag{7.2}$$

with

$$R_d = \frac{1}{(1+d)^i} \tag{7.3}$$

where r_x is the expected change of the maintenance, replacement and operational cost x above inflation, d is the discount rate and $V_{f,t_{buil}(j)}$ is the final value of component j at the end of the calculation period (€).

The **initial investment cost** consists of the construction costs of the building and the coupled HVAC system. To limit the amount of necessary cost data, only those costs that relate to the energy performance of the building are included [262]. Common costs are excluded as they are assumed to be equal for all considered building variants. The annual **maintenance costs** for the heating and the mechanical ventilation system are calculated as a fixed percentage of the initial investment costs as defined in *EN 15459, Annex A* [263]. In line with the cost-optimal study performed by Verbeeck [191], the maintenance costs for the building (envelope) are not included. Maintenance costs are hence only considered for the HVAC system components and the implemented shading devices. When the life expectancy of a certain energy efficiency measure is shorter than the considered life span of the building, **replacement costs** are included in the cost-optimal study for this specific measure. When life expectancy is longer, a **residual value** is calculated for HVAC system components. This way, large fluctuations of the net present costs can be avoided when the life span of HVAC system components considered in different building variants is just slightly shorter or larger than the considered life span of the building. The residual values are determined by a linear depreciation of the initial investment as shown in *Figure 7.1*.

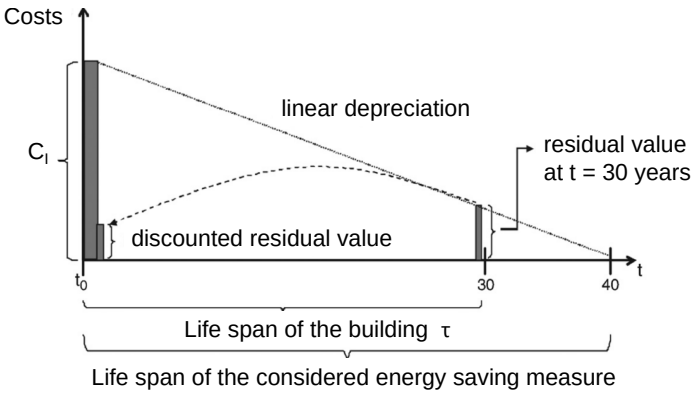

Figure 7.1: Method to calculate the residual values of an energy saving measure with a longer life expectancy than the considered life span of the building [25].

Replacement costs and residual values are considered only for technical components and solar shading devices as the building construction elements are considered to have the same life expectancy as the building [264]. Moreover, **disposal costs** or CO_2 emission costs for natural gas are not considered for this study.

For the **operational energy costs**, only the energy costs related to heating and ventilation are included. Energy use for lighting is not considered as the same lighting and control system is used in all building variants.

Hypotheses and assumptions for the cost calculations

Along the cost-optimal study, many assumptions had to be made. Hereafter, an overview is given of the most important hypotheses and assumptions made regarding amongst others the (energy) price scenarios, the discount rates, the life span of the building (components), etc. All are set in line with both the national guideline [262], the recommendations for the cost-optimal studies as set in the

framework of EPBD [260], and the methodology as applied for the cost-optimal studies performed for non-residential building (including schools) ordered by the Flemish government [25, 20].

In accordance to the EPBD guidelines [262] and in line with the cost-optimal study performed for Flemish school buildings by De Deygere et al. in 2013 [25], a **life span** of 30 years is considered for school buildings. Longer calculation periods are not recommended as assumptions on interest rates and forecasts for energy prices become difficult [259]. The life expectancy of the included HVAC system components and shading devices are set according to *EN 15459, Annex A* [263].
According to the EPBD guidelines [262], the cost data are expressed in real term, so exclude **inflation**. Consequently, likely price changes are to be expressed above the inflation rate. For the **maintenance costs**, it is assumed that the nominal price increases are in line with the general inflation rate (*i.e.* 2%, averaged over the last 10 years [265]) so no additional increases of the prices over time are considered [20]. For the **replacement costs**, a price increase is considered based on the average, annual growth rate of general construction costs. Based on the information found in the ABEX-index [266], an average annual growth rate of 2.4%, or 0.4% above inflation, is found for the past 25 years. As no innovative technologies are included, no large price variations are to be expected over time, so the value for the annual growth rate (*i.e.* 0.4% for real term calculations) is used for projections of the future costs for replacements [125].
The assumptions made regarding the **life expectancy** and the **maintenance costs of the included HVAC system (components)**, based on *EN 15459, Annex A* [263], are summarised in *Table 7.1*.

Table 7.1: Assumed average life expectancy and annual maintenance costs of the included system components.

Component	Life expectancy (years)	Maintenance cost (% of I_c)
radiators	35	1.5
thermostatic radiator valves	17	3
air handling unit	15	4
external louver shading	30	2
external screen shading	30	2
shading - control system	10	2
floor heating	30	2
heating coil	20	2
boiler	20	1.5

As the cost-optimal solution is performed from a microeconomic point of view, all considered costs **include taxes** [25, 20]. All costs calculated along this study include VAT (*i.e.* 21% as only newly built school are considered). **Fiscal cost depreciation** of building investments is not considered within the context of this specific study as schools cannot deduct the cost of the investment and enjoy tax benefits, in contrast to *e.g.* offices. Furthermore, **subsidies and fiscal reduction** related to the building process or the use of the building/systems may be taken into account. For schools, overall, two different types of subsidies are found: general subsidies for the regular financing of school buildings or renovation projects, and subsidies and fiscal reductions specifically related to the implementation of certain construction or energy saving measures. Only the first category is included in

the study. As an elementary school building is considered (*§ 7.3.1*), 70% of the initial investment and replacement costs are subsidised. More detailed information on the applied subsidising procedures for the purchase, the construction and the renovation of school buildings can be found on the web site of the Agency for School Infrastructure (AGIOn) [267].
The discount rate determines the weight placed on investments in the present versus future costs and benefits [125]. From microeconomic point of view, **the discount rate** has to reflect the opportunity cost of capital or the expected rate of return for the building owner [260]. According to the EPBD guidelines [262], the discount rate used along this study is expressed in real terms and is set equal to 3%.

Most of the values set for the input parameters for the cost calculations (*e.g.* discount rate, life expectancy of building and HVAC system components, maintenance costs, etc.) are subjected to large variations due to many influencing factors. A restricted sensitivity analysis is performed for restricted set of input parameters (see *§ 7.6*). The uncertainty due to the likely variations of the other input data is however not assessed in this research.

7.3 School building design variants

7.3.1 Reference school building

The reference school building model used for this study is based on the reference school buildings as defined in *Chapter 2*. The rectangular, elementary school building is chosen because of its simple though representative and common shape and room type profile. Information on the exact size, shape and room type profile can be found in *§ 2.2*. A heavy building structure is assumed.

7.3.2 Energy efficiency measures for the building envelope

To assess the energy saving potential and related variations of the primary energy use of the reference school building, different combinations of commonly used energy saving measures are studied. The insulation and air tightness level of the building envelope, the window type and dimensions, and the type of solar shading are varied. The range and steps of the variations are set in accordance with current regulations and requirements, technical feasibility (*i.e.* survey results presented in *§ 2.3.2* are considered as current best practice) and market availability.

- Regarding the energy saving measures related to the energy performance of the opaque building parts, only the insulation thickness is considered as a variable [25]. As previous cost-optimal studies have shown that the influence of the choice of the insulation material on the results of the cost-optimal study are limited [260], the insulation material and composition of the walls are assumed equal for all considered building variants. The insulation level of the building envelope is altered between an upper limit corresponding to the legal requirements (dd.2015) [18] and a lower limit equal to the current best practice (*§ 2.3.2*). Information on the composition of the walls can be found in *Table 4.1*.
- Two window types are considered: a window that is regularly used in the current building practice ($U_{window,glazing}$ = 1.1 W/(m^{2}K), $U_{window,frame}$ = 1.4 W/(m^{2}K)) and a high performance

window combining high performance glazing ($U_{window,glazing}$ = 0.6 W/(m^{2}K)) with a thermally improved window frame ($U_{window,frame}$ = 0.8 W/(m^{2}K)). The g-value of the glazing is 0.6. No variations of the g-value are assumed.

- The building's air tightness level is varied in 3 discrete steps: n_{50} = 3 ACH, 1 ACH or 0.6 ACH. The upper limit is determined in conformity with the minimum air tightness level required by *NBN−D50−001−1* [120] for buildings using a mechanical ventilation system. The lower limit is set in accordance with the minimum required air tightness level for passive schools: n_{50} = 0.6 ACH [21].
- Three types of shading are considered: no shading, fixed external louvers or automated external screens. The specifications and implemented control systems for the shading devices are described in *§ 4.3.1* and *§ 5.3.2*.

All building variants are assumed to be oriented with the main axis in the East-West orientation. Deterministic boundary conditions for amongst others user's schedule, internal heat gains and ventilation rates are used as set in *Table 4.5* for elementary school buildings.

A summary of the implemented energy saving measures is depicted in *Table 7.2*, resulting in 486 different combinations.

Table 7.2: Overview of the energy saving measures for the building envelope considered in this restricted cost-optimal study of a reference elementary school building.

Energy saving measure	Unit	Values	Simulation code
$\mathbf{U}_{wall}$	**W/(m^{2}K)**	0.24/0.16/0.11	W1/W2/W3
$\mathbf{U}_{floor}$	**W/(m^{2}K)**	0.24/0.20/0.16	F1/F2/F3
$\mathbf{U}_{roof}$	**W/(m^{2}K)**	0.24/0.15/0.11	R1/R2/R3
$\mathbf{U}_{window,glazing}$	**W/(m^{2}K)**	1.1/0.6	G1/G2
$\mathbf{U}_{window,frame}$	**W/(m^{2}K)**	1.4/0.8	
$\mathbf{n}_{50}$	**ACH**	3/1/0.6	A1/A2
shading	**-**	no - slats - automatic screens	S1/S2/S3

All combinations of these building design variants are calculated for two WWR's: WWR = 20% [97] and WWR = 30%. The latter value is equal to the average window-to-wall ratio in schools as found in the survey of the Flemish passive schools (see *Figure 2.11*). The WWR's are not considered as optimisation variables as the window surface area affect - in addition to the investment cost and the energy use - significantly the visual comfort of the building users which is not considered in the cost-optimal objectives.

Finally, to be able to assess the impact of the changes to the calculation method for different ventilation systems (*i.e.* the presence of a heat recovery device) or different heat emission systems (and related temperature regimes), all considered school building variants are coupled to different HVAC systems. Nevertheless, as for this research study refined data on the overall system efficiency $\eta_{overall}$ based on the results of integrated building and HVAC simulations are necessary, only those HVAC systems as studied in *§ 6.3.2* are considered. Furthermore, due to the restrictions related to

the use of an all-air heating system (HVAC4 - see *§ 6.2.5*), only HVAC1 to HVAC3 are included:

- HVAC1: high temperature radiator heating combined with an exhaust ventilation system
- HVAC2: low temperature radiator heating combined with a balanced, mechanical ventilation system with heat recovery
- HVAC3: floor heating in combination with central air heating coils, mechanical ventilation system with heat recovery

Detailed information on the system characteristics and operation can be found in *§ 6.2.1*.

7.4 Cost data

7.4.1 Cost data for the building envelope and for the HVAC system components

For each of the investigated energy saving measures, a cost function is used comprising both the material and labour costs. Secondary costs for amongst others necessary changes to the foundations or windows caused by larger insulation thicknesses are additionally included in the cost functions. Depending on the considered measure, the related costs are expressed as a function of thickness (insulation), area (glazing), length (window frames) or size (boiler, ventilation system).
The data for the construction and HVAC system costs used for this study are founded primarily on an extensive market-based analysis which is conducted by Royal HaskoningDHV and performed in the framework of an ongoing cost-optimal study for non-residential buildings (including schools) ordered by the Flemish government (VEA) [20]. The cost data are based on the evaluation of prices as found in price offers and building contracts for comparable, recently built or renovated building projects. These data are additionally verified by two major building engineering companies in Flanders. As the cost analysis by Royal HaskoningDHV dates from the beginning of 2015 [20], the obtained cost data are considered to be up to date and thus representative for this study. Lacking cost data are found in the work of Parys [125]. Since these cost data date from 2012, all prices are indexed to 2015 prices based on the ABEX-index [266] which indicates the evolution of construction costs in Belgium.
Detailed information on all the costs and cost data curves used for this study can be found in *Appendix C.1*.

7.4.2 Energy costs

The energy costs are calculated according to the EPBD guidelines [262] and in line with the cost-optimal studies for non-residential buildings (including schools) ordered by the Flemish government (VEA) [25, 20]. The energy costs are determined as the current energy prices indexed according to expected energy price changes. The current prices for electricity use and gas consumption are hereby based on the data collected for the second semester of 2014 by Eurostat [268] and are summarised in *Table 7.3*. As schools are liable to pay taxes, all prices include taxes and levies.

Due to the large variety of highly uncertain influencing factors, an accurate prediction of the evolution of energy prices over the building's life span is nearly impossible. Consequently, for cost-optimal

Table 7.3: Energy prices for Belgium as paid by the end user, averaged over the second semester of 2014 and all taxes and levies included, based on the data for non-residential building users (industrial) found in the Eurostat data base [268].

Gas (Eurostat Table nrg_pc_203)		**Electricity (Eurostat Table nrg_pc_205)**	
annual use, GJ/a	**price, €/kWh**	**annual use, MWh/a**	**price, €/kWh**
< 1000	0.0591	< 20	0.2149
< 10 000	0.0512	< 500	0.1742
< 100 000	0.0354	< 2000	0.1309
< 1 000 000	0.0317	< 20000	0.1166
< 4 000 000	0.0295	< 70000	0.0935
> 4 000 000	0.0239	< 150000	0.0935

studies, often different price evolutions are considered to incorporate the uncertainty of the energy price evolution. Likewise, two different energy price scenarios are included within this chapter. A simplified approach is however applied, expressing the price evolution as a constant increase above inflation [25, 20]. For the general cost-optimal study, a 'low' energy price scenario is used, assuming no real price increases for natural gas and electricity meaning that the price increases are set equal to the average price increase or the inflation rate [25, 20]. For the sensitivity analysis (see *§ 7.6*), the impact of a 'high' price scenario, assuming a price increase of 3.5% in real terms for both the gas and electricity prices, is assessed [25, 20].

7.5 Results and discussion

In this section, the results of the analysis of the impact of the changes of the calculation method on the results of a cost-optimal study are discussed. In *§ 7.5.1*, the impact of the applied energy calculation methods on the obtained data clouds and the Pareto fronts is studied. To do so, the results of the cost-optimal study are depicted in cost-optimal diagrams, expressing the net present costs NPC as a function of the primary energy use for heating and ventilation $E_{H,p}$. In *§ 7.5.2*, the impact of the changes of the *quasi-steady-state* calculation methods on the return on investment of each of the implied energy saving measures is determined and it is investigated if the choice of the *quasi-steady-state* calculation method used to assess these energy savings has any influence on the trade-off between the measures.

In schools, 70% of the investment and replacement costs are subsidised [267]. Consequently, the relative share of the energy costs gains importance in the calculation of the net present costs. Hence, the influence of the changes to the *quasi-steady-state* calculation method is expected to be more important in schools compared to other building typologies where no subsidising is foreseen. In contrast, as for this cost-optimal study the start values for the energy efficiency measures are set in accordance with the current energy performance requirements (dd.2015), energy efficient buildings are used as a reference. Consequently, the energy savings and related decreases of the energy costs by further improving the energy efficiency level of the building are limited, which limits the impact of the choice of the energy calculation (*i.e.* original or refined) method on the cost-optimal

calculation results. The impact might become more important for example when comparing alternative energy saving measures for retrofitting of an un-insulated school building, which is however beyond the scope of this research study.

7.5.1 Impact of the changes of the *quasi-steady-state* calculation method on the Pareto optimal solutions

The results of the cost-optimal study, assuming a life span of 30 years, including building subsidies, considering a discount rate of 3% and assuming no real price changes of the energy costs for natural gas and electricity, are depicted in *Figure 7.2* (a) to (d), for varying WWR's and different HVAC systems. The net present cost, calculated according to *Eq. 7.2*, of each combination of energy saving measures is expressed in function of the primary energy use for heating and ventilation. As the results differ depending on the method used for the energy calculations (*i.e.* original or refined calculation method), two different data clouds are obtained and plotted. Moreover, to validate the suggested changes to the calculation method, the results of the cost-optimal study while using dynamic simulations as an input for the heat demand $Q_{H,nd}$ calculations are plotted (black dots).
The results for the obtained Pareto fronts are summarised in *Appendix C.2*, *Table C.4* to *Table C.6*.

Five phenomena are noticed regarding the use of the refined *quasi-steady-state* calculation method. **(i)** In line with the results described in the previous chapters, overall, a better fit is found between the *dynamic* and the *quasi-steady-state* calculation method, when the refined method is used. Some discrepancies remain as shown in the figures, depending on the WWR or the HVAC system installed. These remaining differences can be amongst others explained by the differences in the calculations of the solar heat gains as denoted in *§ 5.2.2* and shown in *Figure 5.2*. **(ii)** The obtained data clouds are shifted to the right and upwards compared to the original calculation results (see *Figure 7.2*). **(iii)** The shape of the Pareto curve (see *Figure 7.2*), the number of Pareto solutions and the economic optima obtained (see *Table C.4* to *Table C.6*) are (quasi) similar for both *quasi-steady-state* calculation methods for HVAC1. For HVAC2 and HVAC3 slightly more differences are found. (**iv**) The shape of the data clouds are slightly different especially noticeable for HVAC2 and HVAC3: the data cloud obtained by the original calculation method is rather compact while for the revised method a more elongated shape is found. Finally, (**v**) the results found for HVAC2 and HVAC3 are similar while the results for HVAC1 are different and slightly more pronounced.

To explain these phenomena, first the impact of the suggested changes of the calculation method on the calculation results for $E_{H,p}$ is studied. As demonstrated in *§ 4.6*, the implementation of more realistic boundary conditions results in a decrease of the ventilation (losses), hence the calculated energy used by the fans according to the refined calculation method is decreased by 2.9 $kWh_{prim}/(m^2.a)$ in case of exhaust ventilation (HVAC1) and by 5.4 $kWh_{prim}/(m^2.a)$ in case of a balanced ventilation system (HVAC2 and HVAC3). In contrast, an increase of the calculation of the heat demand (see *§ 4.6*) and the final use for heating (see *§ 6.4*) is found for the refined method, resulting in an overall increase of $E_{H,p}$. In *Table 7.4*, the average, minimum and maximum differences between the refined and original calculation of the primary energy use for heating and ventilation $\Delta E_{H,p}$ are shown for the various WWR's and HVAC systems. Furthermore, the average relative differences

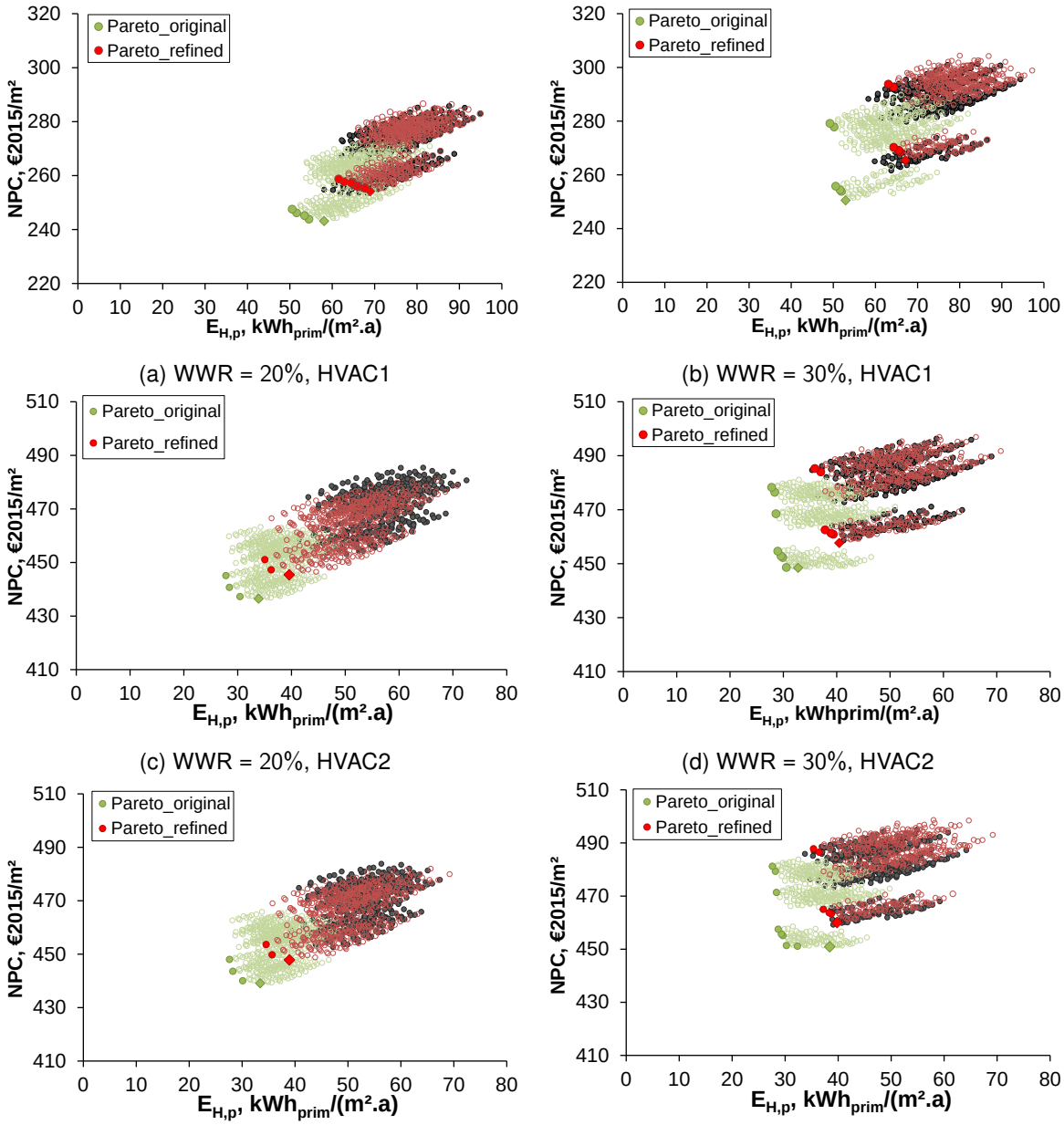

Figure 7.2: Cost diagrams for building variants with different building envelope qualities, coupled to either HVAC1, HVAC2 or HVAC3 and for WWR = 20% and WWR = 30%, expressing the net present costs (€2015/m^2) as a function of the primary energy use (kWh$_{prim}$/m^2). Both values are normalised to the floor area of the building. The results of the original and the refined calculation method are marked in green and red, respectively. For comparison, the results of the cost-optimal study while using dynamic simulations as an input for the heat demand $Q_{H,nd}$ calculations are marked by black dots.

Table 7.4: Overview of the average absolute and relative differences of the primary energy use calculations, normalised to the building floor area, due to the suggested changes of the *quasi-steady-state* method as described in *§ 7.2.1*.

		$\Delta\ \overline{E_{H,p}}$ **kWh$_{prim}$/(m^2.a)**	Δ **E**$_{H,p,min}$ **kWh$_{prim}$/(m^2.a)**	Δ **E**$_{H,p,max}$ **kWh$_{prim}$/(m^2.a)**	$\Delta\ \overline{E_{H,p}}$ %
WWR = 30%	**HVAC1**	+15.1	+11.5	+18.5	+19.9%
	HVAC2	+13.8	+8.1	+19.8	+36.9%
	HVAC3	+13.5	+7.8	+19.4	+31.1%
WWR = 20%	**HVAC1**	+12.2	+8.8	+15.5	+19.0%
	HVAC2	+13.5	+7.2	+20.1	+35.9%
	HVAC3	+13.2	+6.9	+19.7	+35.5%

$\Delta E_{H,p}$,% are depicted, calculated as the ratio of $\Delta E_{H,p}$ and $E_{H,p,original}$. An average increase of the primary energy use for heating and ventilation of ± 20% is found for HVAC1 whereas for HVAC2 and HVAC3, the average differences run up to more than 31%.

The differences between the calculation results for $E_{H,p}$ explain clearly the second mentioned effect: the data cloud is shifted to the right (towards higher energy uses $E_{H,p}$) and upwards (higher energy uses lead to higher energy costs and consequently to higher net present costs of the considered energy saving measures). In practice, this means that an increase of the estimation of the gap towards nearly zero energy buildings and a rise of the assessment of the yearly energy costs (see *Table C.4* and *Table C.6*) for the building user are found. While using the refined calculation method, the yearly costs for natural gas and electricity consumption are about €600 to €900 higher for buildings coupled to HVAC2 and HVAC3. For buildings coupled to HVAC1, the impact is even more significant as the yearly energy cost is increased by €1500 or more.

To explain the third and the fourth mentioned effect, the range of the differences between the energy calculation results $\Delta E_{H,p,max-min}$ are studied. For HVAC1, $\Delta E_{H,p,max-min}$ is approximately 7 kWh$_{prim}$/(m^2.a) (see *Table 7.4*). Consequently, all energy uses are more or less equally increased, so the data cloud is shifted while the shape and the relative position of the data points are more or less maintained. For the building variants with a WWR = 30% and coupled to HVAC1, the same Pareto optimal solutions and economic optima are found for both energy calculation methods (see *Table C.4*). For the building variants with a WWR = 20%, a change of the number of Pareto solutions is found though the same energy saving measures relate to the remaining Pareto front for both energy calculation methods as shown in *Table C.4*. Moreover, the same economic optima are obtained.

For HVAC2 and HVAC3, slightly more variations of the differences between the calculation results are obtained ($\Delta E_{H,p,max-min}$ = ± 12 kWh$_{prim}$/(m^2.a) - *Table 7.4*). Hence, the impact of the changes of the $E_{H,p}$ and the related energy costs E_c is slightly more pronounced compared to HVAC1 which results in a small change of the shape of the data cloud and more differences of the relative positions of the data points. Consequently, for all building variants coupled to HVAC2 and HVAC3, a different number of Pareto optimal solutions and different economic optima are found when the refined energy calculation method is used (see *Table C.5* and *Table C.6*).

The fifth and last effect can be explained by the fact that for HVAC2 and HVAC3 more or less equal changes to the calculation method are suggested. In contrast, for HVAC1, the suggested correction of the overall system efficiency ($\eta_{overall,HVAC3,refined}$ = 0.72 whereas $\eta_{overall,HVAC2,refined}$ = 0.65 and $\eta_{overall,HVAC3,refined}$ = 0.67) is smaller. Moreover, the impact of the changes of the boundary conditions (on the ventilation losses) are assessed differently due to the absence of a heat recovery device.

7.5.2 Impact of the changes to the *quasi-steady-state* calculation method on the hierarchy of energy saving measures

To assess the impact of the changes of the *quasi-steady-state* method on the hierarchy of energy saving measures for the building owner, the return on investment is calculated for all included measures using both the original and refined calculation method. The return on investment of a certain building measure is hereby determined as the ratio of the discounted value of the reduced energy costs and the additional initial investment cost, both related to the implementation of the considered measure. In doing so, each of the included building measures is varied between their maximum and minimum value as described in *Table 7.2*.
The results for an increased level of insulation of the floor, wall, roof and window and an improved air tightness level of the building envelope are plotted in *Figure 7.3*, for both calculation methods, for varying WWR's and for the different HVAC systems. All measures are ranked from the highest to the lowest return on investment as calculated by the refined calculation method.

Overall, *Figure 7.3* shows that, overall, the return on investment is increased when the refined method is used for the energy calculations compared to the original results. The impact on the hierarchy of the measures is however insignificant. In what follows, the results for the calculation of the return on investment are discussed for each of the considered building measures separately.
Regarding the improvement of the insulation level of the opaque building parts, an overall increase of the return on investment is found when the refined *quasi-steady-state* calculation method is used. The magnitude of the increase depends however on the type of the installed HVAC system, and more in particular on the presence of a heat recovery device. Whereas the increase of the return on investment remains limited ($+10.7\%$, on average) for the buildings without a heat recovery device, the increase of the calculation results is much more significant for those cases that have installed a heat recovery device ($+35.3\%$, on average).
Furthermore, the improvement of the air tightness level of the building envelope is assessed differently for buildings with (HVAC2 and HVAC3) and without a heat recovery device (HVAC1). While using the refined method for buildings coupled to HVAC2 or HVAC3, the return on investment is $+34.6\%$ higher compared to the original results, while for HVAC1 the return on investment is decreased by approximately -25.0%.
Regarding the implementation of more energy efficient windows, an overall increase of the return on investment is found for those building with a heat recovery device, while for the buildings without a heat recovery device a slight decrease is found. As the results differ for the various WWR's, the energy saving potential of the implementation of thermally improved windows is calculated additionally. The energy saving potential is hereby calculated as the reduction of the annual primary energy use

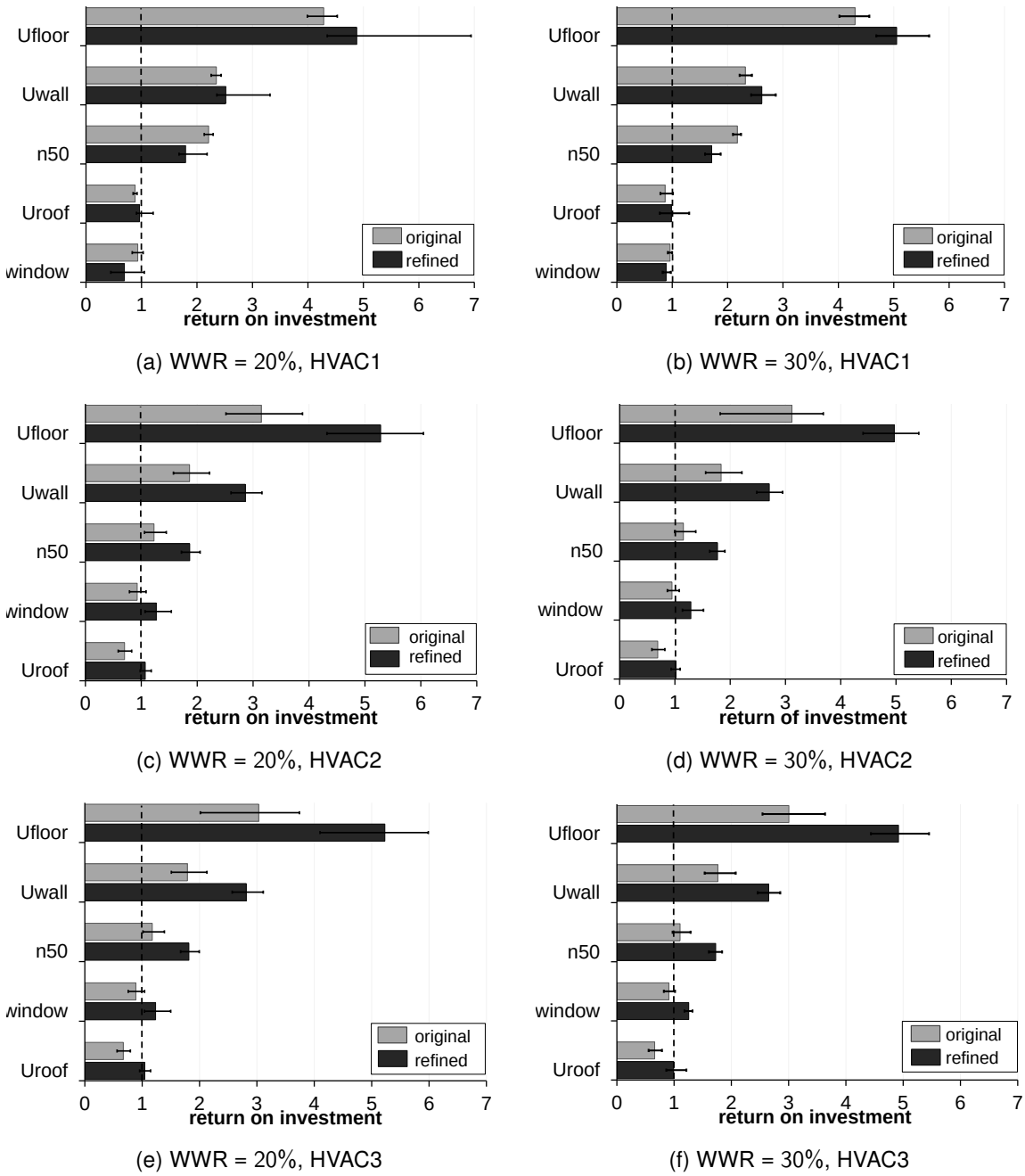

(a) WWR = 20%, HVAC1

(b) WWR = 30%, HVAC1

(c) WWR = 20%, HVAC2

(d) WWR = 30%, HVAC2

(e) WWR = 20%, HVAC3

(f) WWR = 30%, HVAC3

Figure 7.3: Return on investment for various energy saving measures applied in a reference elementary school building coupled to either HVAC1, HVAC2 or HVAC3 and for WWR = 20% and WWR = 30%. The total considered life span of the building is 30 years, the discount rate is 3% and no real price increases for gas and electricity are considered.

due to the implementation of a certain building measure, normalised to the building floor area (see *Eq. 7.4*).

$$\Delta E_{H,p} = E_{H,p,max} - E_{H,p,min} \tag{7.4}$$

The saving potential due to the implementation of triple glazing and thermally improved window frames is depicted in *Figure 7.4*. As shown, the results for the energy saving potential of triple glazing are independent of the coupled HVAC system when the original method is used. In contrast,

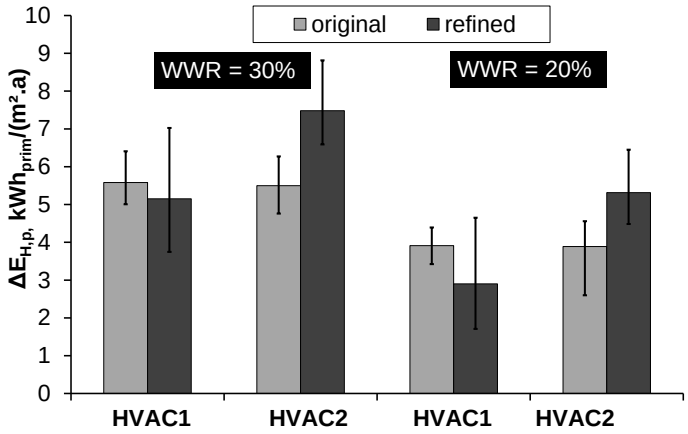

Figure 7.4: Averaged annual primary energy saving potential (kWhmsqa) due to the implementation of thermally improved windows, normalised to the building floor area. The error bars depict the maximum and minimum savings.

while using the refined method, significant differences are found. The energy saving potentials are assessed higher for buildings coupled to HVAC2 compared to buildings coupled to HVAC1.

7.6 Sensitivity analysis

The results of the cost-optimal study described in the previous section assume a life span of the school building of 30 years, include regular subsidies, neglect prices changes of the energy costs for natural gas and electricity and use a discount rate of 3%. As different assumptions might amplify the observed effects of the changes of the calculation methods on the cost-optimal study, a restricted sensitivity analysis is performed, once excluding the granted subsidies (see *§ 7.6.1*) and once considering a 'high' energy price scenario and a different discount rate (see *§ 7.6.2*).

7.6.1 Influence of subsidies

The impact of the exclusion of the subsidies on the results of the cost-optimal study are plotted in *Figure 7.5* for the cost diagrams, expressing the NPC as a function of the primary energy use for heating and ventilation $E_{H,p}$ and in *Figure 7.6* for the calculation results of the return on investment.

When comparing the Pareto fronts plotted in *Figure 7.2* and in *Figure 7.5*, as expected, a significant change is found on the determination of the Pareto optimal solutions when the subsidies for school building projects are excluded for the cost calculations: the number of Pareto solutions is increased and different economic optima are found. Regarding the evaluation of the impact of the changes to the *quasi-steady-state* calculation method on the cost-optimal calculations however, similar results are obtained when the net present costs are calculated with or without subsidies. In both cases, the obtained data clouds are shifted to the right and upwards compared to the original calculation results. Furthermore, for HVAC1, the shape of the Pareto curve and the economic optima obtained are (quasi) similar for both *quasi-steady-state* calculation methods while for HVAC2 and HVAC3 slightly more differences are found between the results for the original and the refined calculation method.

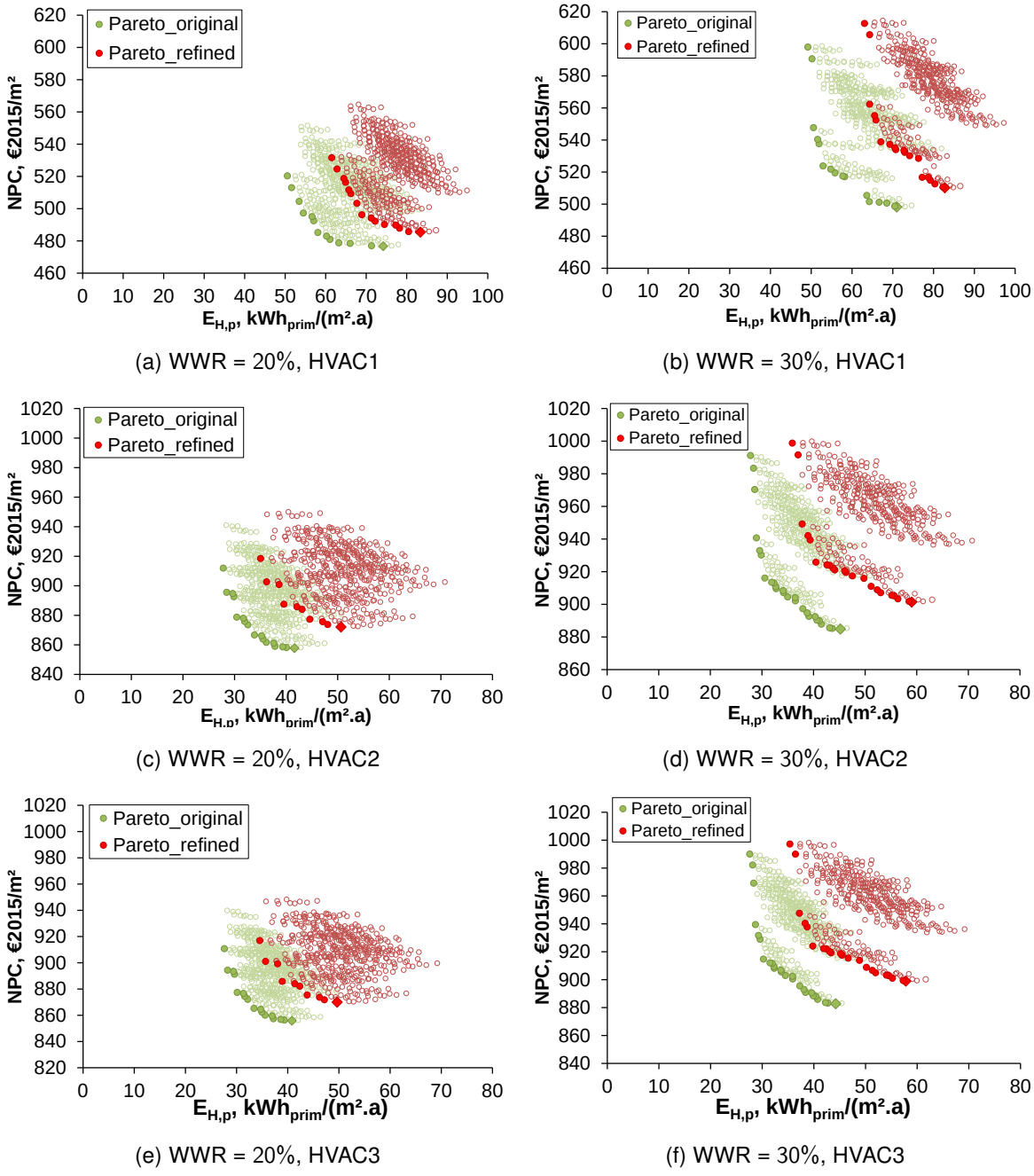

(a) WWR = 20%, HVAC1

(b) WWR = 30%, HVAC1

(c) WWR = 20%, HVAC2

(d) WWR = 30%, HVAC2

(e) WWR = 20%, HVAC3

(f) WWR = 30%, HVAC3

Figure 7.5: Cost diagrams for building variants with different building envelope qualities, coupled to HVAC1, HVAC2 and HVAC3 and for WWR = 20% and WWR = 30%, assuming **no subsidies** paid by the government for school building projects. The net present cost NPC (€2015/m^2) is expressed as a function of the primary energy use (kWh$_{prim}$/m^2), both normalised to the floor area of the building. The results of the original and the refined calculation method are marked in green and blue, respectively.

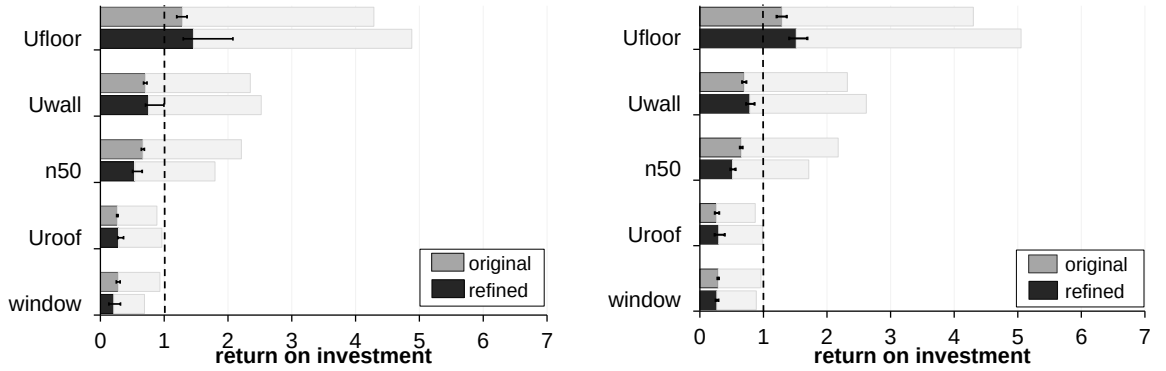

(a) WWR = 20%, HVAC1

(b) WWR = 30%, HVAC1

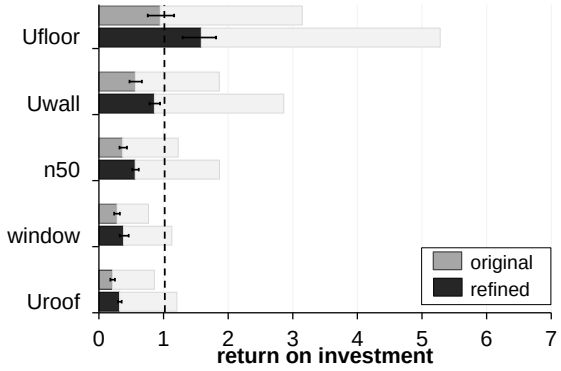

(c) WWR = 20%, HVAC2

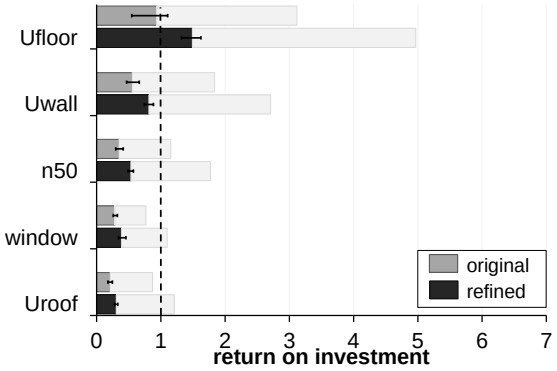

(d) WWR = 30%, HVAC2

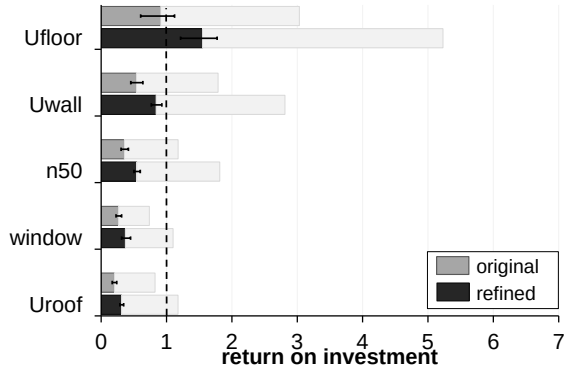

(e) WWR = 20%, HVAC3

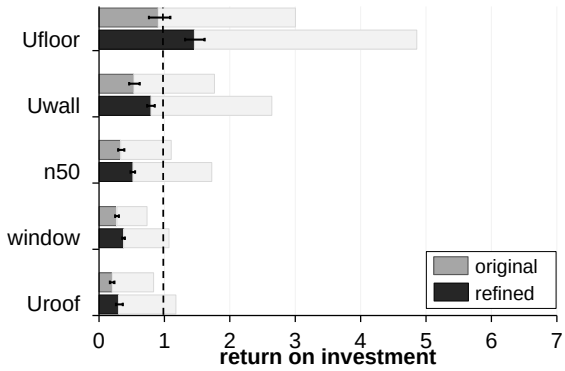

(f) WWR = 30%, HVAC3

Figure 7.6: Return on investment for various energy saving measures applied in a reference elementary school building coupled to HVAC1, HVAC2 and HVAC3 and for WWR = 20% and WWR = 30%. The total considered life span of the building is 30 years, the discount rate is 3%, and no real price increase for gas and electricity and **no subsidies** of the government for the investment and repair of building components are considered.

Likewise, when comparing *Figure 7.3* and *Figure 7.6*, a similar impact of the changes to the calculation method on the results of the return on investment is found for the cost calculations with or without subsidies.

7.6.2 Influence of the discount rate and energy price development

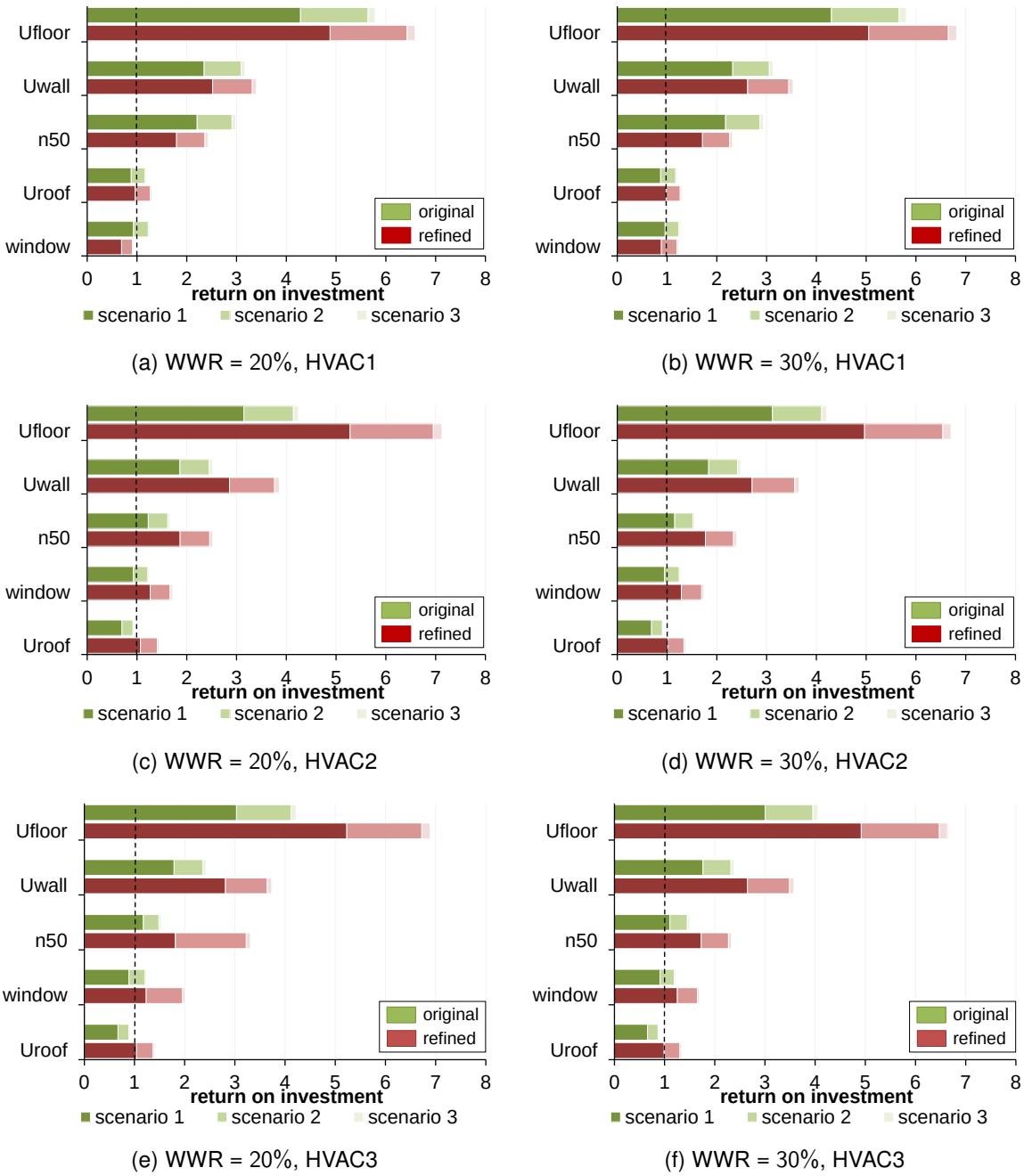

(a) WWR = 20%, HVAC1

(b) WWR = 30%, HVAC1

(c) WWR = 20%, HVAC2

(d) WWR = 30%, HVAC2

(e) WWR = 20%, HVAC3

(f) WWR = 30%, HVAC3

Figure 7.7: Overview of the results of the sensitivity analysis of the calculation of the return on investment assuming 3 difference scenarios: (**1**) discount rate = 3%, (**2**) discount rate = 1% and (**3**) discount rate = 1% and a linear increase of 3.5% for the energy prices.

The values for the discount rate and the energy price development used for the cost-optimal study described in *§ 7.5* are set in line with the specific (national) guidelines for the performance of cost-optimal studies in the context of EPBD [262, 260]. For the sensitivity analysis, an additional 'high'

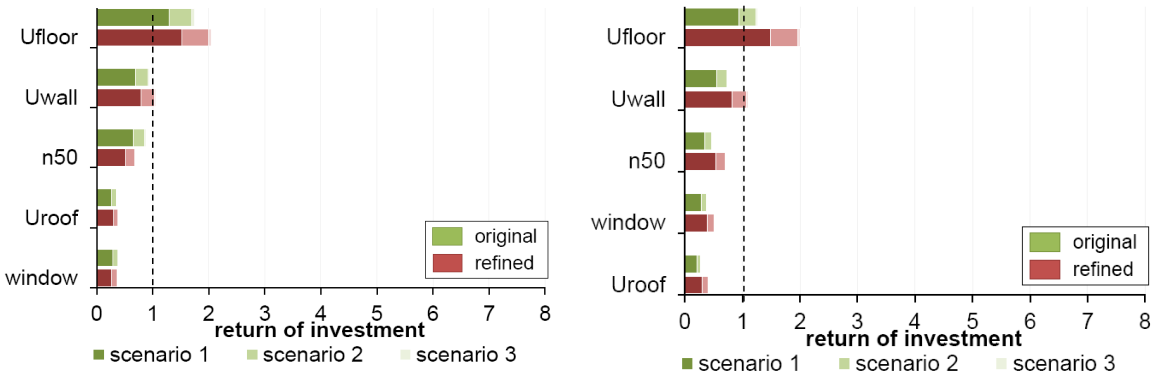

(a) WWR = 30%, HVAC1

(b) WWR = 30%, HVAC2

Figure 7.8: Overview of the results of the sensitivity analysis of the calculation of the return on investment assuming 3 difference scenarios and **excluding the subsidies for school buildings**: (**1**) discount rate = 3%, (**2**) discount rate = 1% and (**3**) discount rate = 1% and a linear increase of 3.5% for the energy prices.

energy price scenario is introduced that assumes a linear increase of the energy prices equal to 3.5%, in line with the assumptions made in a similar cost-optimal study for schools, performed in the context of EPBD [25, 20]. The considered energy price changes are expressed in real terms and are only applied on the energy production component of the energy prices (*i.e.* 71% for gas and 45% for electricity [269]). The taxes, levies and the network fees on the other hand are assumed to be fixed in time [25]. Furthermore, the discount rate is changed. Higher values for the discount rate reduce the impact of long term costs and highlight the benefits on a short term while lower values for the discount rates profit the evaluation of the benefits on a long term. As the choice of the calculation method affects the energy use calculation, and thus the long term costs, a lower value for the discount rate is considered for the sensitivity analysis equal to 1% [25]. Results are plotted in *Figure 7.7*. As both assumptions have an increasing effect on the energy costs, the energy saving potential of the measure is outweighed compared to the results for a discount rate equal to 3% and assuming no energy price changes. Overall, higher estimations for the return on investment are found, hence the effect of the changes of the energy calculation method is amplified. The impact on the ranking of the various measures remains however unchanged.
Additionally, a similar SA is performed, though excluding the subsidies for the construction of school buildings (see *Figure 7.8*). As similar trends are found as shown in *Figure 7.7*, the results of 2 cases (HVAC1 and HVAC2 with a WWR = 30%) are plotted only.

When analysing the results depicted in *Figure 7.6* and *Figure 7.8*, another important general trend is noticed: when subsidies are excluded for the cost calculations, the results for the return on investment are drastically lowered. A further enhancement of the EPBD requirement for schools in Flanders now appear to be mostly cost-ineffective and may therefore - from a strictly economical point of view and provided the implemented cost scenarios and hypotheses on the energy prices and discount rates - be questioned. This is mainly due to the fact that the current energy performance requirements (dd.2015) - used as the reference case for this study - are already rather strict and hence the energy saving potentials are limited. Furthermore, as more energy efficient buildings often require more sophisticated HVAC system technologies, the electricity consumption in these

buildings is increased which limits the overall improvement of the energy performance. Finally, as school buildings are only used - and thus climatised - for a restricted amount of hours per year, the potential of the implemented energy saving measures is not fully benefitted. Note that the EPB Directive [18] requires policy makers to set the minimum energy performance requirements in line with the results of the cost-optimal study. Final decisions on a further enhancement of the energy performance requirements however do not only depend on the economical viability of the energy measures. The reduction of the (embodied) energy use and related ecological impact, and the improvement of the indoor environmental quality are equally important aspects to consider.
Nevertheless, these results are an interesting aspect to consider while (re)organising the structural building financial initiatives or by defining the focus of additional subsidising procedures for (energy efficient) school building projects.

7.7 Conclusion

When the *quasi-steady-state* calculation method for energy assessment calculations is adapted to the typical use and characteristics of schools, an overall increase of the primary energy calculation results is found. As the net present costs of building design variants are increased accordingly, a change of the results for the cost-optimal study is observed. (**i**) An increase of the estimation of the gap towards nearly zero energy buildings is found and an increase of the assessment of the yearly energy costs for the building owner is obtained. (**ii**) In contrast, as the energy use of all data points is more or less equally increased, the relative position of the data points is approximately maintained. Consequently, the shape of the Pareto curves, the number of Pareto solutions and the economic optima obtained are (quasi) equal for both *quasi-steady-state* calculation methods.
To assess the impact on the hierarchy of the building measures, the return on investment is calculated using both the original and refined calculation method. In doing so, the considered building measures are varied between a maximum and minimum value and the related energy savings and additional investment costs are determined. A significant impact is found on the calculation results when the refined calculation method is used, depending on the type of the considered building measure and on the presence of a heat recovery device. Regarding the improvement of the insulation level of the opaque building parts, an overall increase of the return on investment is found when the refined *quasi-steady-state* calculation method is used: an average increase of $+35.3\%$ and $+10.7\%$ is found for buildings with and without a heat recovery device, respectively. Considering the impact of an improved level of air tightness of the building envelope, the return on investment is 34.6% higher for building with and 25.0% lower for buildings without a heat recovery device. Regarding the implementation of more energy efficient windows, an overall increase of the return on investment is found for those buildings with a heat recovery device, while for the buildings without a heat recovery device a slight decrease is found.
Note that these results are valid for the investigated building and HVAC sample, and for the assumptions and hypotheses made for both the energy calculations and for the cost data and price scenarios. A restricted sensitivity analysis shows however that the results are robust for variations in the discount rate, for a 'higher' energy price scenario and for exclusion of subsidies.

Although the impact on the determination of the cost-optimal school design appear to be rather limited (*i.e.* no significant changes of the Pareto Front are noticed), overall, one may conclude that the observed impact of the changes to the *quasi-steady-state* calculation method (*i.e.* general increase of the primary energy use assessment, related energy costs and return on investments) is significant and emphasises the importance of including the suggested revisions in the energy calculation method, especially when it is used for energy rating purposes in a regulatory context.

8

Conclusions and future research work

This dissertation aims at the evaluation of the *quasi-steady-state* monthly calculation method as currently applied in the context of EPBD for school buildings. Flaws, inaccuracies and restrictions are determined and modifications are suggested to obtain a better fit between *quasi-steady-state* and *dynamic* energy calculation results. To do so, this study consists of three main parts. First, a large-scale analysis and description is made of the typical characteristics of the contemporary Flemish school building stock. Second, the impact of these characteristics on the energy use is studied and subsequently translated into some modifications of the *quasi-steady-state* calculation method. Third, the impact of the suggested changes of the *quasi-steady-state* method on the determination of a cost-optimal school design is analysed.

In this last chapter, the main results and conclusions of the study are presented together with the limitations and perspectives for future research.

Main results and conclusions

Analysis of the contemporary school building stock

School buildings have typical operational and architectural characteristics which distinguish educational buildings from other (non-residential) buildings. Occupancy density, ventilation rates and internal heat gains are generally high. Daily school opening hours are limited and frequent holiday periods occur. Furthermore, educational activities imply certain requirements to the architecture and facilities of educational buildings resulting in a large variety of school buildings with different building sizes, geometries, shapes and room type profiles. This diversity on a small scale complicates energy performance evaluation on a larger scale. To generalise the diversity, four different reference models are developed, two for elementary and two for secondary schools, based on the results of a litera-

ture review and an exhaustive statistical survey of recently built or highly renovated school buildings. The size of the reference models is based on the average number of students and dimensions are set in line with the school building subsidizing procedures. For both school types, a representative room type profile is set including class rooms, offices, a teachers' room, a canteen and a kitchen, sanitary, storage rooms and circulation areas. For the elementary schools, a gym is added to the school building model while for the secondary schools laboratories are included instead.
To represent the actual variety of schools, the reference buildings are subsequently combined with a representative range of building (*i.e.* thermal mass, insulation level, air tightness, glazing surface, etc.) and users' related (*i.e.* heating set-points, ventilation rates, HVAC control and operation) characteristics. These are based on an elaborate analysis of a selection of typical school projects and on an exhaustive literature review. Finally, the most frequently used HVAC system types and lighting concepts in high performance, contemporary school buildings in Flanders are determined.

Revision of the quasi-steady-state calculation method

To assess the energy performance of a (school) building design in a regulatory context, the *quasi-steady-state*, monthly Energy Performance Regulations (*EPR*) calculation tool is used in Flanders. When comparing the results of this tool to the results of dynamic simulations however, significant discrepancies are found. Consequently, a series of modifications are suggested to make the calculation model more accurate and suitable to be used for school buildings.
Regarding the energy demand calculations, the impact of the use of standardised input data is studied and new, deterministic values, representative for Flemish schools, are defined. Furthermore, the implementation of the transient thermal behaviour of the building in the *quasi-steady-state* calculation method - and in particular the use of the numerical correlation-based correction factors - is studied and adapted to the typical use of schools. Regarding the method used to transform the heat demand to the final energy use for heating, the interaction between the building and the coupled HVAC systems is studied using integrated, dynamic simulations and it is evaluated if these effects are taken into account properly in the currently applied simplified, subsequential calculation method.

Energy demand calculations

An uncertainty analysis reveals a spread of about 30% of the annual heating demand and 40% of the annual cooling demand due to realistic variations of the users' related boundary conditions for schools, showing the significant (relative) uncertainty of the assessment results arising from the implemented input data used for the *quasi-steady-state* calculation method. These results confirm the need to refine the currently applied boundary conditions and default input data. Especially for passive buildings or net zero energy buildings which need to comply with (very) strict energy performance requirements, a revision is shown to be highly recommended. A sensitivity analysis, based on the Morris method, is performed, to reveal the predominant input parameters (*i.e.* users' and load profiles, comfort settings and the occupant density rate of the class rooms) for which new, more accurate values are determined based on collected field data and monitoring results. The survey reveals a set-point temperature for heating of 17°C for gyms and 21°C in all other school rooms, an occupant density rate of class rooms equal to 3 m^2/pers, target lighting power load in class rooms of 10.6 W/m^2 and an after hour school for equipment and lighting of 5%. As a final result, a set of newly

defined, representative boundary conditions is obtained which is used, directly, for the *dynamic* simulations or is converted into monthly mean input data for the *quasi-steady-state* calculation method

Furthermore, the accuracy of the *quasi-steady-state* calculation method itself and more in particular the implementation of dynamic effects are analysed and modified to the specific use of school buildings. First, the utilisation factors used for the calculation of the heating and cooling balance are adapted. In doing so, the heating and cooling demand, calculated by means of *dynamic* simulations are compared to the results of the monthly calculation method for a series of school building design variants. New, correlation-based numerical parameters are then derived using the black box approach and regression analysis techniques as described in *EN ISO 13790*: $a_{H,0}$ = 1.7 and $\tau_{H,0}$ = 25.7 for the heat balance and $a_{C,0}$ = 2.5 and $\tau_{C,0}$ = 10 for the cooling balance instead of $a_{H/C,0}$ = 1 and $\tau_{C/H,0}$ = 15. When applying these new parameters, overall, a better fit is found between the *dynamic* and *quasi-static* calculation results. The impact differs however for the heating and cooling balance. For the cooling balance, the absolute difference in energy demand is reduced by 70% to 0.15 kWh/(m^2.a), on average. For the heat balance, the impact of the refined utilisation factors is less significant. The averaged absolute difference between the *quasi-static* and *dynamic* energy demand of the investigated building sample is hereby reduced by 2.5%.
The accuracy of the *quasi-steady-state* calculations is simultaneously determined by the method applied to account for system intermittency. In the *EPR* calculation method, the energy saving potential due to intermittent heating or cooling is accounted for by the adjusted temperature approach. A fixed, adjusted monthly mean indoor temperature, independent of the use and characteristics of the building and systems, is used for the calculation of the heating or cooling balance. The results of dynamic simulations performed along this research study reveal however that the saving potentials depend amongst others on the time constant of the building and the applied heating or cooling pattern. Therefore, a suggestion is made to revise the currently applied calculation approach, focusing on the heat balance in particular. A comparative analysis of the results of different *quasi-static* calculation methods and *dynamic* simulations is performed. The results reveal the best fit when the calculation approach as described in *NEN 7120* is applied. This method accounts for intermittent heating by correcting the calculated heat losses instead of adjusting the indoor temperature. Furthermore, separate correction factors are used to account for night time setback and for weekends, both calculated as a function of the length of the period of reduced heating and of the thermal capacity of the building. This method can be further adapted to the typical Flemish school use by resetting the applied default values and the numerical, correlation-based parameters used for the calculation of the aforementioned correction factors.

Energy use calculations

In order to assess the accuracy of the energy use calculations, the impact of the interaction between buildings and their HVAC systems is studied using integrated, dynamic building and system simulations. Hereby, the same simulation approach and overall methodology is used that has already been applied successfully in a similar research study on office buildings. Different building design variants of the rectangular reference building for elementary schools are coupled to four traditional but commonly found HVAC systems in schools. The considered systems differ only in type of ventilation system and secondary systems for heating, while all are coupled to the same primary system

using a condensing gas boiler. The first system comprises radiator heating and an exhaust-only ventilation system without heat recovery. For the second system, the exhaust ventilation system is replaced by a balanced mechanical ventilation systems with heat recovery devices, combined with low temperature radiator heating. For the third system, radiator heating is replaced by a floor heating system in combination with centralised air heating. Finally, the fourth and last considered HVAC system comprises an all-air heating system using both central and local air heating coils.
The dynamic simulation results indicate, for this particular study of rather well insulated buildings, that variations of the emission systems have only a slight impact on the overall HVAC system performance. Furthermore, it is shown that efficiencies decrease significantly when part load ratios of the heating system are low and that the overall performance of the HVAC systems is affected by the building characteristics (*i.e.* energy efficiency of the building envelope, orientation of the building, WWR) although the impact remains limited ($< 10\%$). Subsequently, by comparing the results of the dynamic simulations to the results of *EPR*, it is shown that the final energy use for heating is significantly underestimated by *EPR* (16% or more) compared to the dynamic results, mainly due to highly overestimated generation efficiencies. Whereas the dynamic simulation results demonstrate that the generation efficiencies depend on the hot water (return) temperature and the part load ratios of the heating system, these influences appear not to be taken into account properly in the *EPR* calculation method.
While searching for an alternative, more accurate calculation approach, simple energy estimation models are deduced based on the results of the integrated, dynamic simulations. The heating demand is hereby selected as the independent variable so the influences of parameters such as weather conditions, building and material properties, use, occupancy, etc. are (indirectly) included in the energy use calculations. Based on the results of the analysis of different regression models, the linear models are revealed as the best fit: the average error between the *quasi-static* and *dynamic* energy use calculation results is reduced by 14% to 23%, depending on the considered HVAC system. These results confirm the use of the simplified calculation approach expressing the final energy use as a linear function of the heat demand. However, as significant differences are found compared to the dynamic efficiency values, a revision of the tabulated subsystem efficiencies is recommended.

Impact of the *quasi-steady-state* calculation method on the results of a cost-optimal school building design

Implementing the aforementioned suggested changes to the calculation method, an overall increase of the simulated energy use for heating in schools is observed. As the energy cost and thus the net present cost of a school building design are increased accordingly, a change of the results for the cost optimal study is found, resulting mainly in an increase of the estimation of the gap towards nearly zero energy buildings and an increase of the assessment of the yearly energy costs for the building owner. In contrast, as the energy use of all data points is more or less equally increased, the relative position of the data points is approximately maintained. Consequently, the shape of the Pareto curves, the number of Pareto solutions and the economic optima obtained are (quasi) equal for both *quasi-steady-state* calculation methods, although some small differences are noticed.
Furthermore, the impact of the revision of the calculation method on the return on investment of the

considered building measures is studied. A significant impact is found, depending on the type of the considered building measure and on the presence of a heat recovery device. Regarding the improvement of the insulation level of the opaque building parts, an overall increase of the return on investment is found when the refined *quasi-steady-state* calculation method is used: an average increase of +35.3% and +10.7% is found for buildings with and without a heat recovery device, respectively. Considering the impact of an improved level of air tightness of the building envelope, the return on investment is assessed 34.6% higher in buildings with and 25.0% lower in buildings without a heat recovery. Regarding the implementation of more energy efficient windows, an overall increase of the assessment of the return on investment is found for those buildings with a heat recovery device, while for the buildings without a heat recovery device a slight decrease is found.
A restricted SA shows however that results are robust for variations in the discount rate, for a 'higher' energy price scenario and for exclusion of subsidies.
Considering the overall significant increase of the primary energy use assessment, and hence the increase of the related energy costs and return on investments, the changes to the *quasi-steady-state* calculation method are considered significant, emphasising the importance of including the suggested revisions in the energy calculation method, especially when it is used for energy rating purposes in a regulatory context.

Therefore, as **a final conclusion**, a restricted list of suggestions for revision are formulated, ordered based on their priority, to obtain a more trustworthy *quasi-steady-state* energy assessment method for school buildings:

- Whereas in the current *EPR* method buildings are categorised into (mainly) residential or non-residential buildings, **a more diverse classification of buildings** should be considered. A broader variety of room types should be included and the **related boundary conditions should be determined (more) accurately** based on the specific use and characteristics of the building.
- It is recommended to re-evaluate the currently applied fixed, **subsystem efficiencies** for the energy use calculations. These refinements can be either based on the results of integrated building system simulations or - as good results are obtained for the linear estimation models expressing the final energy use as function of the heat demand - can be restricted to a modification of the subsystem efficiencies based on the detailed CEN/EPB standard *EN 15316*. Especially, the boiler efficiency method of EN 15316 which adds supplementary data to take into account the specific boiler operational conditions appear to be an interesting alternative. Note that before being able to use the linear models, derived in this dissertation, as a reference for revision of the calculation method, further research is necessary to assess the impact of occurring modelling and design uncertainties. Moreover, additional research is necessary to check if the models can be extrapolated to other HVAC system (configurations), control systems, etc. or to other (school) building typologies and (school) building design variants.
- A **revision** of the calculation **approach** used to account for **system intermittency** is recommended. The adjustment factor approach as used in *NEN 7210* offers an interesting alternative for the currently applied adjusted temperature approach as building characteristics and applied heating patterns are better accounted for.
- Finally, new values for **the correlation-based correction factors and default values** used

for the calculation of the utilisation and adjustment factors should be derived and adapted to the typical school buildings' characteristics.

Regarding the calculation for the energy use for cooling, only the impact of the utilisation factor is studied. As however the average error between the *quasi-static* and *dynamic* calculation methods for the investigated school building sample is reduced by 70%, a revision of the currently applied correlation-based correction factor a_0 and τ_0 is highly recommended.

Research restrictions and limitations

In this section, the overall framework and restrictions of the dissertation are summarised.

- The overall aim of this dissertation is to revise the calculation method used for energy compliance checking. Hereby, the research focuses specifically on the impact of the typical use and characteristics of school buildings. General inaccuracies of the method itself, related to *e.g.* the calculation of the quasi-static heat losses and heat gains are roughly mentioned though not addressed in detail throughout this research.

- The research focuses on the Flemish, elementary and secondary school building stock in particular. As the developed reference school building models and implemented boundary conditions are set based on a comprehensive study of a broad range of school building characteristics, the results can be extrapolated to other school forms (*e.g.* technical or vocational schools) on the condition that the organised educational activities are more or less in line with the activities taught in the investigated school building sample. As buildings' and users' characteristics depend on local customs and the specific building typology, the results can however not simply be generalised to other building typologies or other regions. Yet, the research approach used along this dissertation can be used as a reference for similar research studies on other building types or for other regions and countries.

- The research focuses on newly built or highly renovated school buildings which are subjected to the increasingly stringent energy policy and indoor environmental quality requirements. As the older building stock generally does not meet current energy efficiency and comfort requirements, both architectural and building physical characteristics, and HVAC system and lighting concepts of contemporary buildings only are studied. Focusing on the HVAC system selection in particular, only the currently, most commonly used HVAC systems are included due to the work load related to the system sizing procedure and the integrated dynamic simulations. More innovative though less common solutions in schools are not studied.

- Throughout this dissertation, an attempt is made to obtain more realistic energy rating results. Boundary conditions are redefined to approach real schools users' conditions more accurately and are adapted to the typical use and typology of the building based on collected field data and monitoring results. As the energy performance assessment must reflect the energetic

quality of the building and its systems, independently of any occupant and his behaviour, the deterministic approach is maintained. Consequently, the suggested modifications will not improve the accuracy of the model when it is used as a predictive tool to assess real energy use or energy saving potentials.

- In general, a number amount of (integrated) dynamic simulations of school buildings is done. Moreover, a cost-optimal study is performed. These results are however used to judge the accuracy of the currently applied *quasi-steady-state* energy assessment method and emphasise the need for revision of the method. It is not the objective of this research to formulate optimised building concepts for school nor to judge the effectiveness of innovative trends and evolutions. Neither it is the aim to formulate straightforward design guidelines and recommendations on sustainable school building design.

Future research perspectives

Finally, in addition to the results of this study, several research perspectives are revealed which can be further explored.

- The suggested modifications to the *quasi-steady-state* calculation method are entirely based on the results of a comparison with dynamic simulations. The obtained results are not fitted to monitoring data as no accurate monitoring data are available for the considered school building scope. Most of the surveyed buildings are only recently built and thus not yet monitored. Other monitoring results are not representative as the monitored school buildings are only in the initiating phase. Nevertheless, the reliability of the suggested changes to the calculation method and the obtained calculation results would increase if the comparison to the dynamic simulation results could be extended by a comparison with monitoring data.

- Reference buildings are set based on a comprehensive study of the school building characteristics. In doing so, simplifications and abstractions are made. To incorporate the impact of *e.g.* more complex building shapes, larger window-to-wall ratios, etc. further research might include the simulations of some real school buildings.

- In *Chapter 6*, an overall indication is given of the deficiencies of the currently applied *quasi-steady-state* calculation standard *EPR* for final energy use assessment. The detailed results depend however strongly on the design decisions regarding the HVAC system (configurations) and the accuracy of the applied dynamic simulation (model). Before extrapolating the use of the regression models, it is hence important to investigate the impact of these assumptions. The most important sources of uncertainty which should be kept in mind are: (i) the inherent restrictions of the simulation model (*e.g.* use of single air node per zone at a uniform air temperature) and the pragmatic modelling simplifications (*e.g.* the selected resolution of the multi-zonal building model), (ii) the design decisions and simplifications (*e.g.* all components

are assumed to be correctly installed and are connected to well balanced hydraulic or air distribution circuits, HVAC systems are assumed to be implemented and controlled according to current good practice) and (iii) the restrictions of the investigated building and HVAC system sample.

- The study focuses mainly on the calculation of the energy use for heating and ventilation as these are determined as the most dominant energy flows in schools. Due to the more stringent building's energy policy, a decrease of the heating energy use is however to be expected over the next years while active cooling might become necessary, especially in school buildings with lighter building structures or large window-to-wall ratios, or when the users' profile of the school building is changed towards 'Open schools'. Hence, further research might be addressed to the cooling energy flow.

- Lighting and related visual comfort requirement are considered as an important boundary condition along this research study. The suggested changes to the calculation method for the energy use due to lighting are however restricted to a change of the amount of yearly lighting operational hours. The impact of the installed lighting system and various implemented (daylight) control systems on the energy use in schools is not assessed. As the relative share of energy use due to lighting increases in relation to the improvement of the energy efficiency of the building, it would be interesting to address the lighting systems and related energy use in schools in further research.

- While adding extra adjustment and correction factors in relation to the typology and use of the buildings, the *quasi-steady-state* calculation method becomes more complicated. (Part of the) simplicity and transparency, typical for the monthly calculation method, is lost. Furthermore, adapting the *quasi-steady-state* calculation method for a wide range of building typologies is an exhaustive and time-consuming process. Further research can reveal if a change towards the use of the simplified, hourly or fully dynamic calculation method might be a more interesting alternative.

A

Overview of education in Flanders

In Flanders education is mandatory till the age of 18. For children from 2.5 to 6 years (not mandatory) nursery education (ISCED [1] 0) is provided. Primary education (ISCED 1) is aimed at children from 6 to 12 and comprises 6 consecutive years of study. On the one hand, there are autonomous nursery and primary schools providing respectively nursery and primary education exclusively. On the other hand, there are elementary schools offering a combination of both nursery and primary education [270]. Secondary education (ISCED 2/3) is aimed at students aged 12 to 18. It comprises different stages, types of education and study disciplines. From the second stage on, four different education forms can be distinguished:

1. general education (ASO) focusing on broad general education
2. technical education (TSO) specifically focusing on technical subjects
3. art education (KSO) combining broad general education with active art
4. vocational education (BSO) providing practice-oriented education in which young people learn a specific occupation in addition to receiving general education

After secondary school students have, though optional, access to tertiary education (ISCED 4/5). In addition to the mainstream education, special elementary and secondary education is organized for children who need special care due to a physical or mental disability, behavioural or emotional problems, or learning difficulties. An overview of the education facilities is given in

[1] ISCED International Standard of Classification of Education developed by UNESCO to facilitate comparisons of education statistics and indicators across countries on the basis of uniform and internationally agreed definitions

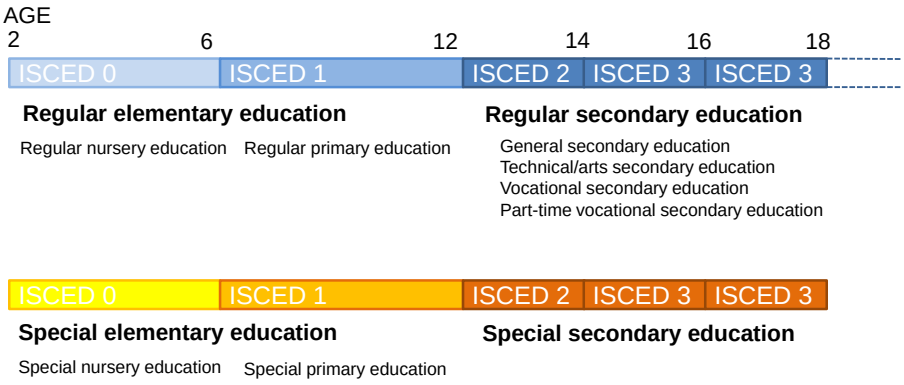

Figure A.1: The Flemish Community's education system related to education facilities [6].

B

Survey results of architectural characteristics of school buildings

A summary of the results of the survey on the architectural characteristics of the Flemish school building stock is depicted in *Table B.1* to *Table B.4* for elementary schools and in *Table B.6* to *Table B.7* for the secondary schools. Results for the space type profile for elementary schools are summarised in *Table B.5*.

Table B.1: Room type profile of elementary schools: survey results for school 1 to 9.

	Elementary school 1		Elementary school 2		Elementary school 3		Elementary school 4		Elementary school 5		Elementary school 6		Elementary school 7		Elementary school 8		Elementary school 9	
Surface area	**m^2**	**%**	**m^2**	**%**	**m^2**	**%**	**m^2**	**%**	**m^2**	**%**	**m^2**	**%**	**m^2**	**%**	**m^2**	**%**	**m^2**	**%**
circulation	470.9	13.6%	268.6	23.3%	112.3	12.5%	263.1	12.8%	56.3	10.1%	657.1	19.5%	414.2	26.2%	98.4	8.4%	300.1	20.0%
laboratory	0.0	0.0%	0.0	0.0%	0.0	0.0%	0.0	0.0%	0.0	0.0%	0.0	0.0%	0.0	0.0%	0.0	0.0%	0.0	0.0%
kitchen	0.0	0.0%	0.0	0.0%	28.2	0.8%	0.0	0.0%	0.0	0.0%	21.1	0.6%	41.4	2.6%	0.0	0.0%	0.0	0.0%
library	0.0	0.0%	0.0	0.0%	0.0	0.0%	45.2	1.3%	0.0	0.0%	0.0	0.0%	0.0	0.0%	0.0	0.0%	0.0	0.0%
changing rooms/showers	0.0	0.0%	0.0	0.0%	0.0	0.0%	33.4	1.0%	0.0	0.0%	54.5	1.6%	4.4	0.3%	0.0	0.0%	37.9	2.5%
gymnasium	0.0	0.0%	0.0	0.0%	0.0	0.0%	265.0	7.6%	0.0	0.0%	58.8	1.8%	0.0	0.0%	549.9	47.0%	0.0	0.0%
sports hall	0.0	0.0%	0.0	0.0%	0.0	0.0%	0.0	0.0%	0.0	0.0%	0.0	0.0%	0.0	0.0%	0.0	0.0%	0.0	0.0%
offices	73.5	2.1%	47.3	1.4%	137.9	4.0%	62.5	1.8%	4.2	0.1%	182.2	5.4%	73.0	4.6%	0.0	0.0%	65.4	4.3%
class	1660.5	47.8%	657.6	18.9%	239.3	6.9%	837.7	24.1%	338.8	9.8%	1405.2	41.8%	555.3	35.1%	241.4	20.6%	801.9	53.3%
technical/storage rooms	451.4	13.0%	114.1	3.3%	101.1	2.9%	148.2	4.3%	60.1	1.7%	116.0	3.5%	141.3	8.9%	135.2	11.6%	13.9	0.9%
teachers' room	63.5	1.8%	0.0	0.0%	52.7	1.5%	27.3	0.8%	0.0	0.0%	90.6	2.7%	0.0	0.0%	36.8	3.1%	54.4	3.6%
polyvalent room	145.0	4.2%	0.0	0.0%	0.0	0.0%	168.5	4.9%	78.5	2.3%	321.9	9.6%	0.0	0.0%	0.0	0.0%	164.7	11.0%
canteen	461.5	13.3%	0.0	0.0%	175.3	5.1%	133.4	3.8%	0.0	0.0%	244.0	7.3%	254.5	16.1%	0.0	0.0%	0.0	0.0%
sanitary	145.0	4.2%	65.2	1.9%	52.4	1.5%	69.3	2.0%	22.1	0.6%	111.4	3.3%	98.6	6.2%	108.6	9.3%	65.1	4.3%
workshop	0.0	0.0%	0.0	0.0%	0.0	0.0%	0.0	0.0%	0.0	0.0%	98.5	2.9%	0.0	0.0%	0.0	0.0%	0.0	0.0%

Table B.2: Room type profile of elementary schools: survey results for school 11 to 18.

	Elementary school 10		Elementary school 11		Elementary school 12		Elementary school 13		Elementary school 14		Elementary school 15		Elementary school 16		Elementary school 17		Elementary school 18	
Surface area	**m^2**	**%**	**m^2**	**%**	**m^2**	**%**	**m^2**	**%**	**m^2**	**%**	**m^2**	**%**	**m^2**	**%**	**m^2**	**%**	**m^2**	**%**
circulation	323.0	10.5%	98.8	9.3%	410.9	18.9%	308.6	17.8%	286.9	22.2%	188.8	13.5%	329.3	20.6%	57.0	21.1%	90.1	13.7%
laboratory	0.0	0.0%	0.0	0.0%	0.0	0.0%	0.0	0.0%	0.0	0.0%	0.0	0.0%	0.0	0.0%	0.0	0.0%	0.0	0.0%
kitchen	54.0	1.8%	31.6	3.0%	31.4	1.4%	29.2	1.7%	0.0	0.0%	11.6	0.8%	0.0	0.0%	0.0	0.0%	0.0	0.0%
library	0.0	0.0%	0.0	0.0%	0.0	0.0%	0.0	0.0%	0.0	0.0%	14.9	1.1%	0.0	0.0%	0.0	0.0%	0.0	0.0%
changing rooms/showers	24.3	0.8%	39.0	3.7%	40.4	1.9%	31.6	1.8%	39.0	3.0%	29.3	2.1%	0.0	0.0%	0.0	0.0%	0.0	0.0%
gymnasium	0.0	0.0%	0.0	0.0%	202.8	9.3%	181.7	10.5%	200.0	15.5%	287.9	20.6%	0.0	0.0%	0.0	0.0%	0.0	0.0%
sports hall	0.0	0.0%	0.0	0.0%	0.0	0.0%	0.0	0.0%	0.0	0.0%	0.0	0.0%	0.0	0.0%	0.0	0.0%	0.0	0.0%
offices	72.8	2.4%	0.0	0.0%	35.2	1.6%	62.6	3.6%	35.7	2.8%	152.5	10.9%	0.0	0.0%	40.8	15.1%	19.7	3.0%
class	1541.2	50.3%	108.0	10.2%	700.5	32.3%	697.2	40.1%	575.2	44.6%	532.7	38.2%	1221.3	76.4%	117.7	43.7%	360.3	54.8%
technical/storage rooms	260.4	8.5%	232.6	21.9%	181.5	8.4%	37.5	2.2%	101.8	7.9%	28.9	2.1%	33.9	2.1%	21.1	7.8%	11.1	1.7%
teachers' room	45.0	1.5%	0.0	0.0%	0.0	0.0%	68.4	3.9%	31.2	2.4%	41.1	2.9%	0.0	0.0%	0.0	0.0%	25.2	3.8%
polyvalent room	285.2	9.3%	285.5	26.9%	355.2	16.4%	0.0	0.0%	0.0	0.0%	58.1	4.2%	0.0	0.0%	0.0	0.0%	111.7	17.0%
canteen	330.5	10.8%	229.0	21.6%	112.5	5.2%	253.2	14.6%	0.0	0.0%	0.0	0.0%	0.0	0.0%	0.0	0.0%	0.0	0.0%
sanitary	127.3	4.2%	36.3	3.4%	101.7	4.7%	67.8	3.9%	20.1	1.6%	50.4	3.6%	13.8	0.9%	33.0	12.2%	39.6	6.0%
workshop	0.0	0.0%	0.0	0.0%	0.0	0.0%	0.0	0.0%	0.0	0.0%	0.0	0.0%	0.0	0.0%	0.0	0.0%	0.0	0.0%

Table B.3: Room type profile of elementary schools: survey results for school 19 to 27.

	Elementary school 19		Elementary school 20		Elementary school 21		Elementary school 22		Elementary school 23		Elementary school 24		Elementary school 25		Elementary school 26		Elementary school 27	
Surface area	**m^2**	**%**	**m^2**	**%**	**m^2**	**%**	**m^2**	**%**	**m^2**	**%**	**m^2**	**%**	**m^2**	**%**	**m^2**	**%**	**m^2**	**%**
circulation	229.5	19.2%	384.9	16.3%	149.8	11.2%	101.5	6.1%	228.6	18.1%	131.6	19.3%	386.4	16.2%	171.0	27.7%	420.1	15.1%
laboratory	0.0	0.0%	0.0	0.0%	0.0	0.0%	0.0	0.0%	0.0	0.0%	0.0	0.0%	0.0	0.0%	0.0	0.0%	0.0	0.0%
kitchen	22.1	1.8%	5.7	0.2%	14.0	1.0%	0.0	0.0%	37.5	3.0%	0.0	0.0%	28.2	1.2%	0.0	0.0%	0.0	0.0%
library	0.0	0.0%	0.0	0.0%	17.0	1.3%	0.0	0.0%	0.0	0.0%	0.0	0.0%	0.0	0.0%	0.0	0.0%	20.6	0.7%
changing rooms/showers	0.0	0.0%	0.0	0.0%	0.0	0.0%	0.0	0.0%	23.6	1.9%	0.0	0.0%	25.7	1.1%	0.0	0.0%	54.7	2.0%
gymnasium	0.0	0.0%	0.0	0.0%	186.3	13.9%	0.0	0.0%	221.7	17.5%	0.0	0.0%	248.7	10.4%	0.0	0.0%	0.0	0.0%
sports hall	0.0	0.0%	0.0	0.0%	0.0	0.0%	0.0	0.0%	0.0	0.0%	0.0	0.0%	0.0	0.0%	0.0	0.0%	1008.0	36.2%
offices	89.4	7.5%	204.2	8.6%	40.8	3.0%	80.7	4.8%	84.3	6.7%	0.0	0.0%	179.9	7.5%	0.0	0.0%	59.6	2.1%
class	659.6	55.2%	1075.9	45.5%	597.9	44.7%	943.2	56.4%	475.3	37.6%	405.5	59.6%	927.9	38.9%	384.0	62.2%	549.3	19.7%
technical/storage rooms	22.2	1.9%	87.8	3.7%	75.9	5.7%	53.4	3.2%	85.8	6.8%	8.9	1.3%	181.9	7.6%	35.2	5.7%	241.4	8.7%
teachers' room	0.0	0.0%	71.6	3.0%	35.3	2.6%	61.3	3.7%	0.0	0.0%	16.3	2.4%	48.4	2.0%	0.0	0.0%	64.8	2.3%
polyvalent room	0.0	0.0%	0.0	0.0%	67.4	5.0%	358.9	21.5%	0.0	0.0%	0.0	0.0%	97.6	4.1%	0.0	0.0%	89.8	3.2%
canteen	132.8	11.1%	427.1	18.1%	86.4	6.5%	0.0	0.0%	50.9	4.0%	66.7	9.8%	174.2	7.3%	0.0	0.0%	221.2	7.9%
sanitary	39.1	3.3%	105.3	4.5%	67.4	5.0%	73.6	4.4%	57.0	4.5%	51.7	7.6%	88.0	3.7%	27.2	4.4%	56.8	2.0%
workshop	0.0	0.0%	0.0	0.0%	0.0	0.0%	0.0	0.0%	0.0	0.0%	0.0	0.0%	0.0	0.0%	0.0	0.0%	0.0	0.0%

Table B.4: Room type profile of elementary schools: survey results for school 28 to 35.

	Elementary school 28		Elementary school 29		Elementary school 30		Elementary school 31		Elementary school 32		Elementary school 33		Elementary school 34		Elementary school 35	
Surface area	**m^2**	**%**	**m^2**	**%**	**m^2**	**%**	**m^2**	**%**	**m^2**	**%**	**m^2**	**%**	**m^2**	**%**	**m^2**	**%**
circulation	7.2	2.1%	0.0	0.0%	312.5	12.6%	202.0	16.8%	225.3	22.6%	151.8	24.8%	330.2	23.0%	267.1	17.2%
laboratory	0.0	0.0%	0.0	0.0%	0.0	0.0%	0.0	0.0%	0.0	0.0%	0.0	0.0%	0.0	0.0%	0.0	0.0%
kitchen	0.0	0.0%	12.4	4.6%	25.4	1.0%	39.7	3.3%	0.0	0.0%	0.0	0.0%	0.0	0.0%	36.5	2.4%
library	0.0	0.0%	0.0	0.0%	0.0	0.0%	0.0	0.0%	0.0	0.0%	0.0	0.0%	0.0	0.0%	0.0	0.0%
changing rooms/showers	0.0	0.0%	0.0	0.0%	0.0	0.0%	0.0	0.0%	0.0	0.0%	0.0	0.0%	14.8	1.0%	10.4	0.7%
gymnasium	0.0	0.0%	0.0	0.0%	0.0	0.0%	0.0	0.0%	0.0	0.0%	0.0	0.0%	0.0	0.0%	0.0	0.0%
sports hall	0.0	0.0%	0.0	0.0%	0.0	0.0%	0.0	0.0%	0.0	0.0%	0.0	0.0%	0.0	0.0%	0.0	0.0%
offices	3.7	1.1%	0.0	0.0%	133.0	5.4%	0.0	0.0%	16.2	1.6%	120.5	19.7%	63.6	4.4%	53.2	3.4%
class	165.8	49.4%	92.8	34.6%	1261.9	50.9%	578.7	48.0%	348.2	34.9%	283.3	46.2%	669.0	46.6%	564.3	36.4%
technical/storage rooms	16.0	4.8%	24.3	9.1%	236.0	9.5%	74.0	6.1%	63.2	6.3%	22.9	3.7%	32.9	2.3%	98.6	6.4%
teachers' room	0.0	0.0%	25.6	9.5%	92.9	3.7%	0.0	0.0%	22.2	2.2%	0.0	0.0%	50.0	3.5%	67.7	4.4%
polyvalent room	90.7	27.0%	73.5	27.4%	196.6	7.9%	298.1	24.8%	106.5	10.7%	0.0	0.0%	153.6	10.7%	194.9	12.6%
canteen	33.4	9.9%	0.0	0.0%	111.1	4.5%	0.0	0.0%	155.6	15.6%	0.0	0.0%	0.0	0.0%	171.9	11.1%
sanitary	19.1	5.7%	39.4	14.7%	110.6	4.5%	12.0	1.0%	61.3	6.1%	34.3	5.6%	120.1	8.4%	84.5	5.5%
workshop	0.0	0.0%	0.0	0.0%	0.0	0.0%	0.0	0.0%	0.0	0.0%	0.0	0.0%	0.0	0.0%	0.0	0.0%

Table B.5: Statistical analysis of the survey results for elementary schools.

	offices	canteen	changing rooms	circulation	class	gymnasium	kitchen	laboratory	library	polyvalent room	sanitary	sports hall	teachers' room	technical/storage rooms	workshop
school 1	2.1%	13.3%		13.6%	47.8%					4.2%	4.2%		1.8%	13.0%	
school 2	4.1%			23.3%	57.0%						5.7%			9.9%	
school 3	15.3%	19.5%		12.5%	26.6%		3.1%				5.8%		5.9%	11.2%	
school 4	3.0%	6.5%	1.6%	12.8%	40.8%	12.9%			2.2%	8.2%	3.4%		1.3%	7.2%	
school 5	0.8%	7.0%		10.1%	60.5%	7.0%					3.9%			10.7%	
school 6	5.4%	7.3%	1.6%	19.5%	41.8%	1.8%	0.6%			9.6%	3.3%		2.7%	3.5%	2.9%
school 7	4.6%	16.1%	0.3%	26.2%	35.1%		2.6%				6.2%			8.9%	
school 8				8.4%	20.6%	47.0%					9.3%		3.1%	11.6%	
school 9	4.3%	5.5%	2.5%	20.0%	53.3%	5.5%					4.3%		3.6%	0.9%	
school 10	1.1%	9.9%		2.1%	49.4%	27.0%					5.7%			4.8%	
school 11		13.7%			34.6%	13.7%	4.6%				14.7%		9.5%	9.1%	
school 12	5.4%	4.5%		12.6%	50.9%	7.9%	1.0%				4.5%		3.7%	9.5%	
school 13	2.4%	10.8%	0.8%	10.5%	50.3%	9.3%	1.8%				4.2%		1.5%	8.5%	
school 14		21.6%	3.7%	9.3%	10.2%	26.9%	3.0%				3.4%			21.9%	
school 15	1.6%	5.2%	1.9%	18.9%	32.3%	9.3%	1.4%			16.4%	4.7%			8.4%	
school 16	3.6%	14.6%	1.8%	17.8%	40.1%	10.5%	1.7%				3.9%		3.9%	2.2%	
school 17	2.8%		3.0%	22.2%	44.6%	15.5%					1.6%		2.4%	7.9%	
school 18	10.9%	4.2%	2.1%	13.5%	38.2%	20.6%	0.8%		1.1%		3.6%		2.9%	2.1%	
school 19				20.6%	76.4%						0.9%			2.1%	
school 20	15.1%			21.1%	43.7%						12.2%			7.8%	
school 21	3.0%	8.5%		13.7%	54.8%	8.5%					6.0%		3.8%	1.7%	
school 22		12.4%		16.8%	48.0%	12.4%	3.3%				1.0%			6.1%	
school 23	1.6%	15.6%		22.6%	34.9%	10.7%					6.1%		2.2%	6.3%	
school 24	19.7%			24.8%	46.2%						5.6%			3.7%	
school 25	7.5%	11.1%		19.2%	55.2%		1.8%				3.3%			1.9%	
school 26	8.6%	18.1%		16.3%	45.5%		0.2%				4.5%		3.0%	3.7%	
school 27	3.0%	6.5%		11.2%	44.7%	13.9%	1.0%		1.3%	5.0%	5.0%		2.6%	5.7%	
school 28	4.8%	10.7%		6.1%	56.4%	10.7%					4.4%		3.7%	3.2%	
school 29	6.7%	4.0%	1.9%	18.1%	37.6%	17.5%	3.0%				4.5%			6.8%	
school 30		9.8%		19.3%	59.6%						7.6%		2.4%	1.3%	
school 31	7.5%	7.3%	1.1%	16.2%	38.9%	10.4%	1.2%			4.1%	3.7%		2.0%	7.6%	
school 32				27.7%	62.2%						4.4%			5.7%	
school 33	2.1%	7.9%	2.0%	15.1%	19.7%				0.7%	3.2%	2.0%	36.2%	2.3%	8.7%	
school 34	4.4%	5.4%	1.0%	23.0%	46.6%	5.4%					8.4%		3.5%	2.3%	
school 35	3.4%	11.1%	0.7%	17.2%	36.4%	12.6%	2.4%				5.5%		4.4%	6.4%	
mean	**5.5%**	**10.3%**	**1.7%**	**16.5%**	**44.0%**	**13.8%**	**2.0%**	**0.0%**	**1.3%**	**7.2%**	**5.1%**	**36.2%**	**3.3%**	**6.6%**	**2.9%**
median	**4.2%**	**9.9%**	**1.8%**	**17.0%**	**44.7%**	**10.7%**	**1.8%**	**0.0%**	**1.2%**	**5.0%**	**4.5%**	**36.2%**	**3.0%**	**6.4%**	**2.9%**
σ	**4.6%**	**4.8%**	**0.9%**	**5.9%**	**13.1%**	**9.5%**	**1.2%**	**0.0%**	**0.6%**	**4.7%**	**2.8%**	**0.0%**	**1.7%**	**4.3%**	**0.0%**
probability	**80.0%**	**80.0%**	**42.9%**	**97.1%**	**100.0%**	**65.7%**	**48.6%**	**0.0%**	**11.4%**	**20.0%**	**100.0%**	**2.9%**	**62.9%**	**100.0%**	**2.9%**

Table B.6: Room type profile of secondary schools: survey results for school 1 to 6.

	Secondary school 1		Secondary school 2		Secondary school 3		Secondary school 4		Secondary school 5		Secondary school 6	
Surface area	**m^2**	**%**	**m^2**	**%**	**m^2**	**%**	**m^2**	**%**	**m^2**	**%**	**m^2**	**%**
circulation	249.6	23.2%	810.3	18.8%	177.5	22.6%	520.8	20.2%	665.3	23.1%	25.0	0.7%
laboratory	0.0	0.0%	0.0	0.0%	0.0	0.0%	0.0	0.0%	0.0	0.0%	234.4	6.4%
kitchen	8.2	0.8%	0.0	0.0%	0.0	0.0%	46.9	1.8%	0.0	0.0%	0.0	0.0%
kitchen (teach)	0.0	0.0%	0.0	0.0%	0.0	0.0%	0.0	0.0%	0.0	0.0%	0.0	0.0%
library	0.0	0.0%	0.0	0.0%	0.0	0.0%	0.0	0.0%	0.0	0.0%	0.0	0.0%
changing rooms/showers	8.2	0.8%	0.0	0.0%	0.0	0.0%	87.4	3.4%	0.0	0.0%	75.3	2.0%
gymnasium	0.0	0.0%	0.0	0.0%	0.0	0.0%	670.2	26.0%	216.2	7.5%	720.0	19.5%
sports hall	0.0	0.0%	0.0	0.0%	0.0	0.0%	0.0	0.0%	0.0	0.0%	0.0	0.0%
administration	0.0	0.0%	246.0	5.7%	12.3	1.6%	95.1	3.7%	34.2	1.2%	204.4	5.5%
class	503.0	46.8%	2402.9	55.9%	421.3	53.6%	794.1	30.8%	1825.9	63.3%	1318.4	35.8%
technical/storage rooms	38.1	3.6%	215.1	5.0%	17.6	2.2%	209.2	8.1%	30.8	1.1%	221.7	6.0%
teachers' room	0.0	0.0%	0.0	0.0%	0.0	0.0%	71.0	2.7%	0.0	0.0%	90.9	2.5%
polyvalent room	213.1	19.8%	498.0	11.6%	0.0	0.0%	0.0	0.0%	59.5	2.1%	669.3	18.2%
canteen	0.0	0.0%	0.0	0.0%	113.8	14.5%	0.0	0.0%	0.0	0.0%	0.0	0.0%
sanitary	53.8	5.0%	128.0	3.0%	44.1	5.6%	87.7	3.4%	52.9	1.8%	125.0	3.4%

Table B.7: Room type profile of secondary schools: survey results for school 7 to 11.

	Secondary school 7		**Secondary school 8**		**Secondary school 9**		**Secondary school 10**		**Secondary school 11**	
Surface area	**m^2**	**%**	**m^2**	**%**	**m^2**	**%**	**m^2**	**%**	**m^2**	**%**
circulation	131.2	10.5%	365.6	21.1%	261.1	8.6%	365.5	22.2%	432.8	23.4%
laboratory	0.0	0.0%	49.3	2.8%	94.0	3.1%	0.0	0.0%	243.0	13.1%
kitchen	28.0	2.2%	10.0	0.6%	0.0	0.0%	33.7	2.1%	5.6	0.3%
kitchen (teach)	0.0	0.0%	0.0	0.0%	0.0	0.0%	0.0	0.0%	193.0	10.4%
library	0.0	0.0%	0.0	0.0%	0.0	0.0%	12.2	0.7%	0.0	0.0%
changing rooms/showers	0.0	0.0%	0.0	0.0%	0.0	0.0%	18.3	1.1%	0.0	0.0%
gymnasium	0.0	0.0%	0.0	0.0%	0.0	0.0%	0.0	0.0%	0.0	0.0%
sports hall	0.0	0.0%	0.0	0.0%	0.0	0.0%	0.0	0.0%	0.0	0.0%
administration	0.0	0.0%	137.2	7.9%	213.7	7.0%	102.1	6.2%	47.9	2.6%
class	561.4	44.7%	952.1	54.8%	1611.7	52.8%	313.0	19.0%	0.0	0.0%
technical/storage rooms	69.8	5.6%	54.5	3.1%	46.4	1.5%	133.4	8.1%	44.0	2.4%
teachers' room	55.9	4.5%	106.0	6.1%	67.6	2.2%	82.5	5.0%	0.0	0.0%
polyvalent room	0.0	0.0%	43.1	2.5%	675.5	22.1%	0.0	0.0%	0.0	0.0%
canteen	342.7	27.3%	0.0	0.0%	0.0	0.0%	573.1	34.9%	823.1	44.4%
sanitary	66.2	5.3%	18.5	1.1%	81.9	2.7%	10.5	0.6%	63.4	3.4%

C

Cost optimal study

C.1 Cost data

The data for the construction costs used for this study, is primarily founded on a market-based analysis which is conducted by Royal HaskoningDHV and performed in the framework of an ongoing cost-optimal study for newly to build non-residential buildings (including schools) ordered by the Flemish government (VEA) [20]. Supplementary data are found in the work of Parys [125]. Since the latter cost data date from 2012, all prices are indexed to 2015 prices based on the ABEX-index [266], which indicates the evolution of construction costs in Belgium.
All costs include material and labor costs and are expressed in €2015.

C.1.1 Costs related to the building envelope

The cost data curves for the **insulation level of the opaque building** parts are plotted in *Figure C.1*.

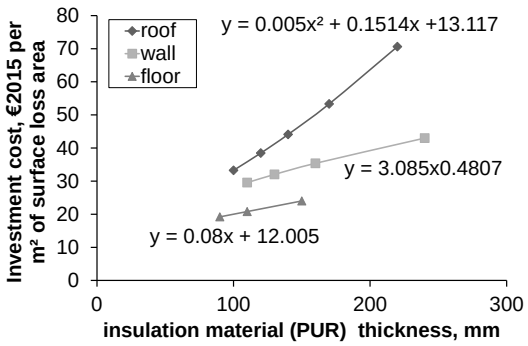

Figure C.1: Investment costs related to the insulation of the opaque building parts, expressed as a function of the insulation thickness (mm) [20].

The cost data for the **windows** is depicted in *Table C.1*. An aluminium window frame is used and a combination of fixed and tilt-and-turn windows is assumed.

Table C.1: Investment costs of the combination of tilt and turn, and fixed windows with an aluminium window frame [20].

Code -	$U_{window,glazing}$ W/(m^{2}K)	$U_{window,frame}$ W/(m^{2}K)	$I_{c,glazing}$ €per m^2 glazing surface	$I_{c,frame}$ €per m^2 window surface
W1	1.1	1.4	54.3	363.0
W2	0.6	0.8	102.3	418.0

The **air tightness level** of the building envelope is shown. This cost is determined by both the costs related to all efforts done to ensure air tightness of the building envelope (*Figure C.2* (a)) and the costs for the execution of the pressurisation test to evaluate the actual air tightness level of the building (*Figure C.2* (b)).

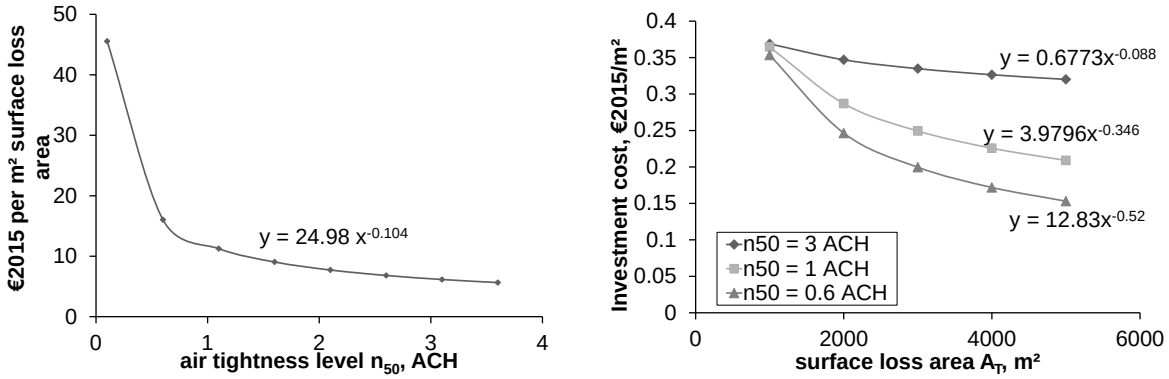

(a) costs air tightness

(b) cost pressurisation test

Figure C.2: Investment costs related to the air tightness of the building envelope [20].

The cost of the implemented **solar shading device** is summarised in *Table C.2*:

Table C.2: Investment costs of solar shading [125, 20].

Code	type of solar shading	control	$I_{c,shading+control}$ € per m^2 shaded window	$I_{c,sensor}$ € per sensor
S1	none	none	-	-
S2	slats	manual	161.7	-
S3	screens	automatically	287.3	274.9

C.1.2 Costs related to the installed HVAC system

The cost data curve for a **gas condensing boiler** is plotted in *Figure C.4*. As the size of the heating system depends strongly on the building's characteristics, a detailed sizing procedure according to *EN 12831* should be performed for each of the investigated building design variants. Detailed design and system sizing procedures are however too time consuming and therefore unfeasible to perform within this cost-optimal study. Therefore, load curves are determined that express the

design heat load capacity of the boiler as a function of the heat demand of the related building. The load curves obtained for this study (see *Figure C.3*) are based on the results of the HVAC system design calculations performed in the previous chapter *§ 6.2.1* .

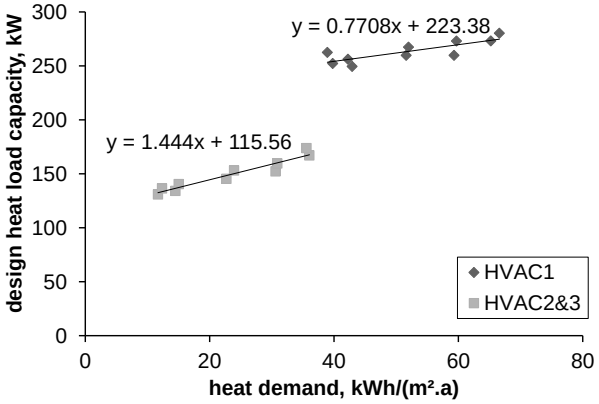

Figure C.3: Design heat load capacity of the gas condensing boiler based on the annual heat demand of the building for the three considered HVAC system configurations (see *§ 6.2.1*).

The investment costs are then expressed as a function of the design heat load capacity of the boiler according to the load curves as set by Royal HaskoningDHV [20]:

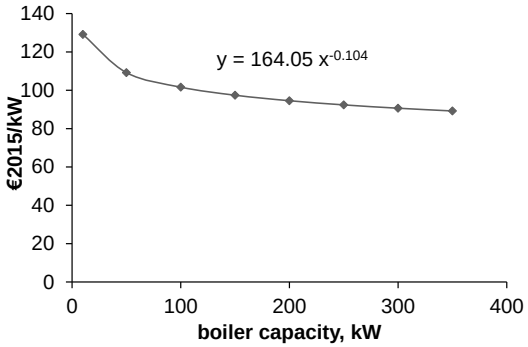

Figure C.4: Investment cost of a gas condensing boiler, expressed as a function of the boiler capacity (kW) [20].

Although the insulation level of the building affects the needed power and the size of the heat distribution and emission system, pragmatic, simplified cost data which express the costs as a function of the net surface floor area of the reference building (m^2), are used in line with the cost data as set by Royal HaskoningDHV which is used for the ongoing cost-optimal study of non-residential buildings (including schools) ordered by the Flemish government (VEA) [20] (see in *Table C.3*).

Table C.3: Investment costs of the heat distribution, control and emission system, expressed as a function of the net surface floor area of the reference building [20].

Type	Measure	Price, €/m^2
control	zonal control	8.9
emission	radiator heating	26.1
	floor heating	29.5

For the ventilation system, cost data as set by Royal HaskoningDHV [20] is used as a reference: a price curve is used, including amongst others the costs for ventilation ducts, vents, fans, and - if present - heat recovery device as a function of the design ventilation flow rate $G_{a,vent}$ (*Figure C.5*). A different price curve is used for an exhaust or balanced mechanical ventilation system. Additionally, the price curve of a cross heat exchanger with a bypass is added.

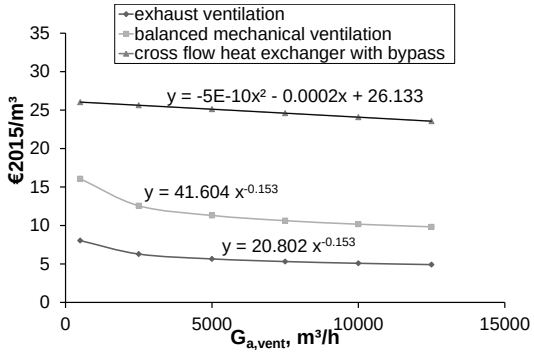

Figure C.5: Investment costs of a ventilation system, heat recovery device and bypass (if present), expressed as a function of the design capacity of the air handling unit [20].

Finally, the cost data curve for the **heating coils** are based on the information found in the work of Parys [125], indexed to 2015 prices. The results are plotted in *Figure C.6*, expressing the investment costs as a function of the heat capacity:

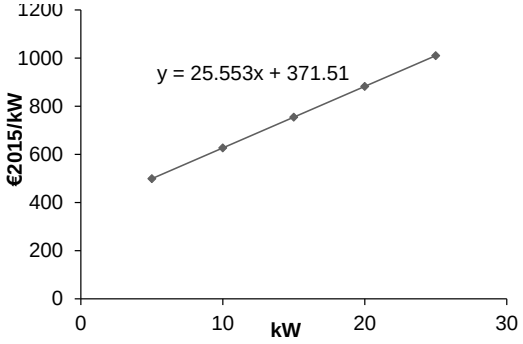

Figure C.6: Investment cost of a heating coil, expressed as a function of the heat capacity (kW) [125].

C.2 Pareto optimal design variants

As shown in *Table C.4* to *Table C.6*, all economic optima and most of the Pareto optimal solutions refer to cases without a shading device. This is caused by the high investment costs of louvers or screens and by the fact that no active cooling is assumed so the positive effect of the implementation of the shading devices on the cooling demand of the building is not validated in the cost-optimal study. In contrast, 45% of the considered building design variants with a WWR = 30% without shading are excluded from the study due to dissatisfying thermal comfort conditions, calculated according to *EN 15251* [47].

Table C.4: Pareto optimal design variants for the reference elementary school building with the main axis in East-West direction, with a **WWR =** 30% and **WWR =** 20%, and coupled to **HVAC1**. Some of the included measures appear on only one of the Pareto fronts (*i.e.* using either the original or refined calculation method). In that case, no data for $E_{H,p}$, NPC and E_c are added to the table. The economic optima, which are the measures with the lowest values for the NPC, are positioned at the top.

								original			refined		
	U_{wall} W/(m²K)	U_{floor} W/(m²K)	U_{roof} W/(m²K)	$U_{window,glazing}$ W/(m²K)	$U_{window,frame}$ W/(m²K)	shading -	n_{50} ACH	$E_{H,p}$ kWh$_{prim}$/(m².a)	NPC €2015/m²	E_c €/a	$E_{H,p}$ kWh$_{prim}$/(m².a)	NPC €2015/m²	E_c €/a
WWR = 30%	0.11	0.2	0.15	0.6	0.8	no	1	52.9	250.5	7189	67.1	265.5	8748
	0.16	0.2	0.11	0.6	0.8	no	1	51.9	253.9	7069	65.9	268.6	8748
	0.11	0.24	0.11	0.6	0.8	no	1	51.6	254.4	7028	65.6	269.1	8564
	0.11	0.24	0.11	0.6	0.8	no	0.6	50.6	255.8	6904	64.3	270.3	8416
	0.11	0.16	0.11	0.6	0.8	automatic screens	1	50.2	277.8	6860	64.3	292.7	8415
	0.11	0.16	0.11	0.6	0.8	automatic screens	0.6	49.2	279.2	6736	63.1	293.8	8262
WWR = 20%	0.11	0.16	0.15	1.1	1.4	no	1	58.1	243.2	7817	69.0	254.2	8975
	0.11	0.16	0.15	1.1	1.4	no	0.6	-	-	-	67.7	255.3	8644
	0.11	0.16	0.15	1.1	1.4	no	1	54.5	243.9	7383	66.2	255.9	8644
	0.11	0.16	0.11	1.1	1.4	no	1	-	-	-	65.7	256.2	8583
	0.11	0.16	0.15	1.1	1.4	no	0.6	53.5	245.2	7255	64.9	256.9	8486
	0.11	0.16	0.11	1.1	1.4	no	0.6	-	-	-	64.5	257.3	8434
	0.11	0.16	0.11	0.6	0.8	no	1	51.6	246.2	7028	62.8	257.7	8231
	0.11	0.16	0.11	0.6	0.8	no	0.6	50.6	247.5	6902	61.5	258.7	8073

Table C.5: Pareto optimal design variants for the reference elementary school building with the main axis in East-West direction, with a **WWR =** 30% and **WWR =** 20%, and coupled to **HVAC2**. Some of the included measures appear on only one of the Pareto fronts (*i.e.* using either the original or refined calculation method). In that case, no data for $E_{H,p}$, NPC and E_c are added to the table. The economic optima, which are the measures with the lowest values for the NPC, are positioned at the top.

								original			**refined**		
	U_{wall} W/(m^{2}K)	U_{floor} W/(m^{2}K)	U_{roof} W/(m^{2}K)	$U_{window,glazing}$ W/(m^{2}K)	$U_{window,frame}$ W/(m^{2}K)	**shading** -	n_{50} ACH	$E_{H,p}$ kWh$_{prim}$/(m^2.a)	NPC €2015/m^2	E_c €/a	$E_{H,p}$ kWh$_{prim}$/(m^2.a)	NPC €2015/m^2	E_c €/a
WWR = 30%	0.11	0.16	0.15	0.6	0.8	no	3	32.8	448.4	5270	-	-	-
	0.11	0.2	0.15	0.6	0.8	no	1	30.6	448.6	5002	40.5	457.7	5910
	0.16	0.2	0.11	0.6	0.8	no	1	29.9	452.3	4920	39.4	460.9	5775
	0.11	0.24	0.11	0.6	0.8	no	1	29.6	452.8	4882	38.9	461.3	5723
	0.11	0.24	0.11	0.6	0.8	no	0.6	29.0	454.6	4806	37.8	462.5	5586
	0.11	0.16	0.11	0.6	0.8	external louvers	3	28.6	468.5	4764	-	-	-
	0.11	0.16	0.11	0.6	0.8	automatic screens	1	28.4	476.4	4738	37.0	484.0	5490
	0.11	0.16	0.11	0.6	0.8	automatic screens	0.6	27.8	478.3	4666	35.9	485.3	5354
WWR = 20%	0.11	0.16	0.15	1.1	1.4	no	1	33.9	436.5	5406	-	-	-
	0.11	0.16	0.15	1.1	1.4	no	1	30.4	437.3	4987	39.6	445.4	5801
	0.11	0.16	0.11	0.6	0.8	no	1	28.5	440.7	4749	36.2	447.3	5394
	0.11	0.16	0.11	0.6	0.8	no	0.6	27.8	445.1	4670	35.1	451.0	5253

Table C.6: Pareto optimal design variants for the reference elementary school building with the main axis in East-West direction, with a **WWR =** 30% and **WWR =** 20%, and coupled to **HVAC3**. Some of the included measures appear on only one of the Pareto fronts (*i.e.* using either the original or refined calculation method). In that case, no data for $E_{H,p}$, NPC and E_c are added to the table. The economic optima, which are the measures with the lowest values for the NPC, are positioned at the top.

								original			refined		
	U_{wall} W/(m^{2}K)	U_{floor} W/(m^{2}K)	U_{roof} W/(m^{2}K)	$U_{window,glazing}$ W/(m^{2}K)	$U_{window,frame}$ W/(m^{2}K)	shading -	n_{50} ACH	$E_{H,p}$ kWh$_{prim}$/(m^2.a)	NPC €2015/m^2	E_c €/a	$E_{H,p}$ kWh$_{prim}$/(m^2.a)	NPC €2015/m^2	E_c €/a
WWR = 30%	0.11	0.20	0.15	1.1	1.4	no	3	38.4	452.6	5955	-	-	-
	0.11	0.16	0.15	0.6	0.8	no	3	32.3	452.8	5219	-	-	-
	0.11	0.2	0.15	0.6	0.8	no	1	30.2	453.0	4963	39.8	461.7	5828
	0.16	0.2	0.11	0.6	0.8	no	1	29.6	456.7	4884	38.7	464.9	5697
	0.11	0.24	0.11	0.6	0.8	no	1	29.3	457.3	4848	38.3	465.4	5647
	0.11	0.24	0.11	0.6	0.8	no	0.6	28.7	459.2	4775	37.2	466.6	5514
	0.11	0.16	0.11	0.6	0.8	slats	3	28.4	473.0	4735	-	-	-
	0.11	0.16	0.11	0.6	0.8	automatic screens	1	28.2	481.0	4711	36.5	488.2	5420
	0.11	0.16	0.11	0.6	0.8	automatic screens	0.6	27.6	482.9	4642	35.4	489.5	5289
WWR = 20%	0.11	0.16	0.15	1.1	1.4	no	1	33.4	440.8	5349	-	-	-
	0.11	0.16	0.15	1.1	1.4	no	1	30.1	441.7	4949	38.9	449.5	5722
	0.11	0.16	0.11	0.6	0.8	no	1	28.3	445.3	4721	35.7	451.4	5328
	0.11	0.16	0.11	0.6	0.8	no	0.6	27.6	449.7	4645	34.6	455.3	5191

D

List of Publications

Articles in international journals

1. **Wauman**, B., Saelens, D., Breesch, H., "The definition of representative boundary conditions for Flemish schools for use in energy assessment methods", *Energy and Buildings*, vol. 87, pp. 1-13, 2015

2. **Wauman**, B., Breesch, H., Saelens, D., "Evaluation of the accuracy of the implementation of dynamic effects in the quasi-steady-state calculation method for school buildings", *Energy and Buildings*, vol. 65, pp. 173-184, 2013

Articles in other academic journals

1. **Wauman**, B., Breesch, H., Saelens, D., "Evaluatie van de energieprestatie van passieve schoolgebouwen - Impact van gebouweigenschappen en randvoorwaarden (in Dutch)", TVVL-Magazine vol:41 issue:5, pp. 58-60, 2012

Peer reviewed papers at international conferences

1. Breesch, H., **Wauman**, B., Klein R., Versele, A., "Determination of boundary conditions in a district sports centre according to the passivehouse standard", in *Proceedings of the 11th REHVA World congress*, 16 - 19 June, (Tampere, Finland), 2013

2. **Wauman**, B., Saelens, D., Breesch, H., "Implementation of realistic boundary conditions - analysis of their effect on the net annual heating demand in passive schools", in *Proceedings of the 9th Nordic Symposium on Building Physics: Vol.3*, 29 May - 2 June, (Tampere, Finland), pp. 1237-1244, 2011

3. **Wauman**, B., Breesch, H., Saelens, D., "Energy performance of passive school buildings: an analysis of building properties and boundary conditions", in *Proceedings of 12th Conference of International Building Performance Simulation Association. Conference of International Building Performance Simulation Association*, 14-16 November, (Sydney, Aus-

tralia), pp. 1737-1744, 2011

4. Versele, A., Voet, J., Claes, K., **Wauman**, B., "Feasible sustainable building for a small development project in South East India", in *Proceedings of World Sustainable Building Conference*, 18 - 21 October, (Helsinki, Finland), 2011

5. **Wauman**, B., Klein, R., Van Loon, S., Baetens, R., Breesch, H., Saelens, D., "Determination of boundary conditions for passive schools: impact on net energy demand for heating and cooling", in *Proceedings of 1st Central European Symposium on building physics*, 13-15 September , (Cracow, Poland), pp. 455-462, 2010

6. **Wauman**, B., Saelens, D., Breesch, H., Poppe, J., Achten, K., Klein, R., Van Loon, S., "Determination of boundary conditions for passive schools: impact on heating/cooling demand (case study)", in *Tagungsband zur 14. Internationalen Passivhaustagung*, 28-29 May, (Dresden, Germany), pp. 239-244, 2010

7. Breesch, H., **Wauman**, B., Poppe, J., Van Loon, S., Baetens, R., Klein, R., Versele, A., Saelens, D., "Determination of boundary conditions for passive schools: impact on net energy demand for heating and cooling", in *Proceedings of the 9th Passive House Symposium*, 3 September, (Brussels, Belgium), pp. 1-8, 2010

Other publications and presentations

1. **Wauman**, B., Breesch, H., "Rapport: Ontwikkelen van specificieke randvoorwaarden voor scholen volgende de passiefhuisstandaard (in Dutch)", Studie in opdracht van AGIOn, 11 January, 2010

E

Curriculum Vitae

Barbara Wauman

Personal information

Date of birth:	July 4, 1982
Place of birth:	St-Niklaas (Belgium)
Nationality:	Belgian
Gender:	female
Family:	Partner Olivier Rombaut, 2 children (Cis Rombaut °2011, Mon Rombaut °2013)
Contact:	barbarawauman@hotmail.com

Education

2004 - 2005	Prevention advisor (level 1) and Environmental coordinator (level A) DVO, Technology campus Ghent, Belgium
2000 - 2004	Master in Industrial Engineering (Building Engineering), University of Leuven, Technology campus Ghent, Belgium
1994 - 2000	Science-Mathematics Berkenboom Humaniora, St-Niklaas Belgium

Present and previous positions

2010 - 2015	present PhD researcher Building Physics Section, Department of Civil Engineering, University of Leuven, Belgium
2005 - 2010	Teaching assistant âĂŞ International Coordinator University of Leuven, Technology campus Ghent, Belgium

References

[1] I. V. S. Mullis, M. O. Martin, P. Foy, and A. Arora, "Results in Mathematics," tech. rep., Chestnut Hill, MA , USA, 2011.

[2] N. Warlop, S. Van Camp, and I. De Meyer, "Wiskundige geletterdheid bij 15 - jarigen (in Dutch)," tech. rep., Ghent University, division of didactics, 2012.

[3] G. Leemans, *De schoolgebouwenmonitor AGIOn (in Dutch)*. 2009.

[4] G. Leemans, "Monitoring the quality of school buildings in Belgium's Flemish community," *CELE Exchange, Vol.2009 Issue 8*, p. 9, 2009.

[5] OECD, "Education at a Glance," tech. rep., OECD, 2004.

[6] G. Leemans and H. von Ahlefeld, "Understanding school building policy and practice in Belgium's Flemish community." 2013.

[7] F. De Deene, K. Loncke, T. Daems, and A. Martens, "Energiegebruik en energiebesparingspotentieel in de basis- en secundaire scholen in Vlaanderen (in Dutch)," 2001.

[8] J. Coolen and K. Knuysen, *Energiezorg in scholen (in Dutch)*. 2007.

[9] Vlaamse Overheid, *Energy use in Flemisch schools in 2005, climate corrected*. Brussels, Belgium: Die Keure, 2007.

[10] M. Stranger, K. D. Brouwere, R. Swinnen, R. Bormans, J. Lauwers, D. Poelmans, and L. Verbeke, "Binnenlucht in Basisscholen (BIBA) (in Dutch)," tech. rep., dienst Milieu & Gezondheid van het departement Leefmilieu, Natuur en Energie (LNE) en team Milieugezondheidszorg van het agentschap Zorg en Gezondheid, Mol, Belgium, 2010.

[11] H. Hens, S. Muyldermans, and W. Sarens, "Energy consumption, thermal comfort and indoor air quality in schools," in *25th AIVC conference 'Ventilation and retrofitting'*, no. 2003, (Prague, Czech Republic), pp. 1–6, 2004.

[12] "http://www.gezondescholen.eu/sites/default/files/cvgs_onderzoek_binnenklimaat_scholen_benelux_2013.pdf."

[13] NBN EN 13779, *Ventilation for non-residential buildings - Performance requirements for ventilation and room-conditioning systems (in Dutch)*. 2010.

[14] "www.lekkerfris.be," *(Date accessed: 2014-04-20)*.

[15] M. Stranger, S. Verbeke, J. Laverge, D. Wuyts, J. Lauwers, K. D. Brouwere, L. Verbeke, D. Poelmans, F. Boonen, A. Janssens, and B. Ingelaere, "Clean air, low energy (2012/MRG/R/363)," tech. rep., Environment, Nature and Energy Department (LNE) and Flemisch Energy Agency (VEA), Mol, Belgium, 2012.

[16] D. Stael, L. Van den Bossche, and A. Janssens, "De luchtkwaliteit in Vlaamse scholen (in Dutch)," *be.passive 03*, pp. 49–50, 2010.

[17] EPBD, "EU, Directive 2002/91/EC of the European Parliaments and of the council of 16 December 2002 on the energy performance of buildings, Official Journal of the European Communities (L1)," 2002.

[18] EPBD, "EU, Directive 2010/31/EU of the European Parliament and of the Council of 19 May 2010 on the energy performance of buildings (recast)," 2010.

[19] W. V. Roelens, T. V. Jonckheere, and K. V. De Baets, "Cijferrapport energieprestatieregelgeving - Procedures en resultaten, geometrische en karakteristieken van het Vlaamse gebouwbestand - periode 2006 - 2012 (in Dutch)," Tech. Rep. April, Vlaams Energie Agentschap (VEA), 2012.

[20] VEA, "EPB-cijfers en statistieken voor EPB-aanvragen ingediend t/m eind 2014 (in Dutch)," tech. rep., 2015.

[21] "B.S.07/12/2007 Decreet betreffende energieprestaties in scholen," 2007.

[22] VEA, "Annex VI Bepalingsmethode van het peil van primair energieverbruik van kantoor- en schoolgebouwen (in Dutch)," 2011.

[23] VEA, "Annex V Bepalingsmethode van het peil van primair energieverbruik van woongebouwen," 2014.

[24] J. Van der Veken, J. Creylman, and T. Lenaerts, “Studie naar kostenoptimale niveaus van de minimumeisen inzake energieprestaties van nieuwe residentiële gebouwen (in Dutch),” Tech. Rep. april, Kenniscentrum Energie, Thomas More Kempen/KU Leuven, Geel, Belgium, 2013.

[25] M. E. De Deygere and E. I. Troch, “Studie naar kostenoptimale energieprestatie-eisen bij niet-residentiële gebouwen (in Dutch),” tech. rep., Vlaams Energie Agentschap (VEA), Brussel, België, 2013.

[26] G. Pernigotto, *Evaluation of building envelope energy performance through extensive simulation and parametrical analysis*. Phd, University of Padova, Italy, 2013.

[27] J. Van der Veken, D. Saelens, G. Verbeeck, and H. Hens, “Comparison of steady-state and dynamic energy simulation programs,” in *International Buildings IX ASHRAE conference on the performance of exterior envelopes of whole buildings*, (Clearwater Beach, Florida, USA), p. 11, 2004.

[28] H. Van Dijk, M. Spiekman, and P. De Wilde, “A monthly method for calculation energy performance in the context of European building regulations,” in *9th International IBPSA Conference*, (Montreal, Canada), pp. 255–262, 2005.

[29] B. Poel, “Energy performance assessment for existing non residential buildings (EPA-NR - EIE/04/125/S07.38651),” tech. rep., Intelligent Energy Europe (EIE), Arnhem, The Netherlands, 2007.

[30] G. Kokogiannakis, *Support for the Integration of Simulation in the European Energy Performance of Buildings Directive*. Phd, University of Strathclyde, 2008.

[31] T. Kalema, G. Johannesson, P. Pylsy, and P. Hagengran, “Accuracy of energy analysis of buildings: a comparison of a monthly energy balance method and simulation methods in calculating the energy consumption and theeffect of thermal mass,” *Journal of Building Physics*, vol. 32, pp. 101–130, Oct. 2008.

[32] J. Jokisalo and J. Kurnitski, “Performance of EN ISO 13790 utilisation factor heat demand calculation method in a cold climate,” *Energy and Buildings*, vol. 39, pp. 236–247, Feb. 2007.

[33] V. Corrado and E. Fabrizio, “A simplified calculation method of the annual energy use for space heating and cooling: Assessment of the dynamic parameters for the Italian building stock and climate,” *Building Physics and Building Engineering*, pp. 645–654, 2006.

[34] V. Corrado and E. Fabrizio, “Assessment of building cooling energy need through a quasi-steady state model: Simplified correlation for gain-loss mismatch,” *Energy and Buildings*, vol. 39, pp. 569–579, May 2007.

[35] M. Sofic, A. Korjenic, and T. Bednar, “Quantification of safety factors for simplified heating and cooling demand calculation methods for Vienna,” *Building Simulation*, vol. 4, pp. 189–204, May 2011.

[36] H. A. Bohez and S. A. Feys, “Exploring the spatial dimension of ’brede scholen’ or community schools in Flanders,” 2014.

[37] ISO, *Energy performance of buildings - calculation of energy use for space heating and cooling ISO/FDIS 13790:2007(E)*. 2008.

[38] T. Loga, C. Kahlert, M. Laidig, and G. Lude, *Räumlich und zeitlich eingeschränkte Beheizung: Korrekturfaktoren zur Berücksichtigung in stationären Energiebilanzverfahren*. Darmstadt, Germany: Institut Wohnen und Umwelt GMBH, 1. auflage ed., 1999.

[39] I. Korolija, *Heating, ventilating and air-conditioning system energy demand coupling with building loads for office buildings*. Phd, De Montfort University, Leicester, UK, 2011.

[40] W. Parys, H. Hens, and D. Saelens, “Impact of refined HVAC systems efficiency determination on EPR energy calculations,” in *9th International Conference on System Simulation in Buildings*, vol. 2, (Liege, Belgium), pp. 1–17, 2014.

[41] L. Peeters, J. Van der Veken, H. Hens, L. Helsen, and W. D’haeseleer, “Control of heating systems in residential buildings: Current practice,” *Energy and Buildings*, vol. 40, pp. 1446–1455, Jan. 2008.

[42] J. Cho, S. Shin, J. Kim, and H. Hong, “Development of an energy evaluation methodology to make multiple predictions of the HVAC&R system energy demand for office buildings,” *Energy and Buildings*, vol. 80, pp. 169–183, Sept. 2014.

[43] DIN V 18599:2007 Part 1-10, “Energy efficiency of Building,” 2007.

[44] NEN 7120, *Energy Performance of buildings - Determination method*. No. april 2011, 2011.

[45] EN 15316-1, *Heating systems in buildings - Method for calculation of system energy requirements and system efficiencies - Part 1: General*. 2007.

[46] EN 124646-1, *Light and lighting - Lighting of work places - Part 1: Indoor work places*. 2003.

[47] EN 15251, *Indoor environmental input parameters for design and assessment of energy performance of buildings addressing air quality, thermal environment, lighting and acoustics*. 2007.

[48] ISO 7730, *Ergonomics of the thermal environment - Analytical determination and interpretation of themal comfort using calculation of the PMV and PPD indices and local thermal comfort criteria*. Aug. 2005.

[49] EN 15316-2-1, *Heating systems in buildings - Method for calculation of system energy requirements and system efficiencies - Part 2-1: Space heating emission systems*. 2007.

[50] M. Deurinck, *Towards more reliable energy saving predictions in the residential building sector*. Phd, KU Leuven, Belgium, 2015.

[51] W. Cyx, N. Renders, M. Van Holm, and S. Verbeke, "IEE TABULA - Typology approach for building stock energy assessment," Tech. Rep. August 2011, Flemish Institue for Technological Research NV (VITO), Mol, Belgium, 2011.

[52] S. P. Corgnati, E. Fabrizio, M. Filippi, and V. Monetti, "Reference buildings for cost optimal analysis: Method of definition and application," *Applied Energy*, vol. 102, pp. 983–993, Feb. 2013.

[53] A. Brandão de Vasconcelos, M. D. Pinheiro, A. Manso, and A. Cabaço, "A Portuguese approach to define reference buildings for cost-optimal methodologies," *Applied Energy*, vol. 140, pp. 316–328, Feb. 2015.

[54] M. Spiekman, S. Alvarez, M. Citterio, P. D'Herdt, H. Erhorn, and H. Erhorn-Kluttig, "Reference buildings for EP calculation studies (ASIEPI WP2)," tech. rep., 2009.

[55] S. Attia, A. Evrard, and E. Gratia, "Development of benchmark models for the Egyptian residential buildings sector," *Applied Energy*, vol. 94, pp. 270–284, June 2012.

[56] E. G. Dascalaki, K. G. Droutsa, C. a. Balaras, and S. Kontoyiannidis, "Building typologies as a tool for assessing the energy performance of residential buildings - A case study for the Hellenic building stock," *Energy and Buildings*, vol. 43, pp. 3400–3409, Dec. 2011.

[57] I. Ballarini, S. P. Corgnati, V. Corrado, and N. Talà, "Definition of building typologies for energy investigations on residential sector by TABULA IEE-project: Application to Italian case studies," in *RoomVent 2011 - 12th International conference on air distribution in rooms*, (Trondheim, Norway).

[58] J. Kragh and K. Wittchen, "Development of two Danish building typologies for residential buildings," *Energy and Buildings*, vol. 68, pp. 79–86, Jan. 2014.

[59] P. Schwehr and R. Fischer, "Building typology and morphology of Swiss multi-family homes 1919 - 1990," Tech. Rep. January, International Energy Agency (IEA), Energy Conservation in Buildings and Community Systems (IEA ECBCS) program Annex 50, Horw, Switzerland, 2010.

[60] A. van den Dobbelsteen, *The Sustainable Office - an exploration of the potential for factor 20 environmental improvement of office accomodation*. Phd, Technical University of Delft, The Netherlands, Technical University of Delft, The Netherlands, 2004.

[61] BMVBS, "Typologie und Bestand beheizter Nichtwohngebäude in Deutschland," Tech. Rep. 16, BMVBS-Online-Publikation 16/2011, 2011.

[62] M. Deru, K. Field, D. Studer, K. Benne, B. Griffith, P. Torcellini, B. Liu, M. Halverson, D. Winiarski, and M. Rosenberg, "Commercial reference building models of the national building stock," Tech. Rep. February 2011, National Laboratory of the US Departement of Energy (NREL), Colorado, USA, 2011.

[63] J. Kneifel, "Life-cycle carbon and cost analysis of energy efficiency measures in new commercial buildings," *Energy and Buildings*, vol. 42, pp. 333–340, Mar. 2010.

[64] P. Hernandez, K. Burke, and J. O. Lewis, "Development of energy performance benchmarks and building energy ratings for non-domestic buildings: An example for Irish primary schools," *Energy and Buildings*, vol. 40, pp. 249–254, Jan. 2008.

[65] J. C. Coolen, G. C. De Bruyn, S. C. Wuyts, E. C. Vanvuchelen, W. E. Coppye, K. E. Achten, and R. E. De Coninck, "Handleiding energiezuinige nieuwbouw voor lokale overheden Deel 2: Maatregelenpakketten (in Dutch)," tech. rep., Vlaamse Overheid, Ministerie van Leefmilieu, Natuur en Energy (LNE), Afdeling Milieu-Informatie en Subsidiëring, Brussels, Belgium, 2007.

[66] S. Pless, P. Torcellini, and N. Long, "Technical support document: development of the advanced energy design guide for K-12 schools - 30 % energy savings technical support document," 2007.

[67] ASHRAE, *Advanced energy design guide K-12 school buildings*. 2007.

[68] U.S. Energy Information Administration (EIA), "2003 Commercial buildings energy consumption survey (CEBCS)," 2003.

[69] B. Su, "School Design and Energy Efficiency," *World Academy of Science, Engineering and Technology*, vol. 5, pp. 423–427, 2011.

[70] D. Curtis, R. Bowen, M. Patel, G. Ruscica, P. Lazzerini, M. De Renzio, S. Zabot, D. Guarino, and A. Cellie, "IEA Annex 15: Energy Efficiency in Schools," tech. rep., International Energy Agency (IEA), Torino, Italy, 1991.

[71] I. Korolija, L. Marjanovic-Halburd, Y. Zhang, and V. I. Hanby, "UK office buildings archetypal model as methodological approach in development of regression models for predicting building energy consumption from heating and cooling demands," *Energy and Buildings*, vol. 60, pp. 152–162, May 2013.

[72] L. Karopka, A. Klöffel, I. Therburg, R. Kopetzky, T. Weber, and S. Kunkel, "Benchmarks für die Energieeffizienz von Nichtwohngebäuden," Tech. Rep. 09, Bundesministerium für Verkehr, Bau and Stadtentwicklunb (BMVBS) - Bundesinstitut für Bau-, Stadt- und Raumforschung (BBSR), Berlin, Germany, 2009.

[73] W. Tian and R. Choudhary, "A probabilistic energy model for non-domestic building sectors applied to analysis of school buildings in greater London," *Energy and Buildings*, vol. 54, pp. 1–11, Nov. 2012.

[74] A. F. Van Bogaert, *Logica en actie in de scholenbouw (in Dutch)*. 1972.

[75] G. Châtel, M. Van Den Driessche, C. Van Gerrewey, T. Vanmeirhaeghe, and B. Verschaffel, *De school als ontwerpopgave School architectuur in Vlaanderen (1995-2005) (in Dutch)*. 2006.

[76] G. Lathouwers and I. Van Heddegem, *Bouw wijs: bouwwijzer voor scholen (in Dutch)*. 2008.

[77] GO!, AGIOn, and Evr-Architecten, *Naar een inspirerende leeromgeving, instrument voor duurzame scholenbouw (in Dutch)*. 2010.

[78] K. Borret, G. Lathouwers, P. Mahieu, A. Malliet, S. Troch, M. Van Den Driessche, and I. Van Heddegem, *De school als bouwheer: gids voor kwaliteitsvolle schoolarchitectuur (in Dutch)*. 2010.

[79] W. P. Feist, O. Kah, R. Pfluger, and P. Heidenreich-Herrman, *Protokollband: Passivhaus-Schulen*. 1 ed., 2006.

[80] C. Marrecau and K. Meyers, *Passiefscholen (in Dutch)*. 2007.

[81] H. Neuckermans, H. Vandevyvere, and A. Van Geystelen, *Onderzoek recente schoolgebouwen in Europa: een stand van zaken (in Dutch)*. 2006.

[82] A. Malliet, C. Robberechts, M. Van Damme, and T. Hens, *Dossier 1: Scholenbouw (in Dutch)*. Brussel, Belgium: Vlaamse Bouwmeester, 2010.

[83] M. Shahrestani, R. Yao, and G. K. Cook, "A review of existing building benchmarks and the development of a set of reference office buildings for England and Wales," *Intelligent Buildings International*, vol. 6, pp. 41–64, Sept. 2014.

[84] Y. Steijns and A. Koutamanis, "A briefing approach to Dutch school design." 2005.

[85] "B.S.09/11/2007 Besluit van de Vlaamse Regering houdende vaststelling van de regels die de behoefte aan nieuwbouw of uitbreiding bepalen en van de fysische en financiële normen voor de schoolgebouwen, internaten en centra voor leerlingenbegeleiding," 2007.

[86] Nationaal Waarborgfonds, "Het gebouwenpark van het gesubsidieerd onderwijs in België. Telling op datum van 1 mei 1986. Raming van behoeften, programmatievoorstel (in Dutch)," 1986.

[87] DIGO, "Scholenbouw in de Vlaamse Gemeenschap. De behoefte aan scholenbouw binnen het gesubsidieerd vrij en officieel onderwijs," 1998.

[88] G. Leemans, "De schoolgebouwenmonitor 2013 - Indicatoren voor de kwaliteit van schoolgebouwen in Vlaanderen (in Dutch)," tech. rep., AGIOn, Brussel, Belgium, 2014.

[89] R. Smet, A. Vannecke, and E. Baeten, *Historiek van het technisch en beroepsonderwijs (1830-1990)*. 2002.

[90] EN 12831, *Heating systems in buildings - Method for calculation of the design heat load*. 2003.

[91] ANSI/ASHRAE Standard 55, *Thermal environmental conditions for human occupancy*. 2013.

[92] FOD, "Koninklijk Besluit 4 juni 2012 - Koninklijk besluit betreffende de thermische omgevingsfactoren B.S. 27 oktober 1934 wet beroepsuitoefeningsverbod," 2012.

[93] Vlaamse Overheid, "Besluit 11 juni 2004 - Besluit van de Vlaamse Regering houdende maatregelen tot bestrijding van de gezondheidsrisico's door verontreiniging van het binnenmilieu," 2004.

[94] L. Bellia, A. Boerstra, F. V. Dijken, E. Ianniello, G. Lopardo, F. Minichiello, and P. Romagnoni, *Indoor Environment and Energy Efficiency in Schools*. Brussels, Belgium: Federation of European Heating, Ventilation, and Air-condition Associations (REHVA), guidebook ed., 2010.

[95] "DBFM Bijlage 10 Outputspecificaties (not published)," 2010.

[96] Agentschap NL, "Programma van eisen Frisse Scholen," Tech. Rep. april, Ministerie van Binnenlandse Zaken en Koninkrijksrelaties, Utrecht, Nederland, 2012.

[97] Departement for Education and Skills, *Building Bulletin 87 - Guidelines for environmental design in schools*, vol. 1. 2003.

[98] "https://www.bloso.be/Pages/Home.aspx," *(Date accessed: 2014-04-20)*.

[99] NEN 2916, *Energieprestatie van utiliteitsgebouwen - Bepalingsmethode*. 2004.

[100] Z. Bakó-Biró, D. Clements-Croome, N. Kochhar, H. Awbi, and M. Williams, "Ventilation rates in schools and pupils' performance," *Building and Environment*, vol. 48, pp. 215–223, Feb. 2012.

[101] P. Wargocki and D. P. Wyon, "Effects of HVAC on student performance," Tech. Rep. October, ASHRAE, 2006.

[102] P. Wargocki and D. Wyon, "The effects of moderately raised classroom temperatures and classroom ventilation rate on the performance of schoolwork by children (RP-1257)," *HVAC and R Research*, vol. 13, pp. 193–220, Mar. 2007.

[103] P. Wargocki and D. P. Wyon, "The effects of outdoor air supply rate and supply air filter condition in classrooms on the performance of schoolwork by children (RP-1257)," *HVAC&R Research*, vol. Vol.13, No, no. March 2007, pp. 165–191, 2011.

[104] D. Clements-Croome, H. Awbi, Z. Bakó-Biró, N. Kochhar, and M. Williams, "Ventilation rates in schools," *Building and Environment*, vol. 43, pp. 362–367, Mar. 2008.

[105] U. Haverinen-Shaughnessy, D. J. Moschandreas, and R. J. Shaughnessy, "Association between substandard classroom ventilation rates and students' academic achievement.," *Indoor air*, vol. 21, pp. 121–31, Apr. 2011.

[106] FOD, "Algemeen reglement voor de arbeidsbescherming Titel II - Algemene bepalingen betreffende de arbeidshygiëne alsmede de veiligheid en de gezondheid van arbeiders," 1947.

[107] Education Funding Agency, *Building Bulletin 101 - Ventilation of school buildings*. No. July, version 1. ed., 2006.

[108] E.-R. Recknagel, Sprenger, and Schramek, *Taschenbuch für Heizung + Klimatechnik*. München, Germany: Oldenbourg Industrieverlag GmbH, 74. auflag ed., 2009.

[109] NPR 1090, "Ventilatie van schoolgebouwen - voorbeelden van oplossingen voor schoolgebouwen (in Dutch)," 2010.

[110] PHI, "Passivhaus Projektierungs Paket (PHPP) version 2007."

[111] ASHRAE, "Thermal Environmental Conditions for Human Occupancy ANSI/ASHRAE Standard 55-2013," 2013.

[112] D. Loe, N. Watson, E. Rowlands, K. Mansfield, and B. Venning, *Building Bulletin 90 - Lighting design for schools*. 1999.

[113] K. Flodberg, *Very low energy office buildings in Sweden - simulations with low internal heat gains*. Licentiate thesis, Lund Unversity, Sweden, Lund, Sweden, 2012.

[114] "www.passivhausprojekte.de," *(Date accessed: 2014-02-13)*.

[115] B. Givoni, "Effectiveness of mass and night ventilation in lowering the indoor daytime temperatures. Part I: 1993 experimental periods," *Energy and Buildings*, vol. 28, pp. 25–32, Aug. 1998.

[116] L. Yang and Y. Li, "Cooling load reduction by using thermal mass and night ventilation," *Energy and Buildings*, vol. 40, pp. 2052–2058, Jan. 2008.

[117] S. Winkel, O. Kah, T. Schulz, J. Schnieders, Z. Bastian, and B. Kaufmann, "Leitfaden für energie- effiziente Bildungsgebäude," tech. rep., Passiv Haus Institut (PHI), Darmstadt, Germany, 2010.

[118] NBN EN ISO 13786, "Thermal performance of building components - Dynamic thermal characteristics - Calculation methods," 2008.

[119] "www.energiesparen.be/epb/welkeeisen," *(Date accessed: 2014-04-20)*.

[120] NBN D 50-001, *Ventilation systems for housings*. 1991.

[121] ASHRAE, *ASHRAE-IESNA. Standard 90.1-2004: Energy standard for buildings except low-rise residential buildings.* 2004.

[122] CIBSE, *Heating, ventilating, air conditioning and refrigeration - CIBSE Guide B*. London, UK: Page Bros. (Norwich) Ltd., 2005.

[123] Passiefhuis-Platform, “Technische installatiewijzer (in Dutch),” 2011.

[124] A. Muzaffar, *Optimization of heating, ventilation, and air-conditioning (HVAC) system configurations*. Phd, University of Engineering & Technology Taxila, Pakistan, 2013.

[125] W. Parys, *Cost optimization of cellular office buildings based on building energy simulation*. Phd, KU Leuven, Belgium, Leuven, Belgium, 2013.

[126] A. Boerstra and J. Kurnitski, “Indoor climate and ventilation of schools,” tech. rep., REHVA, Helsinki, Finland, 2007.

[127] A. Knotzer, “School Vent Cool - Ventilation , cooling and strategies for high performance school renovations,” Tech. Rep. March, AEE - Instute for Sustainable Technologies (AEE INTEC), 2013.

[128] S. J. Emmerich, W. S. Dols, and J. W. Axley, “Natural ventilation review and plan for design and analysis tools,” tech. rep., National Institute of Standards and Technology (NIST), Colorado, USA, 2001.

[129] H. Versteeg, “Onderzoek naar de kwaliteit van het binnenmilieu in basisscholen (in Dutch),” tech. rep., VROM, OCW, SZW en VWS, 2007.

[130] O. Kah, “Schulen im Passivhaus-Standard: Planungsaspekte,” in *Passivhaus-Schulen, Protokollband Nr. 33 des Arbeitskreises kostengünstige Passivhäuser, Phase III*, Darmstadt, Germany: Passivhaus Institut, PHI, 2006.

[131] L. Perez-Lombard, J. Ortiz, and I. R. Maestre, “The map of energy flow in HVAC systems,” *Applied Energy*, vol. 88, pp. 5020–5031, Dec. 2011.

[132] VEA, “Bijlage XII: Systeemeisen (in Dutch),” 2011.

[133] P. Schild and M. Mysen, “Technical Note AIVC 65: Recommendations on specific fan power and fan system efficiency,” tech. rep., 2009.

[134] J. T. M. Rosbach, M. Vonk, F. Duijm, J. T. van Ginkel, U. Gehring, and B. Brunekreef, “A ventilation intervention study in classrooms to improve indoor air quality: the FRESH study.,” *Environmental health : a global access science source*, vol. 12, p. 110, Jan. 2013.

[135] G. E. Stranger M., “Can a ventilation system create a healthier classroom indoor environment in Belgian schools?,” in *12th International Conference on Indoor Air Quality and Climate*, (Austin Texas, USA), 2011.

[136] F. Tariku, S. Cornick, H. Hens, B. Blocken, J. Carmeliet, M. De Paepe, and A. Janssens, “IEA Annex 41: Moisture Engineering Subtask 3 - Boundary Conditions and Whole Building HAM Analysis,” tech. rep., International Energy Agency (IEA), 2007.

[137] W. R. Ryckaert, C. Lootens, J. Geldof, and P. Hanselaer, “Criteria for energy efficient lighting in buildings,” *Energy and Buildings*, vol. 42, pp. 341–347, Mar. 2010.

[138] BSI, “Code of practice for daylighting BS 8206-2,” 2008.

[139] EN 15193, *Energy performance of buildings - Energy requirements for lighting*. 2008.

[140] CEN, *CEN/TR 15615 Explanation of the general relationship between various European standards and the Energy Performance of Buildings Directive (EPBD) - Umbrella Document.* 2006.

[141] B. van Kampen, “CENSE Final Public Report: Leading the CEN standards on energy performance of buildings to practice,” tech. rep., 2010.

[142] H. van Dijk and M. Spiekman, “Energy performance of buildings: Outline for harmonised EP procedures (ENPER - TEBUC),” tech. rep., TNO Building and Construction Research, Delft, The Netherlands, 2004.

[143] K. Arkesteijn, J. Hogeling, and D. van Dijk, “CENSE P90 - The use of the CEN standards to support the EPBD in the EU Member States,” tech. rep., 2008.

[144] B. Wauman, R. Klein, H. Breesch, S. Van Loon, R. Baetens, and D. Saelens, “Determination of boundary conditions for passive schools : impact on net energy demand for heating and cooling,” in *1st Central European Symposium on Building Physics (CESBP), 13-15 September*, (Cracow, Poland), pp. 335–342, 2010.

[145] PASSYS, “Final report of the simplified design tools,” tech. rep., Commission of the European Communities, Directorate General XII, Brussel, België, 1989.

[146] L. Bourdeau and C. Buscarlet, “PASSYS - Development of simplified design tools,” tech. rep., Centre scientifique et technique du batiment (CSTB), Valbonne, France, 1993.

[147] H. van Dijk and C. Arkesteijn, “Windows and space heating requirements: Parameter studies leading to a simplified calculation method,” tech. rep., International Energy Agency (IEA) ECBCS - Annex XII, Delft, The Netherlands, 1987.

[148] Carbon Trust, “Schools - Learning to improve energy efficiency (CTV019),” 2012.

[149] J. Xing, J. Chen, and J. Ling, “Energy consumption of 270 schools in Tianjin, China,” *Frontiers in Energy*, Mar. 2015.

[150] N. L. Tchervilov and N. G. Kaloyanov, “Study on energy efficiency in buildings in the contracting parties of the energy community - Final report,” Tech. Rep. February, Energy Saving International AS (ENSI), 2012.

[151] EN 15316-2-3, *Heating systems in buildings - Method for calculation of system energy requirements and system efficiencies - Part 2-3 : Space heating distribution systems*. 2007.

[152] EN 15316-4-1, *Heating systems in buildings. Method for calculation of system energy requirements and system efficiencies. Space heating generation systems, combustion systems (boilers)*. 2008.

[153] EN 15316-4-2, *Heating systems in buildings - Method for calculation of system energy requirements and system efficiencies - Part 4-2: Space heating generation systems, heat pump systems*. 2008.

[154] EN 15316-4-3, *Heating systems in buildings - Method for calculation of system energy requirements and system efficiencies - Part 4-3 : Heat generation systems , thermal solar systems*. 2007.

[155] M. Shahrestani, R. Yao, and G. K. Cook, “Characterising the energy performance of centralised HVAC&R systems in the UK,” *Energy and Buildings*, vol. 62, pp. 239–247, July 2013.

[156] G. Kokogiannakis, P. Strachan, and J. Clarke, “Comparison of the simplified methods of the ISO 13790 standard and detailed modelling programs in a regulatory context,” *Journal of Building Performance Simulation*, vol. 1, pp. 209–219, Dec. 2010.

[157] I. Korolija, Y. Zhang, L. Marjanovic-Halburd, and V. I. Hanby, “Regression models for predicting UK office building energy consumption from heating and cooling demands,” *Energy and Buildings*, vol. 59, pp. 214–227, Apr. 2013.

[158] D. Crawley, J. Hand, M. Kummert, and B. Griffith, “Contrasting the capabilities of building energy performance simulation programs (version 1.0),” Tech. Rep. July, US Department of Energy, University of Strathclyde Energy Systems Research Unit, University of Wisconsin Solar Energy Laboratory, National Renewable Energy Laboratory, Crawley2005, 2005.

[159] D. Crawley, J. Hand, M. Kummert, and B. Griffith, “Contrasting the capabilities of building energy performance simulation programs,” *Building and Environment*, vol. 43, no. 4, pp. 661–673, 2008.

[160] O. Zogou and A. Stamatelos, *Application of building energy simulation in the sizing and design optimization of an office building and its HVAC equipment*. Nova Science Publishers, Inc., 2009.

[161] S. Klein, W. Beckham, and D. Mitchell, “TRNSYS 17.1: A Transient System Simulation Program, Solar Energy Laboratory, University of Wisconsin, Madison, USA,,” 2010.

[162] G. Mitalas and J. Arseneault, “FORTRAN IV Program to calculate z-transfer functions for the calculation of transient heat transfer through walls and roofs.,” 1972.

[163] K. Chatziangelidis and D. Bouris, “Calculation of the distribution of incoming solar radiation in enclosures,” *Applied Thermal Engineering*, vol. 29, pp. 1096–1105, Apr. 2009.

[164] R. Judkoff and J. Neymark, “International Energy Agency building energy simulation test (BESTEST) and diagnostic method,” Tech. Rep. February, 1995.

[165] D. Saelens, *Enery performance assessment of single storey multiple-skin facades*. Phd, KU Leuven, Belgium, 2002.

[166] “Meteotest. Meteonorm versie 5.1 - Edition 2005.”

[167] NBN B 62-002, *Thermal performances of buildings - Calculation of thermal transmittances of building components and building elements - Calculation of transmission and ventilation heat transfer coefficients*. 2008.

[168] H. Hens, *Toegepaste bouwfysica en installaties in gebouwen: Binnenmilieu, energie, verwarming en ventilatie (in dutch)*. Acco, 2007.

[169] NBN EN ISO 13370, *Thermal performance of buildings - heat transfer via the ground - Calculation methods*. No. September, 2008.

[170] “B.S.28/12/2012 Tranmissiereferentiedocument - Berekening van de warmtedoorgangscoëfficiënt van wanden van gebouwen (U-waarde) en van gebouwen (H-waarde),” 2012.

[171] W. Parys, “Voorstudie zonwering in EPB-context (in Dutch),” tech. rep., KU Leuven, Belgium, 2009.

[172] S. De wit and G. Augenbroe, “Analysis of uncertainty in building design evaluations and its implications,” *Energy and Buildings*, vol. 34, pp. 951–958, Oct. 2002.

[173] I. A. MacDonald, *Quantifying the Effects of Uncertainty in Building Simulation*. Phd, University of Strathclyde, Glasgow, UK, 2002.

[174] Y.-J. Kim, S.-H. Yoon, and C.-S. Park, "Stochastic comparison between simplified energy calculation and dynamic simulation," *Energy and Buildings*, vol. 64, pp. 332–342, Sept. 2013.

[175] C. M. Clevenger and J. Haymaker, "The impact of the building occupant on energy modeling simulations," in *Joint International Conference on Computing and Decision Making in Civil and Building Engineering*, vol. 28, (Montreal, Canada), pp. 1–10, Department of Civil and Environmental Engineering, Stanford University, 2006.

[176] C. M. Clevenger, D. Ph, M. Asce, J. R. Haymaker, and M. Jalili, "Demonstrating the Impact of the Occupant on Building Performance," *Journal of Computing in Civil Engineering*, vol. vol.28, no. February, pp. 99–102, 2014.

[177] V. Corrado and H. E. Mechri, "Uncertainty and sensitivity analysis for building energy rating," *Journal of Building Physics*, vol. 33, pp. 125–156, June 2009.

[178] H. Brohus, P. Heiselberg, A. Simonsen, K. C. Sorensen, and C. Engineering, "Uncertainty of energy consumption assessment of domestic buildings," in *11th International IBPSA Conference*, (Glasgow, Schotland), pp. 1022–1029, 2009.

[179] J. Purdy and I. Beausoleil-Morrison, "The significant factors in modelling residential buildings," in *7th International IBPSA Conference, August 13-15*, (Rio de Janeiro, Brazil), pp. 207–214, 2001.

[180] A. S. Silva and E. Ghisi, "Uncertainty analysis of user behaviour and physical parameters in residential building performance simulation," *Energy and Buildings*, vol. 76, pp. 381–391, June 2014.

[181] J. C. Lam and S. A. M. C. M. Hui, "Sensitivity analysis of energy performance of office buildings," *Building and Environment*, vol. 31, no. I, pp. 27–39, 1996.

[182] F. Domínguez-Muñoz, J. M. Cejudo-López, and A. Carrillo-Andrés, "Uncertainty in peak cooling load calculations," *Energy and Buildings*, vol. 42, pp. 1010–1018, July 2010.

[183] M. Frankel, M. Heater, and J. Heller, "Sensitivity analysis : Relative impact of design , commissioning , maintenance and operational variables on the energy performance of office buildings," in *ACEEE Summer Study on Energy Efficiency in Buildings, August 12-17*, (Pacific Grove, CA, USA), pp. 52–64, 2012.

[184] L. Wang, P. Mathew, and X. Pang, "Uncertainties in energy consumption introduced by building operations and weather for a medium-size office building," *Energy and Buildings*, vol. 53, pp. 152–158, Oct. 2012.

[185] C. Demanuele, T. Tweddell, and M. Davies, "Bridging the gap between predicted and actual energy performance in schools," in *11th World Renewable Energy Congress*, no. September, (Abu Dhabi, UAE), pp. 1–6, 2010.

[186] AGIOn, "Ontwikkelen van specifieke randvoorwaarden voor scholen volgens de passiefhuisstandaard," tech. rep., AGIOn, Brussels, Belgium, 2010.

[187] M. S. De Wit, *Uncertainty in Predictions of Thermal Comfort in Buildings*. Phd, Technical University of Delft, The Netherlands, 2001.

[188] H. Breesch and A. Janssens, "Performance evaluation of passive cooling in office buildings based on uncertainty and sensitivity analysis," *Solar Energy*, vol. 84, pp. 1453–1467, Aug. 2010.

[189] C. J. Hopfe, *Uncertainty and sensitivity analysis in building performance simulation for decision support and design optimization*. Phd, Technical University of Eindhoven, Eindhoven, The Netherlands, 2009.

[190] S. Attia, E. Gratia, A. De Herde, and J. L. Hensen, "Simulation-based decision support tool for early stages of zero-energy building design," *Energy and Buildings*, vol. 49, pp. 2–15, June 2012.

[191] G. Verbeeck, *Optimisation of extremely low energy residential buildings*. Phd, KU Leuven, Belgium, Leuven, Belgium, 2007.

[192] A. Saltelli, K. Chan, and E. Scott, *Sensitivity analysis*. 2001.

[193] "SimLab - Sensitivity Analysis."

[194] M. Morris, "Factorial sampling plans for preliminary computational experiments.," *Technometrics*, vol. 33, pp. 161–174, 1991.

[195] A. Saltelli, M. Ratto, T. Andres, F. Campolongo, and J. Cariboni, *Global sensitivity analysis - The primer*. chichester, UK: John wiley & Sons, Ltd, 2008.

[196] F. Campolongo, J. Cariboni, and A. Saltelli, "An effective screening design for sensitivity analysis of large models," *Environmental Modelling & Software*, vol. 22, pp. 1509–1518, Oct. 2007.

[197] J.-M. Fürbringer and C. Roulet, "Comparison and combination of factorial and Monte-Carlo design in sensitivity analysis," *Building and Environment*, vol. 30, no. 4, pp. 505–519, 1995.

[198] B. Eisenhower, Z. O'Neill, S. Narayanan, V. A. Fonoberov, and I. Mezi, "Comparative study on uncertainty propagation in high performance building design," in *12th Conference of International Building Performance Simulation Association, November 14-16*, (Sydney, Australia), pp. 2785–2792, 2011.

[199] U.S. Environmental Protection Agency (EPA), "DataTrends Energy Use in Office Buildings," 2012.

[200] BBRI, "Kantoor2000 - Studie van energiegebruik en binnenklimaat van kantoren (in Dutch)," tech. rep., BBRI, 2001.

[201] B. Collard and F. Derny, *L'Eclairage dans les écoles*. Jambes, Belgique: Ministère de la Région Wallonne (DGTRE) - Service de l'Energie, 1999.

[202] I. Macdonald and P. Strachan, "Practical application of uncertainty analysis," *Energy and Buildings*, vol. 33, pp. 219–227, Feb. 2001.

[203] J. Van Dromme, S. Vanwelden, H. Breesch, and B. Wauman, *Evaluatie van de energieprestatie in schoolgebouwen: impact van de instellingen voor verwarming en buitenschools gebruik (in Dutch)*. Master thesis, KU Leuven, campus Ghent, 2013.

[204] B. Wauman, H. Breesch, and D. Saelens, "Energy performance of passive schools buildings - An analysis of building properties and boundary conditions," in *12th Conference of International Building Performance Simulation Association*, (Sydney, Australia), pp. 1737 – 1744, 2011.

[205] B. Wauman, H. Breesch, and D. Saelens, "Implementation of realistic boundary conditions : analysis of their effect on the net annual heating demand in passive schools," in *9th Nordic Symposium on Building Physics, May 29 - June 2*, no. Nen 1089, (Tampere, Finland), pp. 1237–1244, 2011.

[206] Eurydice, "Key Data on Learning and Innovation through ICT at School in Europe 2011," tech. rep., Education, Audiovisual and Culture Executive Agency (EACEA), Brussels, Belgium, 2011.

[207] B. Pynoo, S. Kerckaert, J. Eelen, and K. Goeman, "MICTIVO2012: Monitor voor ICT-integratie in het Vlaams onderwijs. Eindrapport OBPWO-project 11.02," tech. rep., Vlaam Ministerie van Onderwijs en Vorming, 2013.

[208] CEC, *Non-residential alternative calculation method (ACM)*. 2008.

[209] "National Calculation Methodology (NCM) modelling guide for buildings other than dwellings in England and Wales," Tech. Rep. January, Department for Communities and Local Government: London, London, UK, 2010.

[210] UCL and DGTRE, "Parameters om het benodigde vermogen voor verlichting te berekenen."

[211] B. Wauman, J. Poppe, S. Van Loon, R. Klein, K. Achten, H. Breesch, and D. Saelens, "Determination of boundary conditions for passive schools : impact on heating and cooling demand," in *14th International Passive House Conference* (P. H. Institut, ed.), (Dresden, Germany), pp. 1–6, 2010.

[212] H. Breesch, B. Wauman, J. Poppe, S. Van Loon, R. Baetens, R. Klein, A. Versele, and D. Saelens, "Determination of boundary conditions for passive schools: impact on net energy demand for heating and cooling," in *9th Passive House Symposium*, (Brussels, Belgium), pp. pp.1–8, 2010.

[213] J. Le Dréau, A. Dawod Selman, P. Heiselberg, and R. Lund Jensen, "Thermal Mass & Dynamic effects, Danish Building Regulation," Tech. Rep. 152, Aalborg University, Department of Civil Engineering, Aalborg, Denmark, 2013.

[214] E. van den Ham and M. Linssen, "Bepaling benuttigingsfactoren voor warmtebronnen en vrije koeling t.b.v. ontwerp NEN 2916 (in Dutch)," tech. rep., Vakgroep Utiliteitsbouw, sectie Bouwfysica, TU Delft, Delft, The Netherlands, 1992.

[215] A. Panek, J. Rucinska, and M. Mijakowski, "Adjustment of parameters used for calculation method applied in certification process in Poland," in *Central Europe Towards Sustainable Buildings (CESB)*, (Prague), 2010.

[216] B. Wauman, H. Breesch, and D. Saelens, "Evaluation of the accuracy of the implementation of dynamic effects in the quasi steady-state calculation method for school buildings," *Energy and Buildings*, vol. 65, pp. 173–184, 2013.

[217] J. Kurnitski, "Indoor air quality in schools - the principal survey and indoor climate measurements (in Finnish)," 1996.

[218] G. Oliveti, N. Arcuri, R. Bruno, and M. De Simone, "An accurate calculation model of solar heat gain through glazed surfaces," *Energy and Buildings*, vol. 43, pp. 269–274, Feb. 2011.

[219] N. Safer, *Modélisation des façades de type de double-peau équipées de protection solaires: approche multi-échelles*. Phd thesis, L'institut de sciences appliquées de Lyon, France, 2006.

[220] V. Corrado, E. Houcem, and E. Fabrizio, "Building energy performance assessment through simplified models: application of the ISO 13790 quasi-steady-state method," *Building Simulation*, pp. 79–86, 2007.

[221] T. Kalamees, J. Vinha, and J. Kurnitski, "Indoor humidity loads and moisture production in lightweight timber-frame detached houses," *Journal of Building Physics*, vol. 29, pp. 219–246, Jan. 2006.

[222] M. Deurinck, D. Saelens, and S. Roels, "Assessment of the physical part of the temperature takeback for residential retrofits," *Energy and Buildings*, vol. 52, pp. 112–121, Sept. 2012.

[223] B. Wauman, H. Breesch, and D. Saelens, "Evaluation of the Energy Performance of Passive Schools - impact of boundary conditions (in dutch)," *TVVL-Magazine vol:41 issue:5*, pp. 58–60, 2012.

[224] J. Van der Veken and H. Hens, "Determination of the heating efficiency at building level," in *Building Physics Symposium*, (Liege, Belgium), pp. 101–104, 2008.

[225] M. Maivel and J. Kurnitski, "Low temperature radiator heating distribution and emission efficiency in residential buildings," *Energy and Buildings*, vol. 69, pp. 224–236, Feb. 2014.

[226] M. Trčka, J. L. Hensen, and M. Wetter, "Co-simulation for performance prediction of integrated building and HVAC systems - An analysis of solution characteristics using a two-body system," *Simulation Modelling Practice and Theory*, vol. 18, pp. 957–970, Aug. 2010.

[227] J. Van der Veken, V. De Meulenaer, and H. Hens, "Eindrapport GBOU - EL2EP PROJECT: Ontwikkeling via levenscyclusoptimalisatie van extreem lage energie- en pollutiewoningen (in Dutch)," tech. rep., 2006.

[228] P. Meijer and R. Verweij, "Energieverbruik per functie voor SenterNovem (in Dutch)," tech. rep., Senternovem, Den Haag, The Netherlands, 2009.

[229] L. Dias Pereira, D. Raimondo, S. P. Corgnati, and M. Gameiro da Silva, "Energy consumption in schools - A review paper," *Renewable and Sustainable Energy Reviews*, vol. 40, pp. 911–922, Dec. 2014.

[230] A. Thewes, S. Maas, F. Scholzen, D. Waldmann, and A. Zürbes, "Field study on the energy consumption of school buildings in Luxembourg," *Energy and Buildings*, vol. 68, pp. 460–470, Jan. 2014.

[231] R. Debruyne, "Rapport nr. 14: ontwerp en dimensionering van centrale-verwarmingsinstallaties met warm water (in Dutch)," Tech. Rep. 14, WTCB, Brussels, Belgium, 2013.

[232] NBN D 30-001, *Centrale verwarming, ventilatie en luchtbehandeling - Gemeenschappelijke eisen voor alle systemen - Warmtegeneratoren en branders*. 1991.

[233] H. Breesch, *Natural night ventilation in office buildings*. Phd, UGent, Belgium, Ghent, Belgium, 2006.

[234] W. Kays and A. London, *Compact heat exchangers*. 3rd ed., 1998.

[235] J. Schietecat, "Vereenvoudigde berekeningsmethode voor een vloerverwarmingssysteem (in Dutch)," 1990.

[236] ASHRAE, *ASHRAE Handbook - Fundamentals (SI Edition)*. 2009.

[237] Taylor Engineering, "Advanced variable air volume system design guide," 2007.

[238] V. Dolisy, B. Fabry, C. Rogiest, and P. André, "Detailed simulation of the control system of the secondary system of an HVAC plant," in *8th International Conference on system simulation in buildings*, (Liège, Belgium), pp. 1–21, 2010.

[239] S. Bertagnolio, *Evidence-based model calibration for efficient energy services*. Phd, University of Liège, Belgium, 2012.

[240] S. Holst, "TRNSYS - Models for radiator heating systems," 1996.

[241] H. Ast, "IEA - Annex 10: Thermostatic valves," tech. rep., Institut für Kernenergetik un Energiesysteme, abt. Heizung, Lüftung-Klimattechnik, Universität Stuttgart, Stuttgart, Germany, 1986.

[242] D. Marchio and O. Morisot, "ConsoClim Cahier des Algorithmes: Modélisation simplifiée d'une batterie chaude," tech. rep., Ecole des Mines de Paris, Centre d'Energétique, Paris, France, 2002.

[243] R. Vandenbulcke, *Optimalisatie van hydronische verwarmingsinstallaties door middel van simulatie*. Phd, UA, University of Antwerp, Belgium, 2013.

[244] M. Bernier, "Non-dimensional pumping power curves for water loop heat pumps," 1999.

[245] M. Haller, L. Konersmann, R. Haberl, A. Dröscher, and E. Frank, "Comparison of different approaches for the simulation of boilers using oil, gas, pellets or wood chips," in *11th International IBPSA Conference*, (Glasgow, Schotland), pp. 732–739, 2009.

[246] M. Haller, "Type 869 Boiler Model for TRNSYS," 2010.

[247] NBN EN 15241, *Ventilation for buildings - Calculation methods for energy losses due to ventilation and infiltration in buildings*. 2007.

[248] B. Olesen, "Radiant floor heating in theory and practice," *ASHRAE Journal*, no. July, pp. 19–24, 2002.

[249] B. Michael, *Methode zur Berechnung und Bewertung des Energieaufwandes für die Nutzenübergabe bei Warmwasserheizanlagen*. PhD thesis, Universität Stuttgart, Germany, 1999.

[250] E. Beusker, C. Stoy, and N. Spiro, "Estimation model and benchmarks for heating energy consumption of schools and sport facilities in Germany," *Building and Environment*, vol. 49, pp. 324–335, Mar. 2012.

[251] H.-x. Zhao and F. Magoulès, "A review on the prediction of building energy consumption," *Renewable and Sustainable Energy Reviews*, vol. 16, pp. 3586–3592, Aug. 2012.

[252] V. Corrado, I. Ballarini, and S. Paduos, "Assessment of Cost-optimal Energy Performance Requirements for the Italian Residential Building Stock," *Energy Procedia*, vol. 45, pp. 443–452, 2014.

[253] J. Kurnitski, A. Saari, T. Kalamees, M. Vuolle, J. Niemelä, and T. Tark, "Cost optimal and nearly zero (nZEB) energy performance calculations for residential buildings with REHVA definition for nZEB national implementation," *Energy and Buildings*, vol. 43, pp. 3279–3288, Nov. 2011.

[254] K. Allacker, *Sustainable building: The development of an evaluation method*. Phd, KU Leuven, Belgium, 2010.

[255] C. Becchio, S. P. Corgnati, E. Fabrizio, and V. Monetti, "The cost optimal methodology applied to an existing office in Italy," *REHVA Journal*, no. October, pp. 18–22, 2013.

[256] E. Pikas, M. Thalfeldt, and J. Kurnitski, "Cost optimal and nearly zero energy building solutions for office buildings," *Energy and Buildings*, vol. 74, pp. 30–42, May 2014.

[257] P. C. and R. D., "Cost Optimal Calculations and Gap Analysis for recast EPBD for Non-Residential Buildings," Tech. Rep. March, AECOM, Department of the environment, community and local government, 2013.

[258] European Commission, "Guidelines accompanying Commission Delegated Regulation (EU) No 244/2012 of 16 January 2012 supplementing Directive 2010/31/EU," 2012.

[259] BPIE, "Cost Optimality - Discussing methology and challenges within the recast EPBD," tech. rep., Brussels, Belgium, 2010.

[260] BPIE, "Implementing the cost-optimal methodology in EU countries: Lessons learned from three case studies," tech. rep., Brussel, België, 2013.

[261] European Commission, "Commission delegated regulation (EU) No 244/2012 of 16 January 2012 supplementing Directive 2010/31/EU," 2012.

[262] Europese Commissie, "Richtsnoeren bij Gedelegeerde Verordening (EU) nr.244/2012 van de Commissie van 16 januari 2012 tot aanvulling van Richtlijn 2010/31/EU (in Dutch)," 2012.

[263] EN 15459, *Energy performance of buildings - Economic evaluation procedure for energy systems in buildings*. 2008.

[264] M. Ferrara, E. Fabrizio, J. Virgone, and M. Filippi, "A simulation-based optimization method for cost-optimal analysis of nearly Zero Energy Buildings," *Energy and Buildings*, vol. 84, pp. 442–457, Aug. 2014.

[265] "http://nl.inflation.eu/inflatiecijfers/belgie/historische-inflatie/cpi-inflatie-belgie.aspx."

[266] "www.abex.be," *(Date accessed: 2015-06-01)*.

[267] "http://www.agion.be/subsidi%C3%ABring.aspx," *(Date accessed: 2015-06-29)*.

[268] "http://ec.europa.eu/eurostat/web/energy/data/database," *(Date accessed: 2015-09-29)*.

[269] VREG, "Marktrapport 2014 (in Dutch)," tech. rep., Vlaamse Regulator van de Elektriciteits- en Gasmarkt (VREG), Brussels, Belgium, 2014.

[270] L. Van Buyten, "Education in flanders, the Flemisch educational landscape in a nutshell," 2005.